

CHEMISTRY OF NEOGENE BASALTS OF BRITISH COLUMBIA AND THE
ADJACENT PACIFIC OCEAN FLOOR: A TEST OF TECTONIC
DISCRIMINATION DIAGRAMS

by

LINDA RUTH ERDMAN

B.Sc. UNIVERSITY OF BRITISH COLUMBIA, 1978

A THESIS SUBMITTED IN PARTIAL FULFILMENT OF
THE REQUIREMENTS FOR THE DEGREE OF
MASTER OF SCIENCE

in

THE FACULTY OF GRADUATE STUDIES
DEPARTMENT OF GEOLOGICAL SCIENCES

We accept this thesis as conforming
to the required standard

THE UNIVERSITY OF BRITISH COLUMBIA

OCTOBER, 1985

© LINDA RUTH ERDMAN, 1985

90

89

In presenting this thesis in partial fulfilment of the requirements for an advanced degree at the The University of British Columbia, I agree that the Library shall make it freely available for reference and study. I further agree that permission for extensive copying of this thesis for scholarly purposes may be granted by the Head of my Department or by his or her representatives. It is understood that copying or publication of this thesis for financial gain shall not be allowed without my written permission.

DEPARTMENT OF GEOLOGICAL SCIENCES

The University of British Columbia
2075 Wesbrook Place
Vancouver, Canada
V6T 1W5

Date: OCTOBER, 1985

ABSTRACT

Seventy-one samples of subalkaline and alkaline basalts from British Columbia and the adjacent Pacific seafloor were analyzed for 33 major, trace and rare earth elements using X-ray fluorescence (XRF) and instrumental neutron activation analysis (INAA). These basalts are all less than 22 Ma in age and come from various magmatic belts, each with a distinct, well-known, tectonic setting; (1) Convergent margin (Garibaldi and Pemberton Belts), (2) Back-arc (Chilcotin Basalts), (3) Hotspot (Anahim Volcanic Belt), (4) Incipient rift (Stikine Volcanic Belt), (5) Arc-trench gap (Alert Bay Volcanic Belt) and (6) Ocean floor (Offshore basalts of the Juan de Fuca-Explorer Ridge Systems). Element abundances and ratios were plotted on eighteen diagrams that have been proposed to discriminate between tectonic settings on the basis of magma chemistry. Although eruption through continental crust has modified the abundances of Ba, Th, U, K and Sr, in most cases this did not affect the ability of the diagrams to distinguish tectonic setting.

On most diagrams basalts from back-arc, hotspot, incipient rift and arc-trench gap settings plotted in the within plate basalt (WPB) field, but distinction between these different WPB settings could not be made. Two samples from the Masset Formation on the Queen Charlotte Islands, included with the Anahim Belt hotspot suite, were consistently classified as convergent margin. Samples from the ocean floor plotted in the N-MORB or E-MORB fields.

Three convergent margin samples from the Pemberton Belt always plotted in the convergent margin field, but on most diagrams all eight samples from the Garibaldi Belt plotted in the WPB field because of their depletion in LIL elements.

La is the only rare earth element obtained by INAA that is essential for identifying the tectonic environment of magma genesis. The ratio La/Nb, is an effective separator of within plate basalts (WPB), including E-MORB, (La/Nb less than 1.2) from convergent margin basalts (La/Nb greater than 2.0). N-MORB lie between the ratios 1.2 and 2.0.

Th, Ta and Hf also obtained by INAA, are important discriminant elements. However, Nb and Zr, obtained by XRF analysis convey much of the same information. The ratio Nb/16 as an estimate of Ta and Zr/39 as an estimate for Hf produced acceptable results on diagrams that originally incorporated Ta and Hf. Effective discrimination can therefore usually be achieved using XRF elements alone.

Convergent margin, within plate and ocean floor tectonic settings were best distinguished on Th-Hf/3-Ta, Ti-Zr-Y and Ti-Zr-Sr, Ti/Y vs. Nb/Y, Th/Yb vs. Ta/Yb, $(\text{Ba/La})_{\text{CH}}$ vs. $(\text{La/Sm})_{\text{CH}}$ and V vs. Ti/1000. Slightly less effective plots were MnO-TiO₂-P₂O₅, La vs. Th, La vs. Nb and K₂O/Yb vs. Ta/Yb. On the other hand TiO₂-K₂O-P₂O₅, MgO-FeO*-Al₂O₃ and La vs. Ba provided little information concerning the tectonic setting of individual samples.

Ti/Cr vs. Ni, Sm/Ce vs. Sr/Ce, Cr vs. Ce/Sr and Cr vs. Y diagrams were useful for distinguishing unfractionated

convergent margin basalts from MORB plus WPB.

Table of Contents

| | |
|--|-------|
| ABSTRACT | ii |
| LIST OF TABLES | x |
| LIST OF FIGURES | xii |
| ACKNOWLEDGMENTS | xvii |
| GLOSSARY | xviii |
| 1. OBJECTIVES | 1 |
| 1.1 SAMPLE SELECTION AND METHODS OF ANALYSIS | 1 |
| 1.2 TECTONIC SETTING | 3 |
| 2. REVIEW OF MAJOR AND TRACE ELEMENT TECTONIC DISCRIMINATION DIAGRAMS | 9 |
| 2.1 CHEMICAL DISTINCTIONS BASED ON MAJOR ELEMENTS | 9 |
| 2.1.1 ALKALINE vs. SUBALKALINE | 9 |
| 2.1.2 THOLEIITIC vs. CALCALKALINE | 11 |
| 2.1.3 OCEANIC vs. NON-OCEANIC | 13 |
| 2.1.3.1 $\text{TiO}_2\text{-K}_2\text{O-P}_2\text{O}_5$ | 13 |
| 2.1.3.2 $\text{MnO-TiO}_2\text{-P}_2\text{O}_5$ | 13 |
| 2.1.3.3 $\text{MgO-FeO}^*\text{-Al}_2\text{O}_3$ | 15 |
| 2.2 TRACE ELEMENT GEOCHEMISTRY | 15 |
| 2.2.1 OCEAN FLOOR BASALTS (MORB) | 17 |
| 2.2.2 OCEAN ISLAND BASALTS (WPB) | 18 |
| 2.2.3 CONVERGENT MARGIN BASALTS (ARC) | 19 |
| 2.3 RARE EARTH ELEMENT GEOCHEMISTRY | 20 |
| 2.4 TRACE ELEMENT DIAGRAMS | 22 |
| 2.4.1 Ti-Zr-Y and Ti-Zr-Sr | 22 |
| 2.4.2 V vs. Ti/1000 | 22 |
| 2.4.3 Ti/Y vs. Nb/Y | 24 |
| 2.4.4 Ti/Cr vs. Ni | 24 |

| | | |
|-------|--|----|
| 2.5 | TRACE AND REE DIAGRAMS | 27 |
| 2.5.1 | Sm/Ce vs. Sr/Ce and Cr vs. Ce/Sr | 27 |
| 2.5.2 | Cr vs. Y | 29 |
| 2.5.3 | (Ba/La) _{CH} vs. (La/Sm) _{CH} | 29 |
| 2.5.4 | La vs. Ba La vs. Th La vs. Nb | 31 |
| 2.5.5 | K ₂ O/Yb vs. Ta/Yb | 34 |
| 2.5.6 | Th/Yb vs. Ta/Yb | 34 |
| 2.5.7 | Th vs. Ta La vs. Ta Th vs. Hf | 34 |
| 2.5.8 | Th-Hf/3-Ta | 36 |
| 2.6 | BULK EARTH NORMALIZED TRACE AND REE DIAGRAMS (BEND) | 40 |
| 2.6.1 | MORB | 41 |
| 2.6.2 | WPB | 41 |
| 2.6.3 | CONVERGENT MARGIN BASALTS | 43 |
| 3. | GARIBALDI and PEMBERTON BELTS | 47 |
| 3.1 | MAJOR ELEMENT CHEMISTRY | 47 |
| 3.2 | DISCRIMINATION DIAGRAMS | 49 |
| 3.2.1 | MAJOR ELEMENT CLASSIFICATIONS | 49 |
| 3.2.2 | TRACE ELEMENT CLASSIFICATIONS | 53 |
| 3.2.3 | TRACE AND REE CLASSIFICATIONS | 53 |
| 3.2.4 | BULK EARTH NORMALIZED DIAGRAMS (BEND) | 63 |
| 3.3 | TRACE ELEMENT CHEMISTRY | 68 |
| 3.3.1 | Th and U | 69 |
| 3.3.2 | TRANSITION ELEMENTS | 70 |
| 3.4 | Sr ISOTOPES | 70 |
| 3.5 | DISCUSSION OF DISCRIMINATION DIAGRAMS | 71 |
| 3.6 | SUMMARY | 73 |

| | | |
|-------|---|-----|
| 4. | CHILCOTIN BASALTS | 78 |
| 4.1 | MAJOR ELEMENT CHEMISTRY | 78 |
| 4.2 | DISCRIMINATION DIAGRAMS | 80 |
| 4.2.1 | MAJOR ELEMENT CLASSIFICATIONS | 80 |
| 4.2.2 | TRACE ELEMENT CLASSIFICATIONS | 82 |
| 4.2.3 | TRACE AND REE CLASSIFICATIONS | 85 |
| 4.2.4 | BULK EARTH NORMALIZED DIAGRAMS (BEND) | 92 |
| 4.3 | TRACE ELEMENT CHEMISTRY | 96 |
| 4.3.1 | Th and U | 97 |
| 4.3.2 | TRANSITION ELEMENTS | 97 |
| 4.4 | Sr ISOTOPES | 98 |
| 4.5 | DISCUSSION OF DISCRIMINATION DIAGRAMS | 98 |
| 4.6 | SUMMARY | 100 |
| 5. | ANAHIM VOLCANIC BELT | 103 |
| 5.1 | MAJOR ELEMENT CHEMISTRY | 103 |
| 5.2 | DISCRIMINATION DIAGRAMS | 105 |
| 5.2.1 | MAJOR ELEMENT CLASSIFICATIONS | 105 |
| 5.2.2 | TRACE ELEMENT CLASSIFICATIONS | 107 |
| 5.2.3 | TRACE AND REE CLASSIFICATIONS | 109 |
| 5.2.4 | BULK EARTH NORMALIZED DIAGRAMS (BEND) | 118 |
| 5.3 | TRACE ELEMENT CHEMISTRY | 121 |
| 5.3.1 | Th AND U | 125 |
| 5.3.2 | TRANSITION ELEMENTS | 125 |
| 5.4 | Sr ISOTOPES | 126 |
| 5.5 | DISCUSSION OF DISCRIMINATION DIAGRAMS | 126 |
| 5.6 | SUMMARY | 129 |
| 6. | STIKINE VOLCANIC BELT | 133 |

| | | |
|-------|---|-----|
| 6.1 | MAJOR ELEMENT CHEMISTRY | 135 |
| 6.2 | DISCRIMINATION DIAGRAMS | 136 |
| 6.2.1 | MAJOR ELEMENT CLASSIFICATIONS | 136 |
| 6.2.2 | TRACE ELEMENT CLASSIFICATIONS | 139 |
| 6.2.3 | TRACE AND REE CLASSIFICATIONS | 139 |
| 6.2.4 | BULK EARTH NORMALIZED DIAGRAMS (BEND) | 147 |
| 6.3 | TRACE ELEMENT CHEMISTRY | 156 |
| 6.3.1 | Th AND U | 157 |
| 6.3.2 | TRANSITION ELEMENTS | 157 |
| 6.4 | Sr ISOTOPES | 158 |
| 6.5 | DISCUSSION OF DISCRIMINATION DIAGRAMS | 159 |
| 6.6 | SUMMARY | 161 |
| 7. | ALERT BAY VOLCANIC BELT | 166 |
| 7.1 | MAJOR ELEMENT CHEMISTRY | 166 |
| 7.2 | DISCRIMINANT DIAGRAMS | 168 |
| 7.2.1 | MAJOR ELEMENT CLASSIFICATIONS | 168 |
| 7.2.2 | TRACE ELEMENT CLASSIFICATIONS | 171 |
| 7.2.3 | TRACE AND REE CLASSIFICATIONS | 171 |
| 7.2.4 | BULK EARTH NORMALIZED DIAGRAMS (BEND) | 176 |
| 7.3 | TRACE ELEMENT CHEMISTRY | 180 |
| 7.3.1 | Th and U | 181 |
| 7.3.2 | TRANSITION ELEMENTS | 181 |
| 7.4 | ISOTOPIC DATA | 181 |
| 7.5 | DISCUSSION OF DISCRIMINATION DIAGRAMS | 182 |
| 7.6 | SUMMARY | 183 |
| 8. | OFFSHORE BASALTS | 186 |
| 8.1 | MAJOR ELEMENT CHEMISTRY | 186 |

| | | |
|-------|--|-----|
| 8.2 | DISCRIMINATION DIAGRAMS | 188 |
| 8.2.1 | MAJOR ELEMENT CLASSIFICATIONS | 188 |
| 8.2.2 | TRACE ELEMENT CLASSIFICATIONS | 192 |
| 8.2.3 | TRACE AND REE CLASSIFICATIONS | 195 |
| 8.2.4 | BULK EARTH NORMALIZED DIAGRAMS (BEND) | 199 |
| 8.3 | TRACE ELEMENT CHEMISTRY | 206 |
| 8.3.1 | Th AND U | 208 |
| 8.3.2 | TRANSITION ELEMENTS | 208 |
| 8.4 | Sr ISOTOPES | 209 |
| 8.5 | DISCUSSION OF DISCRIMINATION DIAGRAMS | 210 |
| 8.6 | SUMMARY | 212 |
| 9. | SUMMARY OF DISCRIMINATION DIAGRAM DISCUSSIONS | 216 |
| 10. | CONCLUSIONS | 227 |
| | REFERENCES | 230 |
| | APPENDIX I - SAMPLE SOURCES AND PREVIOUS ANALYSES | 243 |
| | APPENDIX II - NEUTRON ACTIVATION ANALYSIS | 249 |
| | APPENDIX III - MAJOR AND TRACE ELEMENT ANALYSIS BY XRF | 271 |
| | APPENDIX IV - TA CONTAMINATION | 286 |

LIST OF TABLES

| | | |
|-------------|--|-----|
| TABLE I. | Normalization Values for Bulk Earth Normalized Diagrams | 42 |
| TABLE II. | Garibaldi and Pemberton Belts: Major, trace and rare earth element abundances, Sr iotope ratios and K-Ar dates | 76 |
| TABLE III. | Chilcotin Basalts: Major, trace and rare earth element abundances, Sr iotope ratios and K-Ar dates . 102 | |
| TABLE IV. | Anahim Volcanic Belt: Major, trace and rare earth element abundances, Sr iotope ratios, K-Ar dates and ages | 131 |
| TABLE V. | Stikine Volcanic Belt: Major, trace and rare earth element abundances, Sr iotope ratios, K-Ar dates and ages | 163 |
| TABLE VI. | Alert Bay Volcanic Belt: Major, trace and rare earth element abundances, Sr iotope ratios and K-Ar dates | 185 |
| TABLE VII. | Offshore Basalts: Major, trace and rare earth element abundances, Sr iotope ratios and estimated ages | 214 |
| TABLE VIII. | Classification of Sample Suites Using Discrimination Diagrams | 217 |
| TABLE IX. | Efficiency of Tectonic Discrimination Diagrams | 222 |
| TABLE X. | Element Isotope Data | 251 |
| TABLE XI. | Standard Abundnces of Selected Trace and Rare Earth Elements in Standards Used for INAA | 253 |
| TABLE XII. | Table of Interferences | 257 |

| | | |
|--------------|---|-----|
| TABLE XIII. | Precision of INAA Based on Replicate Analyses | 260 |
| TABLE XIV. | Relative Precisions Based on Replicate Analyses | 264 |
| TABLE XV. | Test of Analytical Accuracy for INAA . | 265 |
| TABLE XVI. | Systematic Error in INAA Analyses . . . | 268 |
| TABLE XVII. | Element Abundances in Intralab Standards WP1 and P1. | 270 |
| TABLE XVIII. | Precision of Major Element Analyses . . | 273 |
| TABLE XIX. | Precision of Trace Element Analyses . . | 277 |
| TABLE XX. | Calculated Abundances of Nb and Ta in Analyzed Basaltic Samples | 290 |
| TABLE XXI. | Abundances of Nb and Ta in Standards (Abbey, 1983). | 293 |
| TABLE XXII. | Abundances of Nb and Ta in Terrestrial Rocks (Wood, 1980) | 294 |

LIST OF FIGURES

| | |
|---|----|
| Fig. 1.1. Neogene volcanic trends of British Columbia and offshore plate boundaries. | 4 |
| Fig. 2.1. $K_2O + Na_2O$ vs. SiO_2 distinguishing alkaline and subalkaline rocks. | 10 |
| Fig. 2.2. AFM diagram separating calcalkaline from tholeiitic volcanic rocks. | 12 |
| Fig. 2.3. FeO^*/MgO vs. SiO_2 diagram separating calcalkaline from tholeiitic volcanic rocks. | 12 |
| Fig. 2.4. $TiO_2-K_2O-P_2O_5$ separating oceanic from non-oceanic basalts. | 14 |
| Fig. 2.5. $MnO-TiO_2-P_2O_5$ with fields for MORB, IAT, CAB, OIT and OIA. | 14 |
| Fig. 2.6. $MgO-FeO^*-Al_2O_3$ diagram distinguishing fields for ARC, CB, OI, N-MORB and E-MORB. | 16 |
| Fig. 2.7. Ti-Zr-Y showing fields for WPB, LKT, OFB and CAB. | 23 |
| Fig. 2.8. Ti-Zr-Sr showing fields for LKT, OFB and CAB. | 23 |
| Fig. 2.9. V vs. $Ti/1000$ distinguishing fields for WPB, MORB and tholeiitic convergent margin basalts. | 25 |
| Fig. 2.10. Ti/Y vs. Nb/Y with fields for WPB, MORB and convergent margin basalt. | 25 |
| Fig. 2.11. Ti/Cr vs. Ni diagram with fields for tholeiitic convergent margin basalt and tholeiitic MORB. | 26 |
| Fig. 2.12. Sm/Ce vs. Sr/Ce distinguishing convergent margin rocks from oceanic volcanic rocks. | 28 |
| Fig. 2.13. Cr vs. Ce/Sr with a field for convergent margin basalts separated from overlapping MORB and WPB fields. | 28 |
| Fig. 2.14. Cr vs. Y with convergent margin, MORB and WPB fields. | 30 |
| Fig. 2.15. $(Ba/La)_{CH}$ vs. $(La/Sm)_{CH}$ diagram distinguishing basalts from convergent margins and oceanic areas (ocean ridge and intraplate). | 32 |
| Fig. 2.16. La vs. Ba with fields for N-MORB, E-MORB plus WPB and orogenic andesites. | 32 |
| Fig. 2.17. La vs. Th with fields for N-MORB, E-MORB plus WPB and orogenic andesites. | 33 |
| Fig. 2.18. La vs. Nb with fields for N-MORB, E-MORB plus WPB and orogenic andesites. | 33 |
| Fig. 2.19. K_2O/Yb vs. Ta/Yb distinguishing convergent margin basalts from slightly overlapping MORB and WPB fields. | 35 |
| Fig. 2.20. Th/Yb vs. Ta/Yb distinguishing convergent margin basalts from slightly overlapping MORB and WPB fields. | 35 |
| Fig. 2.21. Th vs. Ta distinguishing convergent margin basalts from N-MORB plus E-MORB plus WPB. | 37 |
| Fig. 2.22. La vs. Ta with fields for convergent margin basalts, N-MORB and E-MORB. | 37 |
| Fig. 2.23. Th vs. Hf diagram distinguishing fields for WPB, N-MORB and E-MORB. | 38 |

| | | |
|------------|--|----|
| Fig. 2.24. | Th-Hf/3-Ta with fields for N-MORB, E-MORB plus tholeiitic WPB, alkaline WPB and convergent margin basalts. | 39 |
| Fig. 2.25. | BEND patterns for N-MORB and E-MORB. | 44 |
| Fig. 2.26. | BEND patterns for alkaline oceanic WPB, alkaline continental WPB and tholeiitic continental WPB. | 45 |
| Fig. 2.27. | BEND patterns for calcalkaline and alkaline convergent margin basalts. | 46 |
| Fig. 3.1. | Sample location map for the Convergent Margin Suite. | 48 |
| Fig. 3.2. | Total alkalis vs. silica. | 51 |
| Fig. 3.3. | AFM diagram. | 51 |
| Fig. 3.4. | FeO*/NgO vs. SiO ₂ . | 51 |
| Fig. 3.5. | TiO ₂ -K ₂ O-P ₂ O ₅ . | 52 |
| Fig. 3.6. | MnO-TiO ₂ -P ₂ O ₅ . | 52 |
| Fig. 3.7. | MgO-FeO*-Al ₂ O ₃ . | 52 |
| Fig. 3.8. | Ti-Zr-Y. | 54 |
| Fig. 3.9. | Ti-Zr-Sr. | 54 |
| Fig. 3.10. | V vs. Ti/1000. | 54 |
| Fig. 3.11. | Ti/Y vs. Nb/Y. | 55 |
| Fig. 3.12. | Ti/Cr vs. Ni. | 55 |
| Fig. 3.13. | Sm/Ce vs. Sr/Ce. | 57 |
| Fig. 3.14. | Cr vs. Ce/Sr. | 57 |
| Fig. 3.15. | Cr vs. Y. | 58 |
| Fig. 3.16. | La vs. Ba. | 59 |
| Fig. 3.17. | (Ba/La) _{CH} vs. (La/Sm) _{CH} . | 59 |
| Fig. 3.18. | La vs. Th. | 60 |
| Fig. 3.19. | La vs. Nb. | 60 |
| Fig. 3.20. | K ₂ O/Yb vs. Ta*/Yb. | 62 |
| Fig. 3.21. | Th/Yb vs. Ta*/Yb. | 62 |
| Fig. 3.22. | Th-Hf/3-Ta*. | 62 |
| Fig. 3.23. | BEN diagram for samples COQ253, COQ632 and COQ63. | 64 |
| Fig. 3.24. | BEN diagram for samples ELAHO, GARIBALD, CHEAK and MEAGER. | 65 |
| Fig. 3.25. | BEN diagram for samples SALAL1, SALAL2, SALAL3 and SILVERH. | 66 |
| Fig. 3.26. | BEN diagram for samples CAYLEY and SILVERA. | 67 |
| Fig. 4.1. | Sample location map for the Chicotin Basalt Suite. | 79 |
| Fig. 4.2. | Total alkalis vs. silica. | 81 |
| Fig. 4.3. | AFM diagram. | 81 |
| Fig. 4.4. | FeO*/NgO vs. SiO ₂ . | 81 |
| Fig. 4.5. | TiO ₂ -K ₂ O-P ₂ O ₅ . | 83 |
| Fig. 4.6. | MnO-TiO ₂ -P ₂ O ₅ . | 83 |
| Fig. 4.7. | MgO-FeO*-Al ₂ O ₃ . | 83 |
| Fig. 4.8. | Ti-Zr-Y. | 84 |
| Fig. 4.9. | V vs. Ti/1000. | 84 |
| Fig. 4.10. | Ti/Y vs. Nb/Y. | 86 |
| Fig. 4.11. | Ti/Cr vs. Ni. | 86 |

| | | |
|------------|--|----|
| Fig. 4.12. | Cr vs. Ce/Sr. | 87 |
| Fig. 4.13. | Cr vs. Y. | 87 |
| Fig. 4.14. | La vs. Ba. | 89 |
| Fig. 4.15. | (Ba/La) _{CH} vs. (La/Sm) _{CH} | 89 |
| Fig. 4.16. | La vs. Th. | 90 |
| Fig. 4.17. | La vs. Nb. | 90 |
| Fig. 4.18. | K ₂ O/Yb vs. Ta*/Yb. | 91 |
| Fig. 4.19. | Th/Yb vs. Ta*/Yb. | 91 |
| Fig. 4.20. | Th-Hf/3-Ta*. | 91 |
| Fig. 4.21. | BEN diagram for samples QUESW, WOOD LK and BLIZZARD. | 93 |
| Fig. 4.22. | BEN diagram for samples REDSTONE, NAZKO, CAMEL, DOG CK, EDMUND and DEADMAN. | 94 |
| Fig. 4.23. | BEN diagram for samples BULL CAN and CARD. | 95 |

| | | |
|------------|---|-----|
| Fig. 5.1. | Sample location map for the Anahim Volcanic Belt. | 104 |
| Fig. 5.2. | Total alkalis vs. silica. | 106 |
| Fig. 5.3. | AFM diagram. | 106 |
| Fig. 5.4. | FeO*/NgO vs. SiO ₂ | 106 |
| Fig. 5.5. | TiO ₂ -K ₂ O-P ₂ O ₅ | 108 |
| Fig. 5.6. | MnO-TiO ₂ -P ₂ O ₅ | 108 |
| Fig. 5.7. | MgO-FeO*-Al ₂ O ₃ | 108 |
| Fig. 5.8. | Ti-Zr-Y. | 110 |
| Fig. 5.9. | Ti-Zr-Sr. | 110 |
| Fig. 5.10. | V vs. Ti/1000. | 110 |
| Fig. 5.11. | Ti/Y vs. Nb/Y. | 111 |
| Fig. 5.12. | Ti/Cr vs. Ni. | 111 |
| Fig. 5.13. | Sm/Ce vs. Sr/Ce. | 113 |
| Fig. 5.14. | Cr vs. Ce/Sr. | 113 |
| Fig. 5.15. | Cr vs. Y. | 114 |
| Fig. 5.16. | La vs. Ba. | 116 |
| Fig. 5.17. | (Ba/La) _{CH} vs. (La/Sm) _{CH} | 116 |
| Fig. 5.18. | La vs. Th. | 117 |
| Fig. 5.19. | La vs. Nb. | 117 |
| Fig. 5.20. | K ₂ O/Yb vs. Ta*/Yb. | 119 |
| Fig. 5.21. | Th/Yb vs. Ta*/Yb. | 119 |
| Fig. 5.22. | Th-Hf/3-Ta*. | 119 |
| Fig. 5.23. | BEN diagram for samples KITASU, LAKE IS, RAINBOW, ANAHIM, ITCHA1 and ITCHA2. | 120 |
| Fig. 5.24. | BEN diagram for samples ALEX, QUES LK, WGRAYN, SPAN CK and TROPHY. | 122 |
| Fig. 5.25. | BEN diagram for samples MASSET1, MASSET2 and ARIS IS. | 123 |

| | | |
|-----------|--|-----|
| Fig. 6.1. | Sample location map for the Stikine Volcanic Belt. | 134 |
| Fig. 6.2. | Total alkalis vs. silica. | 138 |
| Fig. 6.3. | AFM diagram. | 138 |
| Fig. 6.4. | FeO*/NgO vs. SiO ₂ | 138 |
| Fig. 6.5. | TiO ₂ -K ₂ O-P ₂ O ₅ | 140 |
| Fig. 6.6. | MnO-TiO ₂ -P ₂ O ₅ | 140 |

| | | |
|------------|--|-----|
| Fig. 6.7. | MgO-FeO*-Al ₂ O ₃ . | 140 |
| Fig. 6.8. | Ti-Zr-Y. | 141 |
| Fig. 6.9. | V vs. Ti/1000. | 141 |
| Fig. 6.10. | Ti/Y vs. Nb/Y. | 142 |
| Fig. 6.11. | Ti/Cr vs. Ni. | 142 |
| Fig. 6.12. | Cr vs. Ce/Sr. | 144 |
| Fig. 6.13. | Cr vs. Y. | 144 |
| Fig. 6.14. | La vs. Ba. | 145 |
| Fig. 6.15. | (Ba/La) _{CH} vs. (La/Sm) _{CH} . | 145 |
| Fig. 6.16. | La vs. Th. | 146 |
| Fig. 6.17. | La vs. Nb. | 146 |
| Fig. 6.18. | K ₂ O/Yb vs. Ta*/Yb. | 147 |
| Fig. 6.19. | Th/Yb vs. Ta*/Yb. | 147 |
| Fig. 6.20. | Th-Hf/3-Ta*. | 147 |
| Fig. 6.21. | BEN diagram for samples PRINCER, LEVELD and SATLIN. | 149 |
| Fig. 6.22. | BEN diagram for samples AYNH1, AYNH2 and BOWSER. | 151 |
| Fig. 6.23. | BEN diagram for samples MTDUNN, ISKUT, ISKUTW and BORDERLK. | 152 |
| Fig. 6.24. | BEN diagram for samples EDZ1, SPEC1, SPEC2 and EDZ2. | 153 |
| Fig. 6.25. | BEN diagram for samples NEDZ1, NEDZ2, NEDZ3 and NEDZ4. | 154 |
| Fig. 6.26. | BEN diagram for samples LEVEL1, LEVEL2 and NATLIN. | 155 |
| Fig. 7.1. | Sample location map for the Alert Bay Volcanic Belt. | 167 |
| Fig. 7.2. | Total alkalis vs. silica. | 169 |
| Fig. 7.3. | AFM diagram. | 169 |
| Fig. 7.4. | FeO*/MgO vs. SiO ₂ . | 169 |
| Fig. 7.5. | TiO ₂ -K ₂ O-P ₂ O ₅ . | 170 |
| Fig. 7.6. | MnO-TiO ₂ -P ₂ O ₅ . | 170 |
| Fig. 7.7. | MgO-FeO*-Al ₂ O ₃ . | 170 |
| Fig. 7.8. | Ti-Zr-Y. | 172 |
| Fig. 7.9. | V vs. Ti/1000. | 172 |
| Fig. 7.10. | Ti/Y vs. Nb/Y. | 172 |
| Fig. 7.11. | Ti/Cr vs. Ni. | 173 |
| Fig. 7.12. | Sm/Ce vs. Sr/Ce. | 173 |
| Fig. 7.13. | Cr vs. Ce/Sr. | 174 |
| Fig. 7.14. | Cr vs. Y. | 174 |
| Fig. 7.15. | La vs. Ba. | 175 |
| Fig. 7.16. | (Ba/La) _{CH} vs. (La/Sm) _{CH} . | 175 |
| Fig. 7.17. | La vs. Th. | 177 |
| Fig. 7.18. | La vs. Nb. | 177 |
| Fig. 7.19. | K ₂ O/Yb vs. Ta*/Yb. | 178 |
| Fig. 7.20. | Th/Yb vs. Ta*/Yb. | 178 |
| Fig. 7.21. | Th-Hf/3-Ta*. | 178 |
| Fig. 7.22. | BEN diagram for samples ALERT1, ALERT2 and ALERT3. | 179 |

| | | |
|------------|--|-----|
| Fig. 8.1. | Sample location map for the Ocean Floor Basalt Suite. | 187 |
| Fig. 8.2. | Total alkalis vs. silica. | 190 |
| Fig. 8.3. | AFM diagram. | 190 |
| Fig. 8.4. | FeO*/NgO vs. SiO ₂ . | 190 |
| Fig. 8.5. | TiO ₂ -K ₂ O-P ₂ O ₅ . | 191 |
| Fig. 8.6. | MnO-TiO ₂ -P ₂ O ₅ . | 191 |
| Fig. 8.7. | MgO-FeO*-Al ₂ O ₃ . | 191 |
| Fig. 8.8. | Ti-Zr-Y. | 193 |
| Fig. 8.9. | Ti-Zr-Sr. | 193 |
| Fig. 8.10. | V vs. Ti/1000. | 193 |
| Fig. 8.11. | Ti/Y vs. Nb/Y. | 194 |
| Fig. 8.12. | Ti/Cr vs. Ni. | 194 |
| Fig. 8.13. | Sm/Ce vs. Sr/Ce. | 196 |
| Fig. 8.14. | Cr vs. Ce/Sr. | 196 |
| Fig. 8.15. | Cr vs. Y. | 197 |
| Fig. 8.16. | La vs. Ba. | 198 |
| Fig. 8.17. | (Ba/La) _{CH} vs. (La/Sm) _{CH} . | 198 |
| Fig. 8.18. | La vs. Th. | 200 |
| Fig. 8.19. | La vs. Nb. | 200 |
| Fig. 8.20. | K ₂ O/Yb vs. Ta*/Yb. | 201 |
| Fig. 8.21. | Th/Yb vs. Ta*/Yb. | 201 |
| Fig. 8.22. | Th-Hf/3-Ta*. | 201 |
| Fig. 8.23. | BEN diagram for samples EXMOUNT1, EXMOUNT2 and EXMOUNT3. | 202 |
| Fig. 8.24. | BEN diagram for samples BRBEAR1, BRBEAR2, COBB1 and COBB2. | 204 |
| Fig. 8.25. | BEN diagram for samples SEXRIDGE, PREVRDG, EXRIFT and EXDEEP. | 205 |

ACKNOWLEDGMENTS

I would like to thank Dr. R.L. Armstrong for suggesting the thesis topic, for providing guidance and for critically reviewing the manuscript many times before the final draft. I am also grateful for the comments and suggestions from Drs. R.L. Chase, W.H. Mathews and K. Russell which greatly improved the final manuscript.

Many thanks is extended to NOVATRAK for irradiation of the samples, for letting me use their equipment for INAA and to J. Humphries who spent time teaching me the techniques of INAA. I would also like to thank B. Cousens of the Department of Oceanography for doing the XRF analyses, S. Horsky of the Department of Geology who provided assistance with analytical procedures and R. Berman, G. Nixon, B. Cousens and E. Perkins who wrote the computer programs for data reduction and plotting.

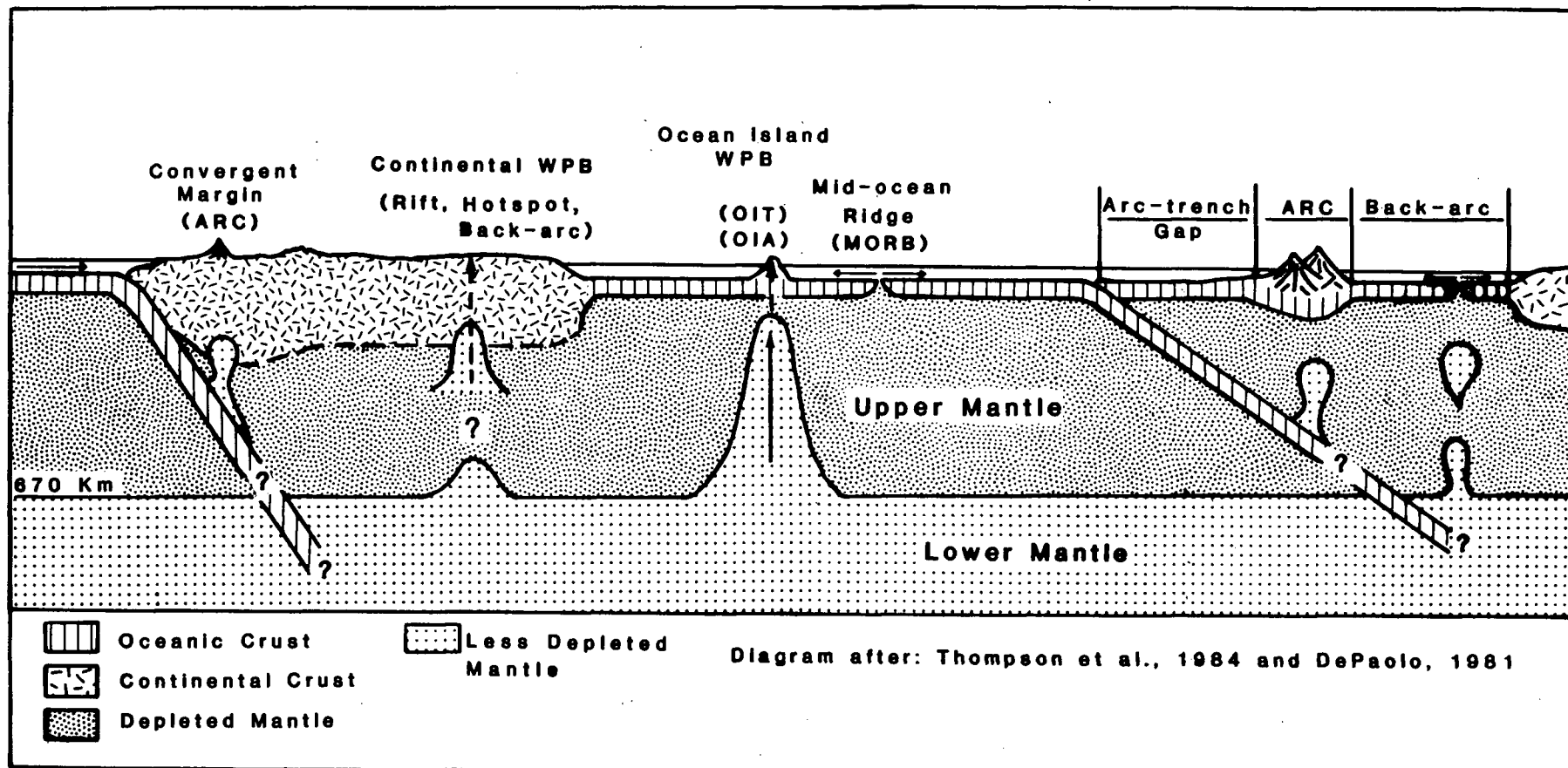
I am indebted to the individuals who collected the samples for their B.Sc., M.Sc., and Ph.D. thesis projects, and by doing so created the research collections from which the samples for this study were selected. Additional samples were provided by Dr. T. Hamilton of the Pacific Geoscience Center and Dr. J. G. Souther of the Geological Survey of Canada.

Funding for this project was from Natural Sciences and Engineering Research Council of Canada operating grant 67-8841 to Dr. R.L. Armstrong and from an NSERC scholarship and Graduate Teaching Assistantship awarded to the author.

GLOSSARY

| | | |
|-------------------|---|--|
| ARC | - | convergent margin = volcanic arc |
| BEND | - | bulk earth normalized diagram |
| CAB | - | calcalkaline basalt |
| CA | - | calcalkaline |
| CB | - | continental basalt |
| E-MORB | - | enriched MORB |
| HREE | - | heavy rare earth element |
| IAT | - | island arc tholeiite |
| INAA | - | instrumental neutron activation analysis |
| LIL | - | large ion lithophile |
| LREE | - | light rare earth element |
| MORB | - | mid-ocean ridge basalt |
| N-MORB | - | normal MORB |
| OFB | - | ocean floor basalt |
| OI | - | ocean island |
| OIA | - | ocean island alkaline |
| OIT | - | ocean island tholeiite |
| REE | - | rare earth element |
| TH | - | tholeiite |
| TH MORB | - | tholeiitic MORB |
| XRF | - | X-ray fluorescence |
| WPB | - | within plate basalt |
| () _{CH} | - | chondrite normalized |

SCHEMATIC DIAGRAM OF TECTONIC SETTING TERMS IN GLOSSARY



1. OBJECTIVES

Tectonic discrimination diagrams which use major and trace element abundances in basaltic rocks have been used to infer tectonic setting. These diagrams were produced using analytical data from unaltered basalts from known tectonic settings, many of them erupted through oceanic crust. In subsequent applications the same diagrams have been used to identify tectonic settings of metamorphosed and/or deformed basic rocks, now incorporated into and often erupted through continental crust. The present investigation was undertaken to:

1. provide more complete chemical data for each suite, and
2. ascertain the applicability of various tectonic discrimination diagrams to suites of Neogene basalts from British Columbia and the adjacent Pacific and Explorer plates which have been erupted in a variety of known tectonic settings.

1.1 SAMPLE SELECTION AND METHODS OF ANALYSIS

The samples studied existed in research collections at U.B.C. and at the G.S.C. in Vancouver. Since this thesis was concerned with discrimination diagrams for basaltic rocks, most samples selected had either a SiO_2 content of less than 55 wt.% (known from previous analyses) or they had been described (verbally) as basalts. These criteria were met for all samples except COQ61 (58.75% SiO_2), CAYLEY (60.34% SiO_2), SILVERA (59.81% SiO_2), ALERT1 (61.15% SiO_2) and

HOODOO (59.18% SiO₂).

Many of the samples chosen for this study had already been described, analyzed by XRF for major and trace elements, and had Sr isotopic determinations and K-Ar dates. A few of them were not previously analyzed. Sample source information and a list of previous analytical work is given in Appendix I.

Incomplete major and trace element data sets were filled in by new XRF analyses and some of the previously analyzed samples were reanalyzed in order to estimate precision of results. Total Fe was measured as Fe₂O₃ and calculated as FeO*. Sample preparation, method of analysis, abundances obtained from duplicate analyses and precision of analyses are given in Appendix III.

Instrumental neutron activation analysis (INAA) (see Appendix II) was used for selected trace and rare earth elements (REE) with the expectation that future studies at U.B.C. might routinely use INAA. Estimates of precision based on replicate analyses are presented in Appendix II, Table XIII, and Table XIV; tests of analytical accuracy are listed in Table XV, and systematic errors in analysis are presented in Table XVI. Because systematic errors were greater than the precision of analysis for La, Hf, Yb and Sc calculated abundances of these elements were revised by an amount equal to the systematic error.

In addition, trace and REE abundances obtained by INAA were determined for intralab standards WP1 and P-1. These

are presented in Appendix II, Table XVII.

Analysis for Ta was unsuccessful because of contamination so Ta abundances were estimated using the ratio Nb/16, denoted Ta*. A more detailed explanation is given in Appendix IV.

1.2 TECTONIC SETTING

The Neogene and younger volcanic trends from western British Columbia and southwestern Yukon, and the present plate boundaries are shown in Figure 1.1. The Queen Charlotte right lateral transform fault which separates the Pacific Plate and North American plates parallels the edge of the continent from southeast Alaska to a triple junction in the vicinity of Delwood Knolls at latitude 50° N. (Yorath and Hyndman, 1983; Riddihough, 1984). Earthquake first motion studies along this fault show almost pure strike-slip motion on a near vertical plane (Milne et al., 1981), however Srivastava (1973), Horn et al., (1981) and Yorath and Hyndman (1983) suggest there may be a component of underthrusting of the Pacific plate beneath the North America plate along the fault zone since Miocene time.

To the north, the Queen Charlotte fault continues into Alaska as the Fairweather fault system (Plafker et al., 1978). Southwest of the triple junction at 50° N, spreading axes (Tuzo Wilson and Delwood Knolls, Explorer Ridge and the Juan de Fuca Ridge) and transform faults (Paul Revere and Sovanco fracture zones) separate the Pacific from Juan de

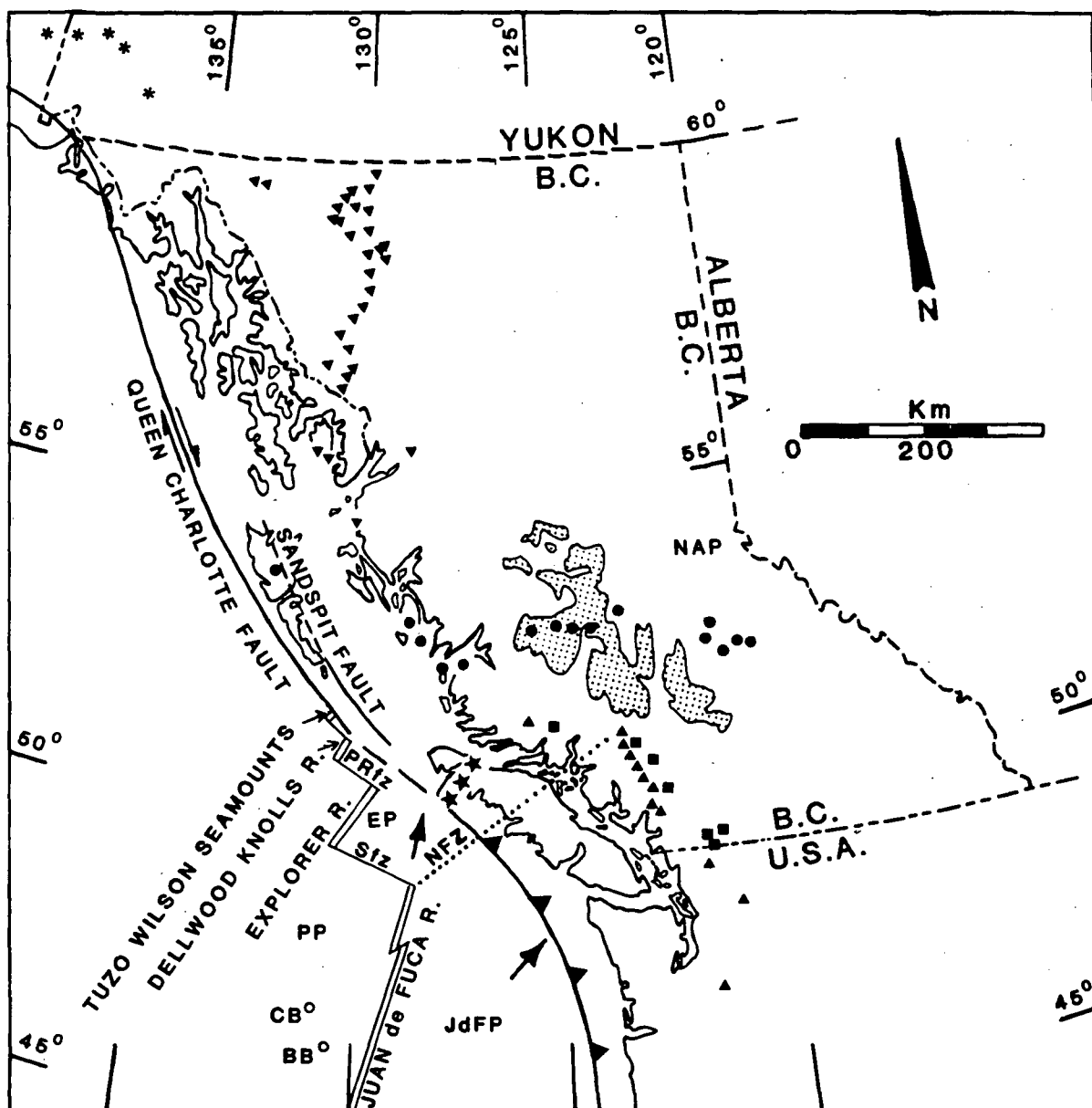


Fig. 1.1. Neogene volcanic trends of British Columbia and southwestern Yukon and present plate tectonic boundaries, showing extent of Garibaldi Volcanic Belt (▲), Pemberton Belt (■), Alert Bay Volcanic Belt (★), Anahim Volcanic Belt (●), Stikine Volcanic Belt (▼) and southeastern Wrangell Volcanic Belt (*). Outlined dotted areas show the extent of the Chilcotin Group Basalts. PP - Pacific plate, EP - Explorer plate, JdFP - Juan de Fuca plate, NAP - North America plate, PRfz - Paul Revere fracture zone (ridge), Sfz - Sovanco fracture zone, NFZ - Nootka fracture zone, CB - Cobb seamount, BB - Brown Bear seamount. Diagram modified from Bevier et al., 1979.

Fuca and Explorer plates. These two smaller plates are separated by the northeasterly trending Nootka left lateral transform fault, which formed in Pliocene time (Riddihough, 1977, Hyndman et al., 1979).

The plate boundary separating the Juan de Fuca and Explorer plates from the North American plate is one of convergence. Although an eastward dipping seismic zone beneath the continent is poorly defined and a major bathymetric trench at the foot of the continental slope is lacking, Riddihough (1979) concludes that the Juan de Fuca-Explorer plates are moving under the North American plate thereby producing the arc type volcanism of the present day Garibaldi Volcanic Belt and the earlier Pemberton Volcanic Belt.

The Quaternary Garibaldi Volcanic Belt comprises a narrow linear chain of volcanic centres that trend approximately N20° W, parallel to and approximately 250 km inland from the Juan de Fuca-North American plate boundary (Green, 1981). Farther northwest, near the Silverthrone Complex, a few volcanic centres of similar age and chemistry lie a similar distance from the convergent plate boundary between Explorer and North American plates.

East of the Garibaldi Belt and following a more northwesterly trend is the largely Miocene Pemberton Volcanic Belt. Bevier et al. (1979) suggest that cessation of volcanism in the Pemberton Belt and the shift to volcanism in the Garibaldi Belt was caused by reorientation

of plate motion about 3 m.y. ago, when the Nootka fracture zone was created.

The Anahim Volcanic Belt runs approximately east-west along latitude 52° N and includes volcanic centres that range in age from 14.5 to less than 0.01 m.y. Three hypotheses have been proposed to explain this magmatic belt. They are:

- magmas rising through deep fractures developed along the northern edge of the subducting Juan de Fuca plate (Stacey, 1974).
- magmas from a mantle hotspot (Bevier et al., 1979).
- magmas generated in an east-west rift zone (Bevier et al., 1979).

Volcanic rocks of the upper Oligocene to lower Miocene Masset Formation occur in the Queen Charlotte Islands and offshore basins to the southeast. Bevier et al. (1979) suggest that these volcanic rocks form the western end of a hotspot trace whose propagation eastward produced the Anahim Volcanic Belt. Northward movement of the Queen Charlotte Islands, after volcanism had occurred, was accomplished by transcurrent motion along the Louscoone Inlet-Sandspit fault systems (Young, 1981; Yorath and Chase, 1981). Other models suggest Masset volcanism is:

- associated with the crustal rifting that generated the first phase of Queen Charlotte Basin subsidence (Yorath and Hyndman, 1983)
- the northwestern end of the Pemberton Volcanic Belt (J.

Souther, oral comm.).

Adjacent to, locally in contact, and coeval with the Anahim Volcanic Belt are the Miocene to Pliocene Chilcotin Group Basalts, forming a lava plain elongate parallel to the continental margin (Bevier, 1982). These lavas were erupted in a back-arc tectonic setting and are contemporaneous with volcanism in the Pemberton arc (Souther, 1977).

The Miocene to Quaternary Stikine Volcanic Belt is situated inland and to the north of the Queen Charlotte Islands and trends toward the northeast, cutting diagonally across the older rocks of the northwesterly trending Coast Mountains and Intermontane Belt. It is believed to be a zone of incipient Cenozoic extension related to transcurrent motion along the adjacent continental margin (Souther, 1977). Near the centre of the Stikine Volcanic Belt is the Edziza-Spectrum Range complex in which alkali basalts to highly fractionated peralkaline rhyolites and trachytes were erupted (Souther, 1977; Souther et al., 1984).

The Wrangell Volcanic Belt, a broad arc that curves around the northern and eastern edge of the St. Elias Mountains in southwest Yukon and southcentral Alaska, results from subduction of the Pacific plate beneath the North American plate (Souther, 1977). Farther to the west the same subduction produces the Aleutian arc system.

The Pliocene Alert Bay Volcanic Belt in northern Vancouver Island, formed during a hiatus in the volcanism of the Pemberton-Garibaldi Volcanic Belts and was likely a

result of magma generation along the edge of the descending Juan de Fuca plate (Armstrong et al., in press).

2. REVIEW OF MAJOR AND TRACE ELEMENT TECTONIC DISCRIMINATION DIAGRAMS

2.1 CHEMICAL DISTINCTIONS BASED ON MAJOR ELEMENTS

Results from conventional bulk chemical analysis of igneous rocks are generally presented as major element oxide percentages by weight, and consequently a variety of tectonic discrimination diagrams have been formulated based entirely on major element chemistry. A complete review of major element geochemical characteristics in MORB, WPB and convergent margin basalts is provided by the Basaltic Volcanism Study Project (1981). Major element chemistry is used to calculate normative mineralogy and to distinguish alkaline from subalkaline and tholeiitic from calcalkaline series rocks (Irvine and Baragar, 1971). As some of the tectonic discrimination diagrams are predicated on separation of alkaline, or tholeiitic, or calcalkaline series rocks, these classifications must first be established.

2.1.1 ALKALINE VS. SUBALKALINE

To distinguish the alkaline from the subalkaline volcanic rock series the alkalis vs. silica ($\text{wt.}\%(\text{Na}_2\text{O} + \text{K}_2\text{O})$ vs. SiO_2) and $Ol'-Ne'-Qz'$ diagrams were used (MacDonald, 1968; Irvine and Baragar, 1971) (Fig. 2.1). Irvine and Baragar considered the $Ol'-Ne'-Qz'$ diagram the most reliable for separating subalkaline from

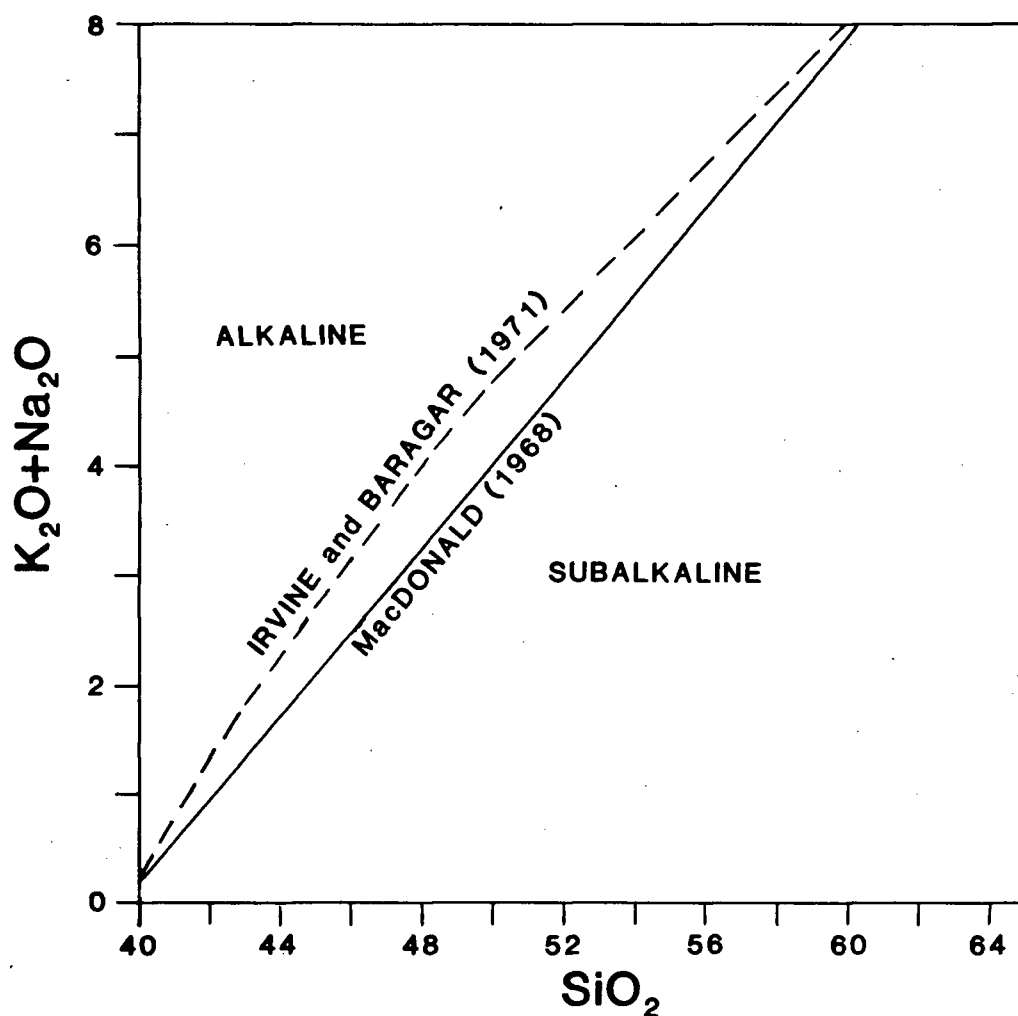
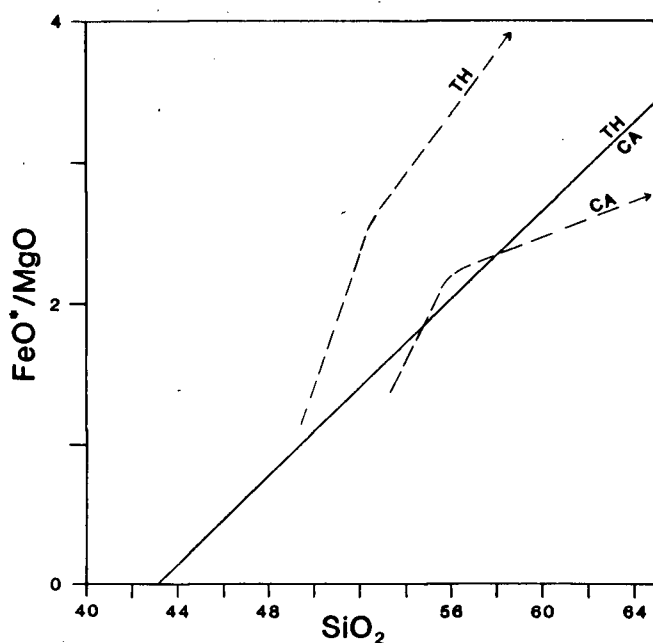
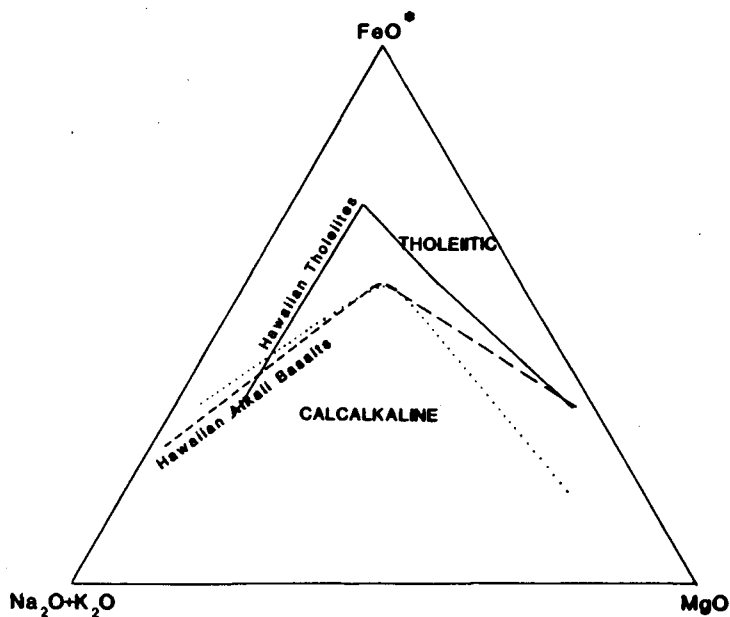


Fig 2.1. $K_2O + Na_2O$ vs. SiO_2 distinguishing alkaline and subalkaline volcanic rocks. The solid line is MacDonald's (1968) dividing line for Hawaiian tholeiitic and alkaline rocks, the dashed curve is Irvine and Baragar's (1971) dividing line for a general distinction between alkaline and subalkaline compositions.

alkaline basalts, therefore in the few cases in this study where the two discrimination diagrams disagreed, *Ol'-Ne'-Qz'* classifications were given the most weight.

2.1.2 THOLEIITIC VS. CALCALKALINE

Subalkaline rocks include both the calcalkaline and the tholeiitic basalt series and were distinguished from one another by Wager and Deer (1939) on the basis of Fe enrichment trends. Pronounced Fe enrichment during differentiation typifies the tholeiitic series while absence of this enrichment typifies the calcalkaline series. This difference is commonly shown on an AFM diagram (Irvine and Baragar, 1971), or on the FeO^*/MgO vs. SiO_2 diagram of Miyashiro (1974) (Figs. 2.2 and 2.3). The latter diagram is more appropriate for suites of differentiated rocks, as trends are more important than individual positions. In addition to lower Fe/Mg ratios Irvine and Baragar noted that calcalkaline basalts and andesites generally contain 16% to 20% Al_2O_3 , whereas similar tholeiitic rocks have only 12% to 16% Al_2O_3 . This was illustrated on a plot of Al_2O_3 vs. normative plagioclase composition, considered by them to be better than the AFM diagram for discriminating tholeiitic from calcalkaline rocks in the basalt-andesite range.



Figs. 2.2 and 2.3. AFM diagram (above) and FeO^*/MgO vs. SiO_2 diagram (below) separating calcalkaline from tholeiitic volcanic rocks. On the AFM diagram the dotted line is from Irvine and Baragar (1971) and the differentiation trends for Hawaiian basalts are from MacDonald and Katsura (1964). The solid line on FeO^*/MgO vs. SiO_2 is from Miyashiro (1974) and the dashed lines are differentiation trends for volcanic suites from Japan (Kuno, 1968).

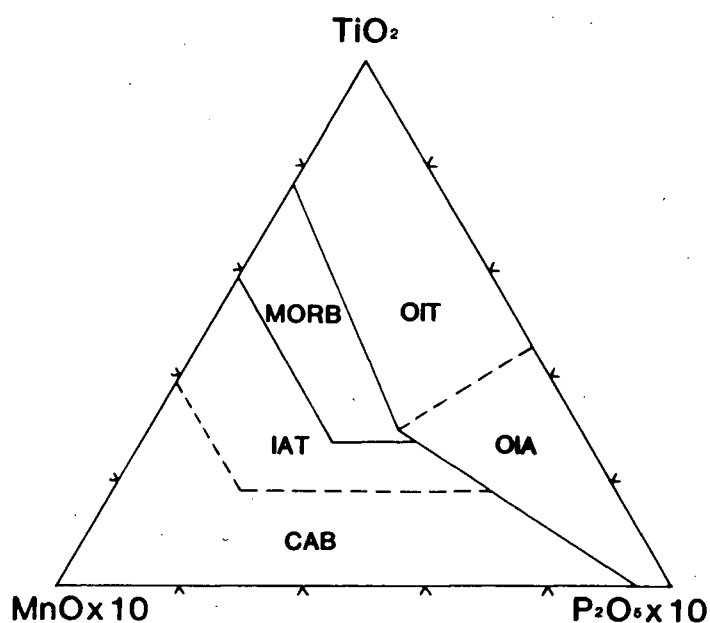
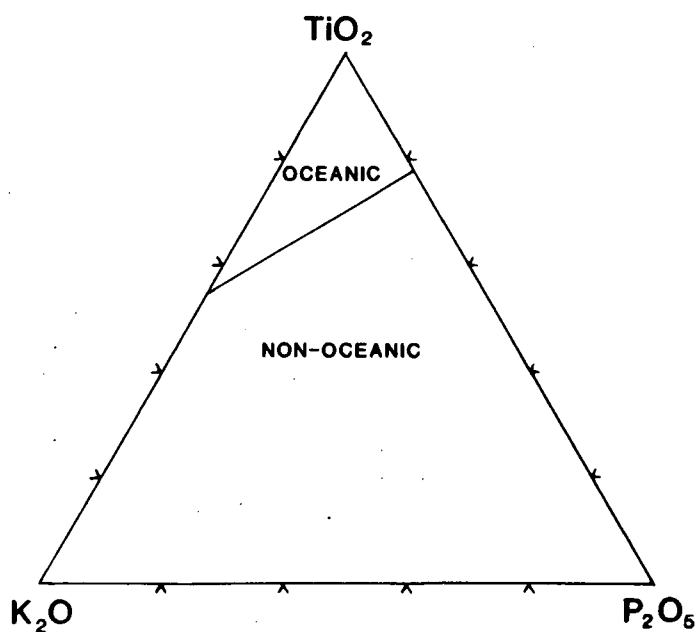
2.1.3 OCEANIC VS. NON-OCEANIC

2.1.3.1 $\text{TiO}_2\text{-K}_2\text{O-P}_2\text{O}_5$

Subalkaline basalts may be separated into oceanic or non-oceanic (continental) environments using a plot of $\text{TiO}_2\text{-K}_2\text{O-P}_2\text{O}_5$ (Figure 2.4) (Pearce et al., 1975). These three oxides effectively discriminated 93% of the oceanic (MORB and WPB) and greater than 80% of the continental basalt data plotted by the above authors. Important exceptions were the Scoresby Sund basalts of East Greenland and the Deccan Plateau basalts of India, both of which plotted in the oceanic field. This supported the suggestion that these exceptions were produced by initial rifting of a continent which generated new sea floor, hence their oceanic character.

2.1.3.2 $\text{MnO-TiO}_2\text{-P}_2\text{O}_5$

Mullen (1983) replaced the K_2O component of the above diagram with MnO and plotted alkaline and subalkaline volcanic rocks which had SiO_2 abundances between 45%-54% (Fig. 2.5). This distinguished five oceanic plate tectonic and petrogenetic environments: MORB, island arc tholeiite (IAT), island arc calcalkaline (CAB), ocean island tholeiite (OIT), and ocean island alkaline (OIA) basalt. Continental tholeiitic WPB's scatter across all of these fields and cannot be resolved from the oceanic basalts as there is no component in this diagram which is more enriched in



Figs. 2.4 and 2.5. TiO_2 - K_2O - P_2O_5 (above) separating oceanic basalts from non-oceanic basalts (Pearce et al., 1975). MnO - TiO_2 - P_2O_5 (below) with fields for MORB, IAT (island arc tholeiite), CAB (island arc calcalkaline), OIT (ocean island tholeiite) and OIA (ocean island alkaline) (Mullen, 1983).

basalts erupted through or associated with continents. Basalts from back-arc basins and rifts generally plot in the ocean island tholeiite field if they are subalkaline, or in the ocean island alkaline field if they are alkaline (Mullen, 1983).

2.1.3.3 MgO-FeO*-Al₂O₃

Pearce et al. (1977) distinguished five different tectonic environments on a MgO-FeO*-Al₂O₃ diagram by plotting analyses of 8400 subalkaline volcanic rocks with silica contents between 51 and 56 wt% (Fig. 2.6). Fields described were:

1. orogenic basalts (ARC)
2. continental basalts (CB)
3. ocean island basalts (OI)
4. ocean ridge/floor basalts (N-MORB), and
5. oceanic islands which are adjacent to or straddling a mid-ocean ridge (E-MORB).

However, none of the tectonic fields had sharp boundaries, especially the orogenic field, which enclosed only 55% of the orogenic data points.

2.2 TRACE ELEMENT GEOCHEMISTRY

Magmas from specific tectonic environments can be distinguished by their characteristic trace and rare earth element concentrations.

In general, abundances of incompatible trace elements are lower in tholeiitic than in alkaline series rocks from

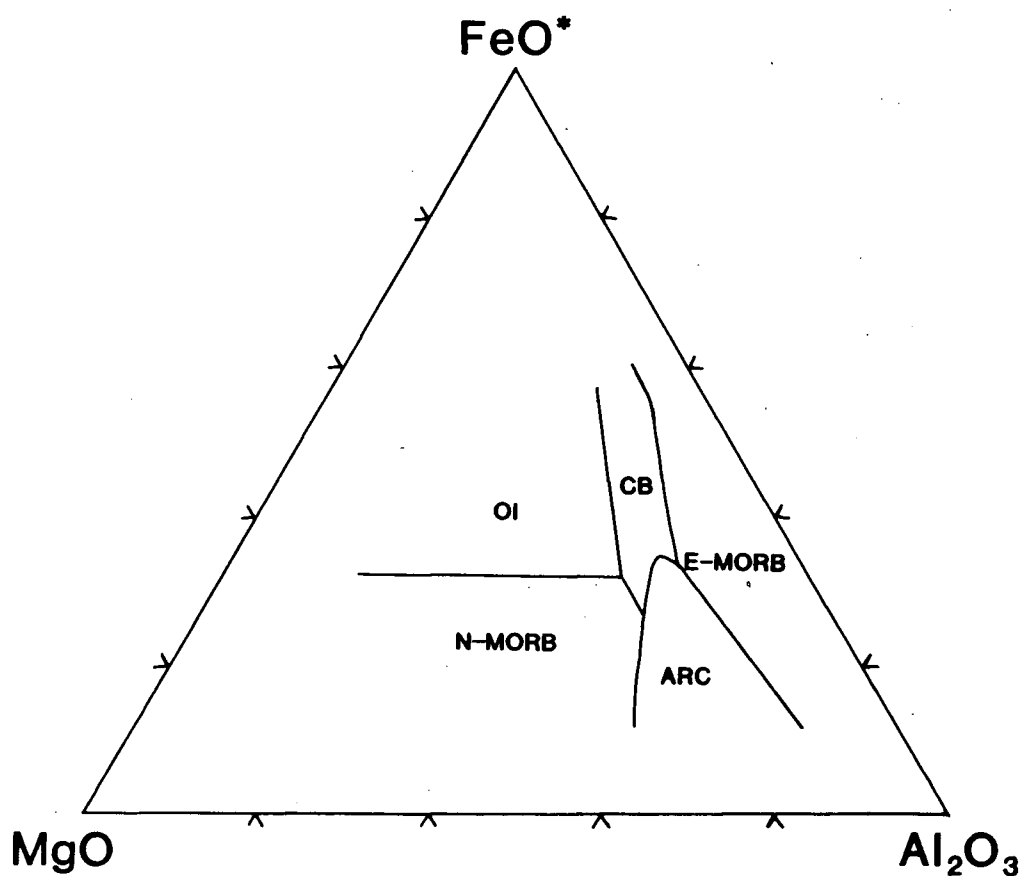


Fig. 2.6. MgO-FeO*-Al₂O₃ diagram distinguishing fields for ARC (convergent margin basalts), CB (continental basalts), OI (ocean island basalts), N-MORB and E-MORB (ocean islands which are adjacent to or straddling a mid-ocean ridge (Pearce et al., 1977)).

the same tectonic environment, but relative interelement enrichments and depletions are similar, providing the source regions were homogeneous and crystal fractionation before eruption was minimal.

In contrast, the compatible (transition) elements Co, Cr, Ni, Sc and V generally have large abundance ranges even within a single suite, and therefore are not very diagnostic of source environments. They are however, important indicators of fractionation. Fractionation of olivine and pyroxene controls Ni and Co content whereas, fractionation of pyroxene \pm Cr-spinel controls Cr abundances (Gast, 1968; Miyashiro and Shido, 1975; Hakli and Wright, 1970). Sc is preferentially incorporated into clinopyroxene and low Sc abundances may indicate high pressure pyroxene fractionation (Basaltic Volcanism Study Project, 1981). Abundances of V are primarily controlled by clinopyroxene fractionation, but under conditions of high fO_2 magnetite is precipitated and this rapidly fractionates V.

2.2.1 OCEAN FLOOR BASALTS (MORB)

N-MORB are depleted in LIL (Ba, Rb, K, Sr and U) relative to all other volcanic rocks, with Ba and Rb being more depleted than K and Sr. Thus, K/Rb and Sr/Rb ratios are generally higher in basalts from N-MORB than ratios from WPB but the N-MORB ratios can be similar to ratios in basalts from convergent margin settings. This is possible because of the enrichment in K and Sr in the

latter basalts. However, N-MORB generally have distinctly higher relative abundances of Nb, Ta, Zr and Hf than the convergent margin basalts (Basaltic Volcanism Study Project, 1981; Sun, 1980).

E-MORB have higher abundances of LIL than N-MORB but they are still depleted relative to basalts from other tectonic environments (Sun et al., 1979; Sun, 1980; Pearce, 1982).

N- and E-MORB abundances for Th and U generally range from 0.1 to 0.7 ppm and 0.05 and 0.3 ppm, respectively, the higher abundances occurring in E-MORB. Th/U ratios range from 2 to 5.

Erlank and Kable (1976) used Zr/Nb ratios from MORB as a measure of source depletion, a low ratio indicating an undepleted source. Most N-MORB have Zr/Nb ratios between 25 and 110, averaging 40 to 50, whereas most E-MORB have Zr/Nb ratios of 15 or less.

2.2.2 OCEAN ISLAND BASALTS (WPB)

WPB have a large range of trace element abundances, nevertheless all trace elements are enriched relative to N- and E-MORB (Thompson et al., 1983; Pearce, 1982).

It is more difficult to chemically distinguish within-plate and subduction-related basalts because abundance ranges completely overlap. Relative to convergent margin basalts oceanic WPB basalts are generally less enriched in Ba, K and Sr, but they are

strongly enriched in Nb relative to Rb and K so that Rb/Nb and K/Nb ratios in WPB are lower.

Tholeiitic oceanic WPB have a Th abundance range between 0.3 and 1.2 ppm and U contents between 0.1 and 0.3 ppm. Alkaline series basalts generally have higher Th abundances (1 to 6 ppm) but U abundances are similar (0.2 to 0.3 ppm). Th/U ratios range from 2 to 5.

Oceanic WPB characteristics are also seen in most continental WPB, but a few continental tholeiites are depleted in Nb relative to Rb and K, and are thus similar to basalts from convergent margins (Dupuy and Dostal, 1984; Thompson et al., 1984; Sun, 1980).

Th and U are enriched in the crust relative to mantle source regions and consequently incorporation of crustal material will increase abundances of both Th and U (Gill, 1981). Thus, very high Th and U contents and high Th/U ratios suggest interaction with continental crust.

2.2.3 CONVERGENT MARGIN BASALTS (ARC)

Relative to both N- and E-MORB convergent margin basalts have higher abundances of LIL (Ba, Rb, K and Sr) but lower abundances of Nb, Ta, Zr and Hf, especially Nb and Ta. Lower Nb and Ta relative abundances also distinguish them from most WPB. Consequently, their Rb/Nb and K/Nb ratios are much higher than ratios from either MORB or WPB (Cullers and Graf, 1984; Kay, 1980;

Pearce, 1982; Kay, 1978 and 1980; White and Patchett, 1984; Hawkesworth et al., 1977; Saunders et al., 1980).

Th and U abundances in oceanic convergent margin basalts correlate positively with K_2O content and magmatic series, from tholeiitic through calcalkaline to shoshonitic, and range from 0.1 to greater than 5 ppm and 0.07 to 1.5 ppm, respectively. Abundances are slightly higher in continental convergent margin basalts. Th/U ratios range from 2 to 5.

Eruption of convergent margin basalts through continental crust further increases abundances of Ba, Rb, K and Sr (Dostal et al., 1977; Jackeš and White, 1972).

2.3 RARE EARTH ELEMENT GEOCHEMISTRY

The group of elements with atomic numbers 57 to 71 all have very similar chemical and physical properties. Light rare earth elements (LREE) have atomic numbers 57-63 (La-Eu) and heavy rare earth elements (HREE) have atomic numbers 64-71 (Gd-Lu). Yttrium (Y) has an atomic number of 39 but is chemically very similar to HREE, therefore it is often included when REE are being discussed.

In general REE are considered to be very incompatible, but clinopyroxene and garnet can fractionate HREE from the liquid, so that only LREE are truly incompatible (Langmuir et al., 1977). $(La/Yb)_{CH}$ ratios indicate the degree of HREE fractionation.

Unlike most other REE Eu^{+3} may be reduced to Eu^{+2} , in which state it can enter plagioclase. Abundance of Eu is therefore controlled by plagioclase fractionation (Cullers and Graf, 1984; Gill, 1981).

N-MORB have low abundances of total REE relative to chondrites and are depleted in LREE relative to HREE.

$(\text{La}/\text{Yb})_{\text{CH}}$ and $(\text{La}/\text{Ce})_{\text{CH}}$ ratios are generally less than 1.0. E-MORB have higher total REE abundances and in most samples $(\text{La}/\text{Yb})_{\text{CH}}$ and $(\text{La}/\text{Ce})_{\text{CH}}$ ratios are greater than 1.0 (Henderson, 1984).

Basalts from convergent margin and within-plate settings have higher abundances of REE than N-MORB, and are usually enriched in LREE relative to HREE, but in most cases REE abundances from these two environments are indistinguishable. A few oceanic island arcs have negative Ce anomalies and can thus be separated from WPB, but as the Ce anomaly is attributed to the subduction of pelagic sediments, convergent margin basalts which have a large proportion of continental detritus entering the trench, i.e. convergent margin basalts sited on continental crust, do not have these distinguishing Ce anomalies (Hole et al., 1984; White and Patchett, 1984). $(\text{La}/\text{Yb})_{\text{CH}}$ ratios in within-plate and convergent margin basalts are generally greater than 1.0, but less than 10.0.

Alkaline series basalts have higher abundances of REE and LREE than subalkaline series basalts and generally have $(\text{La}/\text{Yb})_{\text{CH}}$ ratios greater than 5.0 (Cullers and Graf, 1984).

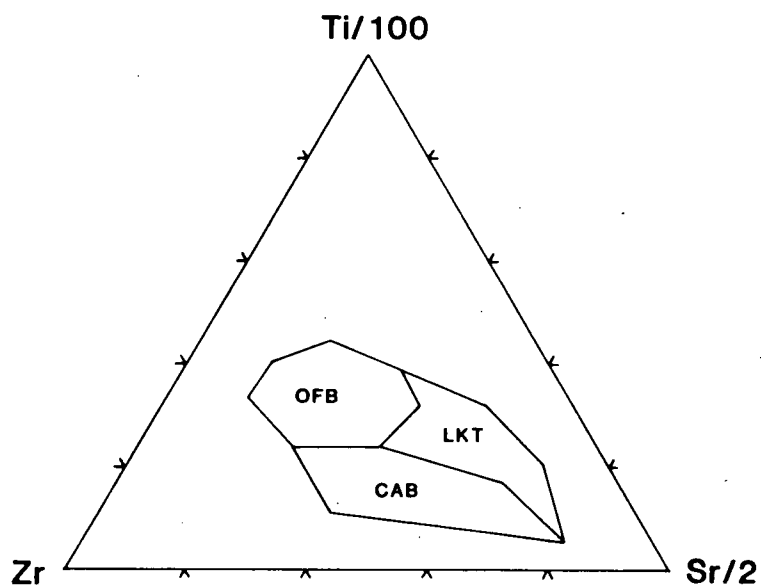
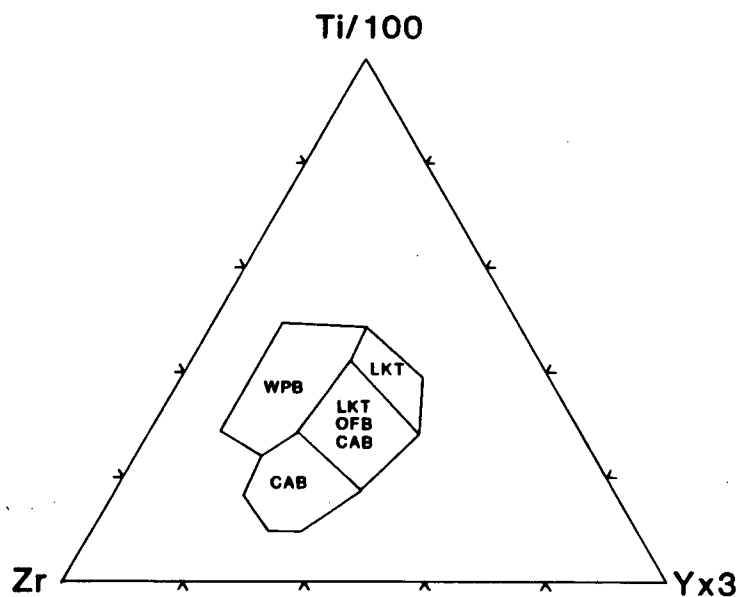
2.4 TRACE ELEMENT DIAGRAMS

2.4.1 TI-ZR-Y AND TI-ZR-SR

Pearce and Cann (1973) plotted data from 300 unaltered basaltic samples and discriminated four different tectonic environments using the elements Ti, Zr, Y and Sr. A Ti-Zr-Y diagram distinguishes WPB from calcalkaline basalts (CAB), low-K tholeiitic basalts (LKT) and ocean floor basalts (OFB). After excluding WPB samples from the data set the latter three tectonic environments are then separated much more effectively using a Ti-Zr-Sr diagram (Figs. 2.7 and 2.8). Note that altered basalts cannot be plotted on the Ti-Zr-Sr diagram and a Ti vs. Zr plot must be used instead (Pearce and Cann, 1973). Holme (1982) argues that some tholeiitic WPB cannot be distinguished from OFB and CAB on the Ti-Zr-Y diagram suggesting this diagram should be used with caution.

2.4.2 V VS. TI/1000

Plotting V vs. Ti/1000 distinguishes suites of tholeiitic and alkaline basaltic rocks from mid-ocean ridges, ocean islands and convergent margins (Fig. 2.9) (Shervais, 1982). Calcalkaline basalts cannot be distinguished because their Ti/V ratios are extremely variable. This plot is based on the crystal/liquid partition coefficient for V which is a function of the



Figs. 2.7 and 2.8. Ti-Zr-Y (above) and Ti-Zr-Sr (below) showing fields for WPB (within-plate basalt), LKT (low-K tholeiite), OFB (ocean floor basalt) and CAB (calcaline basalt) (Pearce and Cann, 1973).

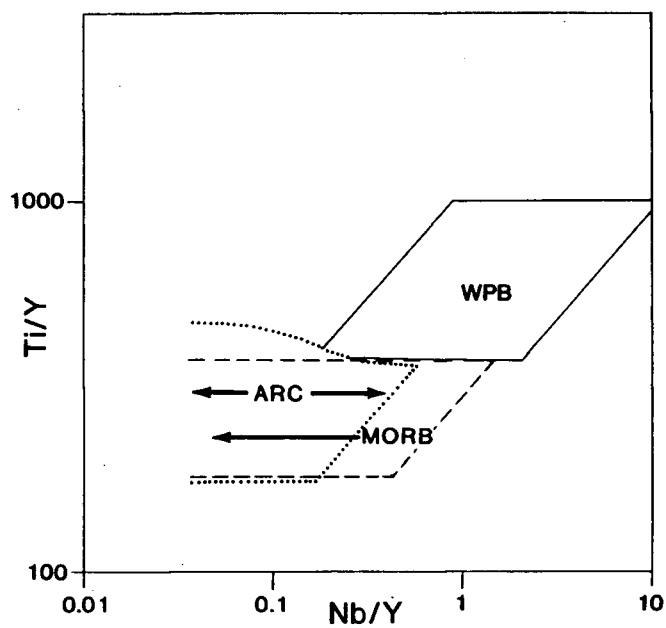
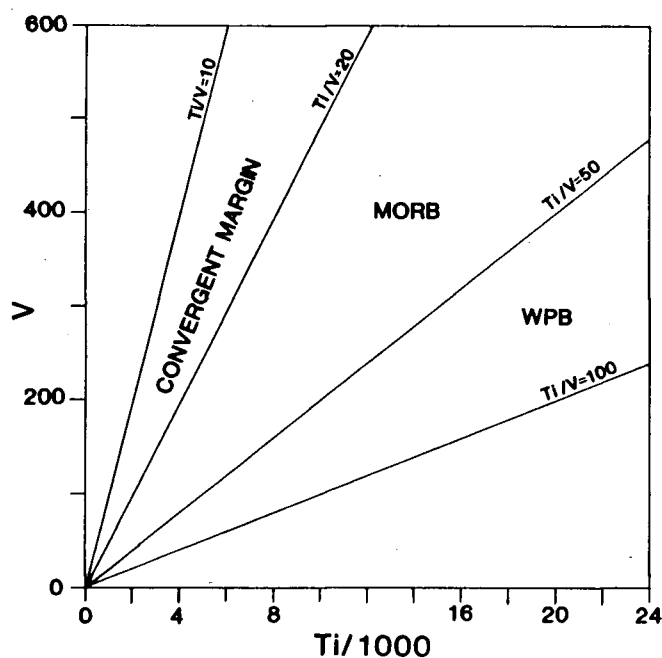
fO_2 of the magma and its source, the degree of partial melting and subsequent fractional crystallization. Arc tholeiites have the smallest Ti/V ratios, 10-20, MORB have Ti/V ratios between 20-50 and most WPB's, whether tholeiitic or alkaline have ratios of 50-100. Basaltic rocks from back-arc basins plot in a field that overlaps both the MORB and arc tholeiite fields, although MORB like abundances and ratios are more common.

2.4.3 TI/Y VS. NB/Y

The Ti/Y vs. Nb/Y diagram distinguishes WPB from MORB and convergent margin basalts but the latter two environments cannot be separated (Fig. 2.10) (Pearce, 1982).

2.4.4 TI/CR VS. NI

Island arc tholeiite and tholeiitic MORB samples with silica contents between 40 and 56 wt% were plotted on a Ti/Cr vs. Ni diagram and an empirical boundary was placed between the two data sets (Fig. 2.11) (Beccaluva et al., 1979). Data from ocean islands were excluded. Although this diagram was designed to distinguish IAT from tholeiitic MORB, it can also be used to distinguish unfractionated WPB samples. These latter samples generally lie within the TH MORB field, whereas most of the more fractionated samples lie within the IAT field. Fractional crystallization of olivine parallels the



Figs. 2.9 and 2.10. V vs. Ti/1000 (above) distinguishing fields for MORB, WPB and tholeiitic convergent margin basalts (Shervais, 1982). Ti/Y vs. Nb/Y (below) with fields for WPB, MORB and convergent margin (ARC) basalts (Pearce, 1982).

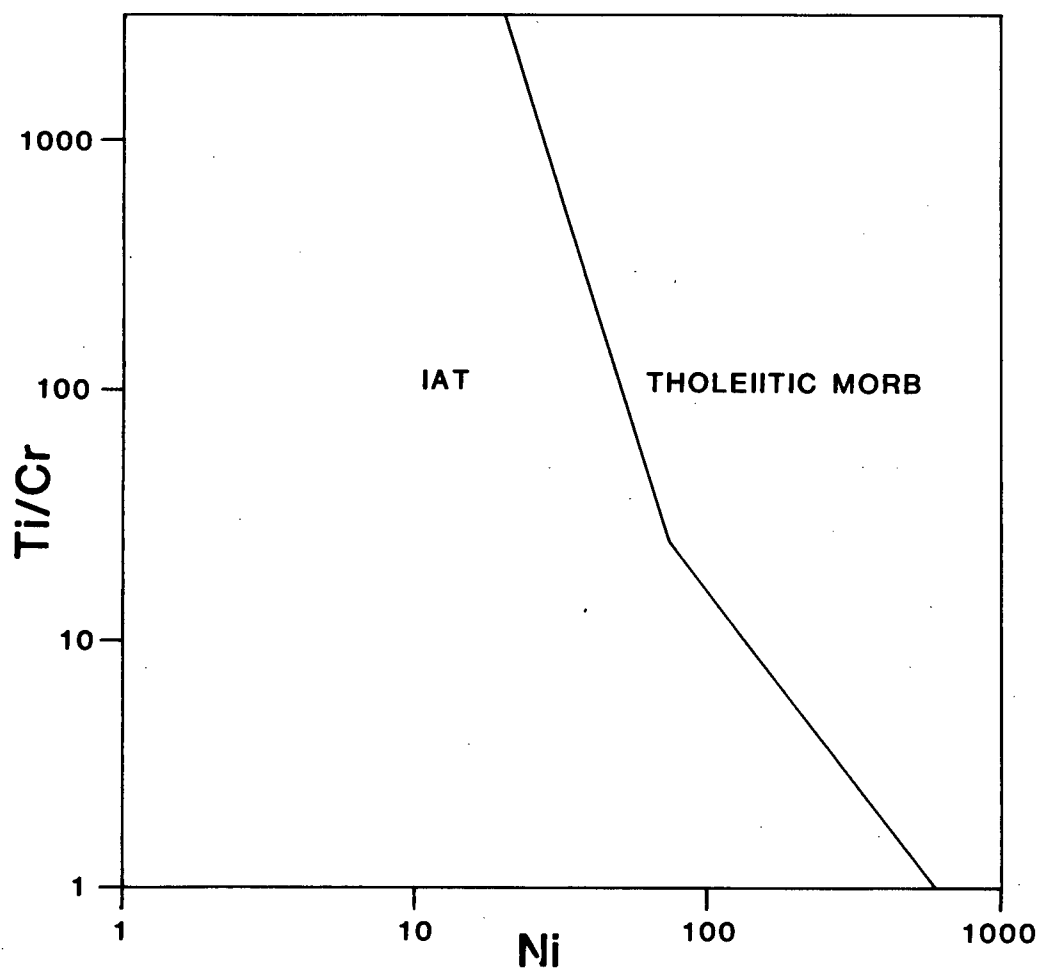


Fig. 2.11. Ti/Cr vs. Ni diagram with fields for tholeiitic convergent margin basalts and tholeiitic MORB (Beccaluva et al., 1979).

boundary, so that more differentiated rocks have increased Ti/Cr ratios and decreased Ni abundances.

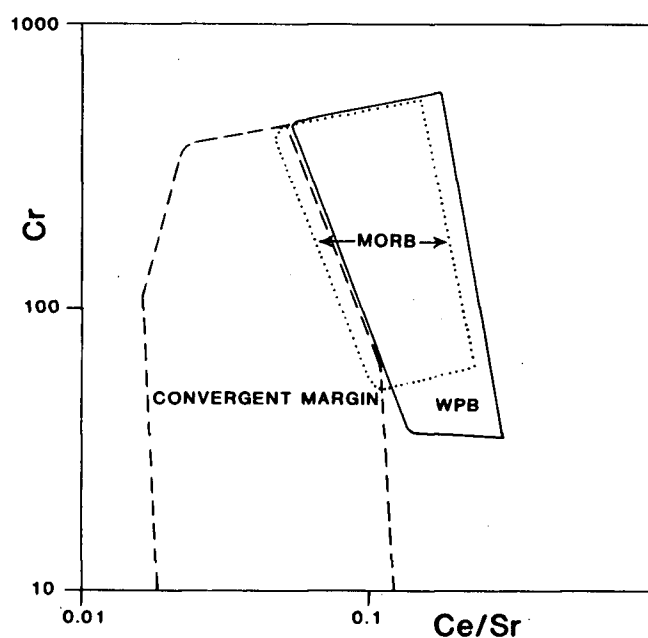
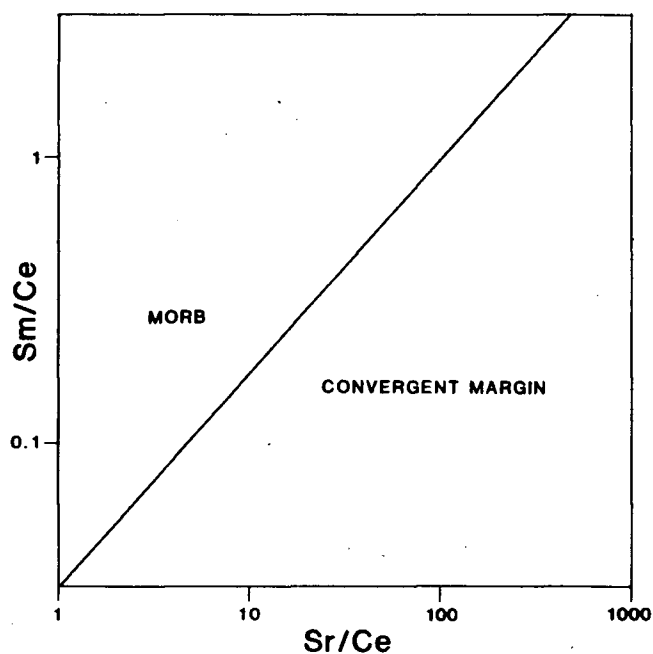
2.5 TRACE AND REE DIAGRAMS

2.5.1 SM/CE VS. SR/CE AND CR VS. CE/SR

The Sm/Ce vs. Sr/Ce and Cr vs. Ce/Sr diagrams both separate convergent margin basalts from MORB ± WPB (Figs. 2.12 and 2.13) (Hawkesworth and Powell, 1980; Pearce, 1982). These diagrams are effective for separating convergent margin basalts for two reasons:

1. Basalts from a convergent margin setting are enriched in Sr relative to MORB.
2. Some convergent margin basalts have negative Ce anomalies.

These two factors contribute to higher Sr/Ce or lower Ce/Sr ratios in convergent margin basalts relative to MORB or WPB. However, extensive plagioclase fractionation can lower the Sr content in a convergent margin basalt, so that points plotting close to the convergent margin- MORB/WPB field boundary line cannot be distinguished with confidence. In addition the Cr vs. Ce/Sr diagram is also affected by olivine and clinopyroxene fractionation.



Figs. 2.12 and 2.13. Sm/Ce vs. Sr/Ce (above) distinguishing convergent margin rocks from oceanic volcanic rocks (Hawkesworth and Powell, 1980). Cr vs. Ce/Sr (below) with a field for convergent margin basalts separated from overlapping MORB and WPB fields (Pearce, 1982).

2.5.2 CR VS. Y

The Cr vs. Y diagram separates convergent margin basalts from MORB and WPB, but both of these latter fields overlap the high Y edge of the convergent margin field (Fig. 2.14) (Pearce, 1982) Therefore, this diagram appears to be useful only as an indicator of olivine and/or pyroxene fractionation, especially in rocks with Y abundances between 28 and 48 ppm.

2.5.3 (Ba/La)_{CH} VS. (La/Sm)_{CH}

A plot of $(\text{Ba/La})_{\text{CH}}$ vs. $(\text{La/Sm})_{\text{CH}}$ can also be used to distinguish basalts from convergent margin and ocean floor environments (Fig. 2.15) (Kay, 1980). Primitive mid-ocean ridge basalts have $(\text{Ba/La})_{\text{CH}}$ ratios less than 1, but as the LREE fractionation ($(\text{La/Sm})_{\text{CH}}$ ratio) increases, the $(\text{Ba/La})_{\text{CH}}$ ratio also increases, to slightly less than 2. In contrast the $(\text{Ba/La})_{\text{CH}}$ ratios of convergent margin basalts are generally higher at low $(\text{La/Sm})_{\text{CH}}$ ratios (less than 1.5) and as the $(\text{La/Sm})_{\text{CH}}$ ratio increases the $(\text{Ba/La})_{\text{CH}}$ ratio decreases. Convergent margin and ocean floor basalts are well separated when the samples are unfractionated, (samples with low $(\text{La/Sm})_{\text{CH}}$ ratios), but as fractionation increases (higher $(\text{La/Sm})_{\text{CH}}$ ratios) data from the two environments overlap (Basaltic Volcanism Study Project, 1981). Back arc basin basalts were also plotted on this diagram but could not be distinguished from convergent

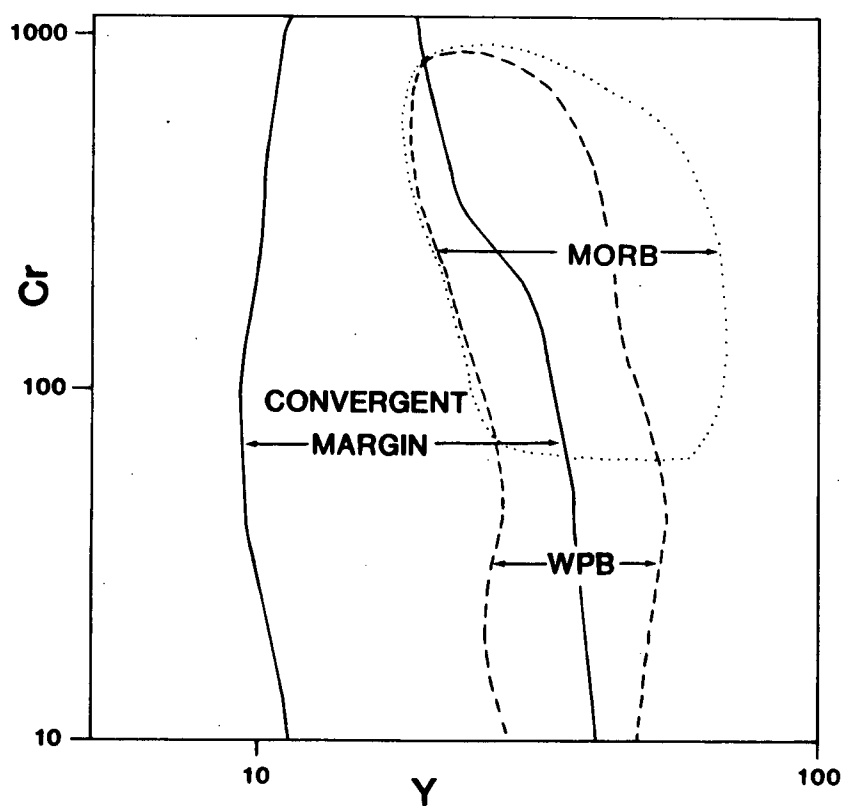


Fig. 2.14. Cr vs. Y with convergent margin, MORB and WPB fields (Pearce, 1982).

margin and/or ocean floor basalts.

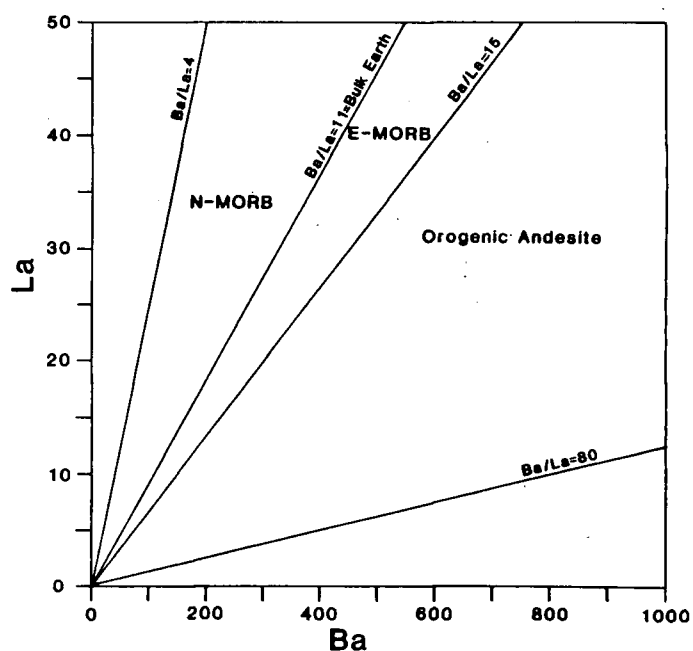
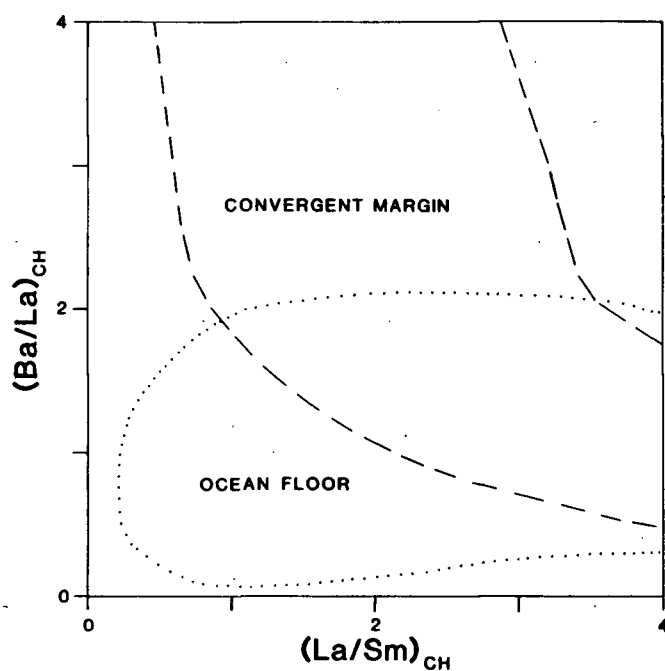
2.5.4 LA VS. BA LA VS. TH LA VS. NB

Plots of La vs. Ba, Th, or Nb separate orogenic andesites from N-MORB or from E-MORB, this latter group including WPB as well (Gill, 1981).

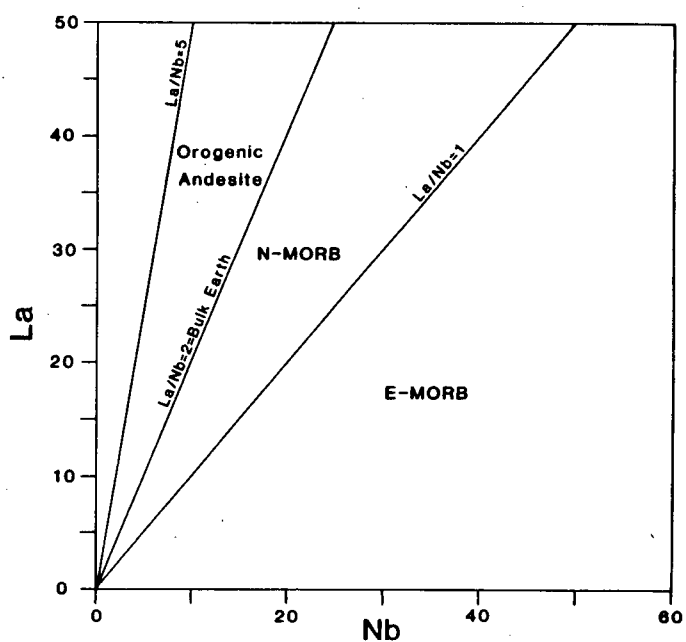
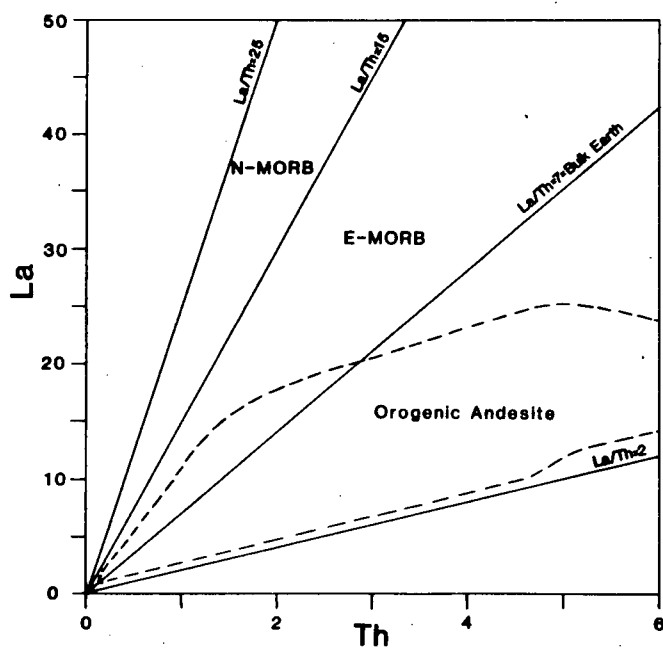
On La vs. Ba, N-MORB have Ba/La ratios between 4 and 11, E-MORB have ratios between 11 and 15 and Ba/La ratios in orogenic andesites range from 15 to 80 (Fig. 2.16) However, when this plot is compared with the $(\text{Ba/La})_{\text{CH}}$ vs. $(\text{La/Sm})_{\text{CH}}$ plot (Figure 2.15) it appears Gill's orogenic field is too rigidly constrained, especially for the more fractionated samples, and there is probably a great deal of overlap between the orogenic and E-MORB fields.

The La vs. Th diagram is very similar to the La vs. Ba plot: N-MORB have La/Th ratios between 25 and 15, E-MORB ratios lie between 15 and 7 and orogenic andesites primarily plot between La/Th ratios of 7 and 2 (Fig. 2.17). At Th contents less than 3 ppm the E-MORB and orogenic fields overlap.

On La vs. Nb orogenic andesites have La/Nb ratios between 2 and 5, N-MORB have ratios between 2 and 1 and La/Nb ratios in E-MORB are less than 1 (Fig 2.18). Histograms of La/Nb ratios in unambiguous examples of convergent margin basalts, oceanic WPB, and continental WPB placed convergent margin basalts between ratios of 1



Figs. 2.15 and 2.16. $(\text{Ba}/\text{La})_{\text{CH}}$ vs. $(\text{La}/\text{Sm})_{\text{CH}}$ diagram (above) distinguishing basalts from convergent margins and oceanic areas (ocean ridge and intraplate) (Kay, 1980). La vs. Ba (below) with fields for N-MORB, E-MORB plus WPB and orogenic andesites (Gill, 1981).



Figs. 2.17 and 2.18. La vs. Th (above) and La vs. Nb (below) with fields for N-MORB, E-MORB and orogenic andesites (Gill, 1981). Ocean islands and continental basalts typically lie in the E-MORB field.

and 5 and continental tholeiitic WPB between 0.5 and 2. Oceanic WPB plus continental alkaline WPB had ratios less than 1.3, but the majority of ratios were less than 1.0 (Thompson et al., 1983).

2.5.5 K₂O/Yb VS. Ta/Yb

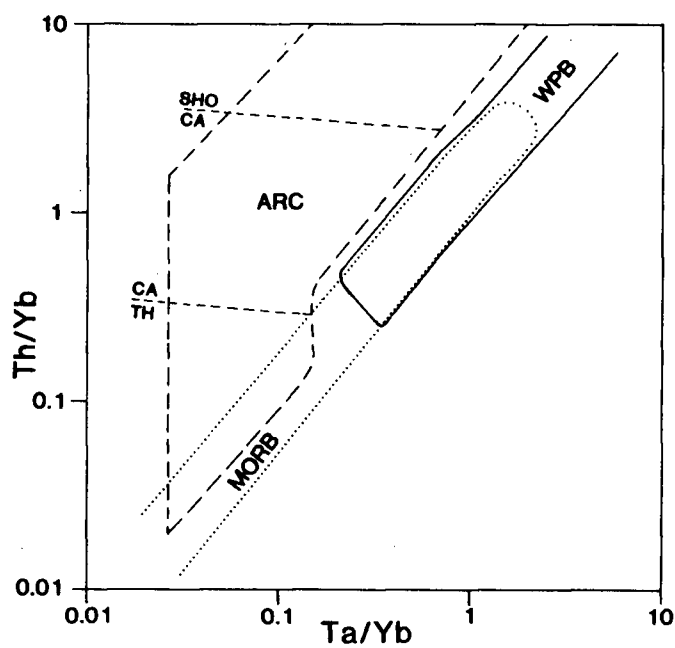
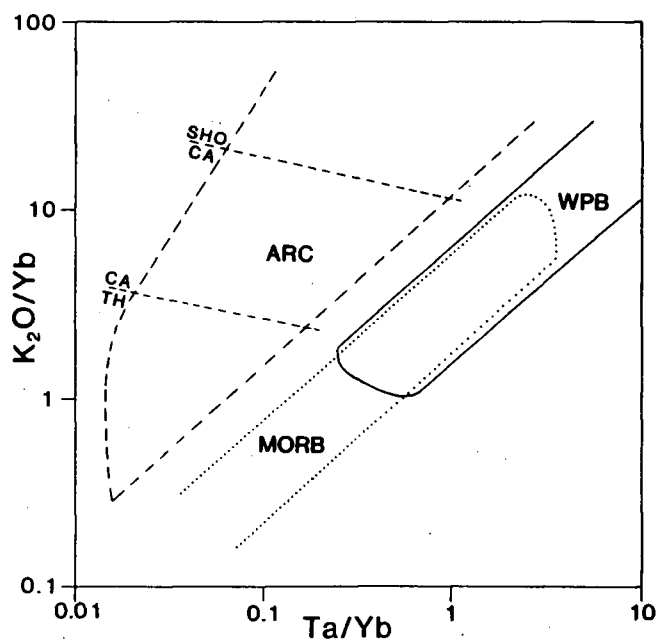
Pearce (1982) plotted K₂O/Yb vs. Ta/Yb to distinguish convergent margin basalts from MORB and WPB (Fig. 2.19). The convergent margin field is further divided into areas for tholeiitic, calcalkaline and shoshonitic basalts. MORB and WPB fields are slightly overlapping.

2.5.6 Th/Yb VS. Ta/Yb

The Th/Yb vs. Ta/Yb diagram is similar to the K₂O/Yb vs. Ta/Yb diagram but because Th is much less mobile in aqueous fluids this diagram is useful when altered rocks are being analyzed (Fig. 2.20) (Pearce, 1982). It has also been suggested that this diagram can distinguish WPB which have been contaminated with continental crust because consequent enrichment in Th displaces WPB into the volcanic arc field (Pearce, 1983).

2.5.7 Th VS. Ta La VS. Ta Th VS. Hf

Wood et al. (1979) plotted three biaxial diagrams using incompatible elements Th, Ta, Hf and La to



Figs. 2.19 and 2.20. K_2O/Yb vs. Ta/Yb (above) and Th/Tb vs. Ta/Yb (below) distinguishing convergent margin basalts (ARC) from slightly overlapping MORB and WPB fields (Pearce, 1982). The convergent margin field is subdivided into TH (tholeiitic), CA (calcalkaline) and SHO (shoshonitic) areas.

distinguish basalt series erupted in different tectonic environments.

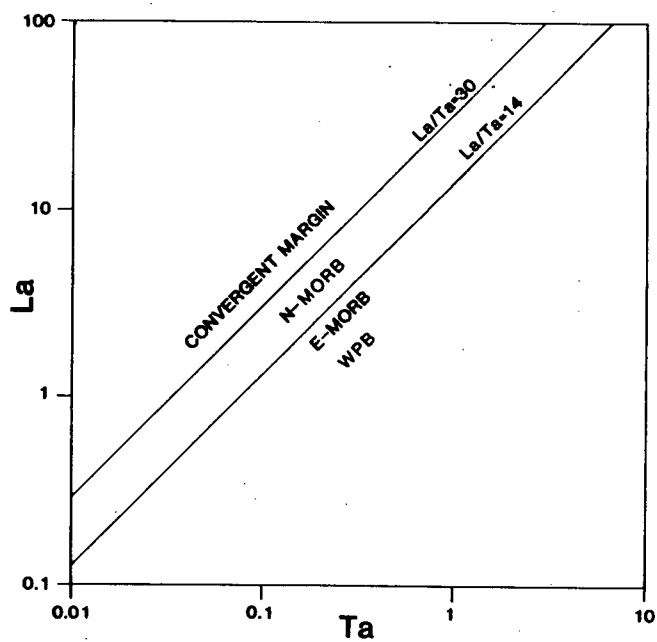
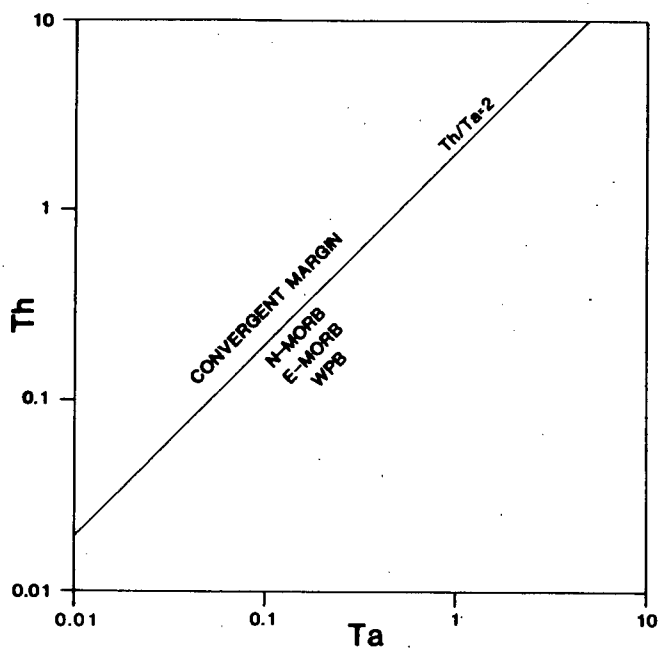
Plotting Th vs. Ta Japanese tholeiitic and calcalkaline lavas were separated from WPB and N- and E-MORB's at a Th/Ta ratio equal to 2 (Fig. 2.21).

Separation of N-MORB from the above grouping is aided by using a plot of La vs. Ta (Fig 2.22). In this plot the Japanese convergent margin samples have La/Ta ratios greater than 30, and WPB and E-MORB have La/Ta ratios less than 14. N-MORB data points plot with La/Ta ratios between 14 and 30.

The Th vs. Hf plot is not used for discriminating Japanese tholeiitic and calcalkaline samples but but it effectively separates WPB from N-MORB from E-MORB (Fig. 2.23). WPB have Hf/Th ratios less than 2.5, N-MORB have Hf/Th ratios greater than 12.5 and E-MORB samples plot in the area between these other two ($12.5 > \text{Hf/Th} > 2.5$)

2.5.8 TH-HF/3-TA

Based on information from the three plots just discussed Wood et al. (1979) and Wood (1980) proposed a triangular discriminant diagram with Th-Hf/3-Ta at the apices (Fig. 2.24). This diagram is not restricted to basalts but can be used for more siliceous rocks as well, and therefore in the remainder of this study the three previous diagrams will not be plotted. Fields distinguished are:



Figs. 2.21 and 2.22. Th vs. Ta (above) and La vs. Ta (below) with fields for Japanese tholeiitic and calcalkaline lavas (convergent margin), WPB plus E-MORB and N-MORB (Wood et al., 1979).

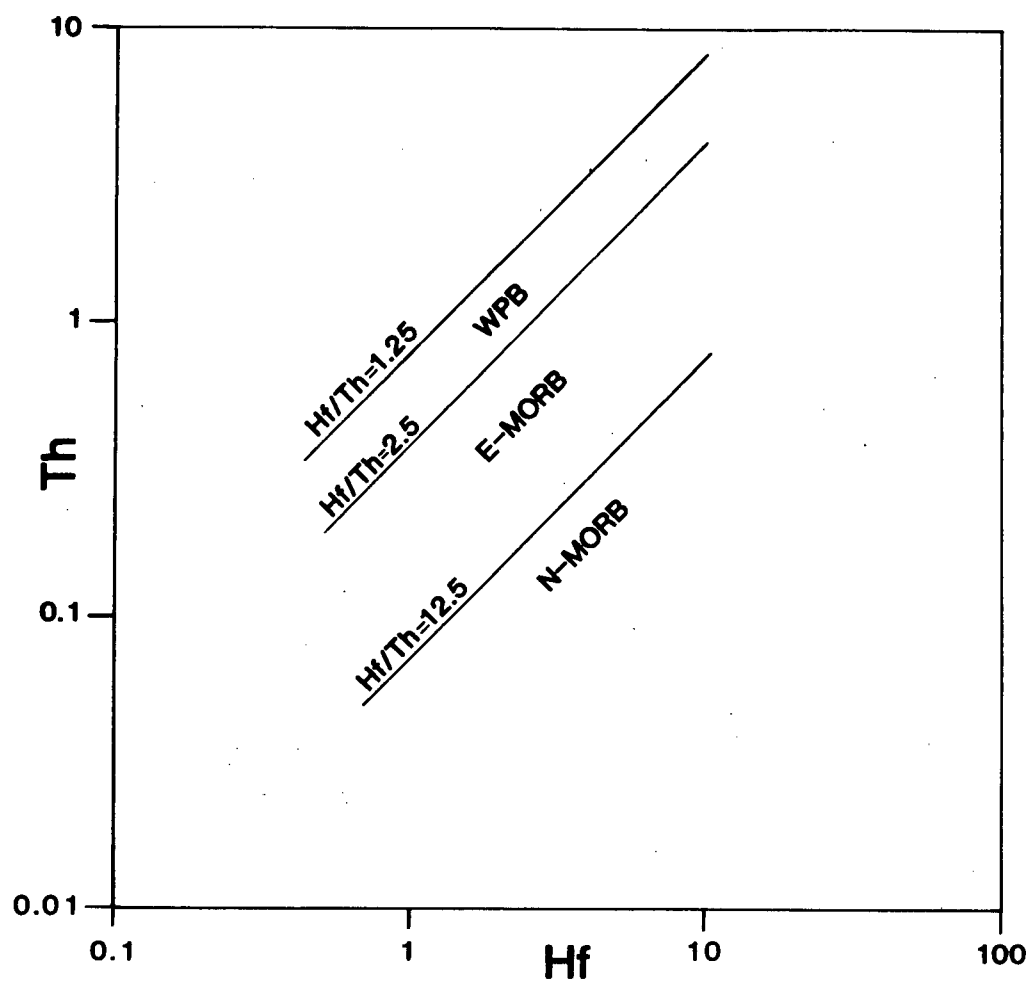


Fig. 2.23. Th vs. Hf diagram distinguishing fields for WPB, N-MORB and E-MORB (Wood et al., 1979).

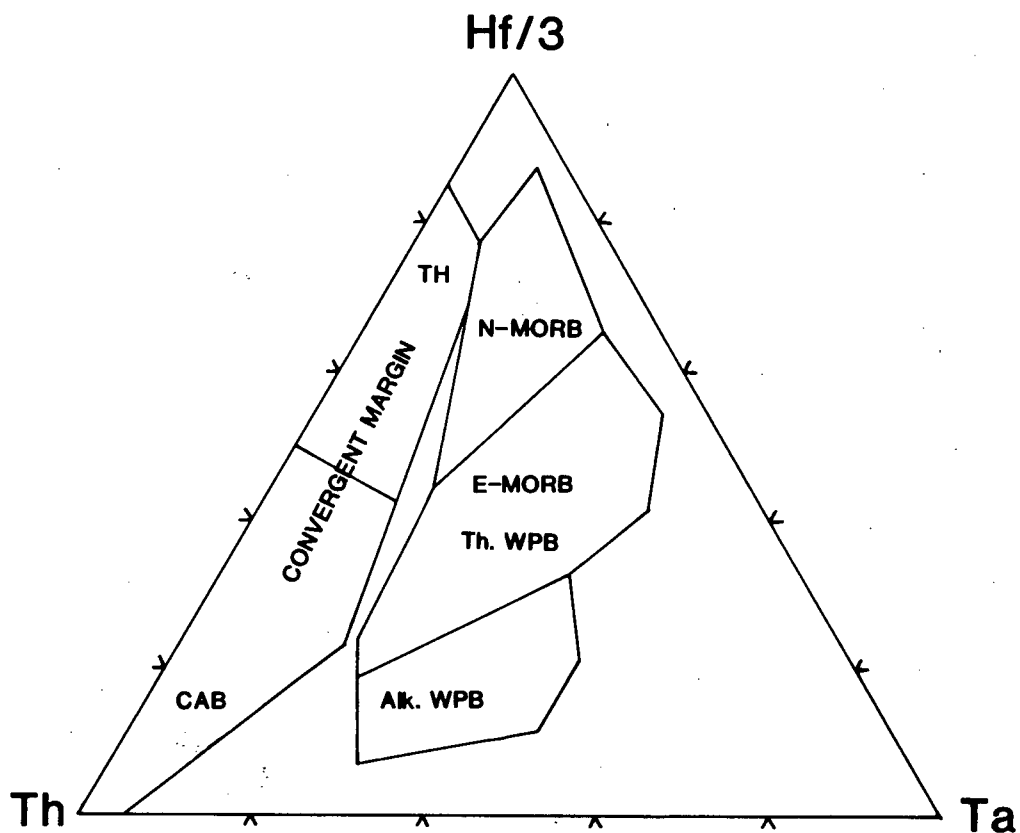


Fig. 2.24. Th-Hf/3-Ta with fields for N-MORB, E-MORB plus tholeiitic WPB, alkaline WPB and convergent margin (Wood, 1980). The convergent margin field is further divided into primitive arc tholeiites (TH) and calcalkaline lavas (CAB).

- A. N-MORB
- B. E-MORB plus tholeiitic WPB
- C. Alkaline WPB
- D. Convergent margins

In addition field D is further divided into a calcalkaline field and a primitive arc tholeiite field by an Hf/Th ratio equal to 3. Possible overlaps exist between field A and B and between fields B and C .

Therefore, any analyzed volcanics which plot close to the boundary lines between these fields cannot be classified with certainty. To discriminate tholeiitic WPB from E-MORB Wood (1980) suggests re-plotting data from field B on a Zr-Ti-Y discriminant diagram (Pearce and Cann, 1973).

2.6 BULK EARTH NORMALIZED TRACE AND REE DIAGRAMS (BEND)

Chondrite normalized REE diagrams allow comparisons to be made between numerous samples which have diverse elemental data, and give information about magma sources and petrogenesis. To increase this information Sun (1980) added selected bulk earth normalized trace element data. The order of the elements is based on their degree of mobility in an aqueous fluid as well as their degree of incompatibility at a small degree of partial melting (Sun, 1980; Pearce, 1983; Thompson et al., 1983).

Following Thompson et al. (1983) the data were normalized to bulk earth abundances, chondritic except for K

and Rb (see Table I for normalization factors). The bulk earth normalized data were then recalculated to make $(Yb)_N = 10.0$. This latter normalization decreases the effects of fractional crystallization of essentially Yb-free phases and makes comparisons of patterns more convenient by spreading them apart without changing their shape (Thompson et al., 1983). For the purposes of discussion these diagrams will be called BEN diagrams or BEND.

Although MORB, WPB and convergent margin basalts have characteristic pattern shapes on BEN diagrams, minor irregularities do occur as a result of variable partial melting and fractional crystallization.

2.6.1 MORB

Ordering from most to least incompatible elements causes the BEND pattern for N-MORB to slope positively from Ba to Y with a shallow concave-up trough from Sm to Ti, and a flat to negative slope from Y to Lu (Fig. 2.25) (Sun, 1980). E-MORB patterns are relatively enriched in LIL. They slope positively from Ba to Nb, slope negatively from Nb to Zr and are similar to N-MORB patterns from Zr to Lu (Fig. 2.25).

2.6.2 WPB

BEND patterns from oceanic WPB and continental alkaline WPB are essentially indistinguishable, with irregular convex-up shapes which 'peak' at Nb (Fig.

TABLE I

NORMALIZATION VALUES FOR BEND

| | |
|-----------------|--------|
| Ba ² | 6.9 |
| Rb ¹ | 0.35 |
| Th ² | 0.042 |
| U ¹ | 0.013 |
| K ¹ | 120.0 |
| Nb ¹ | 0.35 |
| La ² | 0.328 |
| Ce ² | 0.865 |
| Sr ² | 11.8 |
| Nd ² | 0.63 |
| Sm ² | 0.203 |
| Zr ² | 6.84 |
| Hf ² | 0.2 |
| Ti ¹ | 620.0 |
| Eu ³ | 0.0735 |
| Tb ² | 0.052 |
| Y ¹ | 2.0 |
| Yb ² | 0.22 |
| Lu ³ | 0.0322 |

- ¹ Sun (1980)
² Thompson et al.(1983)
³ Henderson (1984)

2.26). However, BEND patterns from continental tholeiites are highly irregular (Fig. 2.26). Some are similar to patterns from oceanic WPB but others have well defined 'troughs' at Nb similar to convergent margin basalts (see below) (Norry and Fitton, 1983; Weaver and Tarney, 1983; Thompson et al., 1983).

2.6.3 CONVERGENT MARGIN BASALTS

In contrast to MORB and WPB most BEND patterns from tholeiitic and calcalkaline convergent margin basalts have 'peaks' at Ba, K, Sr \pm Rb, a 'trough' at Nb, and are concave-up from Sm to Eu (Fig. 2.27). Six out of seven convergent margin basalts studied by White and Patchett (1984) had 'troughs' at Ce, and mixing models for parental oceanic island arc lavas constructed by Hole et al. (1984) also produced negative Ce anomalies. BEND patterns from alkaline series convergent margin basalts grossly resemble patterns from some WPB (Fig. 2.27).

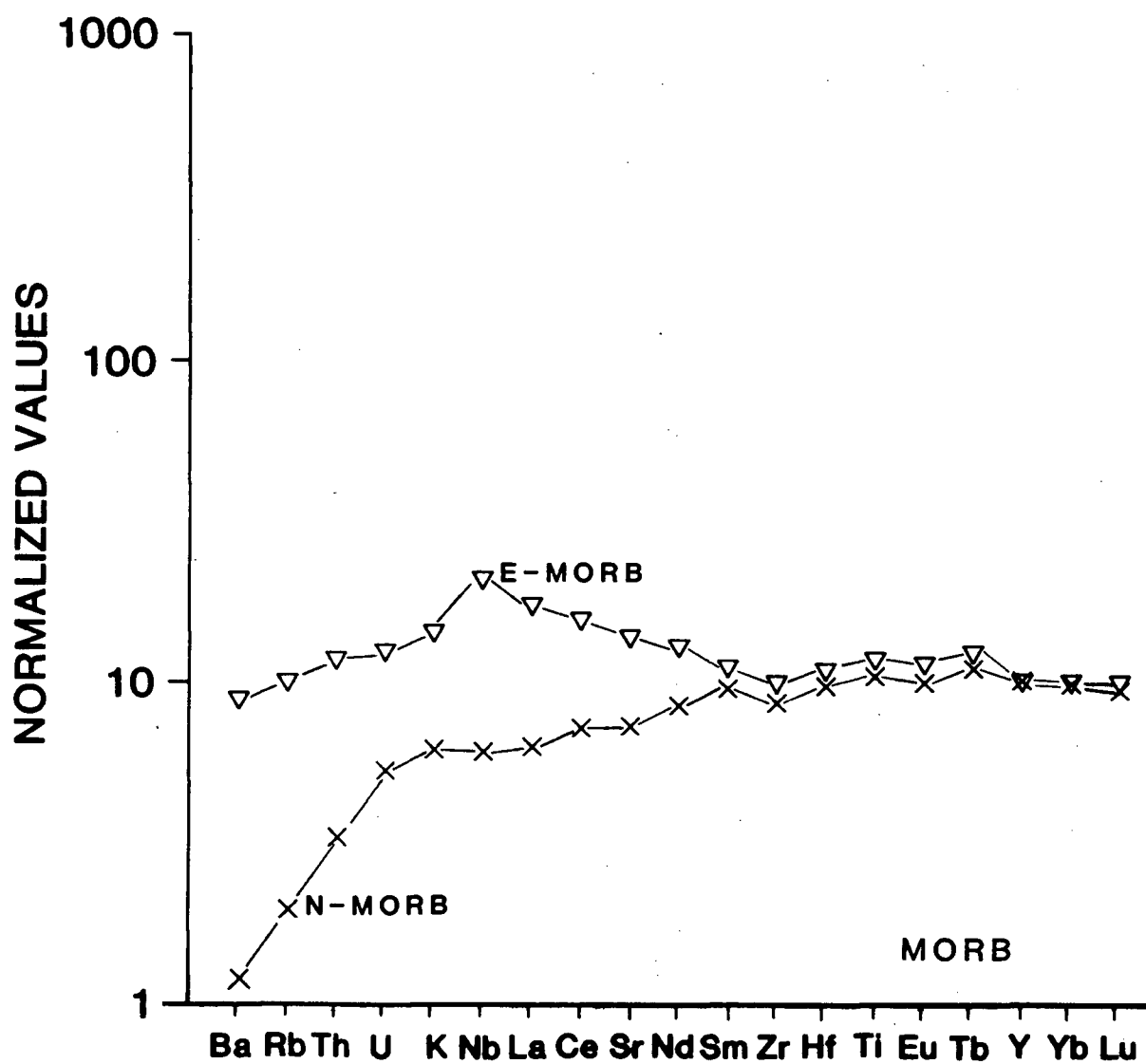


Fig. 2.25. BEND patterns for N-MORB (X) and E-MORB (▽) (Sun, 1980; Sun et al., 1979; White and Bryan, 1977).

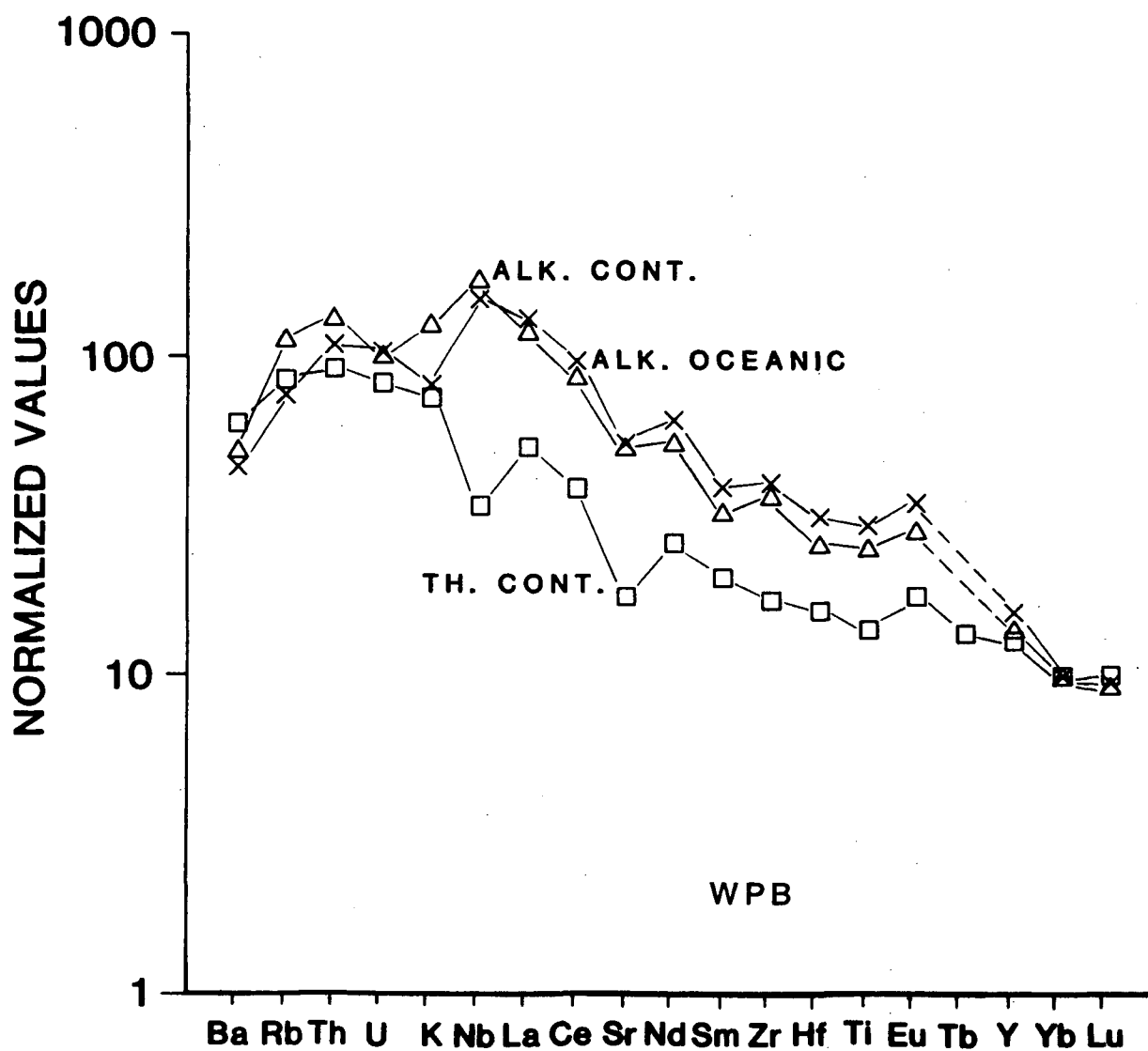


Fig. 2.26. BEND patterns for alkaline oceanic WPB (X), alkaline continental WPB (Δ) and tholeiitic continental WPB (□) (Thompson et al., 1983 and 1984).

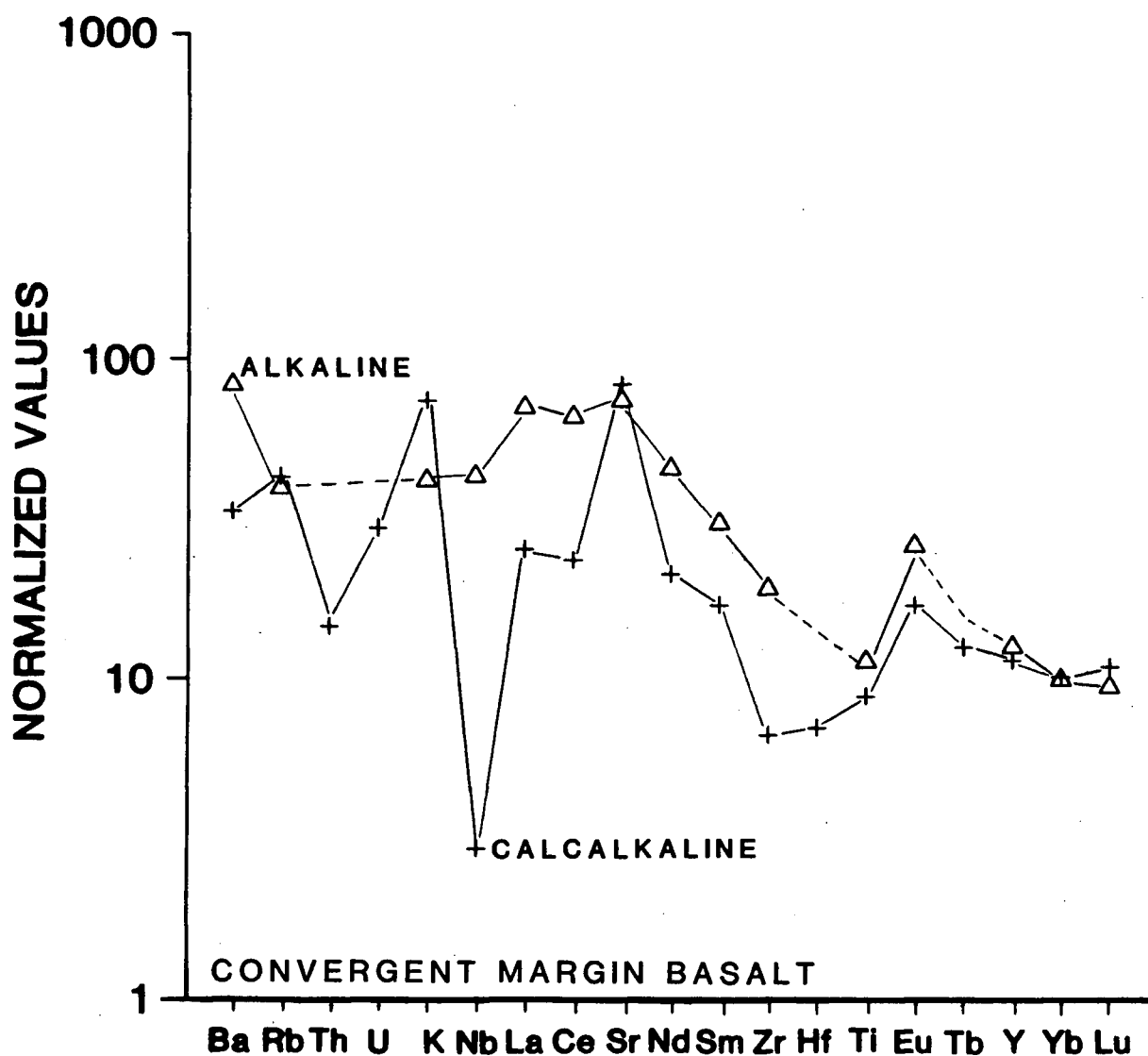


Fig. 2.27. BEND patterns for calcalkaline convergent margin basalt (+) (Basaltic Volcanism Study Project, 1981) and alkaline convergent margin basalt (Δ) (Shimizu and Arculus, 1975).

3. GARIBALDI AND PEMBERTON BELTS

Thirteen samples from two magmatic belts were used to study the convergent margin volcanic rocks in British Columbia. Eight of the samples are from the Quaternary Garibaldi Volcanic Belt east of 125°, two are from Quaternary Mt. Silverthrone, and three are from the Miocene Pemberton Volcanic Belt (Fig. 3.1).

For the purposes of this discussion the two samples from Mt. Silverthrone will be included with the samples from the Garibaldi Volcanic Belt as these two volcanic areas are coeval. At the present time they result from the subduction of different plates, but prior to 3 m.y. ago these plates were joined as one. Therefore any contribution to the erupted magma from the subducting slab should be similar, resulting in comparable geochemical patterns.

Available K-Ar dates from Garibaldi Belt basalts and andesites range from 0.09 Ma to 0.97 Ma (Table II). The three samples from the Coquihalla area had not been dated but Rb-Sr isochron and K-Ar dates from other Coquihalla samples give an age of approximately 22 Ma (Berman, 1979).

3.1 MAJOR ELEMENT CHEMISTRY

Abundances of TiO_2 , Al_2O_3 and P_2O_5 in calcalkaline samples COQ251, COQ632, COQ61, CAYLEY and SILVERA resemble abundances in the average calcalkaline basalt of Jakeš and White (1972) or Gill (1981), but K_2O abundances are slightly higher (Table II). Mg' numbers range from 38 to 52.

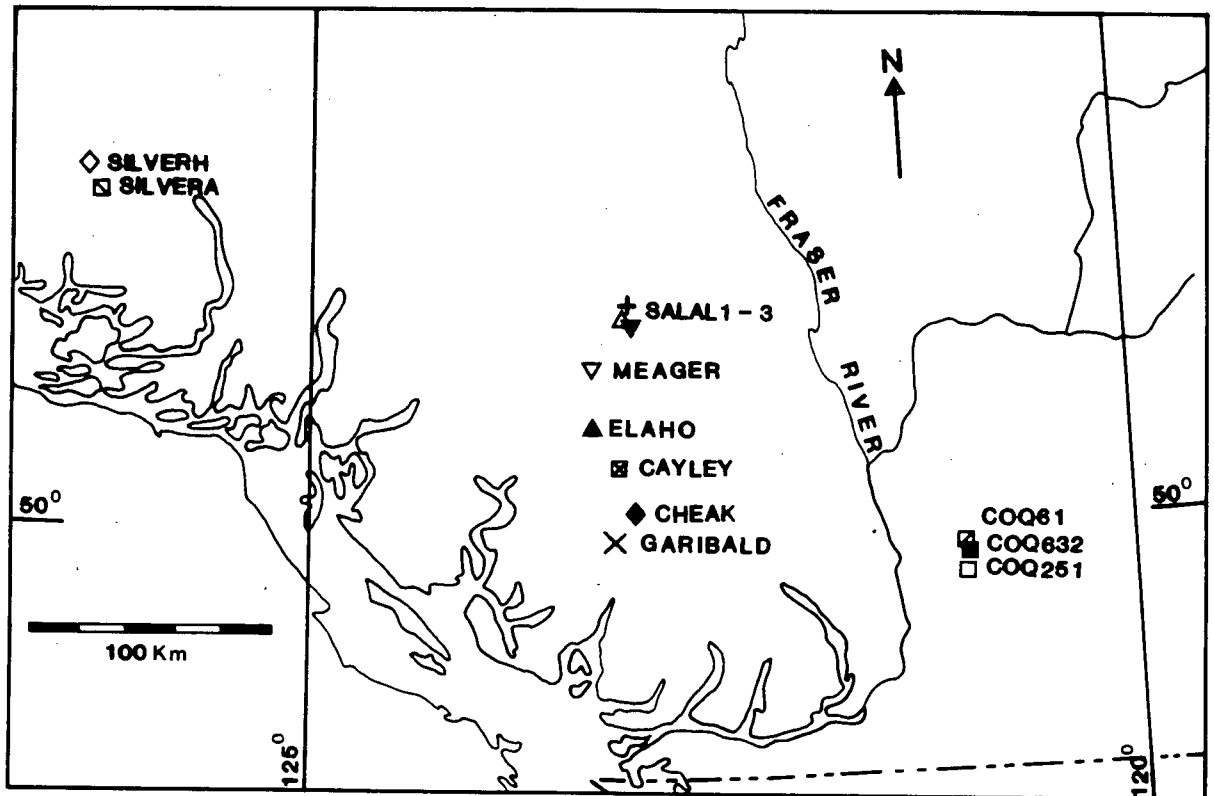


Fig. 3.1. Sample location map for the Convergent Margin Suite. All subsequent diagrams in this chapter use identical symbols.

Garibaldi Belt basalts ELAHO, GARIBALD and CHEAK are enriched in TiO_2 and depleted in Al_2O_3 and K_2O relative to an average arc basalt (Basaltic Volcanism Study Project, 1981) or the Coquihalla basalts (Table II) but P_2O_5 abundances are similar. Mg' numbers lie between 54 and 59.

Sample MEAGER has a TiO_2 content of 1.55 wt.%, similar to TiO_2 abundance in the other three Garibaldi Belt basalt samples, but its abundances of Al_2O_3 , K_2O and P_2O_5 are similar to abundances in the alkaline samples (see below).

Alkaline samples SALAL1, SALAL2, SALAL3 and SILVERH have abundances of TiO_2 , Al_2O_3 and P_2O_5 which are similar to abundances in an average alkaline WPB but K_2O abundances are marginally higher (Thompson et al., 1984; Basaltic Volcanism Study Project, 1981). Mg' numbers range from 41 to 61.

3.2 DISCRIMINATION DIAGRAMS

3.2.1 MAJOR ELEMENT CLASSIFICATIONS

On the total alkalis vs. silica diagram three of the samples are clearly alkaline (SALAL1, SALAL3 and SILVERH), five are clearly subalkaline (CAYLEY, SILVERA, COQ251, COQ632, and COQ61) and the remaining five sit astride MacDonald's (1968) subalkaline and alkaline field boundary (Fig. 3.2).

On $\text{Ol}'\text{-Ne}'\text{-Qz}'$ (not shown) the three alkaline samples are in agreement with the alkalis vs. silica classification, and all remaining samples are classified

as subalkaline. However, SALAL2 will be plotted with the alkaline samples rather than the subalkaline ones because overall it has alkaline trace element chemical characteristics (documented in a later section).

Subalkaline samples plotted on AFM and FeO^*/MgO vs. SiO_2 diagrams straddle the boundary line between tholeiitic and calcalkaline fields (Figs. 3.3 and 3.4), but the lack of a pronounced iron-enrichment trend during differentiation classifies them as calcalkaline.

On Al_2O_3 vs. normative plagioclase composition (not shown) all samples were classified as calcalkaline, except sample MEAGER which was barely tholeiitic.

On TiO_2 - K_2O - P_2O_5 , all subalkaline basaltic samples lie within the non-oceanic field (Fig. 3.5).

On MnO - TiO_2 - P_2O_5 , COQ251 and COQ632 lie within the CAB field, and COQ61 and SALAL2 lie within the IAT field (Fig. 3.6). The remainder lie just within the the OIA field, along the boundary line separating OIA from IAT.

Subalkaline basaltic samples plotted on an MgO - FeO^* - Al_2O_3 diagram lie in two separate groups (Fig. 3.7). COQ251, COQ632 and COQ61 lie within the orogenic field and ELAHO, MEAGER, GARIBALD and CHEAK plot around the triple point between ocean island, continental and ocean ridge/floor fields.

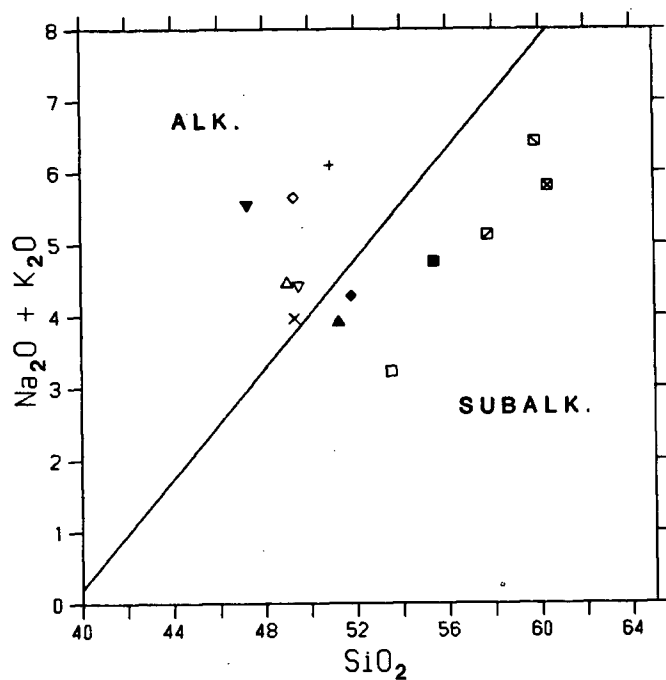
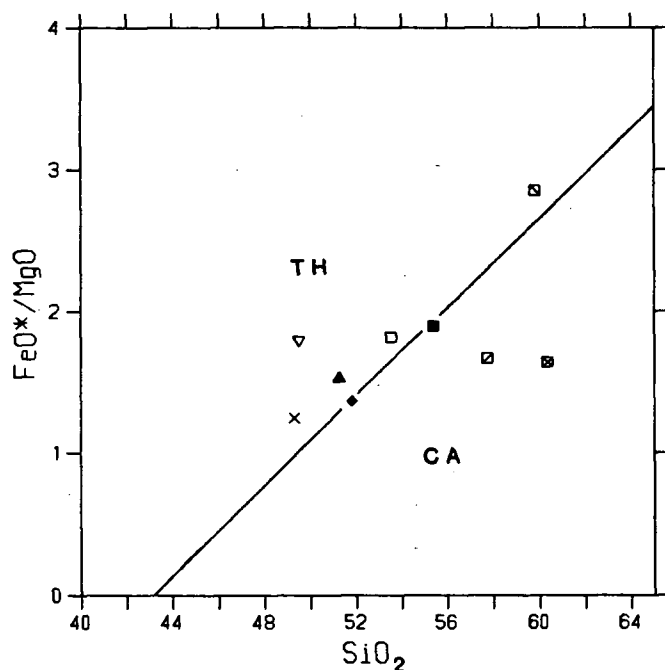
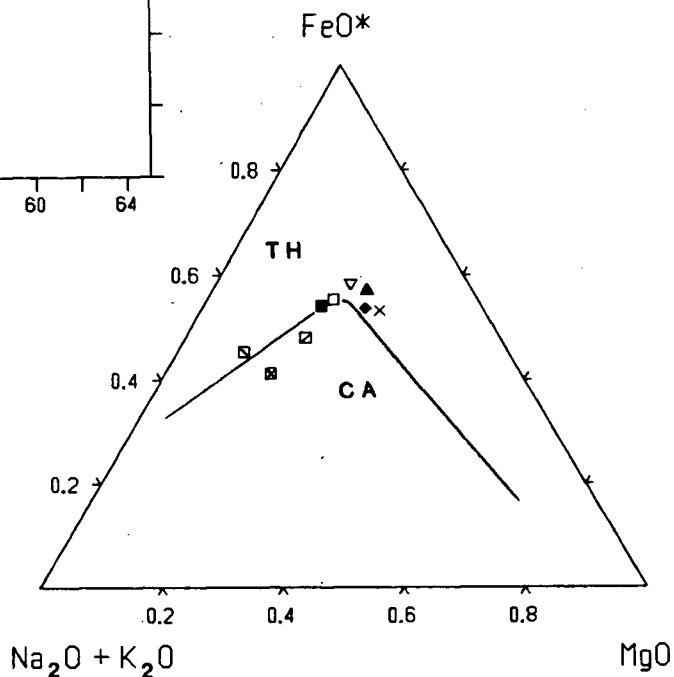


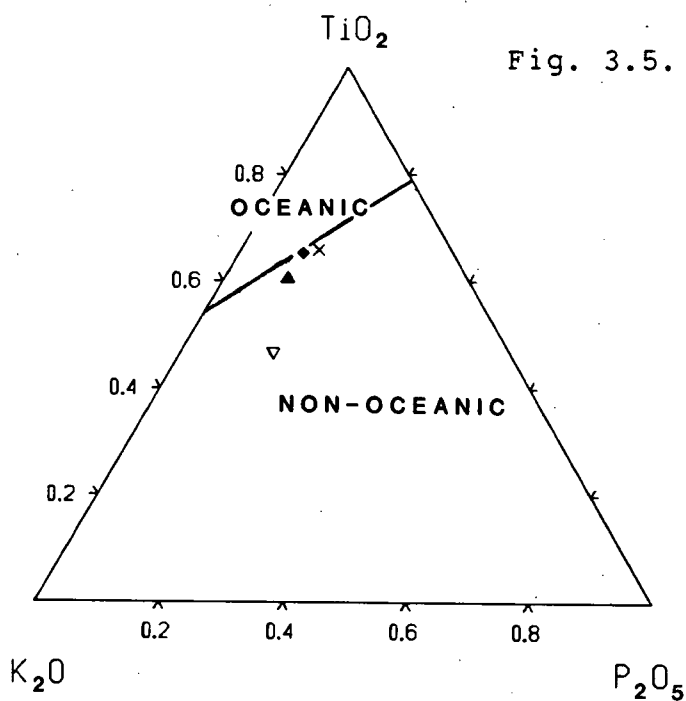
Fig. 3.2. Total alkalis vs. silica. Subalkaline/alkaline boundary from MacDonald (1968).

Fig. 3.3. AFM diagram. Tholeiitic/calcalkaline boundary from Irvine and Baragar (1971).



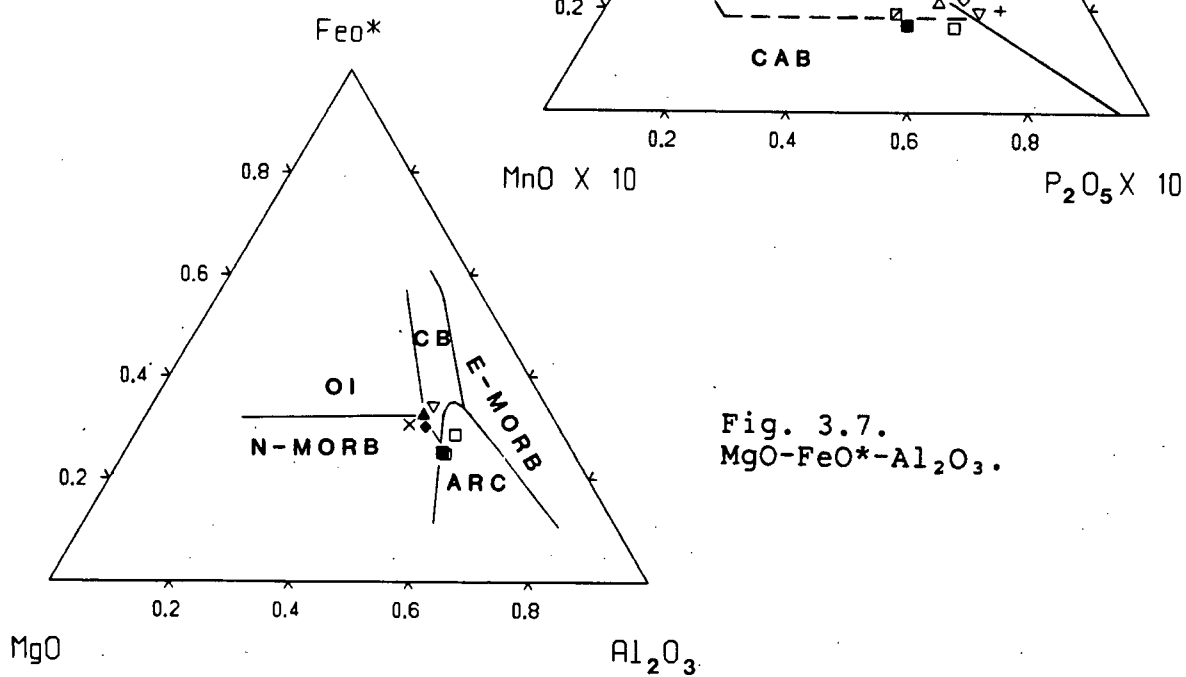
| | |
|------------|-----------|
| ELAHO ▲ | SALAL3 + |
| GARIBALD X | SILVERA □ |
| CHEAK ◆ | SILVERH ◇ |
| MEAGER ▽ | COQ251 □ |
| CAYLEY ▣ | COQ632 ■ |
| SALAL1 ▼ | COQ61 □ |
| SALAL2 △ | |

Fig. 3.4. FeO^*/MgO vs. SiO_2 . Tholeiitic/calcalkaline boundary from Miyashiro (1974).



| | |
|-----------|-----------|
| ELAHO ▲ | SALAL3 + |
| GARBALD X | SILVERA ■ |
| CHEAK ◆ | SILVERH ◇ |
| MEAGER ▽ | COQ251 □ |
| CAYLEY ■ | COQ632 ■ |
| SALAL1 ▽ | COQ61 □ |
| SALAL2 △ | |

Fig. 3.6. MnO - TiO_2 - P_2O_5 .



3.2.2 TRACE ELEMENT CLASSIFICATIONS

On Ti-Zr-Y all Garibaldi Belt samples, except SILVERH, lie within the WPB field along the boundary line separating WPB from LKT-OFB-CAB (Fig. 3.8). Samples COQ251, COQ632 and COQ61 lie within the CAB field on Ti-Zr-Sr, and SILVERH plots just within the LKT field (Fig. 3.9)

Although calcalkaline basaltic samples cannot be distinguished on V vs. Ti/1000 all samples were plotted and two groups are clearly seen (Fig. 3.10). Samples from the Coquihalla Complex lie within the MORB field, toward the convergent margin field boundary, whereas the eight remaining samples lie within or close to the WPB field.

COQ251, COQ632 and COQ61 lie within or adjacent to the overlapping convergent margin-MORB fields on Ti/Y vs. Nb/Y (Fig. 3.11). The eight remaining basaltic samples lie within the WPB field.

Coquihalla samples COQ251, COQ632 and COQ61 lie within the IAT field on Ti/Cr vs. Ni (Fig. 3.12). The remaining basaltic samples lie within the TH MORB field.

3.2.3 TRACE AND REE CLASSIFICATIONS

On Sm/Ce vs. Sr/Ce basaltic samples lie within the convergent margin field (Fig. 3.13).

Most basaltic samples lie within or close to the convergent margin field on Cr vs. Ce/Sr, but SALAL1

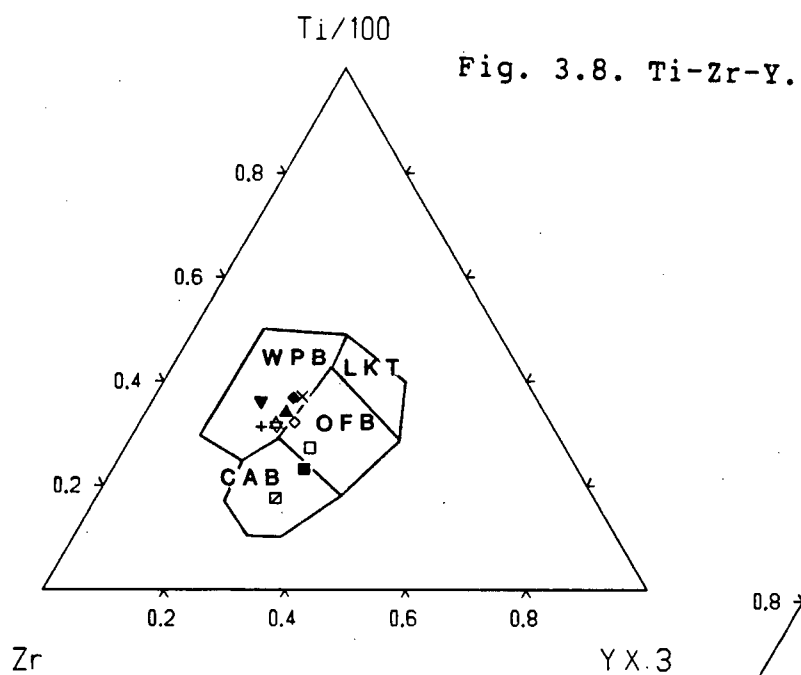


Fig. 3.9. Ti-Zr-Sr.

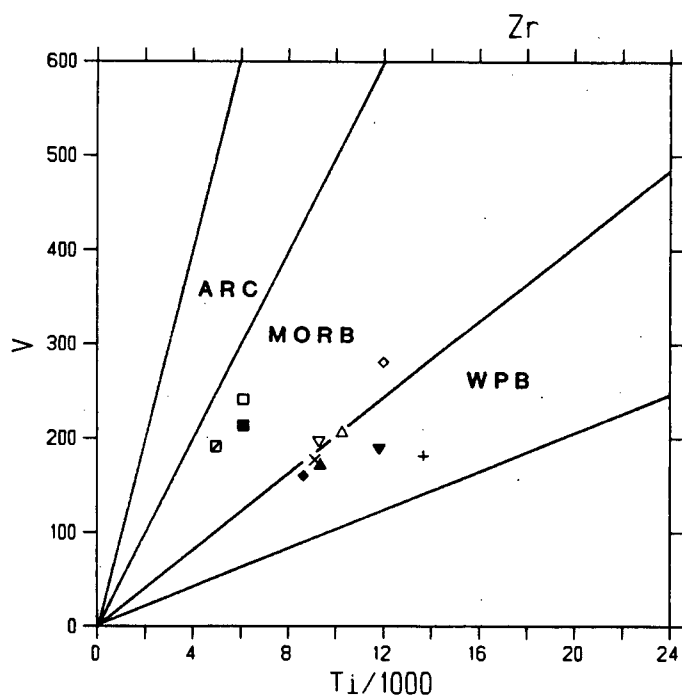
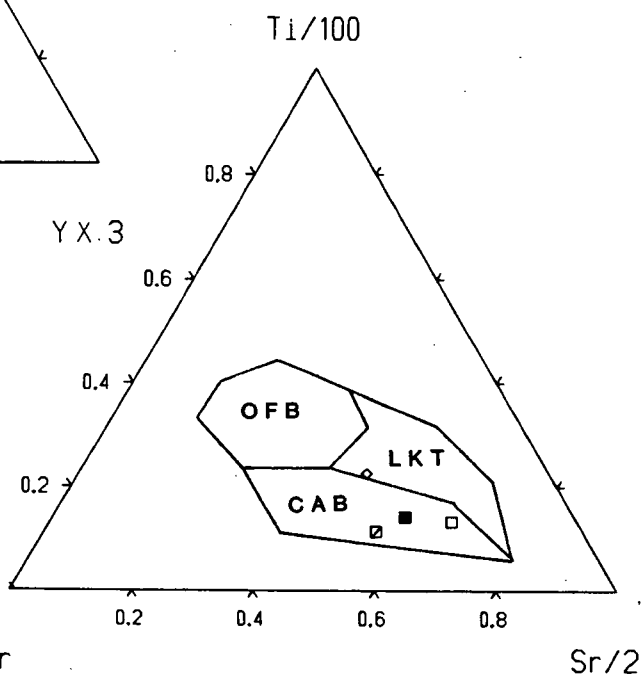
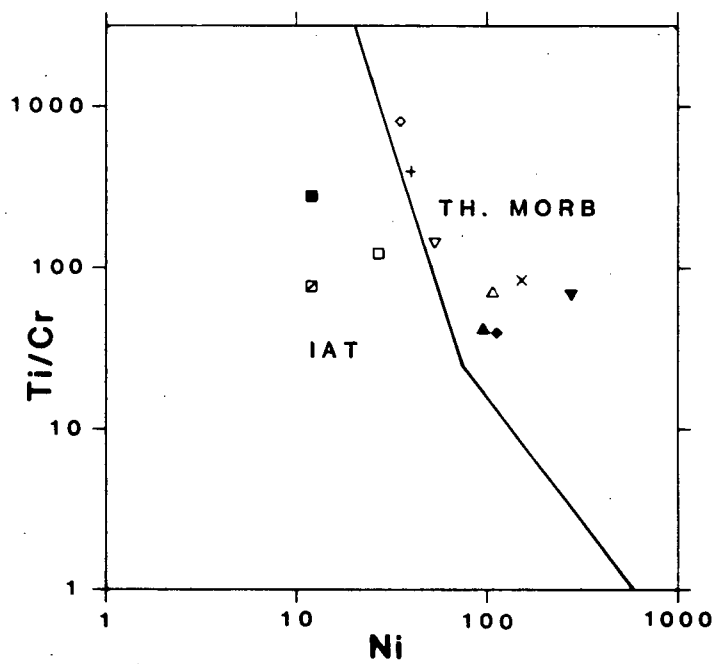
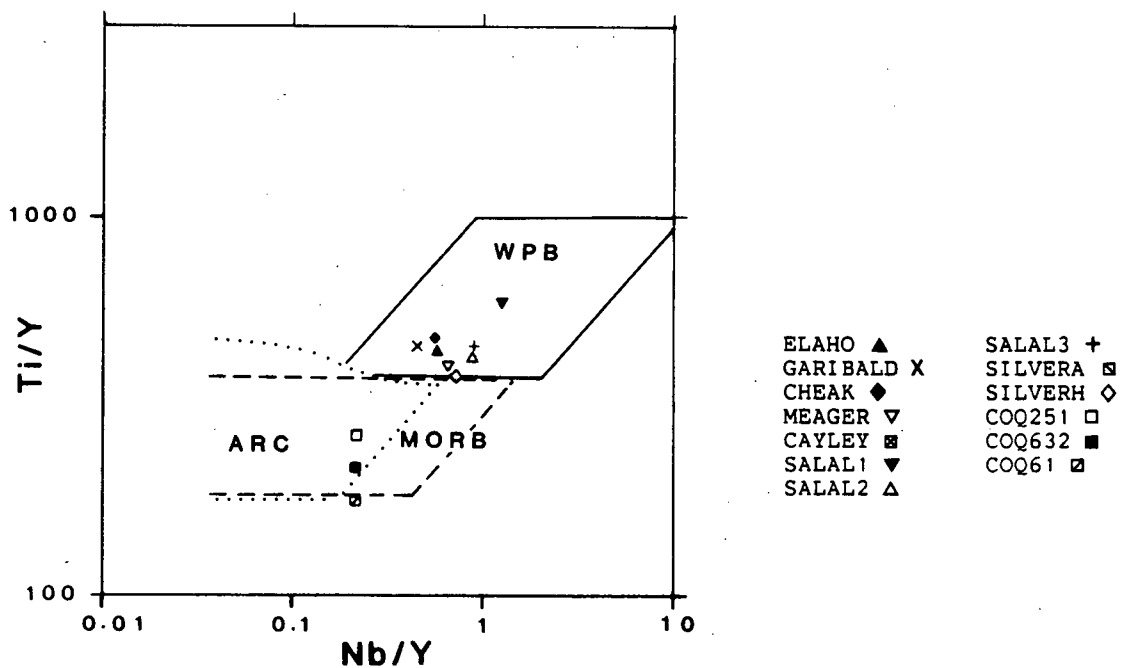


Fig. 3.10. V vs. Ti/1000.

| | |
|------------|-----------|
| ELAHO ▲ | SALAL3 + |
| GARIBALD X | SILVERA □ |
| CHEAK ◆ | SILVERH ◇ |
| MEAGER ▽ | COQ251 □ |
| CAYLEY ▣ | COQ632 ■ |
| SALAL1 ▼ | COQ61 ▣ |
| SALAL2 △ | |



Figs. 3.11 and 3.12. Ti/Y vs. Nb/Y (above) and Ti/Cr vs. Ni (below).

plots in the overlapping MORB-WPB fields (Fig. 3.14).

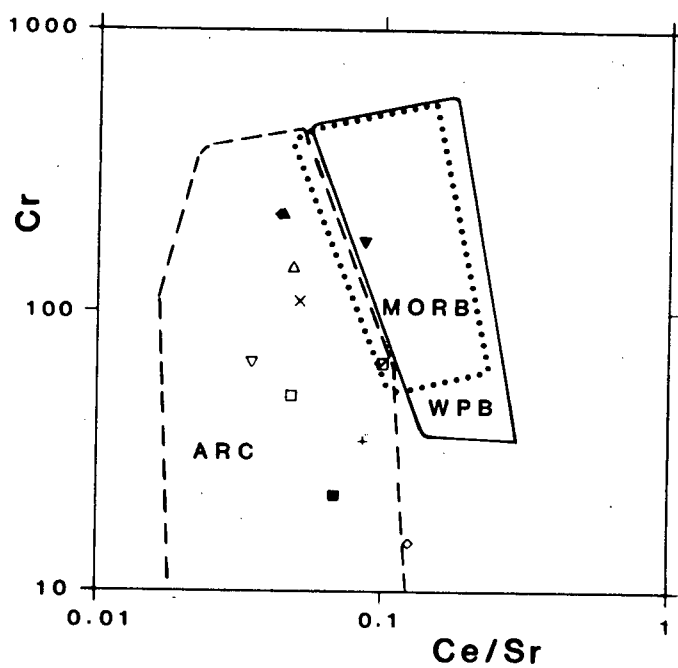
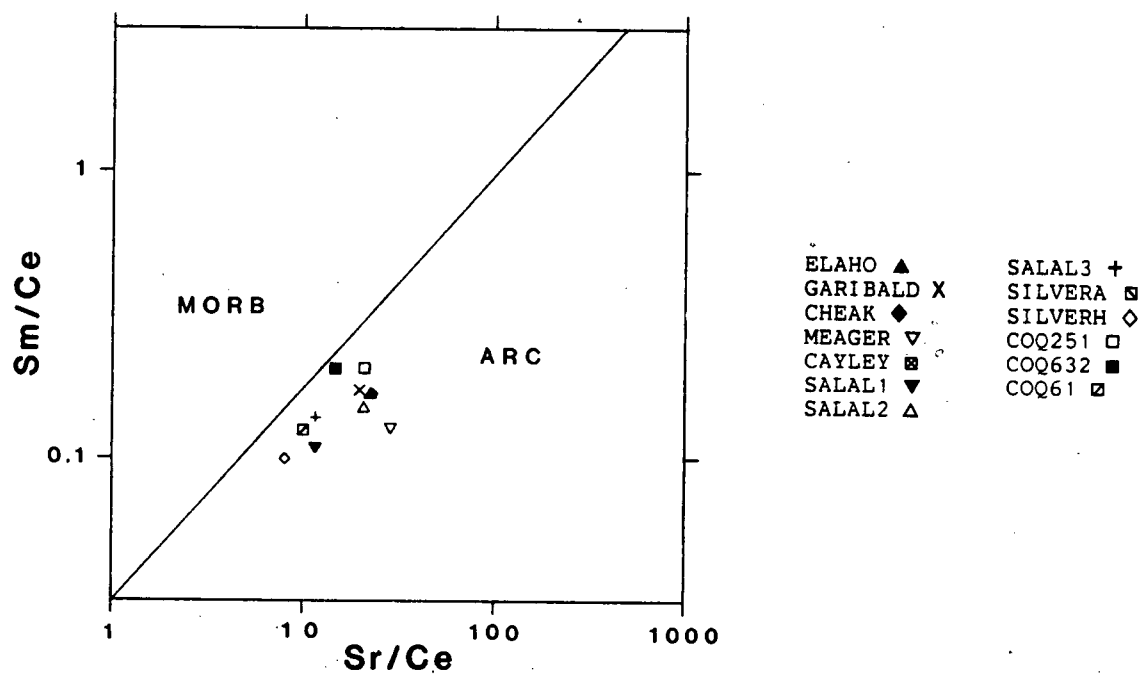
On Cr vs. Y all eleven basaltic samples lie within the convergent margin field, or overlapping WPB-convergent margin fields despite a wide range of Cr abundances (Fig. 3.15).

Both basalts and andesites were plotted on La vs. Ba, La vs. Th and La vs. Nb diagrams.

On La vs. Ba most samples lie within or close to the orogenic andesite field, with Ba/La ratios greater than 15 (Fig. 3.16). SALAL1 and GARIBALD lie within the field for E-MORB. However, on $(\text{Ba/La})_{\text{CH}}$ vs. $(\text{La/Sm})_{\text{CH}}$ only basaltic samples COQ251, COQ632 and COQ61 are clearly classified as convergent margin (Fig. 3.17). The eight remaining basaltic samples lie within the oceanic field. Sample MEAGER and the four alkaline samples have the highest $(\text{La/Sm})_{\text{CH}}$ ratios.

On La vs. Th samples COQ251, COQ632 and COQ61 lie within the orogenic andesite field with La/Th ratios less than 3.3 (Fig. 3.18). Samples MEAGER and SILVERH lie within the N-MORB field, and the eight remaining samples lie within the field for E-MORB. Of these eight, three have Th contents less than 1.5 ppm (ELAHO, GARIBALD and CHEAK) and lie within the area which overlaps with the orogenic andesite field.

COQ251, COQ632, COQ61, CAYLEY and MEAGER lie within the orogenic andesite field on La vs. Nb, with La/Nb ratios between 2 and 5 (Fig. 3.19). Samples SILVERH and



Figs. 3.13 and 3.14. Sm/Ce vs. Sr/Ce (above) and Cr vs. Ce/Sr (below).

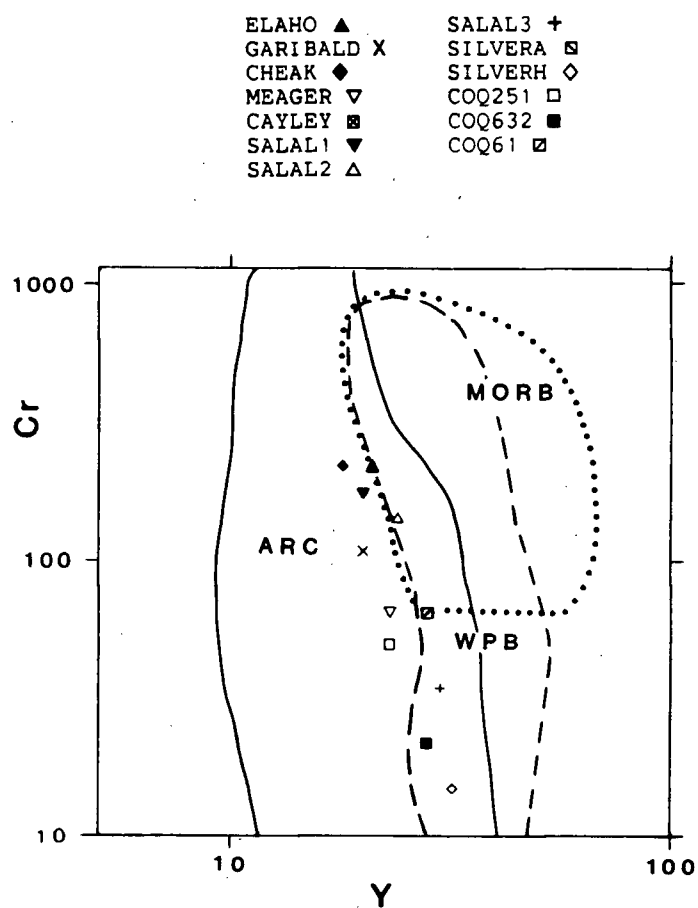
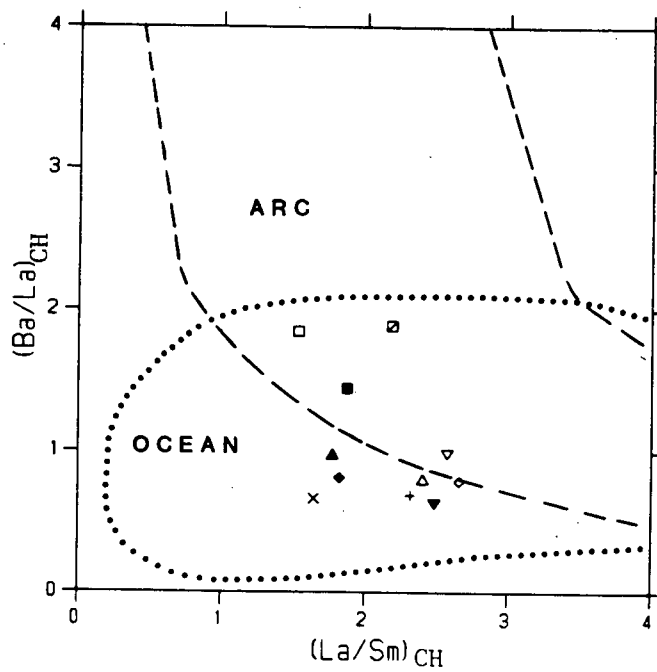
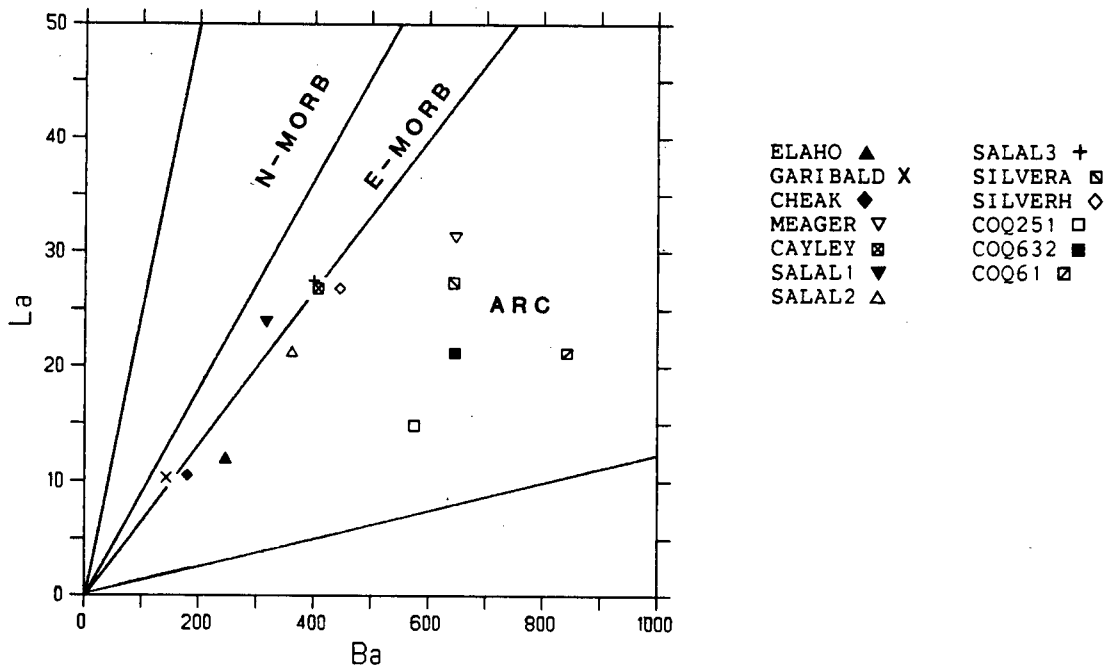
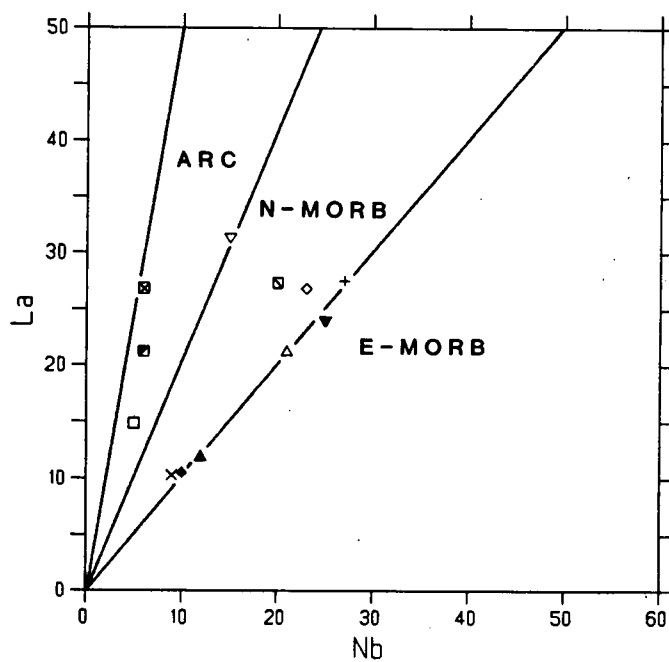
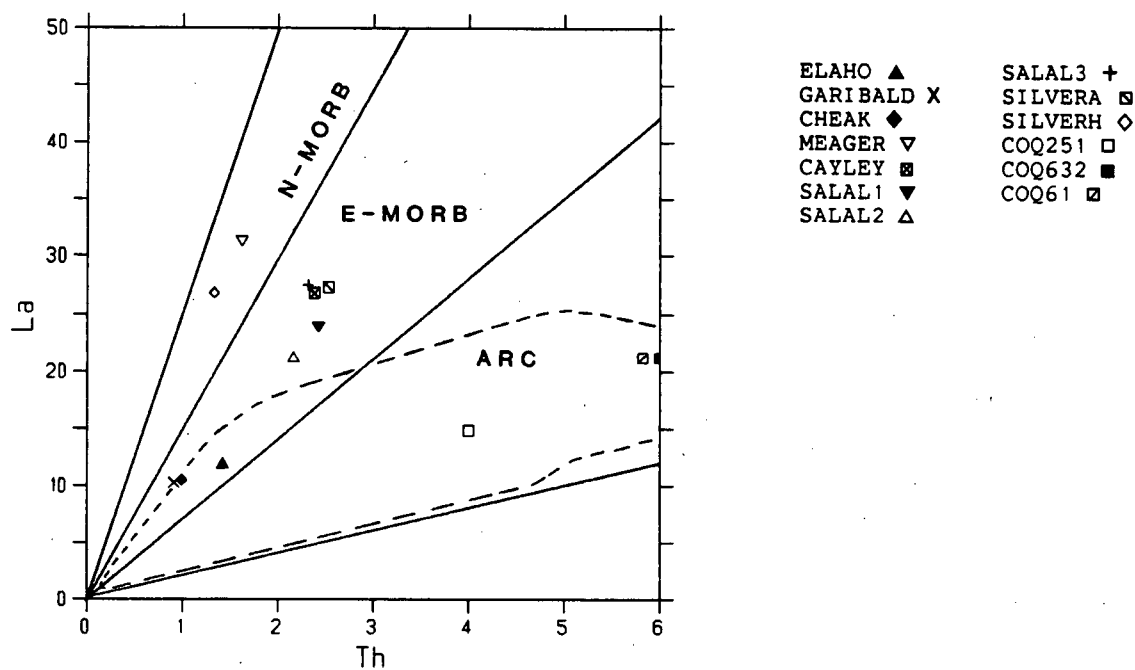


Fig. 3.15. Cr vs. Y.



Figs. 3.16 and 3.17. La vs. Ba (above) and $(Ba/La)_{CH}$ vs. $(La/Sm)_{CH}$ (below).



Figs. 3.18 and 3.19. La vs. Th (above) and La vs. Nb (below).

SILVERA clearly lie within the N-MORB field (La/Nb ratios between 1 and 2) and the remainder lie astride the N-MORB/E-MORB field boundary with La/Nb ratios approximately equal to 1.

Most basalt data plotted on K_2O/Yb vs. Ta^*/Yb lie within the space between the WPB and convergent margin fields (Fig. 3.20). Exceptions are COQ251, COQ632 and COQ61 which lie within the convergent margin field. Samples SALAL1, SALAL2 and SALAL3 have the highest Ta^*/Yb ratios.

On Th/Yb vs. Ta^*/Yb samples COQ251, COQ632 and COQ61 lie within the convergent margin field (Fig. 3.21). All remaining basaltic samples lie within the overlapping MORB-WPB fields.

To plot $Th-Hf/3-Ta^*$ abundances of Hf in samples COQ251, COQ632 and COQ61 were estimated using the ratio $Zr/Hf = 39$. According to Gill (1982) this ratio remains quite constant in basalts from all tectonic environments. On this diagram samples COQ251, COQ632, COQ61 and CAYLEY lie within the convergent margin field (Fig. 3.22). Alkaline samples SALAL1, SALAL2, SALAL3 and SILVERH lie within the alkaline WPB field and the remaining four basalt samples, plus SILVERA, lie within the E-MORB-tholeiitic WPB field.

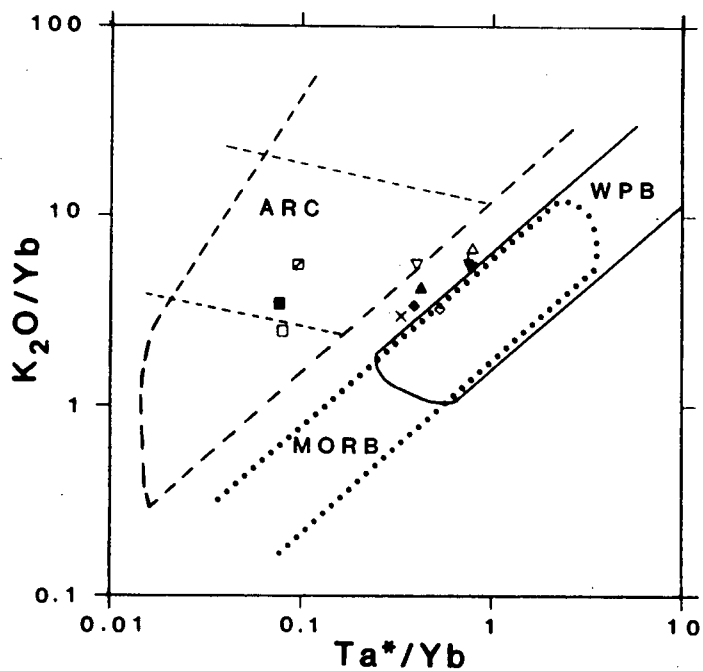


Fig. 3.21. Th/Yb vs. Ta^*/Yb .

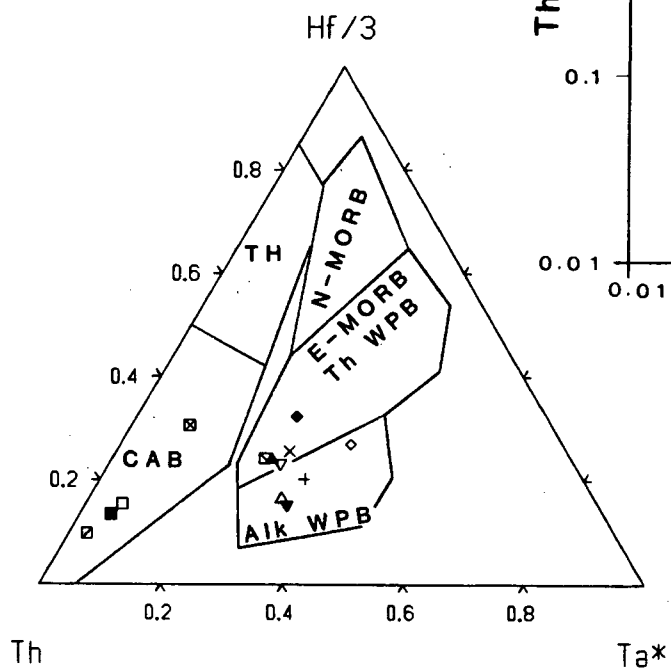
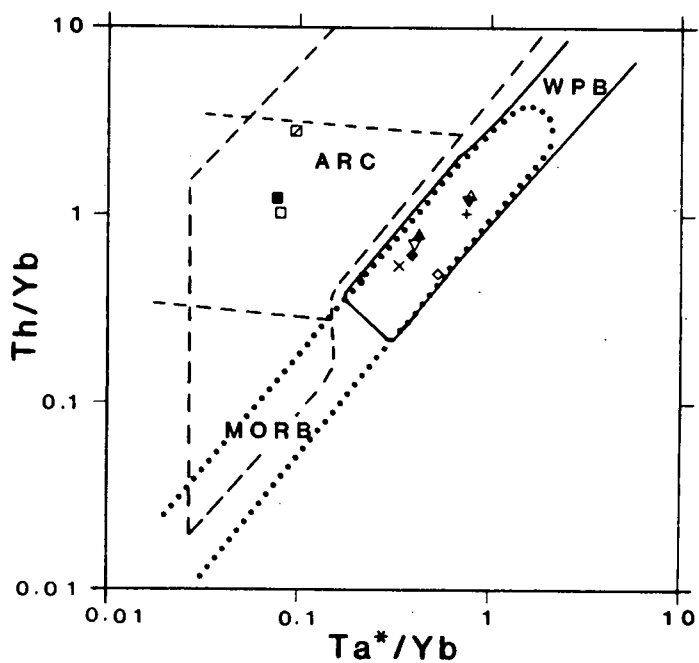


Fig. 3.22. $Th-Hf/3-Ta^*$.

3.2.4 BULK EARTH NORMALIZED DIAGRAMS (BEND)

BEND patterns on Fig. 3.23 are from COQ251, COQ632 and COQ61. Patterns are enriched in Ba, Rb, Th and K relative to LREE, have a pronounced 'trough' at Nb and a less distinct 'trough' at Ti. Eu anomalies are not evident. From Eu to Lu the pattern is fairly flat.

Fig. 3.24 shows BEND patterns for subalkaline Garibaldi Belt basalts, ELAHO, GARIBALD, CHEAK and MEAGER. The first three samples have nearly identical patterns and the latter sample's pattern is grossly similar. All patterns have an irregular, slightly convex-up shape with 'peaks' at Ba, K and Sr and 'troughs' at Nb and Hf. In addition, all patterns have a small 'peak' at Eu so that they have a concave-up 'dip' from Sm to Eu.

BEND patterns on Fig. 3.25 are from Garibaldi Belt hawaiites, SALAL1, SALAL2, SALAL3 and SILVERH. From Ba to Rb the patterns are flat, or have slightly negative slopes, but from Rb to Lu they are irregularly convex-up, with a 'trough' at Hf, so that they have a concave-up dip from Sm to Eu. In addition, SALAL2 has a 'peak' at Sr and SILVERH has a 'trough' at Th. All patterns suggest a positive Eu anomaly, although Tb was not analyzed.

BEND patterns on Fig. 3.26 are from andesitic samples CAYLEY and SILVERA. Both patterns are enriched in LIL relative to HREE, with 'peaks' at Sr, K, Eu \pm Rb

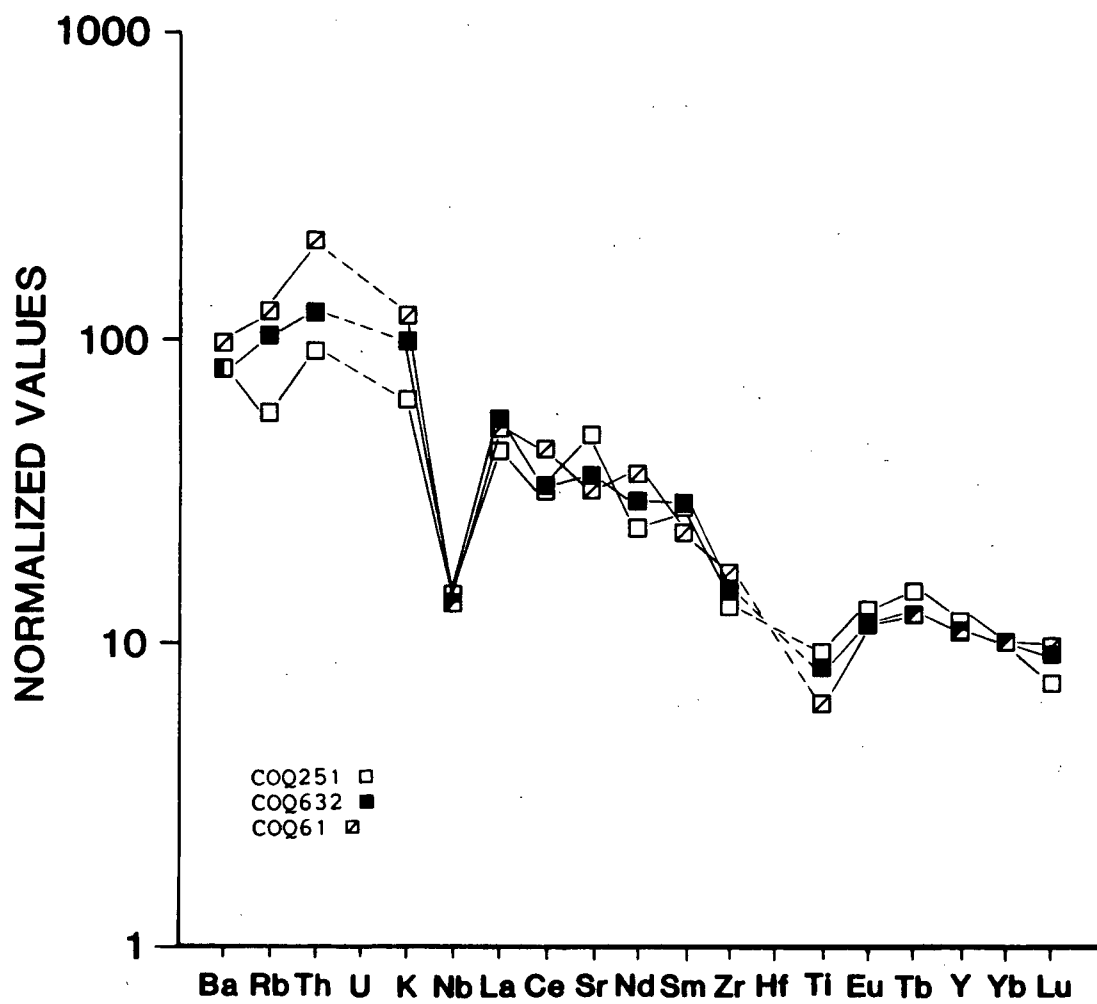


Fig. 3.23. BEN diagram for samples COQ251, COQ632 and COQ61.

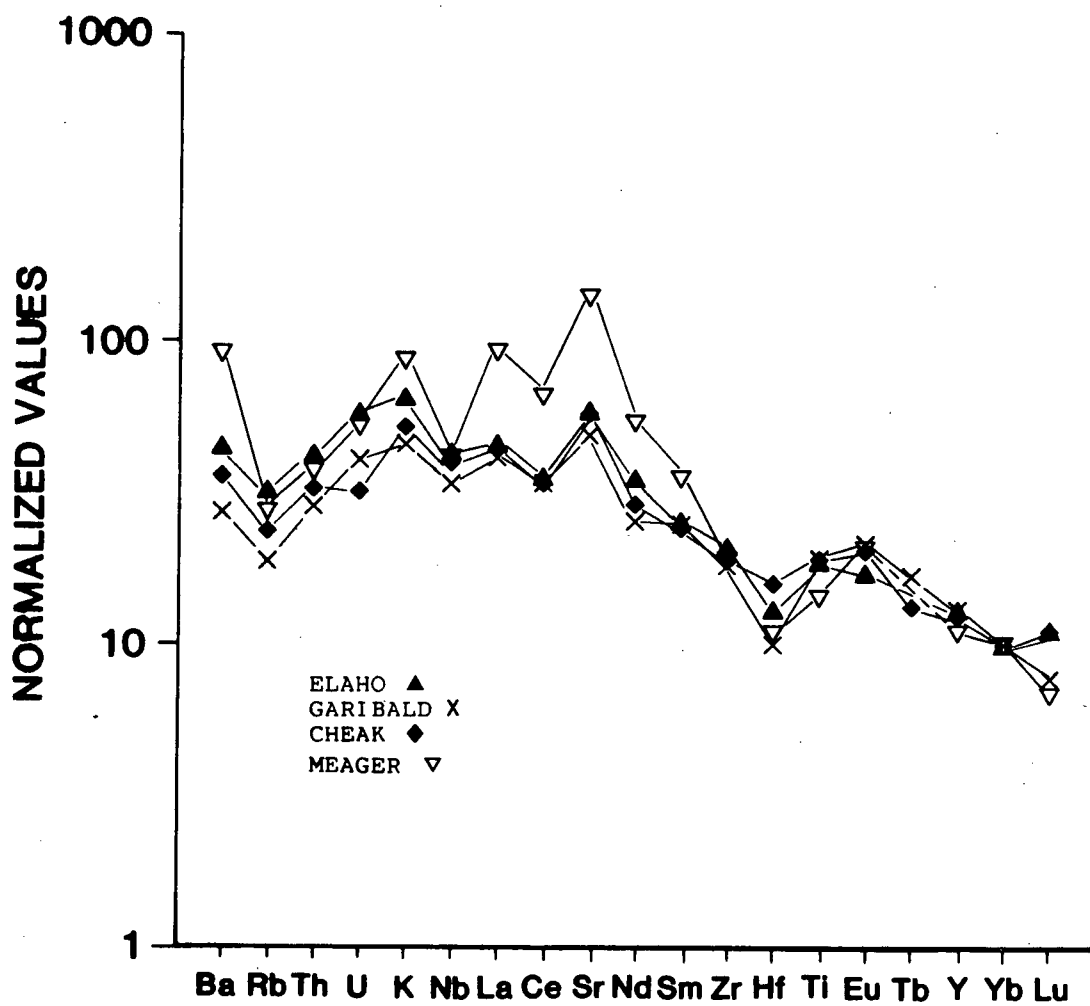


Fig. 3.24. BEN diagram for samples ELAHO, GARIBALD, CHEAK and MEAGER.

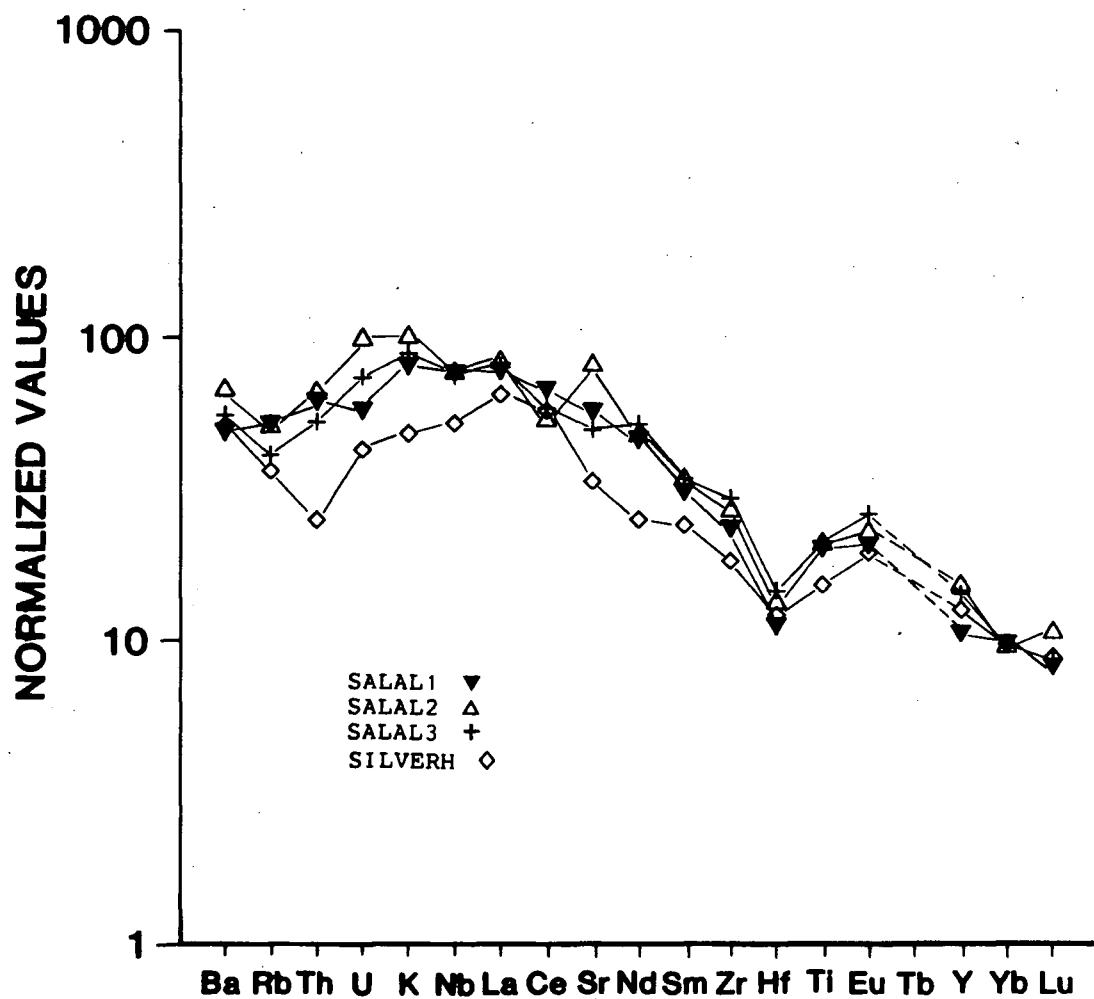


Fig. 3.25. BEN diagram for samples SALAL1, SALAL2, SALAL3 and SILVERH.

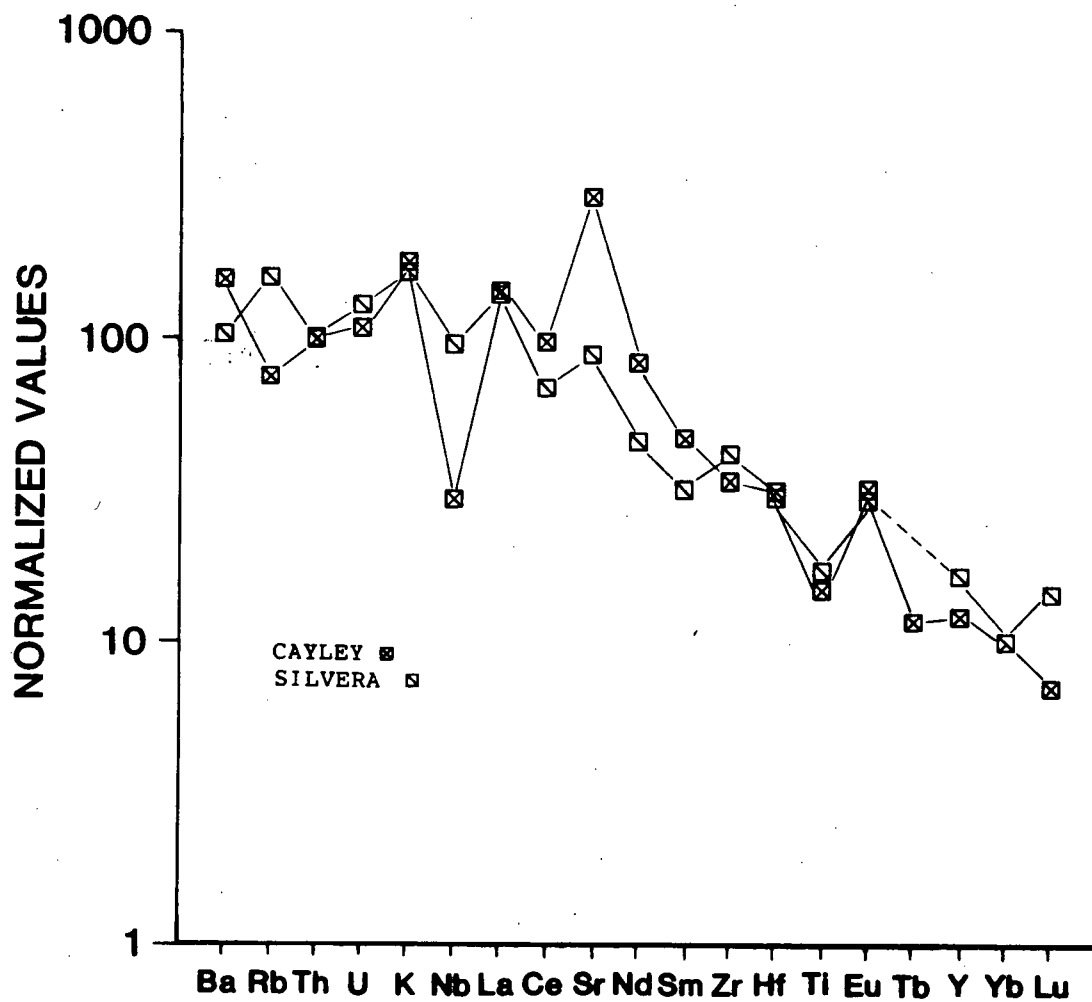


Fig. 3.26. BEN diagram for samples CAYLEY and SILVERA.

and 'troughs' at Nb and Ti. The magnitude of 'peaks' and 'troughs' are much greater in the pattern for CAYLEY.

None of the patterns display negative Ce anomalies.

3.3 TRACE ELEMENT CHEMISTRY

Samples from the Coquihalla Volcanic Complex and andesitic samples CAYLEY and SILVERA from the Garibaldi Belt have abundances of trace and REE and BEND patterns similar to an average calcalkaline convergent margin basalt erupted through continental crust (Thompson et al., 1984; Wilson and Davidson, 1984; Pearce, 1983). La abundances range from 45 to 84 times chondritic, Yb abundances lie between 6 and 13 times chondritic and $(La/Yb)_{CH}$ ratios range from approximately 4 to 14 (Yb abundances estimated for Coquihalla samples). La/Nb ratios are greater than 1.3 and Rb/Nb ratios range from 1.6 to 9, characteristic of convergent margins.

Relative to an 'average' convergent margin basalt basaltic samples ELAHO, GARIBALD and CHEAK are slightly to very depleted in LIL and are enriched in Nb (Basaltic Volcanism Study Project, 1981; Thompson et al., 1984). These three samples have BEND patterns similar to patterns from WPB. La abundances range from 31 to 37 times chondritic, Yb abundances range from 7 to 8 times chondritic and $(La/Yb)_{CH}$ ratios lie between 4.1 and 4.6. La/Nb ratios range from 0.94 to 1.08 and Rb/Nb ratios range from 0.55 to 0.75, more typical of WPB than basalts from convergent margins. Cascade

basaltic lavas also have atypically low Rb/Nb ratios (0.6) and are inferred to have originated within the the mantle wedge (i.e. within-plate) (Leeman and Smith, in preparation).

Basaltic sample MEAGER is slightly to greatly enriched in all trace and REE relative to the other subalkaline Garibaldi Belt basalts. It has an Rb/Nb ratio of 0.66, similar to Rb/Nb from WPB, but its La/Nb ratio of 2.08 is typical of a convergent margin basalt.

Alkaline samples SALAL1, SALAL2, SALAL3 and SILVERH have trace and REE abundances and BEND patterns grossly similar to an average alkaline WPB but Ba abundances are slightly higher (Table II). La abundances range from 65 to 84 times chondritic. Yb abundances lie between 8 and 12 times chondritic and $(La/Yb)_{CH}$ ratios range from 6.6 to 8.6. La/Nb ratios range from 0.9 to 1.2 and Rb/Nb ratios lie between 0.55 and 0.68.

3.3.1 TH AND U

Th abundances in Garibaldi Belt samples lie between 1.0 and 2.5 ppm and U abundances lie between 0.3 and 1.0 ppm (Table II). Th/U ratios are highly variable, range from 1.9 to 3.5 and average 2.6.

Samples from the Coquihalla Volcanic Complex have Th abundances greater than 4 ppm. These samples were not analyzed for U.

3.3.2 TRANSITION ELEMENTS

Cr and Ni abundances and variations in Mg' numbers are presumably controlled by fractionation of olivine \pm clinopyroxene and Cr-spinel. Samples with Mg' numbers greater than 56 (GARIBALD, CHEAK, SALAL1 and SALAL2) also have relatively high abundances of Cr and Ni indicating they are less fractionated than the rest of the samples. Lower Mg' numbers and lower Cr and Ni abundances point to more extensive fractionation.

With the exception of samples CAYLEY and SILVERA, Sc contents range from 17 to 29 ppm and average 22 ppm. Samples CAYLEY AND SILVERA have Sc abundances of 11.2 ppm and 11.6 ppm respectively. They also have the lowest Yb contents and highest $(La/Yb)_{CH}$ ratios. Low Sc abundance suggests high pressure pyroxene fractionation, whereas low contents of Yb suggest a garnet rich residue, perhaps an eclogite.

3.4 SR ISOTOPES

All samples in this study have $^{87}Sr/^{86}Sr$ ratios between 0.7030 ± 0.00007 to 0.7036 ± 0.00008 (Table II). Average $^{87}Sr/^{86}Sr$ ratios of basalts erupted at subduction zones lie between 0.7030 and 0.7040 (Faure, 1977).

3.5 DISCUSSION OF DISCRIMINATION DIAGRAMS

On elemental discrimination diagrams the three calcalkaline samples from the Coquihalla Volcanic Complex always lie within the convergent margin field and on a BEND their patterns have a 'typical' convergent margin shape (Thompson et al., 1984).

Calcalkine andesites CAYLEY and SILVERA could be plotted on only a few diagrams and classifications were not as consistent. On La vs. Th (Fig. 3.18) both CAYLEY and SILVERA lie in the E-MORB field, whereas on the La vs. Nb and Th-Hf/3-Ta* diagrams (Figs. 3.19 and 3.22) CAYLEY lies within the convergent margin field but SILVERA lies within N-MORB and E-MORB (tholeiitic WPB) fields respectively. BEND patterns for both of these samples indicate they are slightly enriched in La relative to a 'typical' convergent margin andesite thereby explaining the La vs. Th classification. The BEND pattern from SILVERA also indicates it is slightly enriched in Nb, relative to a convergent margin basalt, hence the MORB classification on La vs. Nb and Th-Hf/3-Ta*.

In contrast, basalt samples ELAHO, GARIBALD, CHEAK and MEAGER lie within the WPB or E-MORB fields on several of the discrimination diagrams and have BEND patterns with characteristics of both WPB and convergent margin basalt. Relative to a 'typical' convergent margin basalt their higher Ti abundances classifies them as WPB on $\text{TiO}_2\text{-MnO-P}_2\text{O}_5$, Ti-Zr-Y and Ti/Y vs. Nb/Y diagrams and their

undepleted Nb content produces the same classifications on Ti/Y vs. Nb/Y, La vs. Nb, K_2O vs. Ta^*/Yb , Th/Yb vs. Ta^*/Yb and Th-Hf/3- Ta^* diagrams. Atypically low Al_2O_3 abundance is evident on the MgO-FeO*- Al_2O_3 diagram, low Ba content moves them towards or within the WPB fields on La vs. Ba and $(Ba/La)_{CH}$ vs. $(La/Sm)_{CH}$ diagrams and low abundances of Th classify them as WPB on La vs. Th, Th/Yb vs. Ta^*/Yb and Th-Hf/3- Ta^* . On Sm/Ce vs. Sr/Ce, Cr vs. Ce/Sr and Cr vs. Y the samples lie within the convergent margin field because of their Sr and Y abundances. Sr enrichment is caused by either:

- a subduction component (Armstrong, 1971; Kay, 1980; Hole et al., 1984), or
- plagioclase accumulation,

whereas Y depletion is most likely related to a garnet rich source residuum, perhaps an eclogite. This type of arc basalt has been called 'mildly alkaline' or 'transitional' by Best and Brimhall (1974) and 'anomalous' by Pearce (1982). Green (1981) classifies the Garibaldi Belt basalts as 'mildly alkaline'.

Hawaiite samples SALAL1, SALAL2, SALAL3 and SILVERH most often lie within the WPB or E-MORB fields. An exception is the La vs. Ba plot (Fig. 3.16) which classifies them all as convergent margin because of their slight enrichment in Ba. However this enrichment cannot be very significant as it is not evident on $(Ba/La)_{CH}$ vs. $(La/Sm)_{CH}$ (Fig. 3.17). The increased abundance of K_2O results in an ambiguous position

on K_2O/Yb vs. Ta^*/Yb (Fig. 3.20) but on Th/Yb vs. Ta^*/Yb (Fig. 3.21) these four samples are clearly classified as WPB. Data plotted on Cr vs. Ce/Sr (Fig. 3.14) is probably affected by plagioclase, olivine \pm pyroxene and Cr -spinel fractionation. The fractionation of pyroxene \pm Cr -spinel almost certainly controls the position of SALAL3 and SILVERH, whereas plagioclase fractionation (accumulation ?) may be the reason SALAL2 lies within the convergent margin field. However, the lack of a corresponding positive Eu anomaly in this latter sample casts some doubt on this interpretation.

The clearly distinguished alkaline-WPB Garibaldi Belt samples are unusual because members of the alkaline rock series are present only rarely in an arc setting (Delong et al., 1975). In a recent study of the Salal Creek Volcanics Lawrence et al. (1984) relate their alkaline geochemistry to their position at the end of the Garibaldi Volcanic arc and postulate they may be either the consequence of a change from arc to back-arc volcanism, or smaller degrees of melting as volcanic arc magma generation ceases (Jakeš and White, 1969), or a descending plate edge effect (Arculus et al., 1977).

3.6 SUMMARY

The three samples from the Coquihalla Complex (part of the Pemberton Volcanic Arc) belong to the calcalkaline series, lie within the ARC field in all of the tectonic

discrimination diagrams studied and have BEND patterns and La/Nb ratios which are 'typical' of a volcanic arc.

In contrast, basaltic samples from the Garibaldi Belt are transitional (mildly alkaline) in nature and are classified as WPB on many of the studied diagrams. BEND patterns have characteristic convex-up (WPB) shapes and La/Nb and Rb/Nb ratios also suggest a within-plate tectonic setting. Basaltic lavas from the Cascades also display these within-plate geochemical characteristics. This has been interpreted by Leeman and Smith (in prep.) as evidence for a source origin within the mantle wedge overlying the subduction zone.

Andesitic sample CAYLEY is classified as convergent margin on the few diagrams on which it could be plotted and has a BEND pattern and an La/Nb ratio characteristic of a volcanic arc. Andesitic samples SILVERA is more alkaline in nature but still has some convergent margin characteristics.

Basaltic samples from the Salal Creek area of the Garibaldi Belt and one from Mt. Silverthron belong to the alkaline series, lie within the WPB field on almost all of the tectonic discrimination diagrams and have BEND patterns and La/Nb ratios 'typical' of a WPB. Alkaline series rocks are unusual in a convergent margin setting and these are probably related to their position at the end of the Garibaldi Belt (Lawrence et al., 1984).

Both transitional and alkaline Garibaldi Belt samples are enriched in Sr and depleted in Y relative to a 'normal' WPB. Consequently they lie within the ARC field on Sm/Ce vs. Sr/Ce, Ce vs. Ce/Sr and Cr vs. Y. Sr enrichment is either from plagioclase accumulation or related to a subduction component, whereas Y depletion suggests residual garnet in the source.

TABLE II Garibaldi and Pemberton Belts

Major, trace and rare earth element abundances, Sr isotope ratios and K/Ar dates.

| Series Name | ELAHO ¹ CA/Trans Basalt | GARIBALD ² CA/Trans Basalt | CHEAK ³ CA/Trans Basalt | MEAGER ¹ CA/Trans Basalt | CAYLEY Calcalc. Andesite | SALALI ⁴ Alkaline Hawaiite | SALAL2 ⁴ Alkaline Hawaiite | SALAL3 ⁴ Alkaline Hawaiite |
|--------------------------------|--|---|--|---|--------------------------------|---|---|---|
| LAT. | 50 26.97 | 49 58.3 | 50 03.0 | 50 40.2 | 50 12.1 | 50 47.0 | 50 47.5 | 50 47.9 |
| LONG. | 123 34.88 | 123 09 | 123 08.0 | 123 34.95 | 123 18.4 | 123 22.6 | 123 21 | 123 23.5 |
| SiO ₂ | 51.24 | 49.30 | 51.82 | 49.50 | 60.34 | 47.27 | 49.00 | 50.92 |
| TiO ₂ | 1.56 | 1.52 | 1.44 | 1.55 | 0.89 | 1.97 | 1.71 | 2.28 |
| Al ₂ O ₃ | 15.77 | 15.55 | 15.94 | 16.30 | 16.64 | 14.37 | 15.99 | 16.96 |
| Fe ₂ O ₃ | 1.91 | 11.78 | 1.45 | 4.04 | 5.60 | 1.75 | 1.64 | 1.64 |
| FeO | 9.46 | 0.0 | 8.77 | 8.11 | 0.0 | 9.94 | 9.29 | 9.29 |
| MnO | 0.15 | 0.14 | 0.14 | 0.15 | 0.09 | 0.19 | 0.19 | 0.17 |
| MgO | 7.28 | 8.56 | 7.43 | 6.59 | 3.10 | 9.92 | 7.79 | 4.28 |
| CaO | 8.42 | 8.90 | 8.51 | 8.85 | 7.27 | 8.62 | 9.48 | 7.61 |
| Na ₂ O | 3.18 | 3.46 | 3.73 | 3.11 | 4.44 | 4.43 | 3.34 | 4.76 |
| K ₂ O | 0.75 | 0.50 | 0.54 | 1.29 | 1.36 | 1.09 | 1.13 | 1.33 |
| P ₂ O ₅ | 0.26 | 0.29 | 0.23 | 0.50 | 0.27 | 0.46 | 0.43 | 0.75 |
| H ₂ O | N/A | 0.22 | 0.49 | N/A | N/A | 0.07 | 0.27 | 0.13 |
| Ba | 247.0 | 143.0 | 179.0 | 647.0 | 407.0 | 317.0 | 362.0 | 400.0 |
| Rb | 9.0 | 5.0 | 6.0 | 10.0 | 15.0 | 17.0 | 14.0 | 15.0 |
| Th | 1.4 | 0.9 | 1.0 | 1.6 | 2.4 | 2.4 | 2.2 | 2.3 |
| U | 0.6 | 0.4 | 0.3 | 0.7 | 0.8 | 0.7 | 1.0 | 1.0 |
| Nb | 12.0 | 9.0 | 10.0 | 15.0 | 6.0 | 25.0 | 21.0 | 27.0 |
| La | 12.0 | 10.3 | 10.5 | 31.3 | 26.8 | 23.9 | 21.3 | 27.5 |
| Ce | 24.7 | 22.3 | 21.2 | 59.0 | 48.2 | 54.8 | 36.3 | 52.8 |
| Sr | 554.0 | 437.0 | 489.0 | 1695.0 | 1944.0 | 634.0 | 749.0 | 613.0 |
| Nd | 17.8 | 12.2 | 13.2 | 35.3 | 30.0 | 27.5 | 23.6 | 34.3 |
| Sm | 4.2 | 3.9 | 3.6 | 7.5 | 5.5 | 5.9 | 5.5 | 7.3 |
| Zr | 116.0 | 95.0 | 94.0 | 137.0 | 134.0 | 152.0 | 145.0 | 212.0 |
| Hf | 2.1 | 1.5 | 2.3 | 2.3 | 3.6 | 2.1 | 2.1 | 3.1 |
| Eu | 1.0 | 1.2 | 1.1 | 1.6 | 1.4 | 1.4 | 1.3 | 2.0 |
| Tb | N/A | 0.6 | 0.5 | N/A | 0.3 | N/A | N/A | N/A |
| Y | 21.0 | 20.0 | 18.0 | 23.0 | 14.0 | 20.0 | 24.0 | 30.0 |
| Yb | 1.8 | 1.7 | 1.6 | 2.3 | 1.3 | 2.0 | 1.7 | 2.3 |
| Lu | 0.3 | 0.2 | 0.3 | 0.2 | 0.1 | 0.3 | 0.3 | 0.3 |
| Co | 36.0 | 54.0 | 56.0 | 30.0 | 27.0 | 51.0 | 42.0 | 30.0 |
| Cr | 221.0 | 108.4 | 219.0 | 65.5 | 16.3 | 174.3 | 143.1 | 34.6 |
| Cu | 39.0 | 56.0 | 37.0 | 67.0 | 66.0 | 60.0 | 60.0 | 38.0 |
| Ni | 95.0 | 152.0 | 112.0 | 53.0 | 25.0 | 277.0 | 107.0 | 40.0 |
| Sc | 22.1 | 21.4 | 18.0 | 23.7 | 11.2 | 22.4 | 24.9 | 18.6 |
| V | 173.0 | 177.0 | 160.0 | 196.0 | 104.0 | 188.0 | 207.0 | 181.0 |
| V ⁸⁷ | 0.7031 | N/A | N/A | 0.7036 | N/A | 0.7033 | N/A | 0.7030 |
| Sr ⁸⁶ | | | | | | | | |
| K/Rb | 691.75 | 830.10 | 747.09 | 1070.83 | 752.62 | 532.24 | 670.01 | 736.02 |
| (La/Yb) _{CH} | 4.54 | 4.10 | 4.40 | 9.04 | 14.18 | 7.90 | 8.61 | 8.20 |
| La/Nb | 1.00 | 1.14 | 1.05 | 2.09 | 4.47 | 0.96 | 1.01 | 1.02 |
| Mg' | 54 | 59 | 57 | 50 | 52 | 61 | 56 | 41 |
| K/Ar DATE (Ma) | 0.14±0.1 | < 1 | < 1 | 0.09±0.06 | < 1 | 0.59±0.05 | < 1 | 0.97±0.05 |

continued.....

| | SILVERA | SILVERH | COQ251 | COQ632 | COQ61 |
|------------------------------------|-------------------|--------------------|-----------------|-----------------|-----------------|
| Series Name | Calcalc. Andesite | Alkaline Hawaiiite | Calcalc. Basalt | Calcalc. Basalt | Calcalc. Basalt |
| LAT. | 51 24.5 | 51 33.25 | 49 53 | 49 53 | 49 54 |
| LONG. | 126 15.25 | 126 21.5 | 121 04 | 121 05 | 121 04 |
| SiO ₂ | 59.81 | 49.30 | 53.53 | 55.40 | 57.75 |
| TiO ₂ | 1.08 | 2.00 | 1.02 | 1.02 | 0.83 |
| Al ₂ O ₃ | 17.14 | 16.22 | 16.38 | 16.34 | 15.38 |
| Fe ₂ O ₃ | 6.55 | 12.10 | 8.89 | 8.38 | 8.05 |
| FeO | 0.0 | 0.0 | 0.0 | 0.0 | 0.0 |
| MnO | 0.10 | 0.18 | 0.19 | 0.15 | 0.14 |
| MgO | 2.04 | 5.08 | 6.75 | 5.47 | 6.11 |
| CaO | 6.67 | 8.95 | 9.70 | 8.12 | 6.42 |
| Na ₂ O | 4.88 | 4.76 | 2.26 | 3.08 | 2.96 |
| K ₂ O | 1.54 | 0.88 | 0.96 | 1.67 | 2.16 |
| P ₂ O ₅ | 0.28 | 0.53 | 0.31 | 0.37 | 0.21 |
| H ₂ O | N/A | N/A | 1.10 | 0.47 | 2.32 |
| Ba | 644.0 | 445.0 | 576.0 | 646.0 | 842.0 |
| Rb | 33.0 | 16.0 | 21.0 | 42.0 | 54.0 |
| Th | 2.5 | 1.3 | 4.0 | 6.0 | 11.0 |
| U | 1.0 | 0.7 | N/A | N/A | N/A |
| Nb | 20.0 | 23.0 | 5.0 | 6.0 | 6.0 |
| La | 27.4 | 26.8 | 14.8 | 21.2 | 21.2 |
| Ce | 35.6 | 62.6 | 29.0 | 34.0 | 48.0 |
| Sr | 625.0 | 502.0 | 605.0 | 500.0 | 479.0 |
| Nd | 17.4 | 20.1 | 16.0 | 22.0 | 29.0 |
| Sm | 3.9 | 6.2 | 6.0 | 7.0 | 6.0 |
| Zr | 172.0 | 159.0 | 95.0 | 120.0 | 149.0 |
| Hf | 3.6 | 3.1 | N/A | N/A | N/A |
| Eu | 1.3 | 1.8 | 1.0 | 1.0 | 1.1 |
| Tb | N/A | N/A | 0.7 | 0.8 | 0.8 |
| Y | 20.0 | 32.0 | 23.0 | 28.0 | 28.0 |
| Yb | 1.3 | 2.7 | 2.4* | 2.7* | 2.9* |
| Lu | 0.3 | 0.4 | 0.3 | 0.4 | 0.4 |
| Co | 44.0 | 63.0 | 58.0 | 41.0 | 45.0 |
| Cr | 9.1 | 15.0 | 50.0 | 22.0 | 65.0 |
| Cu | 37.0 | 21.0 | 28.0 | 26.0 | 28.0 |
| Ni | 14.0 | 35.0 | 27.0 | 12.0 | 12.0 |
| Sc | 11.6 | 28.7 | 22.1 | 23.0 | 17.5 |
| V | 132.0 | 280.0 | 241.0 | 213.0 | 191.0 |
| ⁸⁷ Sr/ ⁸⁶ Sr | 0.7036 | 0.7036 | 0.7036 | N/A | N/A |
| K/Rb | 387.38 | 456.55 | 379.47 | 330.06 | 332.04 |
| (La/Yb) _{CH} | 13.79 | 6.64 | 4.14* | 5.27* | 4.90* |
| La/Nb | 1.37 | 1.17 | 2.97 | 3.53 | 3.53 |
| Mg' | 38 | 45 | 50 | 48 | 52 |
| K/Ar DATE (Ma) | 0.4 ± 0.1 | 0.95 ± 0.2 | ~22 | ~22 | ~22 |

Major element abundances from:

- ¹Anderson (1975)
²Green (1981)
³Feisinger (1975)
⁴Lawrence (1979)

*Estimated from BEND

N/A = not analyzed

4. CHILCOTIN BASALTS

Eleven samples of the Miocene to Pliocene Chilcotin Group basalts were selected for analysis (Fig. 4.1). The basalts were generated in a back-arc tectonic setting due to asthenospheric upwelling evidently related to the Pemberton and Garibaldi arcs. In addition the upwelling may have been influenced by the proximity of the Anahim hot-spot (Bevier, 1982).

According to Bevier (1982), the bulk of the Chilcotin basalts are 6 to 10 Ma old with an earlier episode of basaltic volcanism at 19 to 25 Ma and a later episode at 2 to 3 Ma. Samples selected for this study range in age from 2.2 to 18.1 Ma (Table III).

4.1 MAJOR ELEMENT CHEMISTRY

Abundances of major element oxides in Chilcotin Group basalts (Table III) resemble abundances from oceanic WPB (Basaltic Volcanism Study Project, 1981). Total alkalis range from 3.23 to 5.06 wt. %, the highest abundance in sample WOOD LK. P_2O_5 abundances in samples DOG CK, BULL CAN and CAMEL are similar to P_2O_5 abundances in MORB from the Nazca Plate, East Pacific Rise or mid-Indian Ocean Ridge, whereas P_2O_5 abundances in the eight remaining samples are higher, within the range of oceanic WPB (Rhodes et al., 1976; Sun et al., 1979; Mullen, 1983). Mg' numbers range from 40 to 60 and average 53, suggesting the basalts are not primary and have fractionated on their way to the surface.

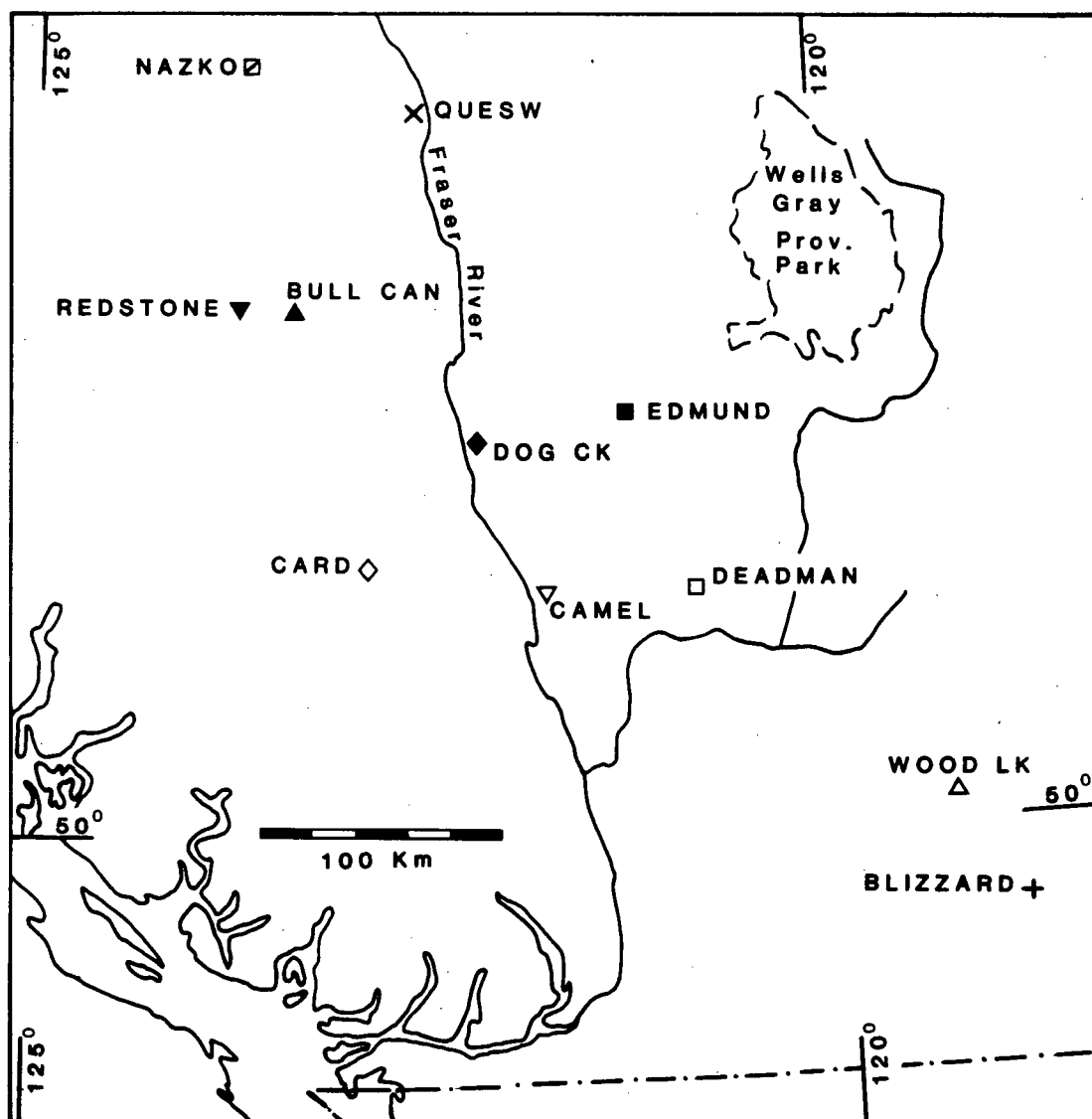


Fig. 4.1. Sample location map for the Chilcotin Basalt Suite. All subsequent diagrams in this chapter use identical symbols.

4.2 DISCRIMINATION DIAGRAMS

4.2.1 MAJOR ELEMENT CLASSIFICATIONS

On total alkalis vs. silica one sample, WOOD LK, is distinctly alkaline and the remainder lie straddling MacDonald's (1968) boundary between alkaline and subalkaline fields (Fig. 4.2). The $Ol'-Ne'-Qz'$ diagram identifies three samples as alkaline (CAMEL, EDMUND and WOOD LK) and the rest as subalkaline (REDSTONE, BULL CAN, NAZKO, QUESW, CARD, DOG CK, DEADMAN and BLIZZARD).

AFM and FeO^*/MgO vs. SiO_2 diagrams show all subalkaline samples from the alkalis vs. silica diagram to be tholeiitic (Figs. 4.3 and 4.4).

On Al_2O_3 vs. normative plagioclase sample BULL CAN is sufficiently aluminous to be classified as calcalkaline.

Petrography of the Chilcotin Basalts, described by Bevier (1982), indicates they contain only one pyroxene, a clinopyroxene. This is characteristic of an alkaline basalt, but normative mineralogy classifies most of them as olivine tholeiites (Yoder and Tilley, 1962; Irvine and Baragar, 1971), therefore, Bevier prefers to call these basalts transitional. In this study all basalts are transitional except WOOD LK which is classified as a nepheline normative alkaline basalt.

On $TiO_2-K_2O-P_2O_5$ three of the ten transitional samples clearly lie within the non-oceanic field, three

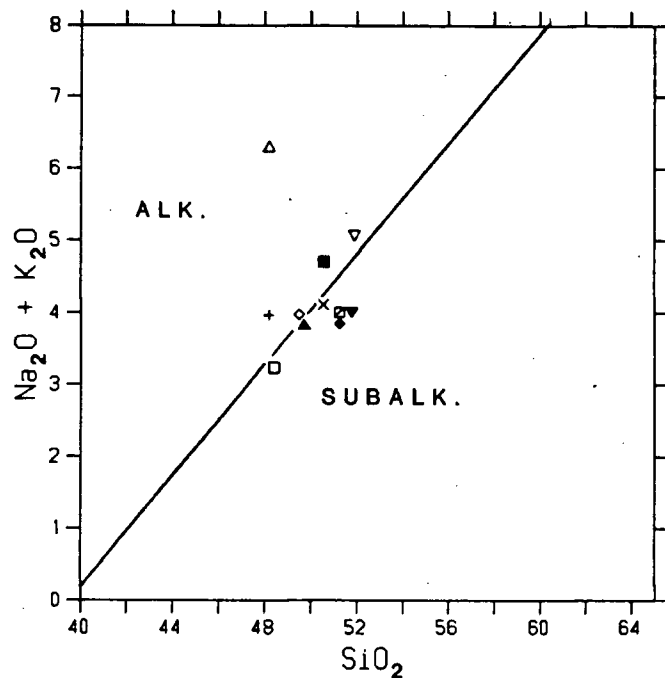


Fig. 4.2. Total alkalis vs. silica. Subalkaline/alkaline boundary from MacDonald (1968).

Fig. 4.3. AFM diagram. Tholeiitic/calcalkaline boundary from Irvine and Baragar (1971).

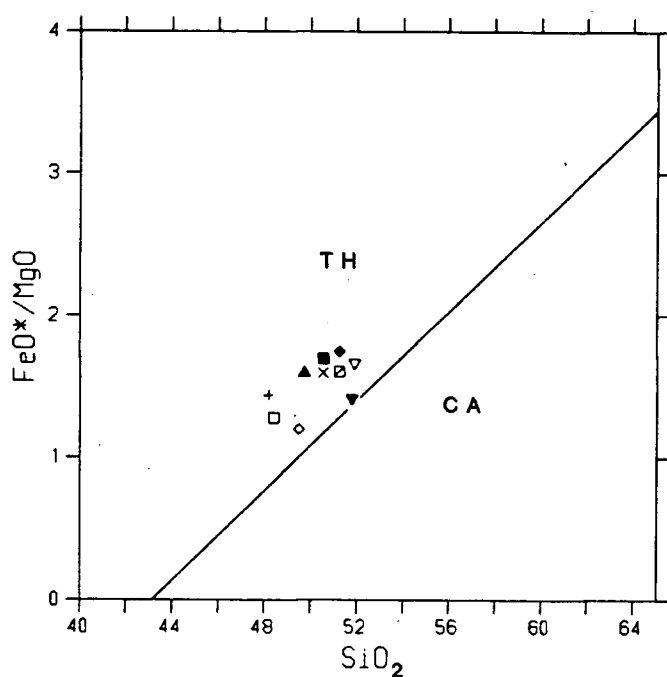
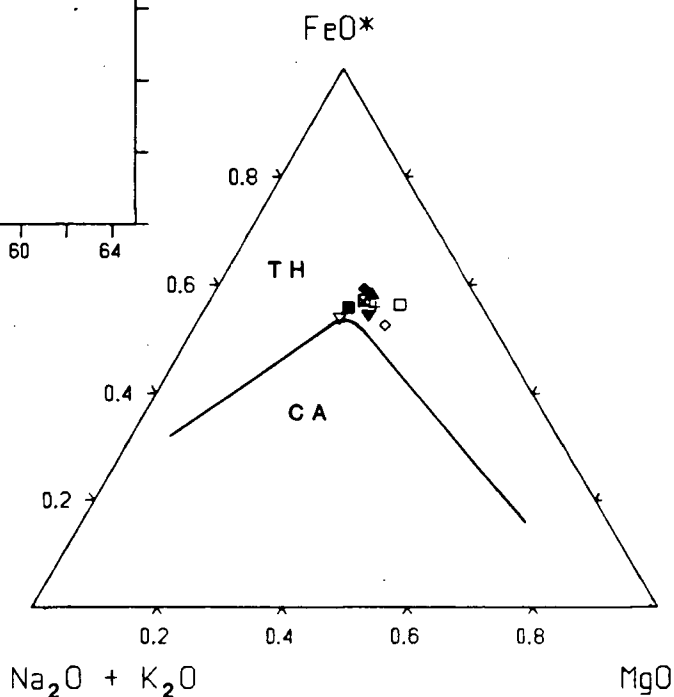


Fig. 4.4. FeO^*/MgO vs. SiO_2 . Tholeiitic/calcalkaline boundary from Miyashiro (1974).

| | |
|------------|------------|
| REDSTONE ▽ | BULL CAN ▲ |
| NAZKO □ | QUESW × |
| CARD ◇ | CAMEL ▽ |
| DOG CK ◆ | EDMUND ■ |
| DEADMAN □ | WOOD LK ▲ |
| BLIZZARD + | |

lie within the oceanic field and the remaining four straddle the boundary line dividing these two fields (Fig. 4.5).

On $\text{MnO-TiO}_2\text{-P}_2\text{O}_5$ samples CARD, QUESW and WOOD LK clearly lie within the OIA field and CAMEL and DOG CK are classified as MORB (Fig. 4.6). BULL CAN lies on the MORB-IAT field boundary and the five remaining samples lie within the OIA field, along the OIA-IAT field boundary.

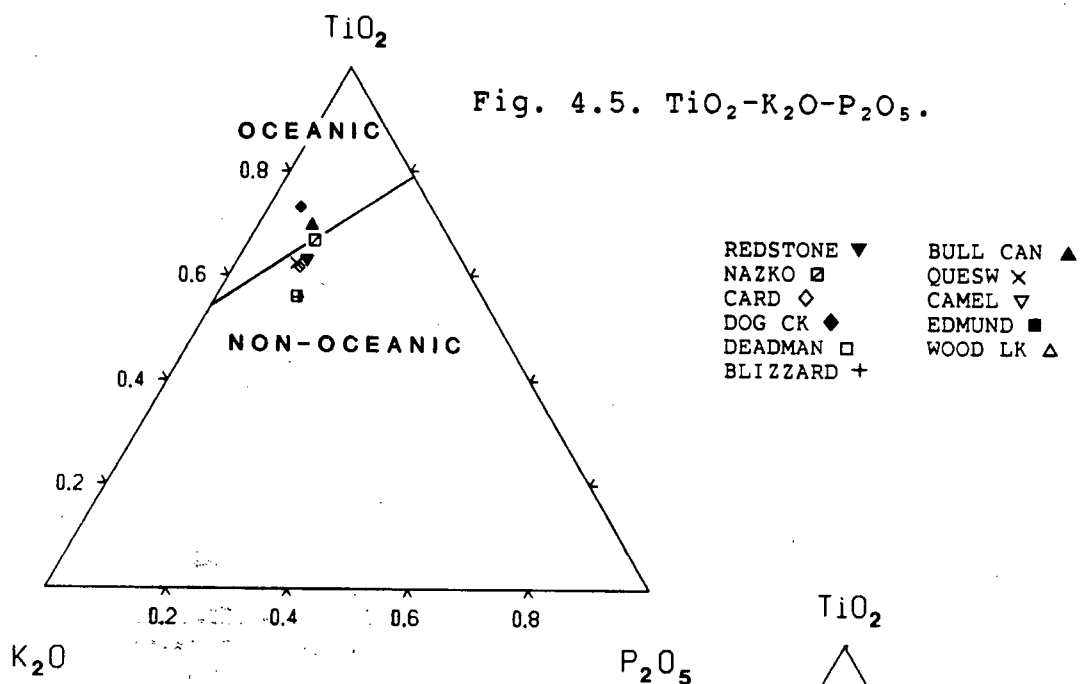
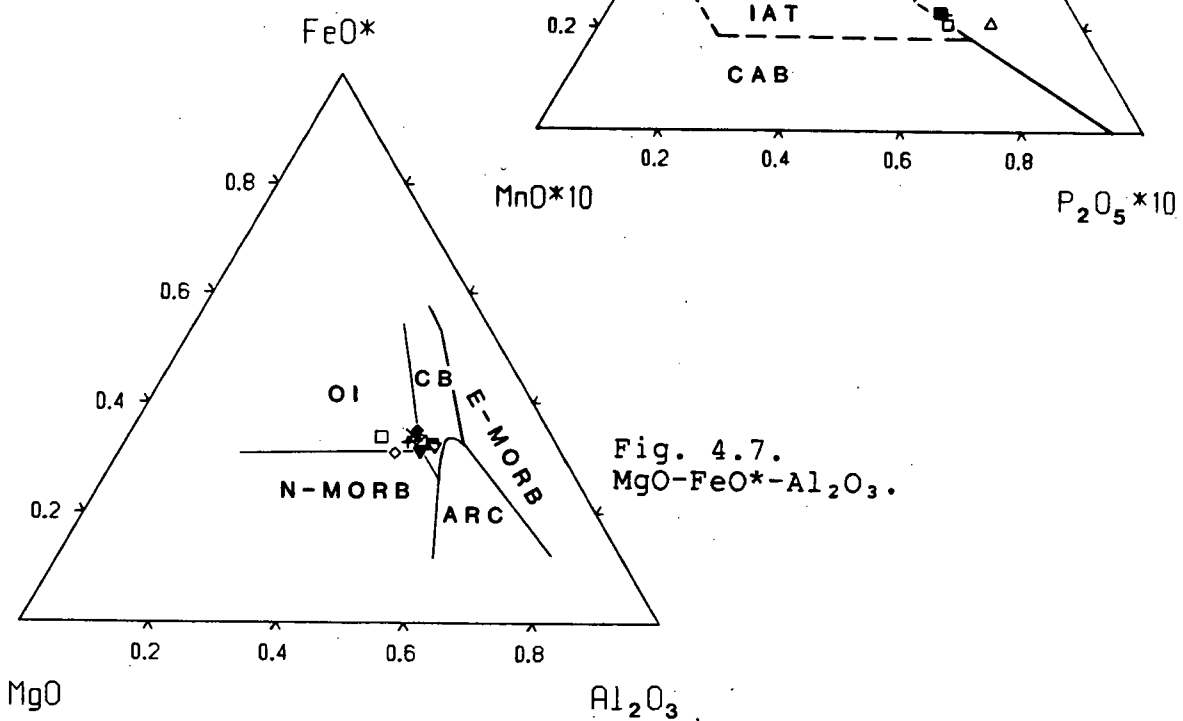
On $\text{FeO}^*\text{-MgO-Al}_2\text{O}_3$ eight transitional samples lie around the triple point between continental, ocean island and N-MORB fields (Fig. 4.7). CARD straddles the boundary separating ocean island and N-MORB and DEADMAN lies within the ocean island field.

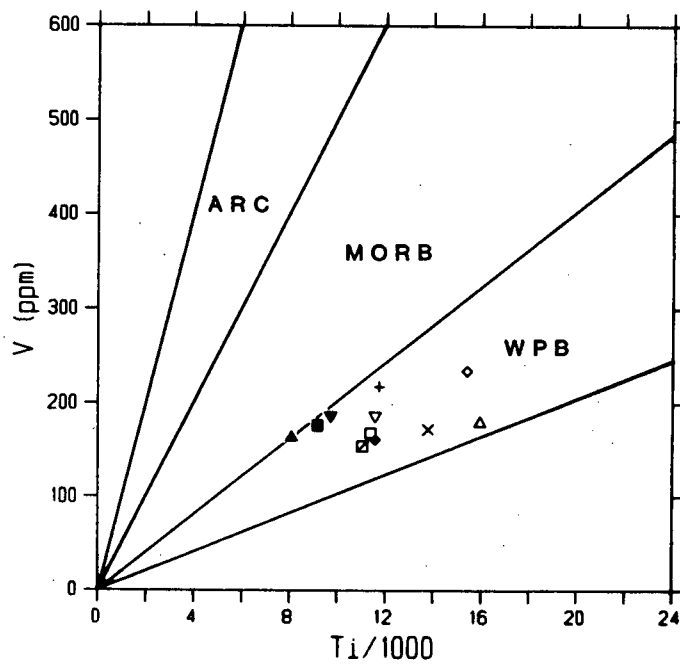
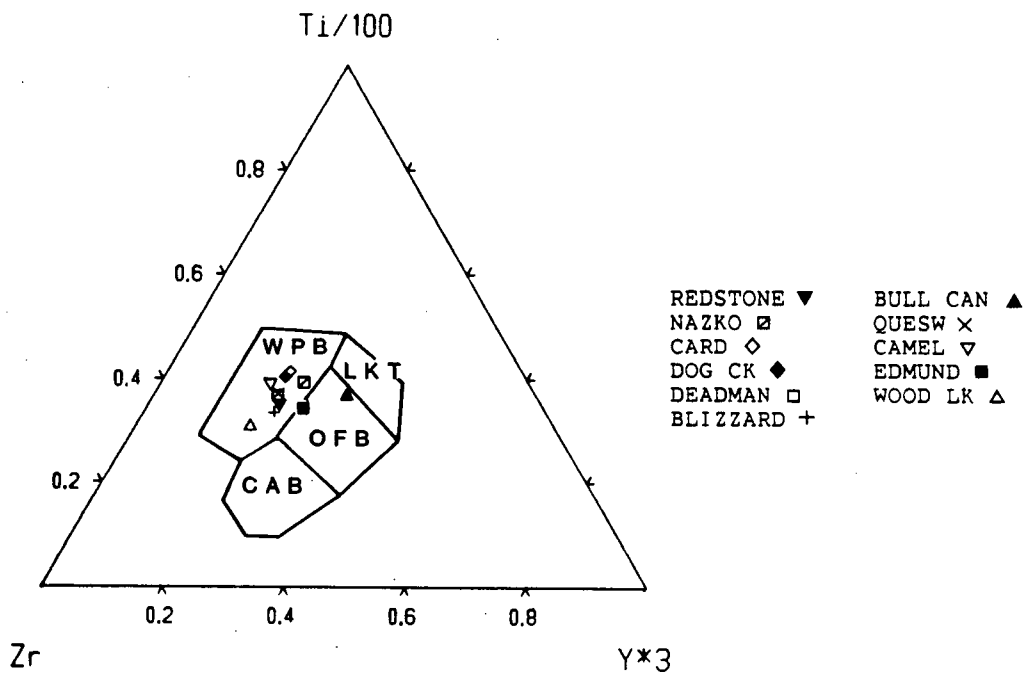
4.2.2 TRACE ELEMENT CLASSIFICATIONS

Except for BULL CAN, all samples lie within or close to the WPB field on Ti-Zr-Y (Fig. 4.8). BULL CAN clearly lies within the field containing OFB, LKT and CAB. On Ti-Zr-Sr it lies within the LKT field (not shown).

On V vs. Ti/1000 all samples have Ti/V ratios between nearly 50 and 100 and lie within the WPB field (Fig. 4.9). REDSTONE, BULL CAN and EDMUND lie close to the boundary between the MORB and WPB fields.

Ten of the eleven samples lie within the WPB field on Ti/Y vs. Nb/Y (Fig. 4.10). Sample BULL CAN has

Fig. 4.6. MnO - TiO_2 - P_2O_5 .Fig. 4.7. MgO - FeO^* - Al_2O_3 .



Figs. 4.8. and 4.9. Ti-Zr-Y (above) and V vs. $Ti/1000$ (below). (below).

slightly lower Ti/Y and Nb/Y ratios and lies just within the field of overlapping MORB and convergent margin basalts.

On Ti/Cr vs. Ni most samples have approximately the same Ti/Cr ratio and lie within the TH MORB field, but BLIZZARD has a slightly lower abundance of Ni and lies just within the IAT field (Fig. 4.11). WOOD LK has a much higher Ti/Cr ratio and lies far from the other samples, adjacent to the IAT-TH MORB field boundary.

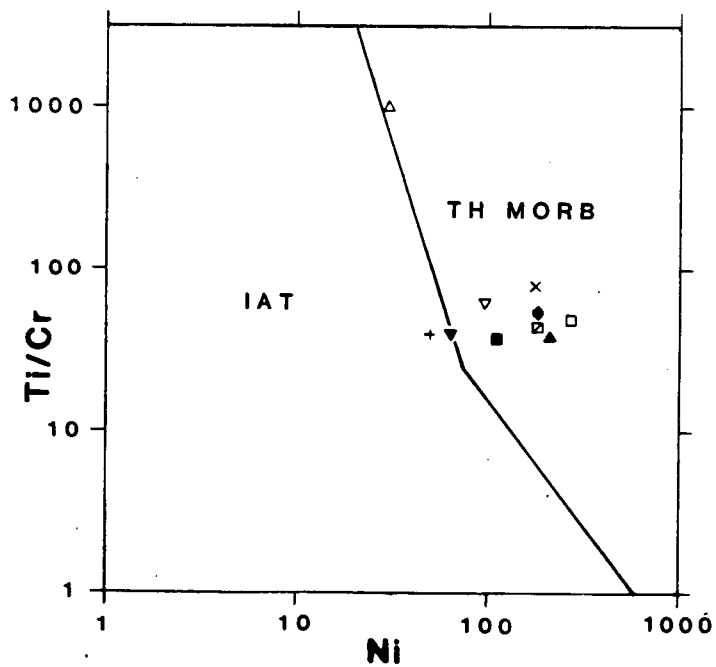
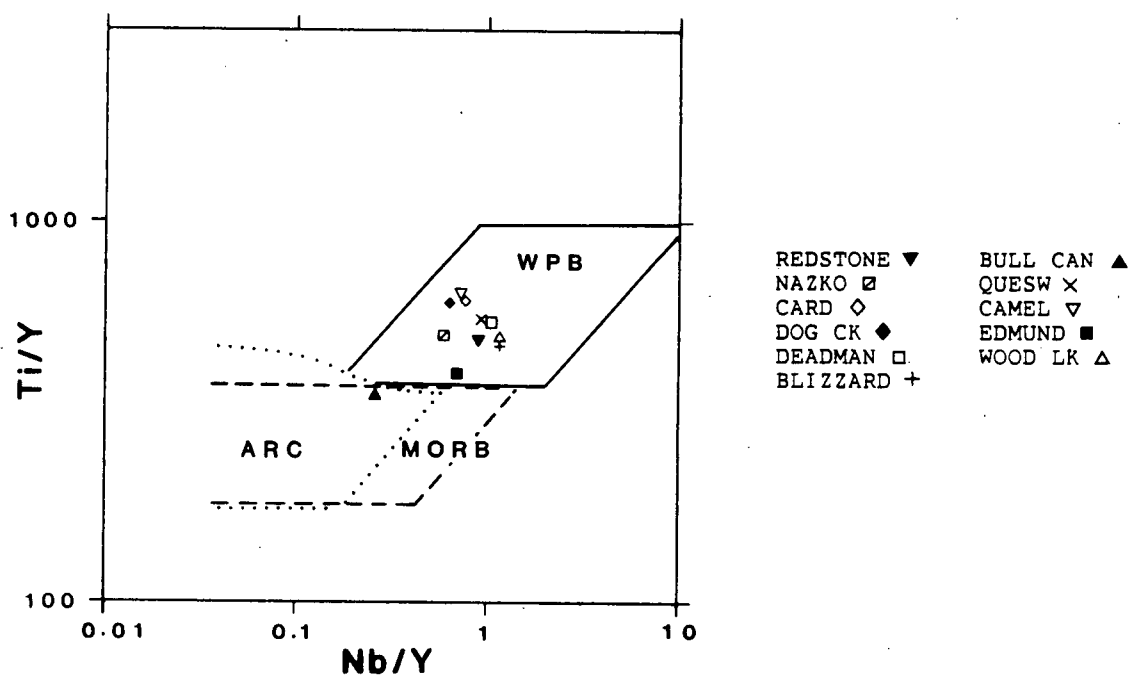
4.2.3 TRACE AND REE CLASSIFICATIONS

Sm/Ce vs. Sr/Ce was not plotted because this diagram does not have a WPB field.

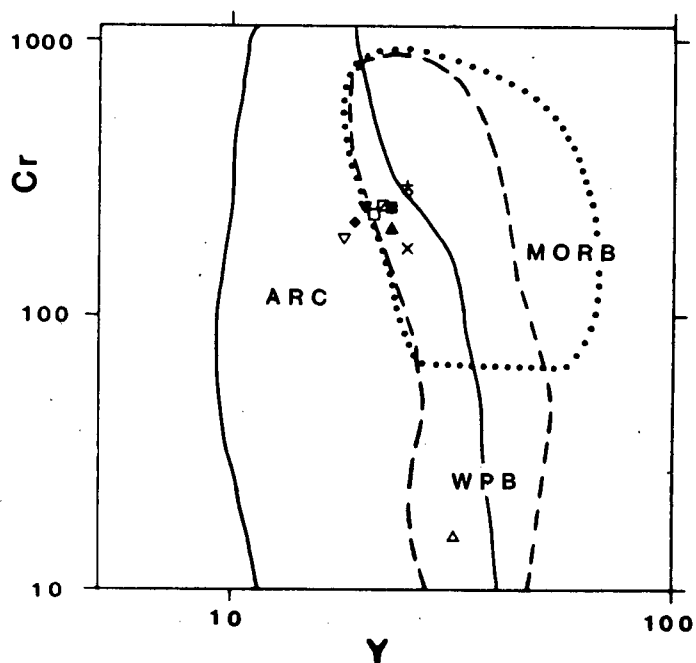
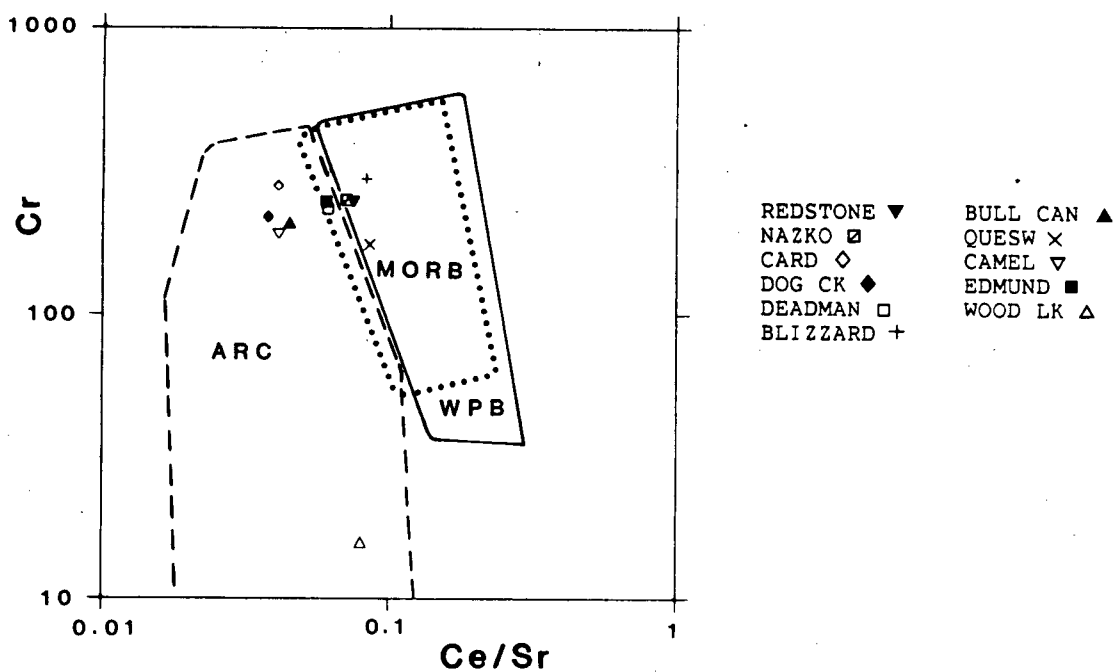
On Cr vs. Ce/Sr ten of the eleven samples lie in a broad band near the top of the diagram (Fig. 4.12). Of these ten, six lie within the overlapping MORB-WPB or ARC-MORB fields and four clearly lie within the convergent margin field. WOOD LK has a much lower Cr content and lies within the convergent margin field, far from the other ten samples.

On Cr vs. Y ten samples lie within or close to the overlapping convergent margin-WPB fields (Fig. 4.13). As on Fig 4.12 WOOD LK lies far from the other ten samples.

On La vs. Ba eight samples have Ba/La ratios greater than 15 and lie within the orogenic andesite field (Fig. 4.14). BLIZZARD lies straddling the boundary between the orogenic andesite and WPB fields, and



Figs. 4.10 and 4.11. Ti/Y vs. Nb/Y (above) and Ti/Cr vs. Ni (below).



Figs. 4.12 and 4.13. Cr vs. Ce/Sr (above) and Cr vs. Y (below).

REDSTONE and WOOD LK lie within the WPB field.

On $(\text{Ba/La})_{\text{CH}}$ vs. $(\text{La/Sm})_{\text{CH}}$ all samples lie within the ocean field (Fig. 4.15). Two of these, CARD and CAMEL, lie within the area which overlaps with the convergent margin field.

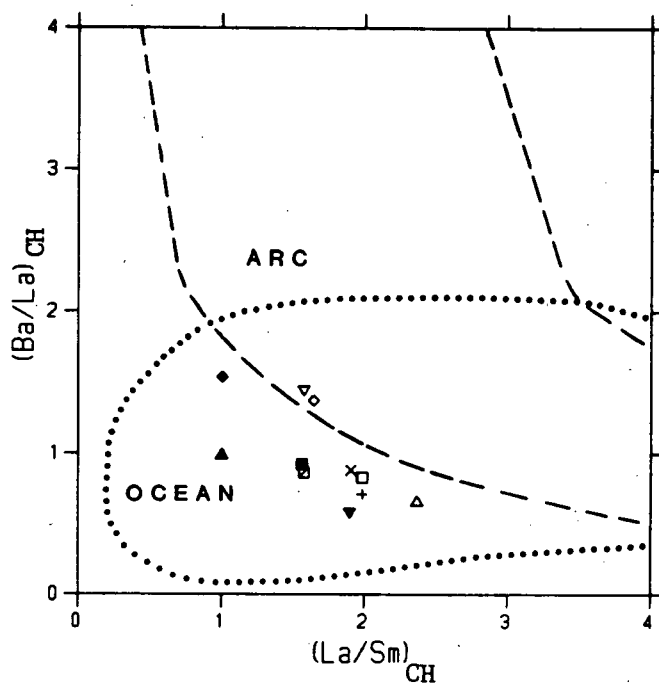
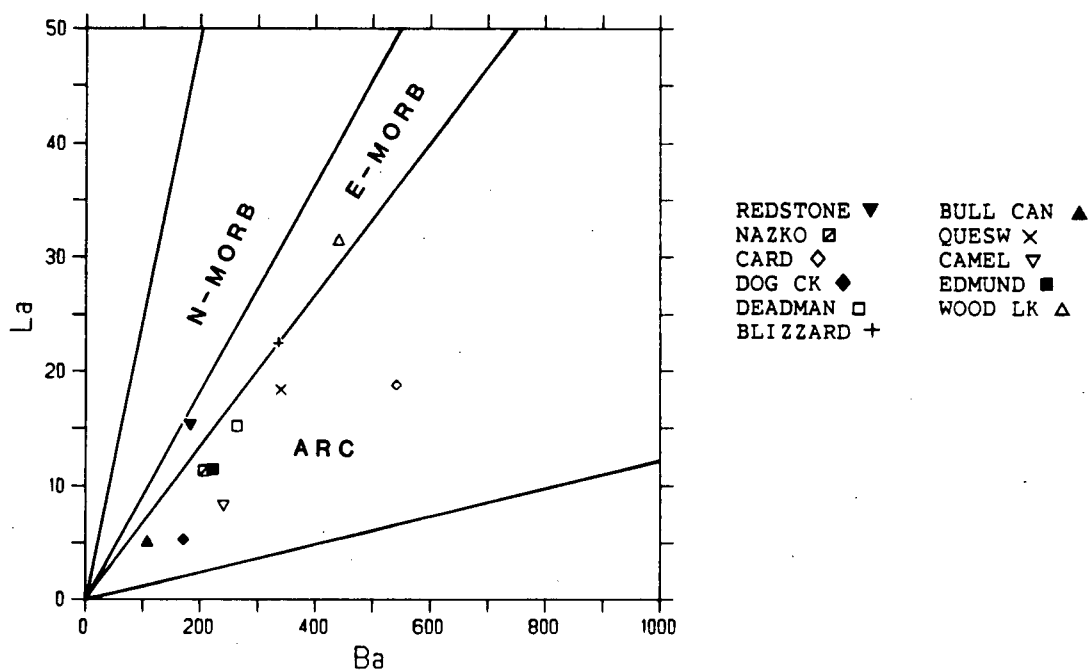
On La vs. Th, WOOD LK lies within the WPB field but the remaining ten samples lie within or close to the orogenic andesite field (Fig. 4.16). However, eight of these ten have La/Th ratios between nearly seven and ten and lie within the overlapping orogenic andesite-WPB fields.

On La vs. Nb ten samples lie within the WPB field, with La/Nb ratios less than 1 (Fig. 4.17). CARD lies astride the N-MORB-WPB field boundary.

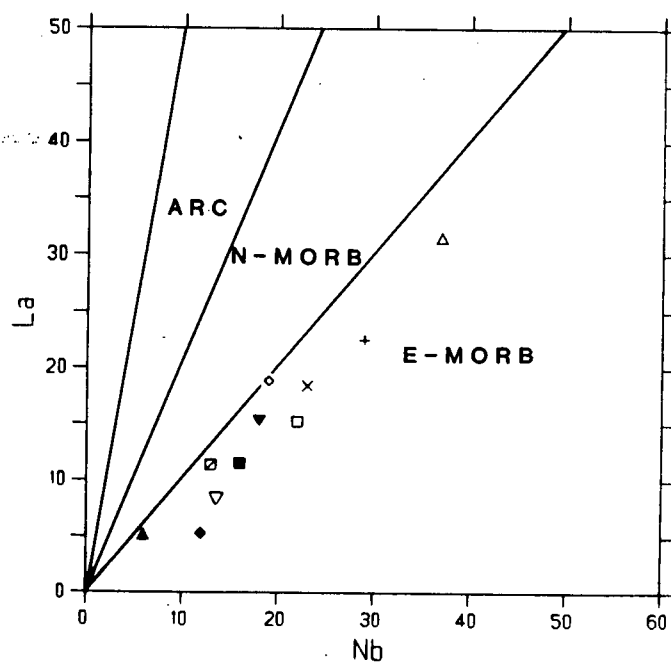
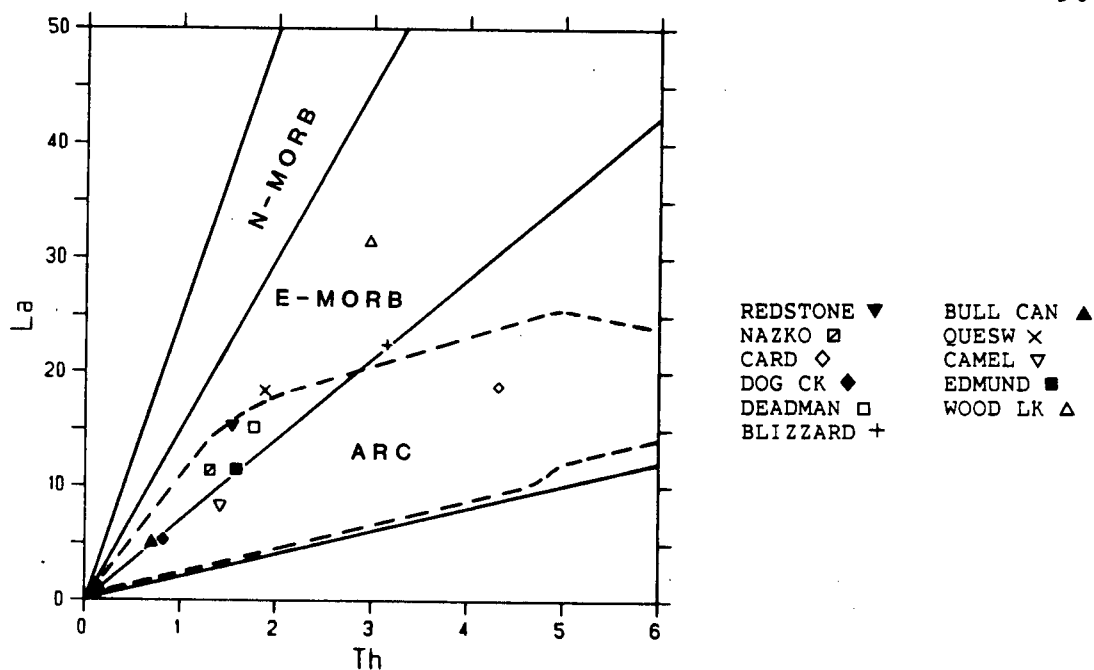
On $\text{K}_2\text{O/Yb}$ vs. Ta^*/Yb most samples lie within or close to the area between the convergent margin and MORB-WPB fields (Fig. 4.18). A few samples lie just within the overlapping MORB-WPB field, along that field's upper boundary line.

All samples except CARD lie within the WPB field on Th/Yb vs. Ta^*/Yb (Fig. 4.19). CARD has a slightly higher Th/Yb ratio and lies on the lower boundary line of the convergent margin field.

On Th-Hf/3-Ta* all samples except CARD lie within the fields for tholeiitic and alkaline WPB (Fig. 4.20). CARD plots away from the other samples, towards Th and lies on the convergent margin field boundary.



Figs. 4.14 and 4.15. La vs. Ba (above) and $(Ba/La)_{CH}$ vs. $(La/Sm)_{CH}$ (below).



Figs. 4.16 and 4.17. La vs. Th (above) and La vs. Nb (below).

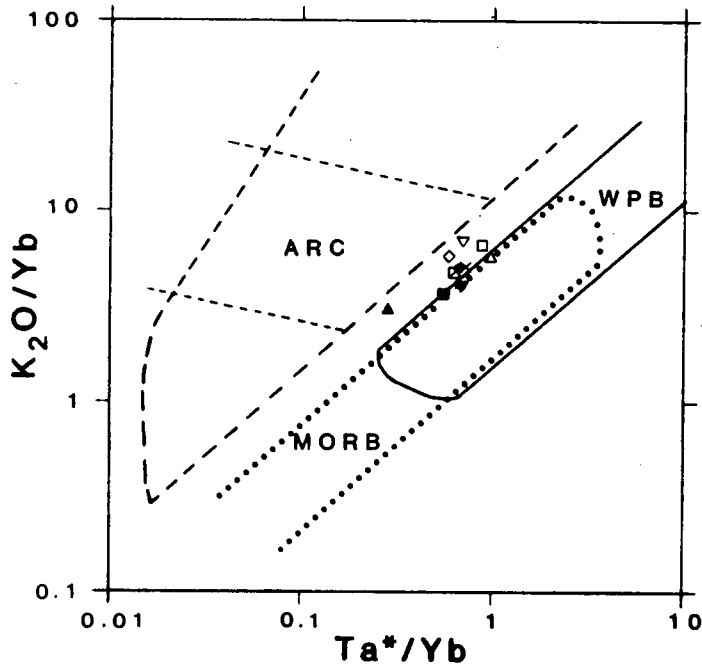
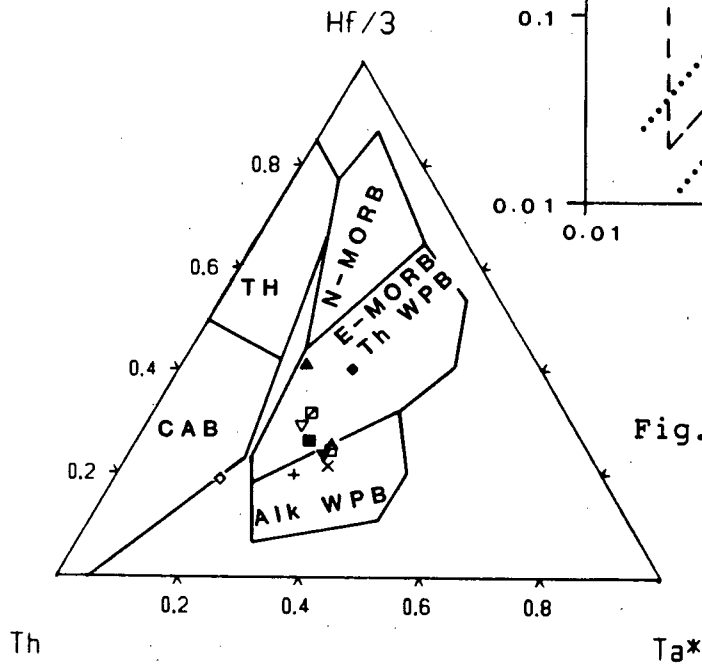
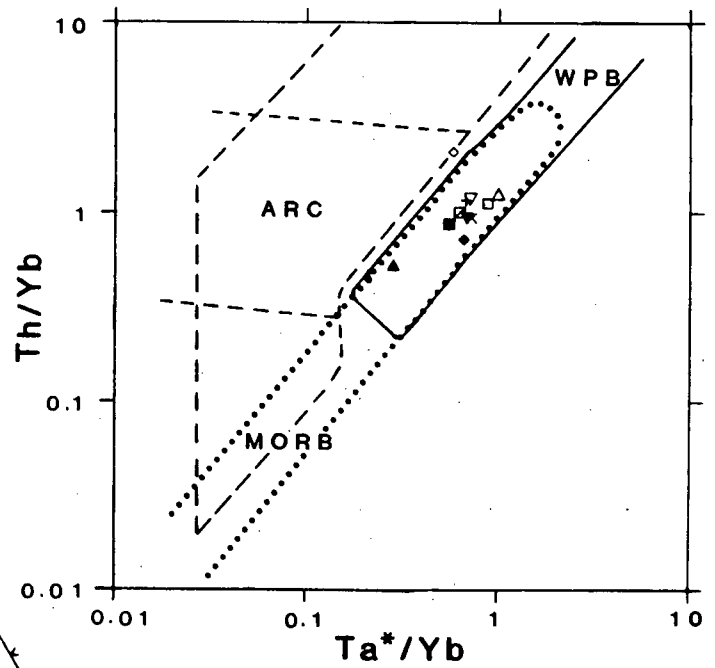


Fig. 4.19. Th/Yb vs. Ta^*/Yb .



4.2.4 BULK EARTH NORMALIZED DIAGRAMS (BEND)

Element data plotted on BEND distinguishes three groups of samples (Figs. 4.21, 4.22 and 4.23).

The BEND patterns on Fig. 4.21 are from alkaline sample WOOD LK, and transitional samples QUESW and BLIZZARD. These patterns have convex-up shapes which peak at Nb or K, and have fairly regular negative slopes from La to Lu, with a concave-up dip from Sm to Eu. WOOD LK has a moderate 'trough' at Nd and QUESW is slightly enriched in Ba relative to Rb. All samples have small positive Eu anomalies.

BEND patterns on Fig. 4.22 are from samples REDSTONE, NAZKO, CAMEL, DOG CK, EDMUND, and DEADMAN. All patterns have convex-up shapes which 'peak' at K (NAZKO, CAMEL, DOG CK, EDMUND and DEADMAN) or Nb (REDSTONE). The patterns are nearly flat from La to Sm, are flat to shallow concave-up from Sm to Eu and have negative slopes from Eu to Lu. All patterns have a small to large 'peak' at Sr (Sr enrichment), but they do not have a corresponding 'peak' at Eu. NAZKO and EDMUND are slightly enriched in Ba relative to Rb and CAMEL is enriched in LIL relative to Zr, Hf, Ti and REE.

BEND patterns on Fig. 4.23 are from samples CARD and BULL CAN. Both patterns show enrichment in Ba relative to Rb, enrichment in Sr (Sr 'peak') and have convex-up 'humps' from Rb to Nb, indicating relative enrichment in Th, U and K. CARD has a 'peak' at Eu but

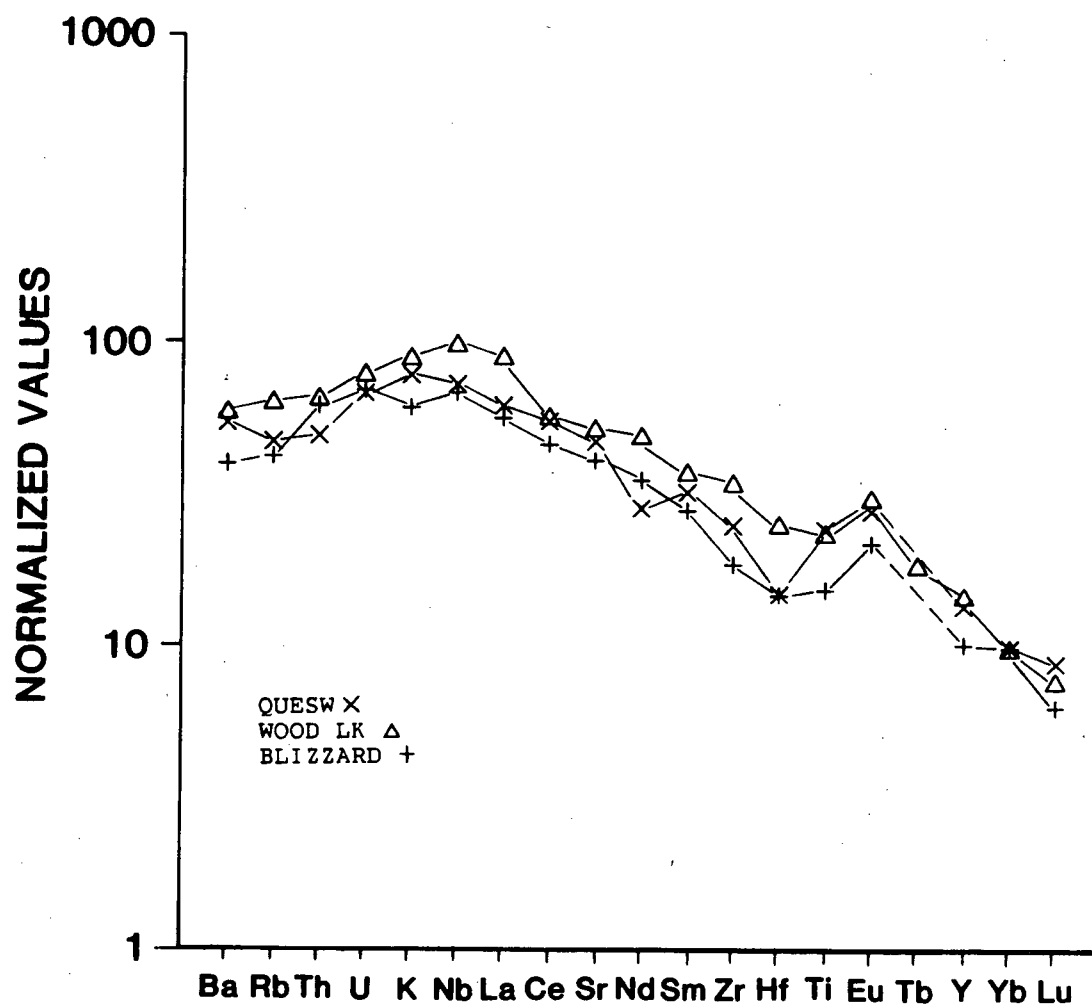


Fig. 4.21. BEN diagram for samples QUESW, WOOD LK and BLIZZARD.

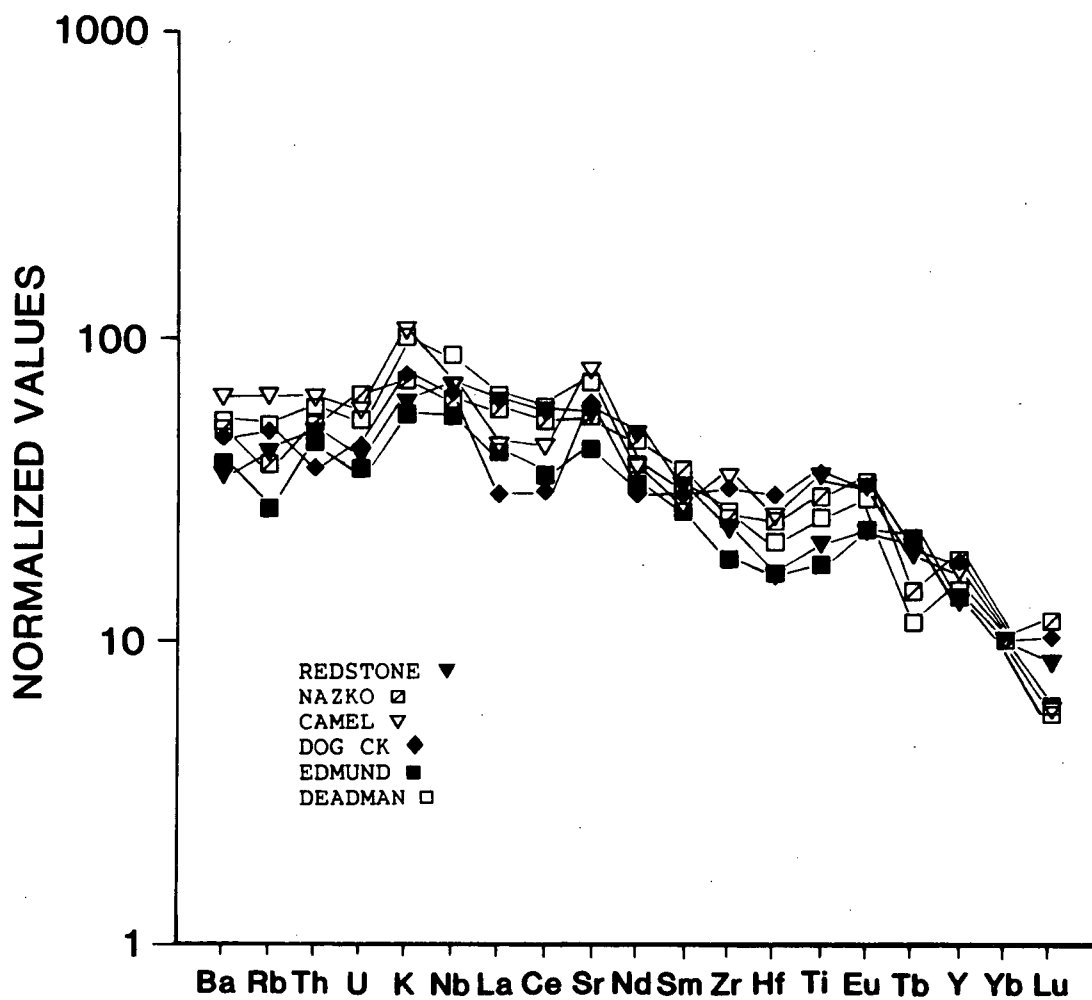


Fig. 4.22. BEN diagram for samples REDSTONE, NAZKO, CAMEL, DOG CK, EDMUND and DEADMAN.

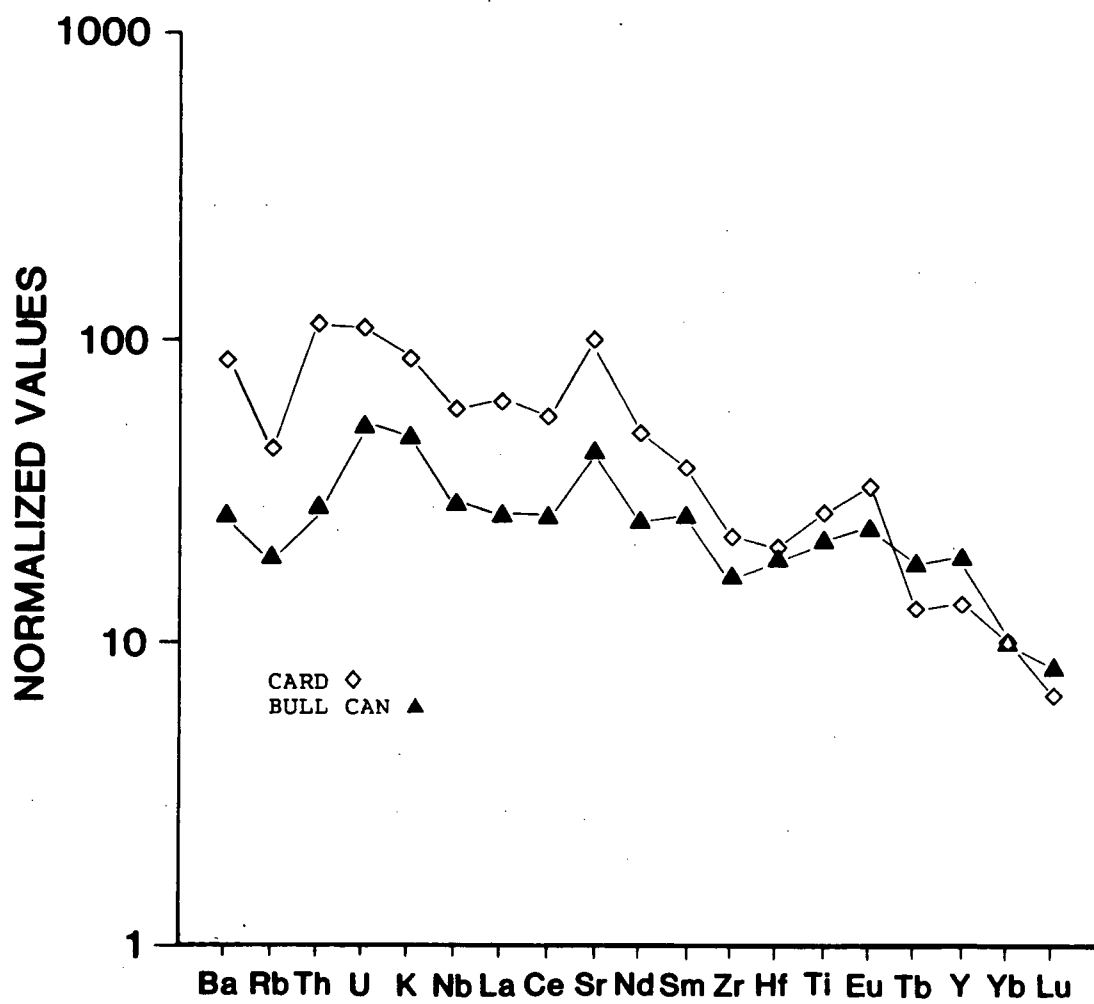


Fig. 4.23. BEN diagram for samples BULL CAN and CARD.

BULL CAN does not. Fig. 4.22.

4.3 TRACE ELEMENT CHEMISTRY

Transitional samples QUESW and BLIZZARD have abundances of trace and REE similar to abundances in an alkaline oceanic WPB and have BEND patterns similar to the pattern from alkaline sample WOOD LK (Fig. 4.21), but major element chemistry and normative mineralogy classifies them as tholeiites. Thus their trace element chemistry is consistent with their transitional nature. The eight remaining transitional samples have lower trace element abundances, similar to a tholeiitic oceanic WPB but relative to a tholeiitic oceanic WPB their LREE abundances are lower (Thompson et al., 1984).

The ten transitional samples have La abundances ranging from 16 to 69 times chondritic, Yb abundances from 5 to 13 times chondritic and $(La/Yb)_{CH}$ ratios between 3.09 and 6.5. Nine of the ten samples have La/Nb ratios ranging from 0.44 to 0.85, resembling La/Nb ratios in oceanic WPB, but CARD has a ratio of 0.99, within the range of either oceanic WPB or convergent margin basalt (Thompson et al., 1983).

In general alkaline sample WOOD LK has the highest abundances of trace and rare earth elements in this suite (CARD has higher abundances of Ba, Th, U and Sr). Its La content is 96 times chondritic, Yb content is 11 times chondritic and $(La/Yb)_{CH}$ ratio is 8.93. La/Nb equals 0.85.

4.3.1 TH AND U

Th abundances range from 0.7 ppm to 1.9 ppm in samples REDSTONE, BULL CAN, NAZKO, QUESW, CAMEL, DOG CK, EDMUND and DEADMAN, and from 3.0 to 4.3 ppm in CARD, WOOD LK and BLIZZARD (Table III). U abundances are less than or equal to 0.5 ppm in the first eight samples listed above, and greater than or equal to 1.1 ppm in the latter three samples. Both Th and U abundances are higher than abundances in an average oceanic WPB but Th/U ratios which range from 1.75 to 3.95 and average 2.9, are similar to ratios in many oceanic WPB (Basaltic Volcanism Study Project, 1981).

4.3.2 TRANSITION ELEMENTS

Abundances of Cr and Ni in most Chilcotin Group lavas range from 175 to 296 ppm and 50 to 271 ppm respectively. As Ni abundance negatively correlates with Mg' number, Bevier (1982) concludes that none of the Chilcotin basalts are primary magmas, but were derived by partial melting of a spinel peridotite with 10 - 15 % of subsequent olivine fractionation. Sample WOOD LK, which has an Mg' number of 40, has the lowest Cr and Ni abundances in this suite (Cr = 15.7 ppm, Ni = 30 ppm). These values presumably indicate loss of olivine which included Cr-spinel.

Sc abundances range from 19.4 to 26.8 ppm and average 23.5 ppm.

4.4 SR ISOTOPES

$^{87}\text{Sr}/^{86}\text{Sr}$ ratios were not available from samples REDSTONE, NAZKO, EDMUND and WOOD LK. Excluding CARD ($^{87}\text{Sr}/^{86}\text{Sr} = 0.7042$), the remaining five samples have Sr isotope ratios between 0.70316 ± 8 and 0.70346 ± 6 (Table III). These ratios are within the range of $^{87}\text{Sr}/^{86}\text{Sr}$ ratios from oceanic WPB (Faure, 1977).

4.5 DISCUSSION OF DISCRIMINATION DIAGRAMS

On $\text{K}_2\text{O}/\text{Yb}$ vs. Ta^*/Yb (Fig. 4.18) all samples lie within or close to the area between convergent margin and MORB-WPB, but on Th/Yb vs. Ta^*/Yb (Fig. 4.19) all samples, excluding CARD lie within the MORB-WPB field. This implies the Chilcotin basalts are slightly enriched in K relative to Nb and suggests interaction with a K-rich metasomatic fluid. K enrichment is also evident from BEND patterns. As well, all samples except REDSTONE and WOOD LK lie within the convergent margin field on La vs. Ba (Fig. 4.14) but on $(\text{Ba}/\text{La})_{\text{CH}}$ vs. $(\text{La}/\text{Sm})_{\text{CH}}$ (Fig. 4.15) these 'convergent margin' samples lie within the ocean(WPB) field. Therefore, although some samples are enriched in Ba relative to Rb (metasomatism?, analytical error?) Ba enrichment relative to La is not great enough to affect the $(\text{Ba}/\text{La})_{\text{CH}}$ vs. $(\text{La}/\text{Sm})_{\text{CH}}$ diagram.

Samples CAMEL, BULL CAN and DOG CK are classified as oceanic or MORB on $\text{TiO}_2\text{-K}_2\text{O-P}_2\text{O}_5$ (Fig. 4.5) and $\text{MnO-TiO}_2\text{-P}_2\text{O}_5$ (Fig. 4.6), and as convergent margin basalts

on Cr vs. Ce/Sr (Fig. 4.12). These classifications reflect their relative depletion in P_2O_5 and enrichment in Sr.

Enrichment in Sr suggests either:

- metasomatism,
- plagioclase accumulation,
- low pressure fractionation of phases other than plagioclase (eg. olivine, pyroxene), or
- interaction with continental crust (contamination).

Lack of positive Eu anomalies and 'average' WPB Sr isotope ratios support neither of these latter two suggestions.

BULL CAN also lies within or close to the MORB field on many of the other diagrams because of its low elemental abundances. This suggests a depleted source region, perhaps depleted during a previous melting event.

Both CAMEL and DOG CK lie within the convergent margin field on Cr vs. Y (Fig. 4.13) because of their depletion in Y relative to the rest of the sample suite. This suggests a garnet rich source residuum. W.H. Mathews (oral comm., 1985) thinks these two samples are likely to have had a common source, at or north of DOG CK.

CARD also lies within the convergent margin field on $(Ba/La)_{CH}$ vs. $(La/Sm)_{CH}$ and La vs. Th, as well as on Cr vs. Ce/Sr (Fig. 4.12), and lies astride the convergent margin field boundary on La vs. Nb (Fig. 4.17), Th/Yb vs. Ta*/Yb (Fig. 4.19) and Th-Hf/3-Ta* (Fig. 4.20). The convergent margin classification is caused by this samples relative enrichment in Ba, Th, K and Sr and slight depletion in Nb.

CARD, the most 'orogenic', is nearest to the coeval Pemberton arc and may have inherited an LIL rich component from the subducting slab. In recent years slab components in back-arc basins and even ocean islands have been suggested by McKenzie and O'Nions (1983), Cohen and O'Nions (1982) and Thompson et al. (1983, 1984). Additional evidence arguing for a slab component in CARD is suggested by its relatively high $^{87}\text{Sr}/^{86}\text{Sr}$ ratio of 0.7042. Alternatively these characteristics may be caused by crustal contamination (Dupuy and Dostal, 1984).

4.6 SUMMARY

The Chilcotin Group basalt samples have tholeiitic/transitional chemistry, except sample WOOD LK which is classified as a nepheline normative alkaline basalt. Major, trace and rare earth element abundances are generally similar to abundances in a tholeiitic oceanic WPB, and on most tectonic discrimination diagrams these samples lie within the WPB field. Some of the diagrams imply an enrichment in Ba, K \pm Sr and Th, suggesting interaction with an alkali rich metasomatic fluid. BULL CAN comes from a depleted source with some of the chemical characteristics of a MORB.

Excluding CARD, Sr isotope ratios imply no interaction with the continental crust. CARD has both an Sr isotope ratio and some geochemical characteristics of either;

- crustally contaminated WPB, or

- the presence of a subduction - related component.

TABLE III. Chilcotin Basalts

Major, trace and rare earth element abundances, Sr isotope ratios and K/Ar dates.

| | REDSTONE | BULL CAN | NAZKO | QUESW | CARD | CAMEL | DOG CK | EDMUND | DEADMAN | WOOD LK | BLIZZARD |
|------------------------------------|-------------------|-------------------|-------------------|------------------|-------------------|------------------|-------------------|------------------|-------------------|--------------------|------------------|
| Series Name | Thol/Trans Basalt | Thol/Trans Basalt | Thol/Trans Basalt | Alk/Trans Basalt | Thol/Trans Basalt | Alk/Trans Basalt | Thol/Trans Basalt | Alk/Trans Basalt | Thol/Trans Basalt | Alkaline Hawaiiite | Alk/Trans Basalt |
| LAT. | 52 07.2 | 52 05.5 | 53 03.67 | 52 56.6 | 51 05.47 | 50 58.2 | 51 35.0 | 51 36.8 | 50 58.0 | 50 03.6 | 49 37.5 |
| LONG. | 123 40.0 | 123 23.3 | 123 34.67 | 122 33.5 | 122 57.53 | 121 55.4 | 122 15.0 | 121 22.7 | 120 58.0 | 119 21.0 | 118 55.0 |
| SiO ₂ | 51.77 | 49.71 | 51.24 | 50.54 | 49.50 | 51.89 | 51.25 | 50.55 | 48.41 | 48.19 | 48.19 |
| TiO ₂ | 1.62 | 1.35 | 1.84 | 2.30 | 2.57 | 1.93 | 1.93 | 1.53 | 1.90 | 2.66 | 1.96 |
| Al ₂ O ₃ | 15.08 | 15.58 | 15.07 | 14.44 | 14.84 | 15.25 | 14.69 | 15.64 | 14.62 | 16.01 | 15.31 |
| Fe ₂ O ₃ | 11.02 | 13.20 | 12.12 | 12.43 | 11.84 | 11.04 | 12.82 | 11.78 | 13.84 | 13.65 | 12.70 |
| FeO | 0.0 | 0.0 | 0.0 | 0.0 | 0.0 | 0.0 | 0.0 | 0.0 | 0.0 | 0.0 | 0.0 |
| MnO | 0.15 | 0.17 | 0.16 | 0.17 | 0.14 | 0.14 | 0.16 | 0.16 | 0.18 | 0.18 | 0.18 |
| MgO | 7.10 | 7.42 | 6.82 | 7.04 | 8.95 | 6.02 | 6.70 | 6.28 | 9.81 | 4.60 | 7.99 |
| CaO | 8.96 | 8.56 | 8.46 | 8.59 | 7.72 | 8.51 | 8.47 | 8.95 | 7.54 | 7.60 | 9.21 |
| Na ₂ O | 3.34 | 3.42 | 3.38 | 3.09 | 2.82 | 4.25 | 3.27 | 4.03 | 2.19 | 4.93 | 2.89 |
| K ₂ O | 0.66 | 0.41 | 0.62 | 1.02 | 1.15 | 0.81 | 0.57 | 0.67 | 1.04 | 1.38 | 1.07 |
| P ₂ O ₅ | 0.30 | 0.17 | 0.30 | 0.37 | 0.46 | 0.15 | 0.14 | 0.42 | 0.45 | 0.80 | 0.48 |
| H ₂ O | N/A | N/A | N/A | 0.55 | N/A | N/A | N/A | N/A | N/A | N/A | N/A |
| Ba | 183.0 | 108.0 | 206.0 | 340.0 | 541.0 | 235.0 | 170.0 | 222.0 | 264.0 | 440.0 | 336.0 |
| Rb | 11.0 | 4.0 | 8.0 | 15.0 | 14.0 | 12.0 | 9.0 | 8.0 | 13.0 | 24.0 | 18.0 |
| Th | 1.5 | 0.7 | 1.3 | 1.9 | 4.3 | 1.4 | 0.8 | 1.6 | 1.8 | 3.0 | 3.1 |
| U | 0.4 | 0.4 | 0.5 | 0.8 | 1.3 | 0.4 | 0.3 | 0.4 | 0.5 | 1.1 | 1.1 |
| Nb | 18.0 | 6.0 | 13.0 | 23.0 | 19.0 | 13.0 | 12.0 | 16.0 | 22.0 | 37.0 | 29.0 |
| La | 15.2 | 5.2 | 11.3 | 18.4 | 18.8 | 7.8 | 5.3 | 11.4 | 15.2 | 31.6 | 22.5 |
| Ce | 37.1 | 13.4 | 27.3 | 43.2 | 44.3 | 20.2 | 14.1 | 25.3 | 36.7 | 53.2 | 48.8 |
| Sr | 496.0 | 300.0 | 387.0 | 508.0 | 1086.0 | 491.0 | 375.0 | 421.0 | 601.0 | 664.0 | 589.0 |
| Nd | 22.8 | 9.5 | 17.2 | 16.4 | 28.6 | 12.6 | 10.1 | 17.2 | 17.3 | 33.6 | 27.2 |
| Sm | 5.0 | 3.2 | 4.4 | 6.0 | 7.1 | 3.1 | 3.2 | 4.5 | 4.7 | 8.2 | 7.0 |
| Zr | 120.0 | 68.0 | 104.0 | 157.0 | 142.0 | 127.0 | 114.0 | 106.0 | 132.0 | 256.0 | 157.0 |
| Hf | 2.4 | 2.3 | 3.0 | 2.7 | 3.8 | 2.8 | 3.2 | 2.8 | 3.1 | 5.5 | 3.6 |
| Eu | 1.3 | 1.1 | 1.5 | 1.9 | 2.2 | 1.3 | 1.2 | 1.4 | 1.6 | 2.5 | 2.0 |
| Tb | 0.7 | 0.5 | 0.4 | N/A | 0.6 | 0.5 | 0.5 | 0.9 | 0.4 | 1.0 | N/A |
| Y | 20.0 | 23.0 | 22.0 | 25.0 | 25.0 | 18.0 | 19.0 | 23.0 | 21.0 | 32.0 | 25.0 |
| Yb | 1.6 | 1.3 | 1.3 | 2.0 | 2.1 | 1.2 | 1.1 | 1.8 | 1.6 | 2.4 | 2.7 |
| Lu | 0.2 | 0.2 | 0.2 | 0.3 | 0.2 | 0.1 | 0.2 | 0.2 | 0.1 | 0.3 | 0.3 |
| Co | 60.0 | 50.0 | 56.0 | 45.0 | 51.0 | 41.0 | 48.0 | 49.0 | 61.0 | 45.0 | 40.0 |
| Cr | 245.9 | 207.8 | 250.0 | 175.4 | 279.9 | 189.6 | 217.9 | 245.9 | 232.8 | 15.7 | 296.3 |
| Cu | 61.0 | 59.0 | 101.0 | 77.0 | 170.0 | 26.0 | 43.0 | 35.0 | 69.0 | 30.0 | 38.0 |
| Ni | 64.0 | 211.0 | 181.0 | 176.0 | 182.0 | 96.0 | 183.0 | 111.0 | 271.0 | 30.0 | 50.0 |
| Sc | 20.6 | 23.0 | 22.3 | 21.2 | 21.1 | 22.4 | 22.1 | 24.4 | 18.2 | 17.9 | 24.7 |
| V | 185.0 | 165.0 | 154.0 | 172.0 | 234.0 | 185.0 | 161.0 | 176.0 | 168.0 | 181.0 | 217.0 |
| ⁸⁷ Sr/ ⁸⁶ Sr | N/A | 0.70346 | N/A | 0.7034 | 0.7042 | 0.70320 | 0.70316 | N/A | 0.70316 | N/A | 0.7033 |
| K/Rb | 498.06 | 850.85 | 643.33 | 564.47 | 681.87 | 560.32 | 525.73 | 695.21 | 664.08 | 477.31 | 493.45 |
| (La/Yb) _{CH} | 6.23 | 2.62 | 5.85 | 6.17 | 6.12 | 12.29 | 3.09 | 4.24 | 6.48 | 8.93 | 5.61 |
| La/Nb | 0.85 | 0.86 | 0.87 | 0.80 | 0.99 | 1.65 | 0.44 | 0.71 | 0.69 | 0.85 | 0.78 |
| Mg' | 56 | 53 | 53 | 53 | 60 | 52 | 51 | 51 | 58 | 40 | 55 |
| K/Ar date (Ma) | N/A | 6.1 ± 0.2 | 6.3 ± 0.3 | 8.7 ± 0.6 | 18.1 ± 0.6 | 2.2 ± 0.3 | 2.9 ± 0.2 | 7.8 ± 0.3 | 8.2 ± 0.3 | 14.8 ± 1.5 | 5.0 ± 0.5 |

N/A = not analyzed

5. ANAHIM VOLCANIC BELT

Nine samples from the Anahim Volcanic Belt west of the Fraser River were selected for analysis (Fig. 5.1). Two of these nine are from the Masset Formation on the Queen Charlotte Islands to determine if they are chemically similar to basalts from the Anahim Belt in central British Columbia because Bevier et al. (1979) suggest the Masset volcanics may form the western end of the Anahim hotspot trace. An additional five samples from volcanic centers east of the Fraser River were included in this suite, as these locations are often placed on figures which define the Anahim Belt (Bevier, 1978). However, recent work by C. Hickson (oral comm., 1984) suggests eruptions from the Anahim hotspot source end in the vicinity of the Nazko Cones, west of Quesnel, and J.E. Souther (in press) speculates that a second hotspot trace forms this eastward continuation.

Samples from this suite range in age from 23.8 Ma to 0.28 Ma (Table IV). The oldest dates are from the Masset Formation and the youngest age is from a sample located in Wells Gray Park.

5.1 MAJOR ELEMENT CHEMISTRY

Major element oxide abundances (Table IV) generally lie within the range of major element abundances in oceanic tholeiitic and alkaline WPB (Basaltic Volcanism Study Project, 1981; Carmichael et al., 1974). Mg' numbers divide

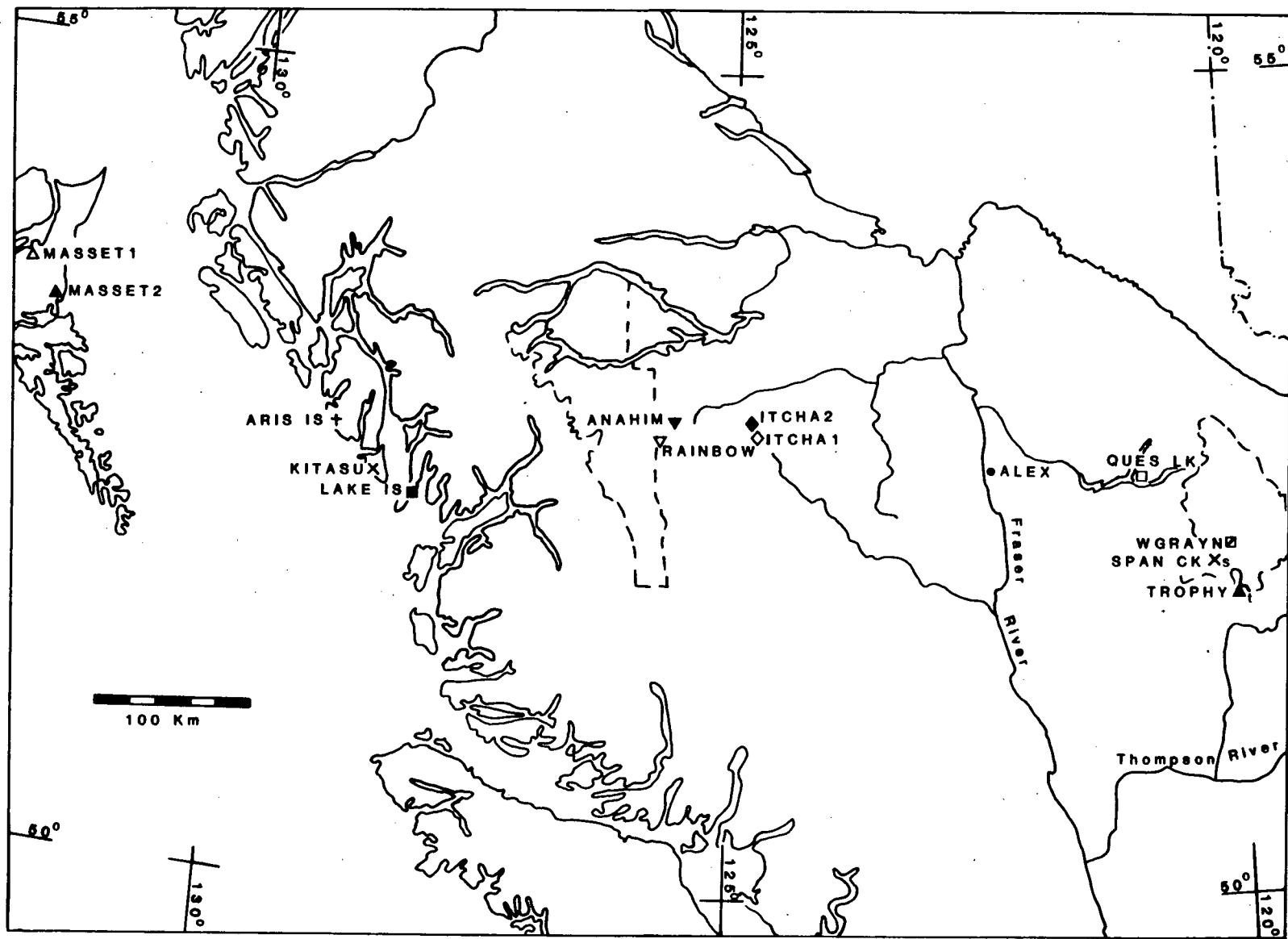


Fig 5.1. Sample location map for the Anahim Volcanic Belt. All subsequent diagrams in this chapter use identical symbols.

the samples into two groups. The nine samples west of the Fraser River plus ALEX have Mg' numbers between 30 and 56, whereas the four remaining samples, in and near Wells Gray Park, have Mg' numbers between 56 and 62. Thus, these latter four samples are less fractionated (more primitive).

5.2 DISCRIMINATION DIAGRAMS

5.2.1 MAJOR ELEMENT CLASSIFICATIONS

On the total alkalis vs. silica diagram eight of the fourteen samples clearly lie within the alkaline field, five plot astride MacDonalds (1968) subalkaline/alkaline field boundary and one (ALEX) is clearly subalkaline (Fig. 5.2). *Ol'-Ne'-Qz'* (not shown) classifies nine samples as alkaline (ARIS IS, KITASU, LAKE IS, RAINBOW, ANAHIM, ITCHA1, ITCHA2, SPAN CK and TROPHY) and the remaining five as subalkaline. A petrographic study of TROPHY by Fiesinger (1975) suggests it should be classified as transitional.

On AFM and FeO^*/MgO vs. SiO_2 diagrams, subalkaline and transitional basaltic samples lie within the tholeiitic fields (Figs. 5.3 and 5.4).

Al_2O_3 vs. normative plagioclase (not shown) confirms the AFM discrimination except for samples MASSET1 and MASSET2 which were sufficiently aluminous to be classified as calcalkaline.

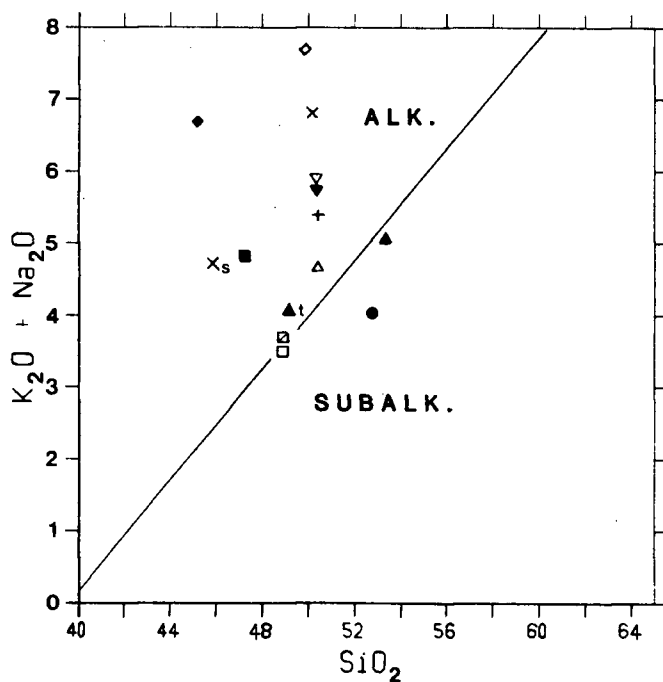


Fig. 5.2. Total alkalis vs. silica. Subalkaline/alkaline boundary from MacDonald (1968).

Fig. 5.3. AFM diagram. Tholeiitic/calcalkaline boundary from Irvine and Baragar (1971).

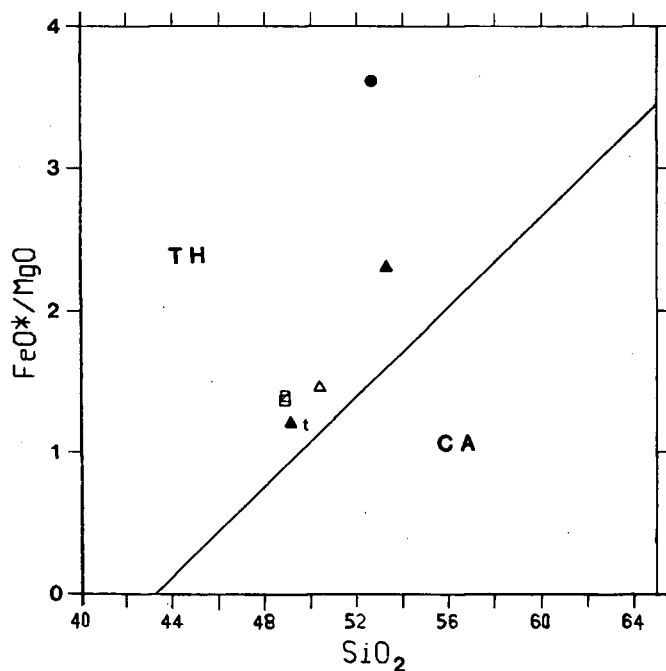
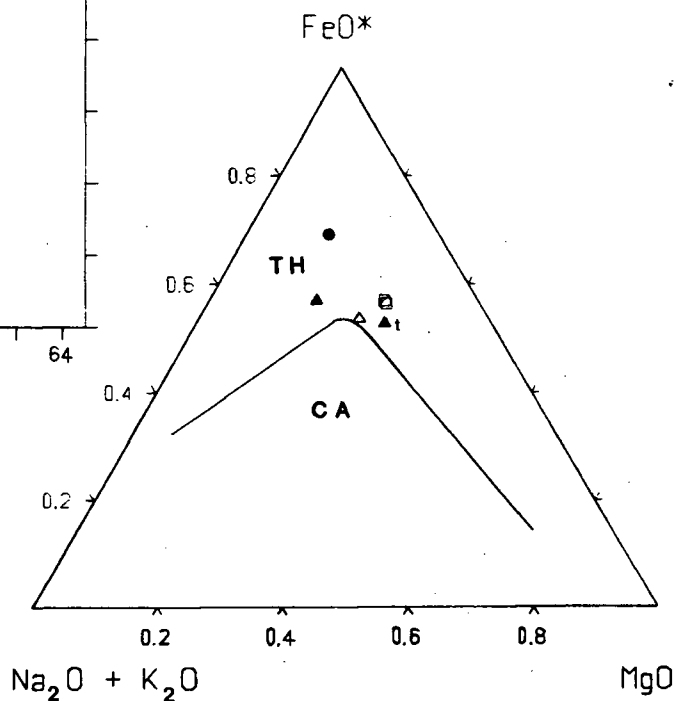


Fig. 5.4. FeO^*/MgO vs. SiO_2 . Tholeiitic/calcalkaline boundary from Miyashiro (1974).

| | |
|-----------------------------|---------------------------|
| MASSET1 Δ | MASSET2 Δ |
| ARIS IS $+$ | KITASU \times |
| LAKE IS \blacksquare | RAINBOW ∇ |
| ANAHIM \blacktriangledown | ITCHA1 \diamond |
| ITCHA2 \blacklozenge | ALEX \bullet |
| QUES LK \square | WGRAYN \boxplus |
| SPAN CK \times_s | TROPHY \blacktriangle_t |

Because $\text{TiO}_2\text{-K}_2\text{O-P}_2\text{O}_5$ can only be used for subalkaline samples with total alkalis less than or equal to 20% on an AFM diagram samples MASSET1 and MASSET2 were excluded. The four remaining samples lie close to the boundary line between the oceanic and non-oceanic fields (Fig. 5.5). ALEX and WGRAYN lie within the oceanic field, TROPHY lies within the non-oceanic field and QUES LK lies on the boundary line.

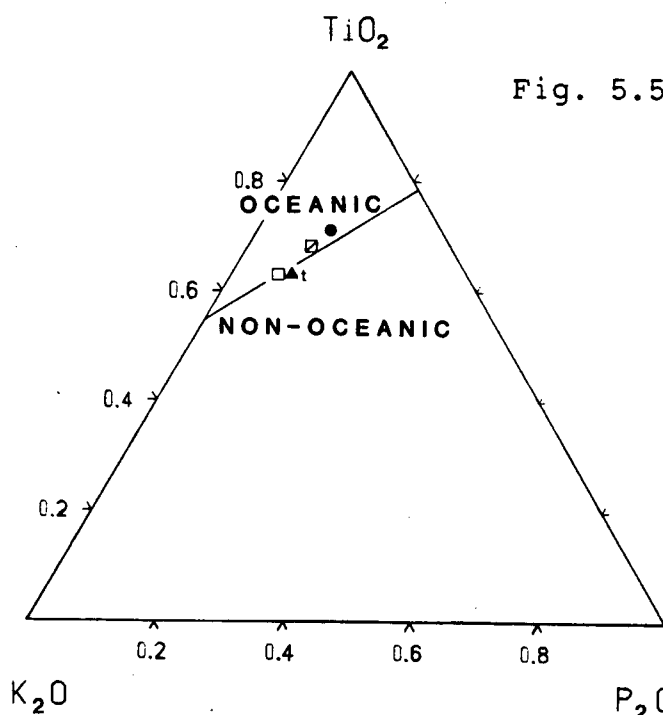
Most samples plotted on $\text{MnO-TiO}_2\text{-P}_2\text{O}_5$ lie within the OIA field (Fig. 5.6). Exceptions are:

- ANAHIM which lies within the OIT field.
- QUES LK which lies within the MORB field.
- TROPHY which lies on the boundary line between the MORB and IAT fields, and
- MASSET1 which lies on the boundary between the IAT and CAB fields.

On $\text{MgO-FeO}^*\text{-Al}_2\text{O}_3$, four subalkaline and transitional samples straddle the boundary between the ocean island (OI) and MORB fields, MASSET2 lies within the orogenic (ARC) field and ALEX lies at the approximate center of the continental field (Fig. 5.7). Thus this diagram is inconclusive.

5.2.2 TRACE ELEMENT CLASSIFICATIONS

Eleven of the fourteen samples plot within the WPB field on Ti-Zr-Y (Fig. 5.8). The three remaining samples were replotted on Ti-Zr-Sr (Fig. 5.9). On this latter

Fig. 5.5. TiO_2 - K_2O - P_2O_5 .

| | |
|-----------------------------|---------------------------|
| MASSET1 Δ | MASSET2 \blacktriangle |
| ARIS IS $+$ | KITASU \times |
| LAKE IS \blacksquare | RAINBOW ∇ |
| ANAHIM \blacktriangledown | ITCHA1 \diamond |
| ITCHA2 \diamond | ALEX \bullet |
| QUES LK \square | WGRAYN \square |
| SPAN CK \times_s | TROPHY \blacktriangle_t |

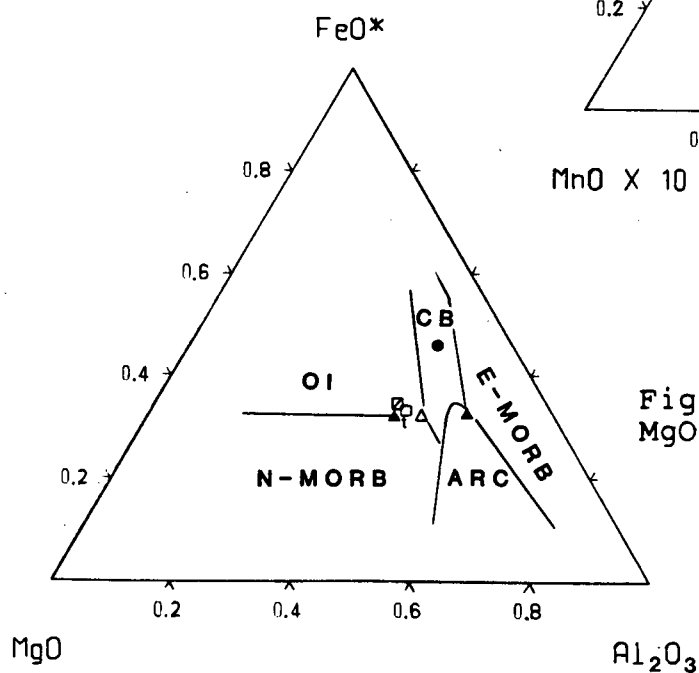
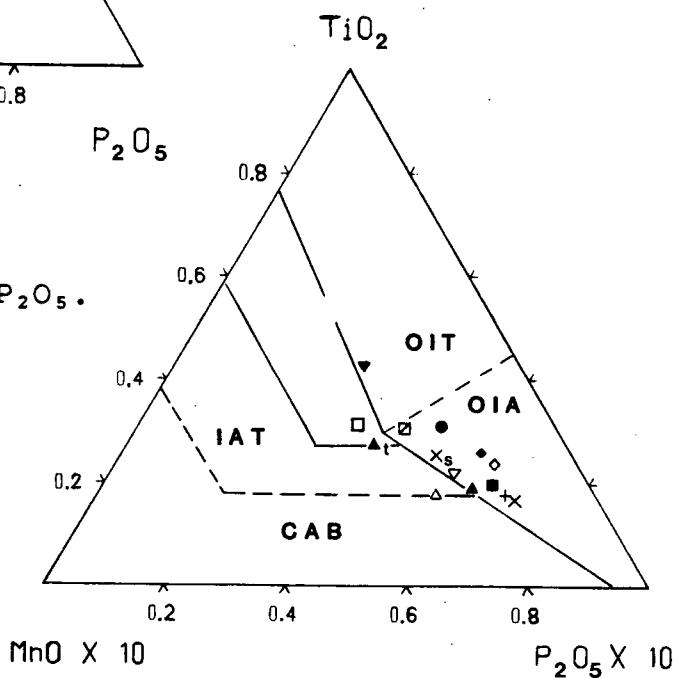
Fig. 5.6. MnO - TiO_2 - P_2O_5 .Fig. 5.7.
 MgO - FeO^* - Al_2O_3 .

diagram calcalkaline samples MASSET1 and MASSET2 lie within the CAB field and sample LAKE IS lies within the OFB field, adjacent to the OFB-CAB field boundary.

V vs. $Ti/1000$ cannot discriminate samples belonging to the calcalkaline series, therefore MASSET1 and MASSET2 were excluded from this plot. Eleven of the remaining twelve samples have Ti/V ratios greater than 50 and plot within the WPB field (Fig. 5.10). ARIS IS lies within the MORB field with a Ti/V ratio of 48.

On Ti/Y vs. Nb/Y samples MASSET1 and MASSET2 plot within the field for MORB, adjacent to the MORB-convergent margin field boundary (Fig. 5.11). Three of the remaining twelve samples (ARIS IS, KITASU and LAKE IS) have relatively low Ti/Y ratios and plot astride the lower boundary of the WPB field. The other nine samples are clearly classified as WPB.

Samples MASSET1, LAKE IS, RAINBOW, ITCHA1 and ALEX plot within the IAT field on the Ti/Cr vs. Ni diagram (Fig. 5.12). MASSET2 and KITASU lie on the field boundary and the remaining seven samples plot within the TH MORB field. This diagram does not have a field for WPB.

5.2.3 TRACE AND REE CLASSIFICATIONS

Only the two samples from the Masset Formation were plotted on Sm/Ce vs. Sr/Ce because this diagram was designed to classify convergent margin basalts, and does

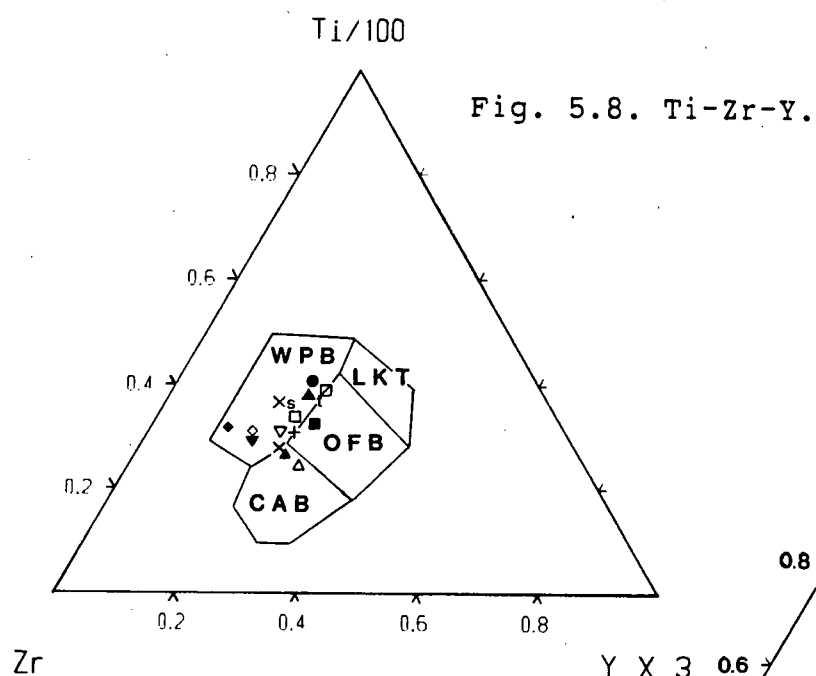


Fig. 5.9. Ti-Zr-Sr.

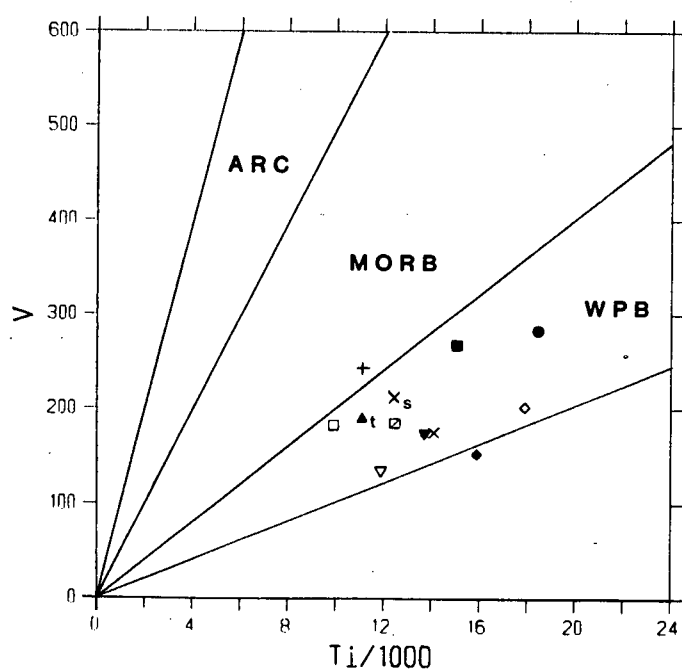
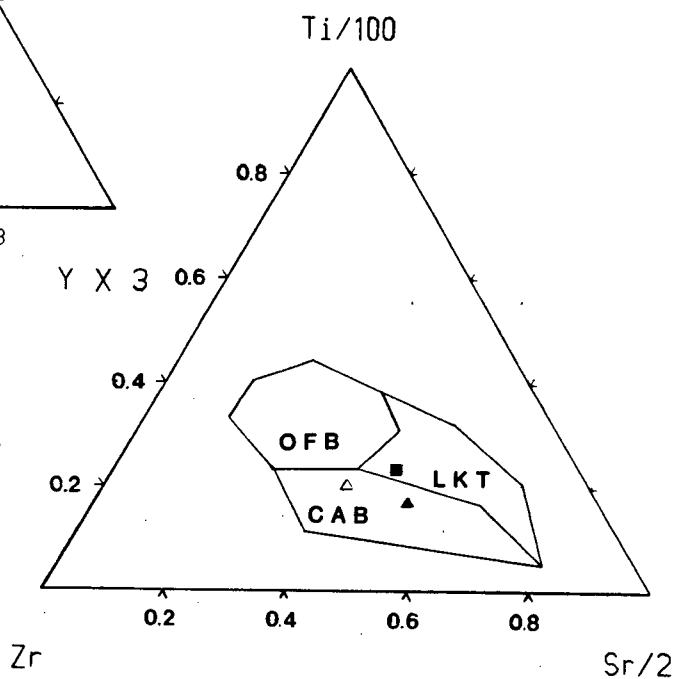
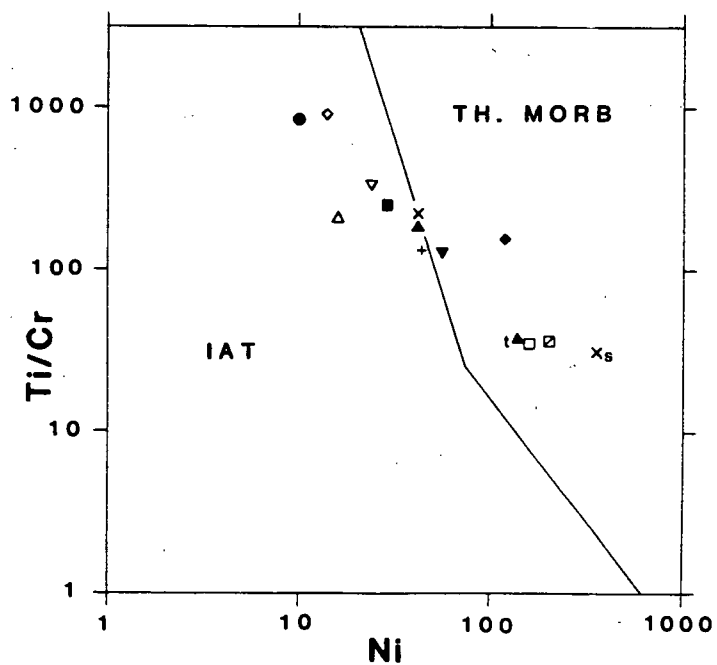
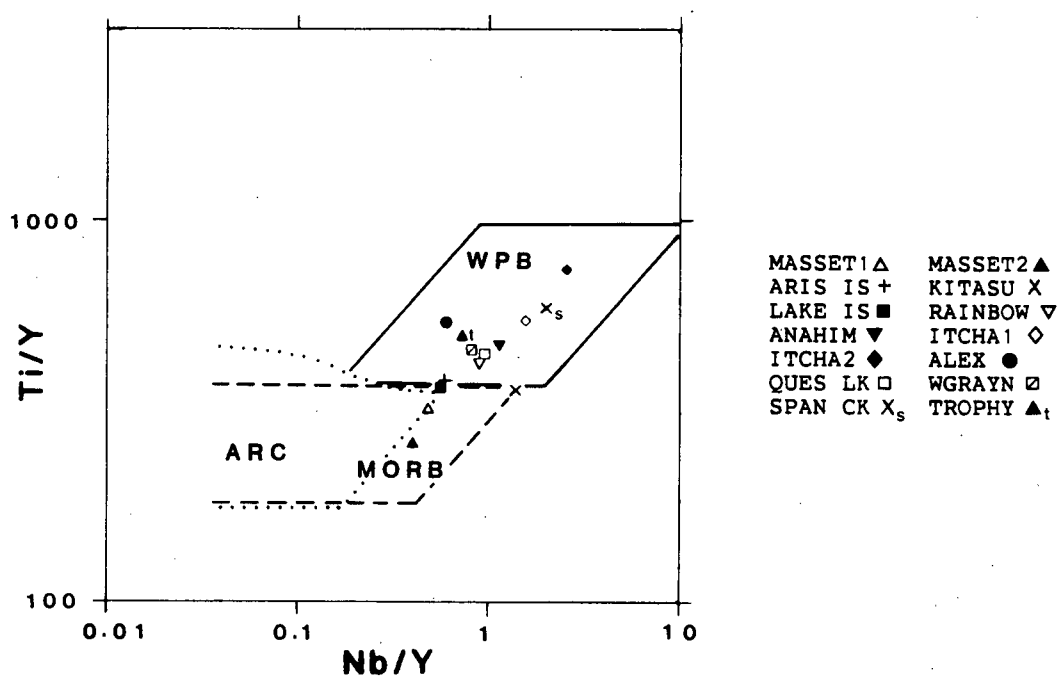


Fig. 5.10. V vs. Ti/1000.

| | |
|-----------------------------|---------------------------|
| MASSET1 Δ | MASSET2 \blacktriangle |
| ARIS IS $+$ | KITASU \times |
| LAKE IS \blacksquare | RAINBOW ∇ |
| ANAHIM \blacktriangledown | ITCHA1 \diamond |
| ITCHA2 \blacklozenge | ALEX \bullet |
| QUES LK \square | WGRAYN \boxtimes |
| SPAN CK \times_s | TROPHY \blacktriangle_t |



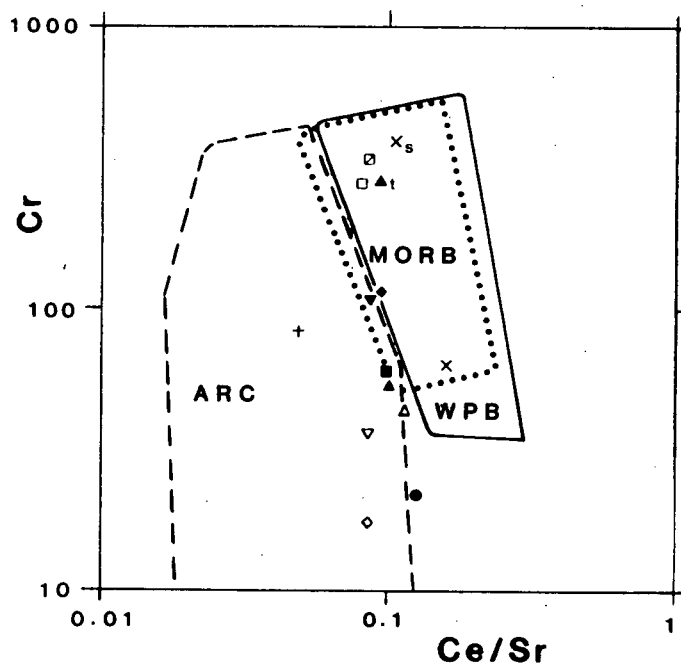
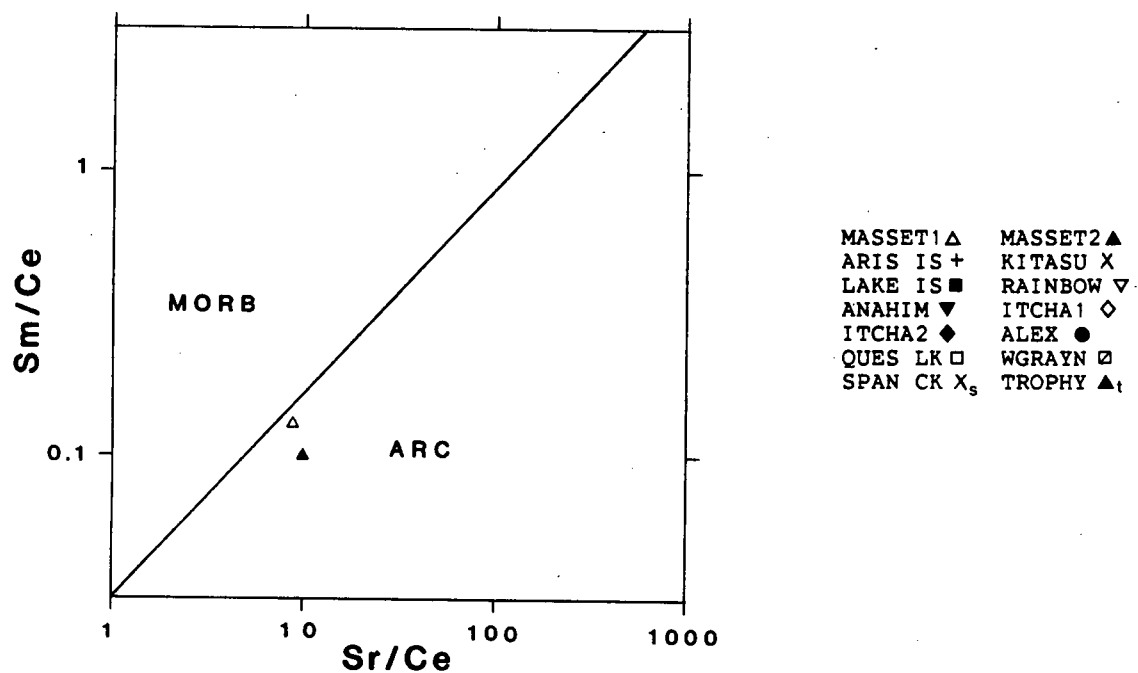
Figs. 5.11 and 5.12. Ti/Y vs. Nb/Y (above) and Ti/Cr vs. Ni (below).

not have a WPB field (Fig. 5.13). MASSET 1 and MASSET2 lie within the convergent margin field.

On Cr vs. Ce/Sr six samples lie within the overlapping MORB-WPB fields (Fig. 5.14). Four of these six from east of the Fraser River and lie removed from all of the remaining samples. The other eight samples lie within or close to the convergent margin field. Seven of these eight samples have Ce/Sr ratios which are similar to ratios from the samples which plot in the MORB-WPB fields, but they are depleted in Cr, thus their convergent margin classification. The eighth sample, ARIS IS, has a much lower Ce/Sr ratio than the other thirteen samples and lies at the center of the convergent margin field.

On Cr vs. Y all samples lie within the field for WPB (Fig. 5.15). MASSET1, MASSET2, ITCHA1, RAINBOW and ALEX lie within the area which overlaps with the convergent margin field, ARIS IS, ANAHIM, ITCHA2, QUES LK, SPAN CK and TROPHY lie within the overlapping WPB-MORB- convergent margin fields and WGRAYN lies within the overlapping WPB-MORB fields.

On La vs. Ba eight samples lie within the orogenic andesite field with Ba/La ratios greater than 15 (Fig. 5.16). KITASU and ITCHA2 have Ba/La ratios less than 11 and lie within the N-MORB field and the remaining four (RAINBOW, ITCHA1, QUES LK and WGRAYN) lie within the E-MORB (WPB) field.



Figs. 5.13 and 5.14. Sm/Ce vs. Sr/Ce (above) and Cr vs. Ce/Sr (below).

| | | | |
|---------|----------------|---------|----------------|
| MASSET1 | △ | MASSET2 | ▲ |
| ARIS IS | + | KITASU | X |
| LAKE IS | ■ | RAINBOW | ▽ |
| ANAHIM | ▼ | ITCHA1 | ◇ |
| ITCHA2 | ◆ | ALEX | ● |
| QUES LK | □ | WGRAYN | ⊠ |
| SPAN CK | X _s | TROPHY | ▲ _t |

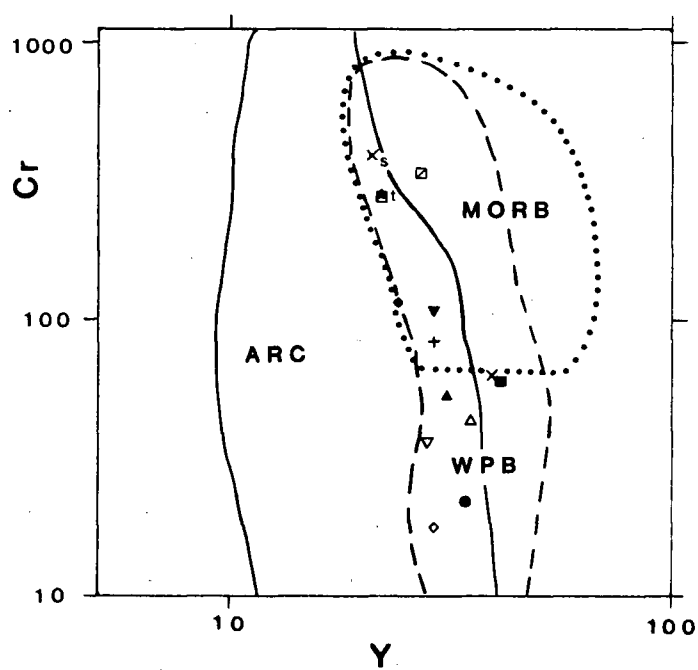


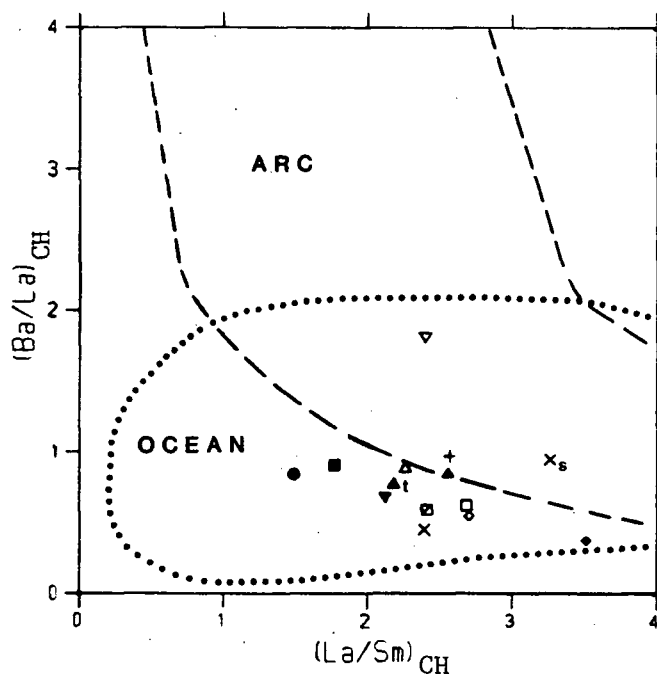
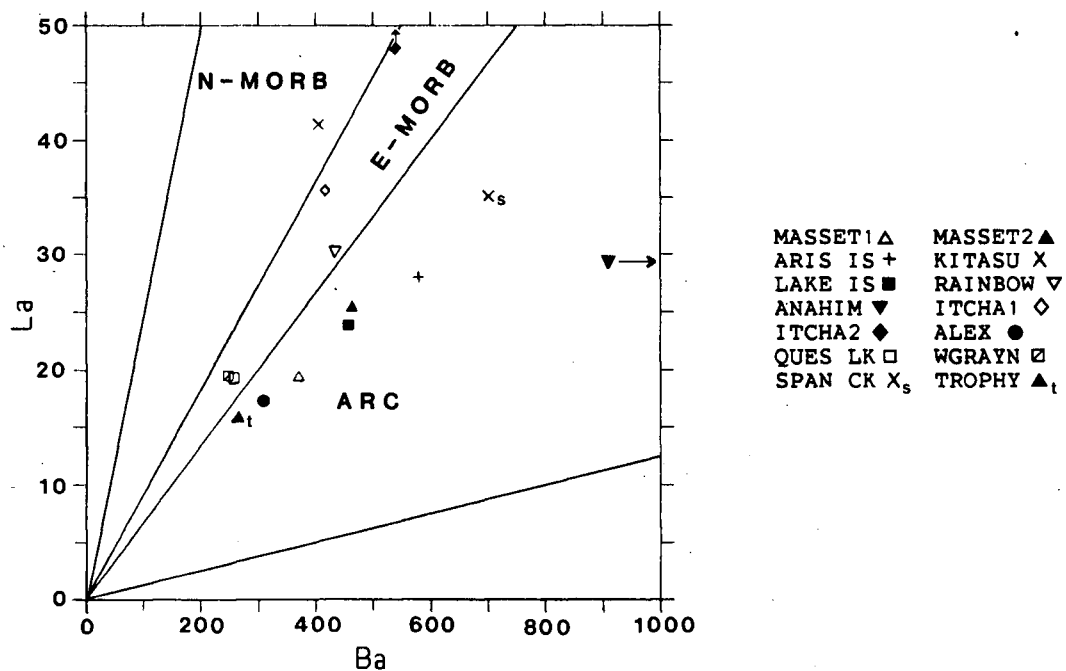
Fig. 5.15. Cr vs. Y.

On $(\text{Ba/La})_{\text{CH}}$ vs. $(\text{La/Sm})_{\text{CH}}$ nine of the fourteen samples clearly lie within the ocean field (Fig. 5.17). MASSET1 and MASSET2 lie within the ocean field adjacent to the ocean-ARC field boundary, ARIS IS and SPAN CK lie just within the overlapping ocean-ARC fields and RAINBOW lies far from the other thirteen samples, clearly within the ARC field.

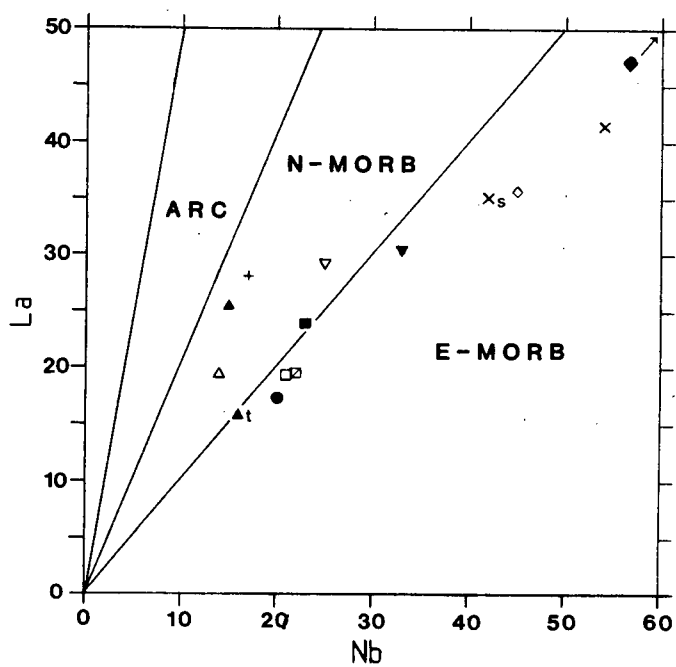
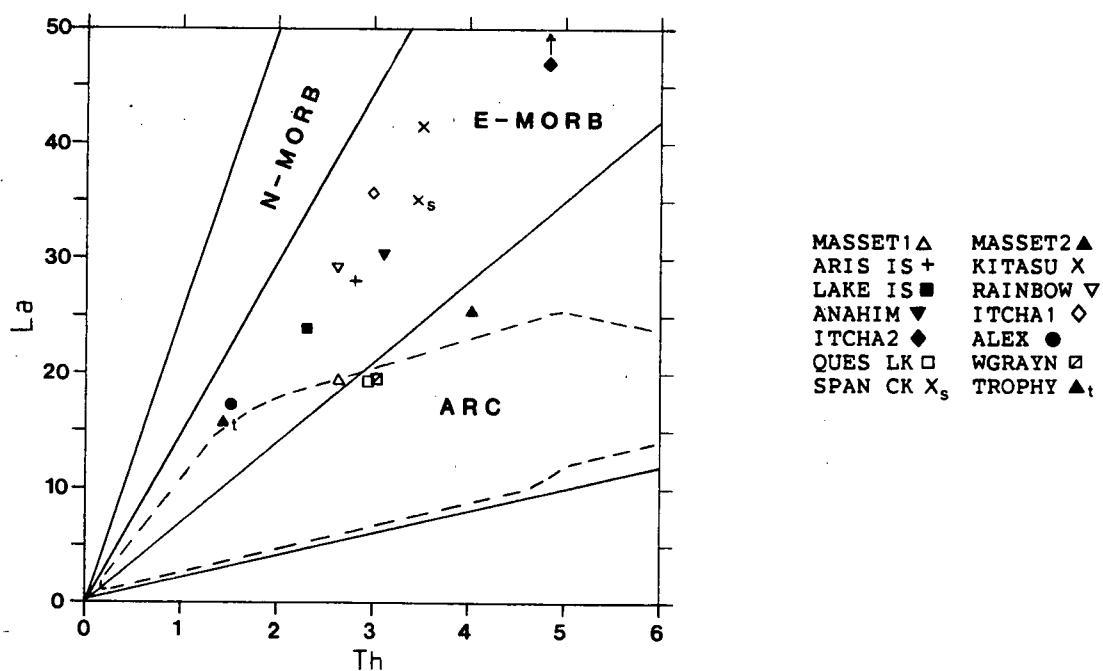
On La vs. Th eleven samples lie within the E-MORB (WPB) field with La/Th ratios greater than 7 (Fig. 5.18). The remaining three (MASSET2, QUES LK and WGRAYN) have La/Th ratios less than 7. MASSET1, QUES LK and WGRAYN lie just within the orogenic andesite field boundary.

On La vs. Nb nine samples have La/Nb ratios less than 1 and lie within the E-MORB (WPB) field (Fig. 5.19). The remaining five samples (MASSET1, MASSET2, ARIS IS, RAINBOW and ITCHA2) have La/Nb ratios between 1 and 2 and lie within the N-MORB field.

On K_2O vs. Ta^*/Yb samples lie within: (a) the overlapping MORB-WPB fields, and (b) the area between the overlapping MORB-WPB fields and the convergent margin field (Fig. 5.20). Samples which lie within this latter area are MASSET1, MASSET2, ARIS IS, RAINBOW, ANAHIM and TROPHY. They have the same range of Ta^*/Yb ratios as the other eight samples but their $\text{K}_2\text{O}/\text{Yb}$ ratios are higher.



Figs. 5.16 and 5.17. La vs. Ba (above) and $(Ba/La)_{CH}$ vs. $(La/Sm)_{CH}$ (below).



Figs. 5.18 and 5.19. La vs. Th (above) and La vs. Nb (below).

On Th/Yb vs. Ta*/Yb MASSET1, MASSET2 and ARIS IS have the highest Th/Yb ratios and lie 'above' the WPB field (Fig. 5.21). MASSET2 has a sufficiently high Th/Yb ratio to lie within the convergent margin field. The remaining twelve samples lie within the overlapping MORB-WPB fields.

On Th-Hf/3-Ta* eleven of the thirteen samples lie within the alkaline WPB and E-MORB- tholeiitic WPB fields (Fig. 5.22) The remaining three samples, MASSET1, MASSET2 and ARIS IS, lie towards and within the CAB field.

5.2.4 BULK EARTH NORMALIZED DIAGRAMS (BEND)

Trace and rare earth element data plotted on BEN diagrams divides the samples into three groups (Figures 5.23, 5.24 and 5.25).

Samples KITASU, LAKE IS, RAINBOW, ANAHIM, ITCHA1 and ITCHA2 are plotted on Fig. 5.23. Their BEND patterns are grossly similar with convex-up shapes peaking at Nb (KITASU, ITCHA1), K (RAINBOW, ANAHIM) or La (LAKE IS, ITCHA2). A large 'peak' at La is unusual. Both LAKE IS and RAINBOW are enriched in Ba relative to Rb. All patterns have large positive Eu anomalies, but none of them have correlative positive Sr anomalies. In fact, KITASU and LAKE IS display negative Sr anomalies! The pattern for LAKE IS is fairly flat from Ba to La in contrast to the other five patterns which have a

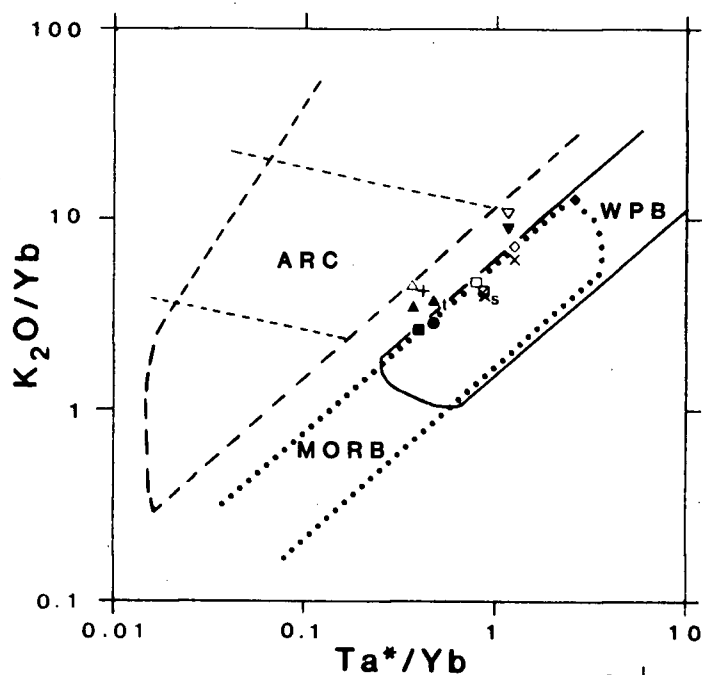


Fig. 5.21. Th/Yb vs. Ta^*/Yb .

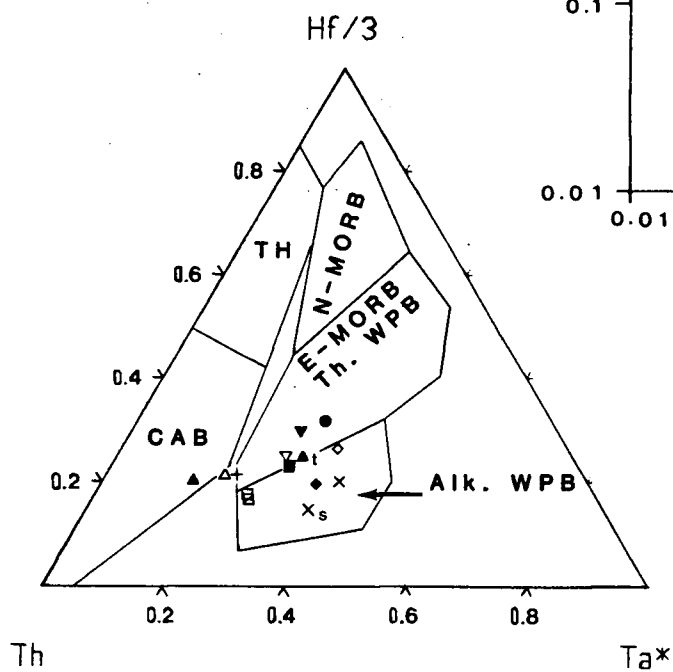
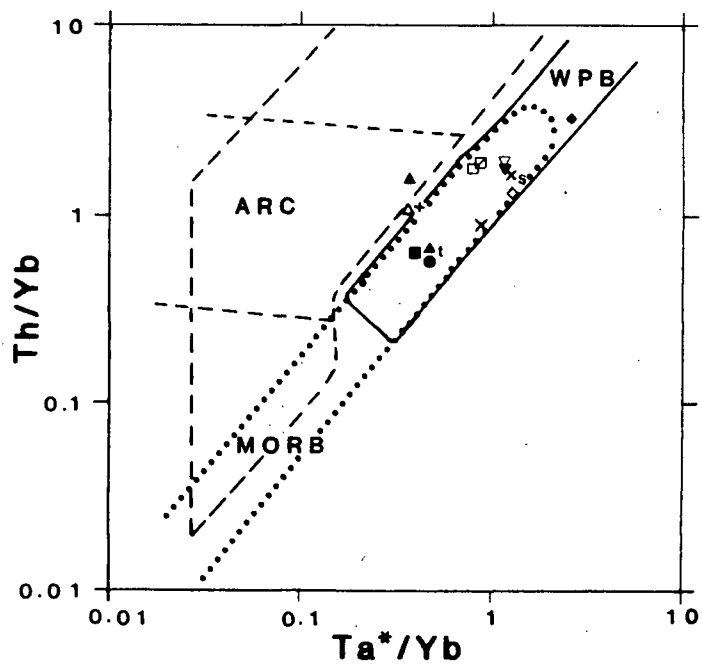


Fig. 5.22. $Th-Hf/3-Ta^*$.

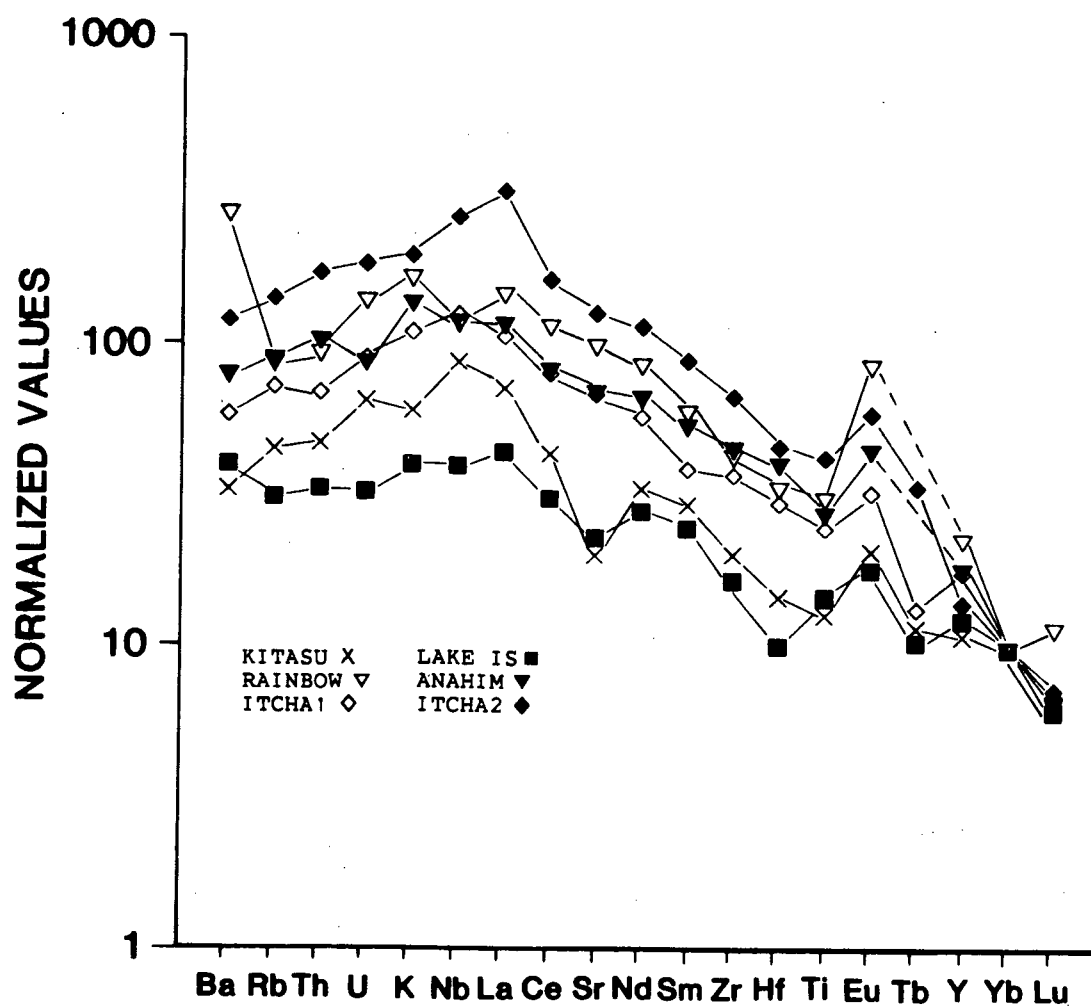


Fig. 5.23. BEN diagram for samples KITASU, LAKE IS, RAINBOW, ANAHIM, ITCHA1 and ITCHA2.

distinctly positive slope.

BEND patterns on Fig. 5.24 are from the five locations east of the Fraser River; ALEX, QUES LK, WGRAYN, SPAN CK and TROPHY. Patterns are similar to those on Fig. 5.23, but Fig. 5.24 patterns are more irregular from Ba to La, and they all have a concave-up dip from Sm to Ti. All samples, excluding QUES LK, are enriched in Ba relative to Rb and WGRAYN is enriched in Th and U. All patterns have small positive Eu anomalies and ALEX has a 'trough' at Sr. The patterns from TROPHY and ALEX are almost identical and are grossly similar to the pattern from LAKE IS on Fig. 5.23.

BEND patterns on Figure 5.25 are from samples MASSET1, MASSET2 and ARIS IS. This latter sample has 'peaks' at Ba and Sr, but barring these two exceptions the three patterns are nearly identical. They are all slightly enriched in LIL relative to La, have a 'trough' at Nb and are slightly depleted in Hf and Ti relative to Y. All patterns have small positive Eu anomalies.

5.3 TRACE ELEMENT CHEMISTRY

All samples from Figs. 5.23 and 5.24 have abundances of trace and REE and BEND patterns which are similar to those from oceanic and some continental WPB (Thompson et al., 1983; Kay, 1984) (Table IV). Samples belonging to the alkaline series generally have higher abundances of LIL and LREE than the tholeiitic and transitional samples. Most La

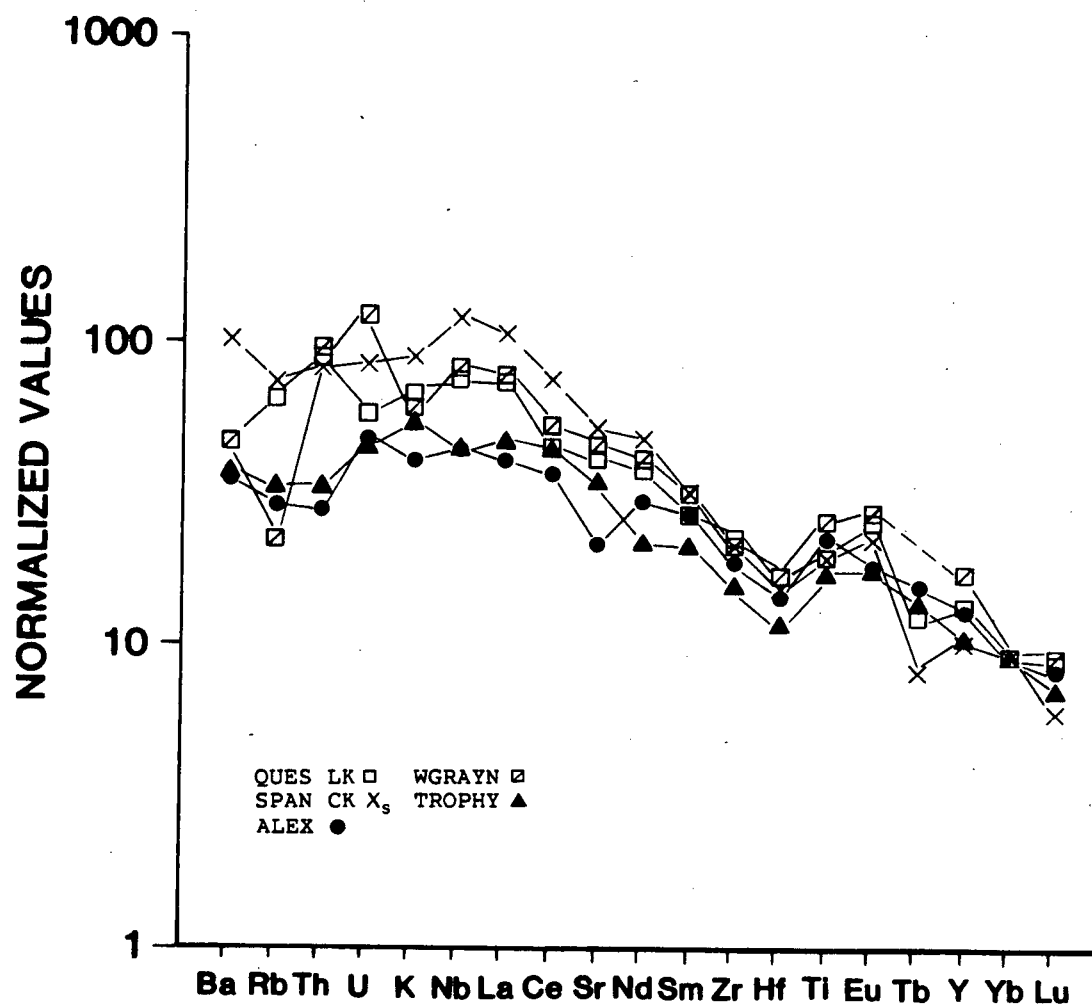


Fig. 5.24. BEN diagram for samples ALEX, QUES LK, WGRAYN, SPAN CK and TROPHY.

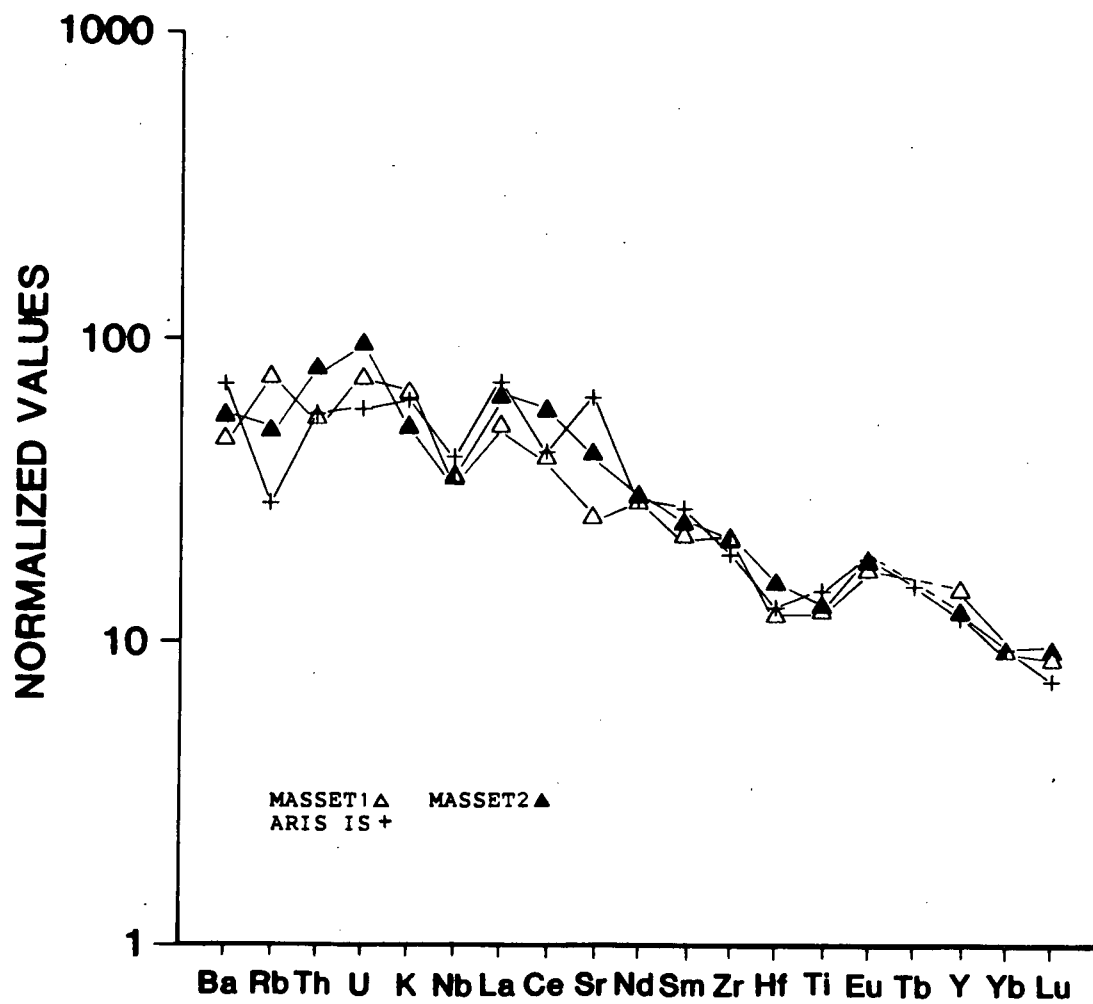


Fig. 5.25. BEN diagram for samples MASSET1, MASSET2 and ARIS IS.

abundances lie between 48 and 59 times chondritic in the tholeiitic/transitional samples and 72 to 126 times chondritic in the alkaline samples. Sample ITCHA2 is an exception with an La content of 211 times chondritic which results in this samples unusually shaped BEND pattern. In the tholeiitic/transitional samples Yb abundances range from 7 to 12.5 times chondritic and are within the range of Yb abundances in the alkaline samples; Yb = 6 to 18 times chondritic. Excluding ITCHA2, $(La/Yb)_{CH}$ ratios lie between 4.41 and 14.38 in the alkaline samples, and 4.36 to 8.23 in the tholeiitic/transitional samples. Alkaline samples KITASU and LAKE IS are enriched in HREE relative to the remaining five alkaline samples, explaining their lower $(La/Yb)_{CH}$ ratios, which are more like those from the tholeiitic/transitional samples. ITCHA2 has a $(La/Yb)_{CH}$ ratio of 31.30 because of its enrichment in La. La/Nb ratios range from 0.75 to 1.10, within the range of ratios from OIB (Thompson et al, 1983).

The three samples from Fig. 5.25 have trace and REE abundances and BEND patterns which are grossly similar to either continental WPB contaminated with continental crust, or convergent margin basalts (Dupuy and Dostal, 1984; Thompson et al., 1983). La abundances range from 59 to 86 times chondritic, Yb contents lie between 11 and 12 times chondritic and $(La/Yb)_{CH}$ ratios from 5.43 to 7.44. These samples have La/Nb ratios which lie between 1.3 and 1.6, providing additional evidence for either of the above

alternatives.

5.3.1 TH AND U

Abundances of Th range from 1.4 to 4.8 ppm and U abundances lie between 0.6 and 1.6 ppm. Th/U ratios range from 1.87 to 4.92 and average 2.77. There is no correlation between Th and U abundances or ratios and a samples age or geographic location.

5.3.2 TRANSITION ELEMENTS

Abundances of Cr and Ni in samples QUES LK, WGRAYN, SPAN CK and TROPHY are higher than Cr and Ni abundances in the remaining ten basalts, suggesting fractionation of olivine, clinopyroxene \pm Cr-Spinel was more important in the petrogenesis of the latter basalts than in the former. ANAHIM, which has an Ni content of 56 ppm, and Cr content of 108 ppm, presumably fractionated more olivine than either clinopyroxene or Cr-spinel.

Sc contents divide the samples into two groups: (A) Sc greater than 20 ppm, and (B) Sc less than 16.5 ppm. Samples ANAHIM, ITCHA1 and ITCHA2 belong to the latter group. Low Sc contents suggest a history involving high pressure pyroxene fractionation (Basaltic Volcanism Study Project, 1981).

5.4 SR ISOTOPES

Excluding MASSET1, MASSET2 and ARIS IS, available Sr isotopic data does not distinguish samples west of the Fraser from those to the east. Both western and eastern samples have $^{87}\text{Sr}/^{86}\text{Sr}$ ratios ranging from 0.7030 to 0.7035 (Table IV). Average ratios of oceanic WPB range from 0.7028 to 0.706 (Faure, 1977).

Sr isotopic ratios for MASSET1, MASSET2 AND ARIS IS are 0.7039, 0.7040 and 0.7042 respectively. These ratios are distinctly higher than ratios from the other eleven samples, and are similar to ratios from convergent margin settings, but they are still within the range of oceanic WPB.

5.5 DISCUSSION OF DISCRIMINATION DIAGRAMS

On most elemental discrimination diagrams, the eleven tholeiitic, alkaline and transitional samples from Figs. 5.23 and 5.24 plot as WPB or E-MORB, and their BEND patterns have convex-up WPB-like shapes. However on some of the diagrams a few of these samples lie within N-MORB or convergent margin fields. These latter classifications generally occur only sporadically and therefore they do not seem significant for discrimination purposes. For example, ITCHA2 lies within the N-MORB field on La vs. Ba (Fig. 5.16) because of its very high abundance of La, RAINBOW appears to be from a convergent margin setting on $(\text{Ba}/\text{La})_{\text{CH}}$ vs. $(\text{La}/\text{Sm})_{\text{CH}}$ (Fig. 5.17) because it is enriched in Ba, QUES LK and WGRAYN lie within the orogenic field on La vs. Th (Fig.

5.18) because of their relative enrichment in Th and RAINBOW, ANAHIM and TROPHY lie 'above' the WPB field on K_2O/Yb vs. Ta^*/Yb (Fig. 5.20) because they are slightly enriched in K_2O . Olivine and pyroxene \pm Cr-spinel fractionation lower Cr abundance in LAKE IS, ANAHIM, RAINBOW, ITCHA1, ITCHA2 and ALEX so that they lie within or close to the convergent margin field on Cr vs. Ce/Sr (Fig. 5.14) even though their Ce/Sr ratios are within the range of ratios from the samples classified as WPB.

The biggest exception to the WPB (E-MORB) classification comes from the La vs. Ba diagram (Fig. 5.16). On this diagram six of the eleven samples discussed above lie within the orogenic andesite field. However on the $(Ba/La)_{CH}$ vs. $(La/Sm)_{CH}$ diagram (Fig. 5.17) only RAINBOW is unequivocally classified as convergent margin because of its high abundance of Ba. This discrepancy casts some doubt on the validity of the La vs. Ba field boundaries, especially when this diagram is applied to basalts.

Alkaline samples KITASU and LAKE IS do not always plot with the four other alkaline Anahim Belt samples from west of the Fraser River. This suggests that if the source for KITASU and LAKE IS was the Anahim hotspot, it must have been heterogeneous and changing with time.

The three tholeiitic and transitional samples in and near Wells Gray Park generally plot in a group separate from the four alkaline samples west of the Fraser River (RAINBOW, ANAHIM, ITCHA1 and ITCHA2), and alkaline sample SPAN CK,

also from Wells Gray Park, plots near the other "Wells Gray" samples on many of the diagrams. Tholeiitic sample ALEX, from east of the Fraser River, generally plots with the four samples just discussed, except on diagrams affected by olivine and pyroxene fractionation (i.e. diagrams using Cr or Ni). In an attempt to explain why samples east of the Fraser River plot separately from samples west of the Fraser River the following three suggestions are offered:

- tholeiitic basalts characteristically have lower abundances of most elements relative to alkaline basalts;
- the source was heterogeneous;
- the source for the five samples east of the Fraser River was not the Anahim hotspot (C.J. Hickson, oral comm., 1985; J.E. Souther, in press).

Calcalkaline samples MASSET1 and MASSET2 and alkaline sample ARIS IS plot within or towards the convergent margin field on many of the diagrams, have BEND patterns with some of the characteristics of subduction related basalts (high LIL with respect to La and Nb and Ti depletion), La/Nb ratios greater than 1.3 and $^{87}\text{Sr}/^{86}\text{Sr}$ ratios greater than 0.7039. On some diagrams ARIS IS plots separately from MASSET1 and MASSET2 and close to KITASU and/or LAKE IS. This latter grouping of samples is seen on MnO-TiO₂-P₂O₅, Ti-Zr-Y, V vs. Ti/1000, Ti/Y vs. Nb/Y, Ti/Cr vs. Ni and La vs. Ba diagrams. This suggests that ARIS IS may have originated in a source chemically similar to the KITASU and

LAKE IS source, but there were slight modifications towards a 'convergent margin' chemistry.

The convergent margin affinity observed in MASSET1, MASSET2 and ARIS IS decreases from west to east and with time, suggesting this chemistry is perhaps related to:

- possible oblique subduction of the Pacific plate along the Queen Charlotte fault which may have been occurring at that time, or
- volcanism in the Pemberton Arc (J. Souther, oral comm., 1985).

Alternatively, Dupuy and Dostal (1984) suggest WPB BEND patterns similar to convergent margin patterns may be produced by varying degrees of crustal contamination. This alternative might be tested with additional O, Nd, and Pb isotopic data.

5.6 SUMMARY

Basalt samples from the Anahim Volcanic Belt west of the Fraser River belong to the alkaline series and are classified as WPB. Basalt samples from east of the Fraser River belong primarily to the tholeiitic series, although one sample is alkaline, and they too are classified as WPB. These latter samples, excluding ALEX, are more 'primitive' than the 'western' samples.

Chemistry and Sr isotope ratios lend no support to the suggestion that 'western' (Anahim Belt) and 'eastern' samples came from different sources. The observed chemical

differences may easily be related to abundance differences in tholeiitic vs. alkaline series rocks.

Chemical differences which on a few diagrams separate alkaline samples KITASU and LAKE IS from the remaining alkaline samples suggest a heterogeneous hotspot which changed with time.

Two basaltic samples from the Masset Formation on the Queen Charlotte Islands belong to the calcalkaline series and have chemical characteristics and Sr isotope ratios grossly similar to a convergent margin basalt. Alkaline sample, ARIS IS, from the mainland also has some convergent margin characteristics.

Chemistry of the Masset Formation samples suggest their source was not the Anahim hotspot, however crustal contamination of the hotspot magma could have caused the convergent margin-like chemistry. Alternatively, Masset basalts may be related to the Pemberton Arc or they may have been produced by the possible oblique subduction of the Pacific plate along the Queen Charlotte Fault. However, as oblique subduction is only established from recent plate movements (< 6 Ma) this latter possibility is only speculatively applied here.

TABLE IV ANAHIM VOLCANIC BELT

Major, trace and rare earth element abundances, Sr isotope ratios, K/Ar dates and ages.

| Series Name | MASSET1 Calcalk. Basalt | MASSET2 Calcalk. Bas/And | ARIS IS Alkaline Hawaiite | KITASU Alkaline Hawaiite | LAKE IS Alkaline Hawaiite | RAINBOW ¹ Alkaline Hawaiite | ANAHIM ¹ Alkaline Hawaiite |
|--------------------------------|-------------------------------|--------------------------------|---------------------------------|--------------------------------|---------------------------------|--|---|
| LAT. | 53 30.6 | 53 24.6 | 52 42.0 | 52 29.5 | 52 21.3 | 52 44.6 | 52 45.15 |
| LONG. | 132 20.0 | 131 55.5 | 129 15.5 | 128 43.5 | 128 21.0 | 125 44.6 | 125 37.10 |
| SiO ₂ | 50.38 | 53.31 | 50.38 | 50.15 | 47.24 | 50.30 | 50.33 |
| TiO ₂ | 1.54 | 1.68 | 1.85 | 2.35 | 2.51 | 1.98 | 2.29 |
| Al ₂ O ₃ | 15.28 | 16.13 | 16.53 | 15.18 | 13.91 | 16.54 | 16.17 |
| Fe ₂ O ₃ | 11.95 | 11.03 | 9.90 | 13.07 | 16.20 | 12.89 | 12.84 |
| FeO | N/A | N/A | N/A | N/A | N/A | N/A | N/A |
| MnO | 0.22 | 0.17 | 0.15 | 0.19 | 0.20 | 0.19 | 0.14 |
| MgO | 7.39 | 4.30 | 6.46 | 3.66 | 6.31 | 3.18 | 4.32 |
| CaO | 8.08 | 7.78 | 8.64 | 7.62 | 8.00 | 8.52 | 8.01 |
| Na ₂ O | 3.58 | 4.18 | 4.33 | 5.27 | 3.86 | 4.43 | 4.16 |
| K ₂ O | 1.10 | 0.89 | 1.07 | 1.55 | 0.96 | 1.46 | 1.57 |
| P ₂ O ₅ | 0.47 | 0.53 | 0.69 | 0.96 | 0.81 | 0.51 | 0.17 |
| H ₂ O | N/A | N/A | N/A | N/A | N/A | N/A | 0.74 |
| Ba | 370.0 | 463.0 | 579.0 | 404.0 | 457.0 | 1113.0 | 434.0 |
| Rb | 30.0 | 21.0 | 12.0 | 28.0 | 18.0 | 19.0 | 24.0 |
| Th | 2.6 | 4.0 | 2.8 | 3.5 | 2.3 | 2.6 | 3.1 |
| U | 1.1 | 1.5 | 0.9 | 1.5 | 0.7 | 1.1 | 0.9 |
| Nb | 14.0 | 15.0 | 17.0 | 54.0 | 23.0 | 25.0 | 33.0 |
| La | 19.5 | 25.5 | 28.1 | 41.4 | 23.9 | 29.2 | 30.3 |
| Ce | 40.6 | 60.7 | 43.8 | 66.8 | 44.2 | 60.6 | 56.9 |
| Sr | 355.0 | 601.0 | 898.0 | 420.0 | 449.0 | 714.0 | 659.0 |
| Nd | 22.3 | 22.3 | 22.5 | 37.4 | 29.4 | 33.2 | 33.7 |
| Sm | 5.3 | 6.2 | 6.8 | 10.7 | 8.3 | 7.5 | 8.8 |
| Zr | 176.0 | 182.0 | 161.0 | 246.0 | 188.0 | 181.0 | 250.0 |
| Hf | 2.9 | 3.9 | 3.2 | 5.2 | 3.4 | 4.1 | 6.5 |
| Eu | 1.5 | 1.7 | 1.7 | 2.7 | 2.2 | 3.9 | 2.6 |
| Tb | N/A | N/A | 0.9 | 1.0 | 0.8 | N/A | N/A |
| Y | 35.0 | 31.0 | 29.0 | 39.0 | 41.0 | 28.0 | 29.0 |
| Yb | 2.4 | 2.5 | 2.5 | 3.9 | 3.6 | 1.4 | 1.8 |
| Lu | 0.3 | 0.4 | 0.3 | 0.4 | 0.3 | 0.2 | 0.2 |
| Co | 26.0 | 31.0 | 21.0 | 28.0 | 25.0 | 26.0 | 32.0 |
| Cr | 44.0 | 54.0 | 84.0 | 63.4 | 60.3 | 36.2 | 107.7 |
| Cu | 78.0 | 102.0 | 86.0 | 43.0 | 46.0 | 65.0 | 70.0 |
| Ni | 16.0 | 42.0 | 44.0 | 42.0 | 29.0 | 24.0 | 56.0 |
| Sc | 24.0 | 20.0 | 22.0 | 21.4 | 33.2 | 21.8 | 16.2 |
| V | 250.0 | 169.0 | 242.0 | 174.0 | 266.0 | 133.0 | 172.0 |
| Sr ⁸⁷ ₈₆ | 0.7039 | 0.7040 | 0.7042 | 0.7026 | 0.7035 | 0.7032 | 0.7032 |
| K/Rb | 304.37 | 351.80 | 740.17 | 459.52 | 442.72 | 637.87 | 543.02 |
| (La/Yb) _{CH} | 5.43 | 6.77 | 7.44 | 7.16 | 4.41 | 14.38 | 11.49 |
| La/Nb | 1.39 | 1.70 | 1.65 | 0.77 | 1.04 | 1.17 | 0.92 |
| Mg' | 55 | 44 | 56 | 36 | 44 | 33 | 40 |

Dates and 23.8 ± 0.8 19.8 ± 0.7 ~14 ~14 ~14 7.9 ± 0.3 6.7 ± 0.3
Ages (Ma).

N/A = not analyzed

continued.....

| | ITCHA1 | ITCHA2 | ALEX | QUES LK | WGRAYN ² | SPAN CK | TROPHY ² |
|--------------------------------|--------------------|-------------------|--------------|--------------|---------------------|-------------------|---------------------|
| Series Name | Alkaline Mugearite | Alkaline Hawaiite | Thol. Basalt | Thol. Basalt | Thol. Basalt | Alkaline Basanite | Thol/Trans Basalt |
| LAT. | 52 42.0 | 52 45.0 | 52 38.7 | 52 39.5 | 52 05 | 52.01.7 | 51 50 |
| LONG. | 124 45.0 | 124 49.2 | 122 27.0 | 120 59.25 | 120 03 | 120.19.75 | 120 00. |
| SiO ₂ | 49.84 | 45.17 | 52.70 | 48.88 | 48.89 | 45.80 | 49.13 |
| TiO ₂ | 2.65 | 2.98 | 3.08 | 1.65 | 2.08 | 2.07 | 1.85 |
| Al ₂ O ₃ | 16.57 | 14.09 | 12.67 | 15.02 | 14.13 | 13.94 | 14.25 |
| Fe ₂ O ₃ | 11.53 | 14.26 | 15.53 | 12.89 | 2.19 | 13.02 | 1.23 |
| FeO | N/A | N/A | N/A | N/A | 10.05 | N/A | 10.03 |
| MnO | 0.15 | 0.17 | 0.19 | 0.17 | 0.17 | 0.18 | 0.21 |
| MgO | 3.60 | 8.14 | 3.87 | 8.52 | 8.66 | 10.92 | 9.21 |
| CaO | 7.28 | 7.85 | 7.42 | 9.19 | 9.83 | 8.94 | 9.74 |
| Na ₂ O | 6.06 | 4.78 | 3.28 | 2.71 | 3.02 | 3.41 | 3.28 |
| K ₂ O | 1.63 | 1.90 | 0.75 | 0.78 | 0.67 | 1.30 | 0.80 |
| P ₂ O ₅ | 0.69 | 0.68 | 0.50 | 0.19 | 0.30 | 0.42 | 0.27 |
| H ₂ O | N/A | N/A | N/A | N/A | 0.84 | N/A | 0.40 |
| Ba | 416.0 | 553.0 | 307.0 | 257.0 | 247.0 | 701.0 | 264.0 |
| Rb | 26.0 | 33.0 | 13.0 | 18.0 | 6.0 | 26.0 | 12.0 |
| Th | 3.0 | 4.8 | 1.5 | 2.9 | 3.0 | 3.5 | 1.4 |
| U | 1.2 | 1.6 | 0.8 | 0.6 | 1.2 | 1.1 | 0.6 |
| Nb | 45.0 | 61.0 | 20.0 | 21.0 | 22.0 | 42.0 | 16.0 |
| La | 35.7 | 69.1 | 17.3 | 19.3 | 19.5 | 35.1 | 15.9 |
| Ce | 71.4 | 94.6 | 41.4 | 31.3 | 35.3 | 65.7 | 39.4 |
| Sr | 835.0 | 1004.0 | 330.0 | 391.0 | 415.0 | 625.0 | 421.0 |
| Nd | 37.6 | 48.7 | 24.7 | 19.2 | 20.1 | 30.8 | 14.2 |
| Sm | 8.1 | 12.1 | 7.2 | 4.4 | 5.0 | 6.6 | 4.5 |
| Zr | 263.0 | 312.0 | 169.0 | 126.0 | 114.0 | 150.0 | 112.0 |
| Hf | 6.2 | 6.3 | 3.8 | 2.8 | 2.6 | 3.2 | 2.4 |
| Eu | 2.5 | 2.9 | 1.8 | 1.5 | 1.6 | 1.7 | 1.4 |
| Tb | 0.7 | 1.1 | 1.0 | 0.5 | N/A | 0.4 | 0.7 |
| Y | 29.0 | 24.0 | 34.0 | 22.0 | 27.0 | 21.0 | 22.0 |
| Yb | 2.3 | 1.5 | 2.7 | 1.7 | 1.6 | 2.1 | 2.1 |
| Lu | 0.2 | 0.2 | 0.4 | 0.2 | 0.2 | 0.2 | 0.2 |
| Co | 29.0 | 121.0 | 33.0 | 100.0 | 86.0 | 59.0 | 112.0 |
| Cr | 17.6 | 115.7 | 21.9 | 279.3 | 339.5 | 393.9 | 287.5 |
| Cu | 33.0 | 79.0 | 24.0 | 52.0 | 47.0 | 69.0 | 38.0 |
| Ni | 14.0 | 119.0 | 10.0 | 160.0 | 203.0 | 357.0 | 139.0 |
| Sc | 13.6 | 15.5 | 25.5 | 23.7 | 24.0 | 22.7 | 21.7 |
| V | 152.0 | 201.0 | 282.0 | 182.0 | 184.0 | 211.0 | 190.0 |
| Sr ⁸⁷ ₈₆ | 0.7030 | N/A | 0.7030 | N/A | 0.7034 | 0.7035 | 0.7032 |
| K/Rb | 520.41 | 477.94 | 478.90 | 359.71 | 926.94 | 415.05 | 553.40 |
| (La/Yb) _{CH} | 10.58 | 31.30 | 4.36 | 7.81 | 8.23 | 11.20 | 5.05 |
| La/Nb | 0.79 | 1.13 | 0.87 | 0.92 | 0.89 | 0.84 | 0.99 |
| Mg' | 38 | 53 | 33 | 57 | 56 | 62 | 60 |

Major element abundances from:

¹ Bevier, 1978

² Fiesinger, 1975

Dates and 0.78 ± 0.07
Ages (Ma).

N/A = not analyzed

6. STIKINE VOLCANIC BELT

The Stikine Volcanic Belt is believed to be zone of incipient late Cenozoic extension related to transcurrent motion along the adjacent continental margin (Souther, 1977). Large volumes of alkaline basalts to peralkaline rhyolites form the basaltic shields, composite domes, flows and central volcanoes of the Mount Edziza Volcanic Complex, Level Mountain and Hart Peaks (Souther et al., 1984; Hamilton, 1981). Hoodoo Mountain, a differentiated volcanic complex to the south, is not as voluminous. The remainder of the Stikine Volcanic Belt is comprised of small monogenetic cones and lava flows (Souther et al., 1984; R.L. Armstrong, pers. comm., 1985).

Twenty-two samples from the Stikine Volcanic Belt were selected for analysis (Fig. 6.1) Four are from the Mt. Edziza Volcanic Complex and another four are from residual basalt caps and valley flows north and northeast of Mt. Edziza at approximately 58° N. Three samples are from the Level Mountain volcano, west of Dease Lake and two are from near Atlin. One sample comes from an isolated cone in the northwest part of the Bowser Basin, two were collected from the recent Aiyansh River flow in the southwest Bowser Basin and one is from a dyke located just to the north of Prince Rupert. Four of the five remaining samples are from monogenetic volcanic centers in the Sikine region northwest of Stewart and the fifth is from Hoodoo Mountain.

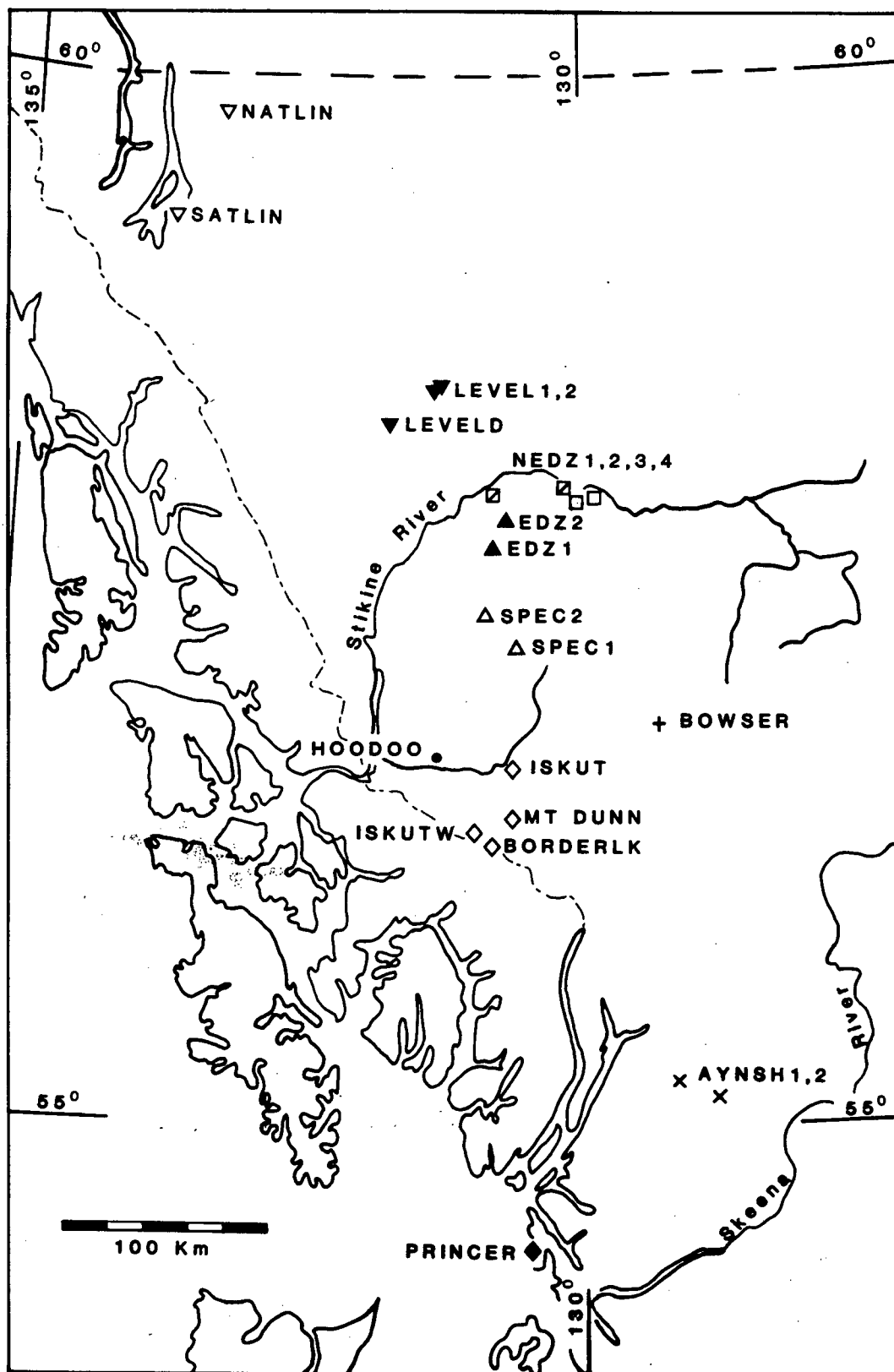


Fig. 6.1. Sample location map for the Stikine Volcanic Belt.

K-Ar dates from samples in the Mount Edziza Volcanic Complex and locations just to the north range from 0.507 ± 0.070 to 7.8 ± 0.3 Ma (Table V), BOWSER has a K-Ar date of 1.6 ± 0.3 Ma and samples PRINCER and SATLIN have been dated at 7.2 ± 0.8 and 16.5 ± 3.1 Ma respectively (U.B.C. K-Ar lab). C^{14} dates obtained from the Aiyansh lava flow give an age of 220 years (Sutherland-Brown, 1969). Samples from near the Iskut River (BORDERLK, ISKUTW, MT DUNN and ISKUT) are approximately 0.04 Ma old and HOODOO has been dated at 0.02 ± 0.013 Ma (U.B.C. K-Ar lab). The three samples from Level Mountain have not been dated but other samples from Level Mountain have K-Ar dates of 5.8 to 14.9 Ma.

6.1 MAJOR ELEMENT CHEMISTRY

Abundances of major elements in most of the basaltic samples are very similar to abundances in an average Hawaiian alkali olivine basalt (MacDonald, 1968), or the alkaline Anahim Belt volcanics (this study) (Table V). Mg' numbers range from 32 to 58, the lowest numbers from AYNSh1 and AYNSh2.

Samples PRINCER and SATLIN are distinguished from the remainder of the suite by lower total alkalis at a given SiO_2 content, as well as lower abundances of TiO_2 . PRINCER has an Mg' number of 61, indicating it is the least fractionated sample in this suite.

Abundances of most major elements in LEVELD are generally similar to abundances in PRINCER and SATLIN, but

its TiO_2 content is higher.

HOODOO has a higher abundance of SiO_2 (59 wt%), very low abundances of TiO_2 , MgO , and CaO and a molecular excess of $(\text{Na}_2\text{O}+\text{K}_2\text{O})$ over Al_2O_3 . Both acmite and sodium metasilicate appear in its list of normative minerals, distinguishing it as peralkaline (MacDonald, 1974; Carmichael et al., 1974), and its differentiation index of 80 identifies it as a trachyte (Thompson et al., 1972; Thornton and Tuttle, 1960). Trace element abundances are also characteristic of a highly fractionated peralkaline lava (Ferrara and Treuil, 1974). Its Ba and Sr abundances are less than 1 ppm, the transition elements (Co, Cr, Cu, Ni, Sc, and V) occur in very low abundances and it is greatly enriched in Rb, Th, U, K, Nb, Zr, Hf and all REE's, except Eu. These peralkaline chemical characteristics preclude comparisons with the Stikine basalt suite, therefore it will not be plotted on any of the tectonic discrimination diagrams.

6.2 DISCRIMINATION DIAGRAMS

6.2.1 MAJOR ELEMENT CLASSIFICATIONS

On total alkalis vs. silica one sample (PRINCER) lies on MacDonald's (1968) dividing line between the subalkaline and alkaline fields, two (LEVELD and SATLIN) lie just within the alkaline field close to the dividing line and the remaining eighteen samples lie within the

alkaline field (Fig. 6.2). On $Ol'-Ne'-Qz'$ (not shown) PRINCER, SPEC1, NEDZ1 and SATLIN are classified as subalkaline and the remainder are classified as alkaline.

Samples SPEC1 and NEDZ1, classified as subalkaline on $Ol'-Ne'-Qz'$, but not on alkalis vs. silica, have major element abundances which are indistinguishable from alkaline samples ISKUT and BORDERLK. In contrast, sample LEVELD, which is alkaline on $Ol'-Ne'-Qz'$, and barely alkaline on alkalis vs. silica, has abundances of K_2O and P_2O_5 which are similar to abundances in tholeiitic samples PRINCER and SATLIN. Because of these contrasting elemental and normative mineral classifications these three samples will be called transitional and plotted with the subalkaline samples from $Ol'-Ne'-Qz'$.

All five subalkaline and transitional samples belong to the tholeiitic series on AFM and FeO^*/MgO vs. SiO_2 (Figs. 6.3 and 6.4).

On the AFM diagram, all five samples have total alkalis less than 20% so all of them can be plotted on $TiO_2-K_2O-P_2O_5$ (Fig. 6.5). Four of the five lie within the non-oceanic field, but LEVELD clearly lies within the oceanic field.

On $MnO-TiO_2-P_2O_5$ ISKUTW lies just within the OIT field, but the remaining twenty samples lie within the OIA field (Fig. 6.6).

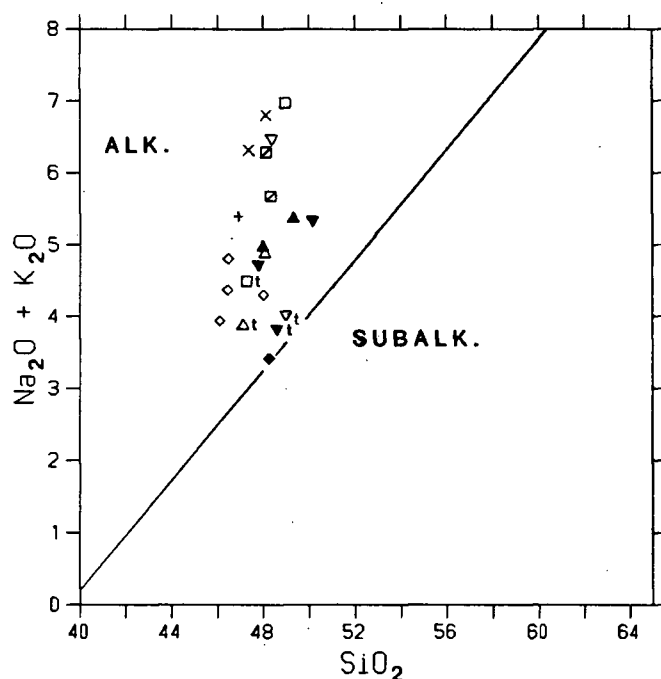


Fig. 6.2. Total alkalis vs. silica. Subalkaline/alkaline boundary from MacDonald (1968).

| | |
|------------|-----------|
| AYNSH1 X | AYNSH2 X |
| PRINCER ◆ | MT DUNN ◇ |
| ISKUT ◇ | ISKUTW ◇ |
| BORDERLK ◇ | BOWSER + |
| EDZ1 ▲ | EDZ2 ▲ |
| SPEC1 ▲ | SPEC2 ▲ |
| NEDZ1 □ | NEDZ2 □ |
| NEDZ3 □ | NEDZ4 □ |
| LEVEL1 ▼ | LEVEL2 ▼ |
| LEVELD ▼ | SATLIN ▼ |
| NATLIN ▼ | |

Fig. 6.3. AFM diagram. Tholeiitic/calcalkaline boundary from Irvine and Baragar (1971).

| |
|-----------|
| PRINCER ◆ |
| SPEC1 ▲ |
| NEDZ1 □ |
| LEVELD ▼ |
| SATLIN ▼ |

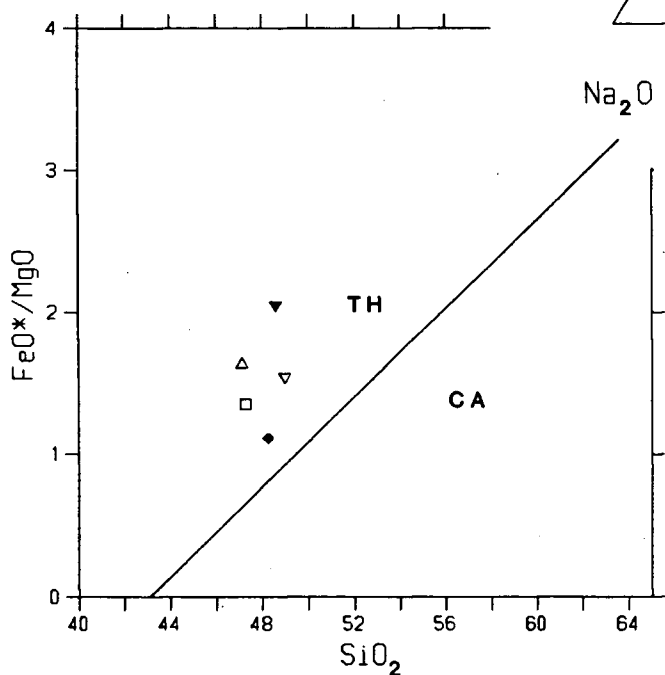
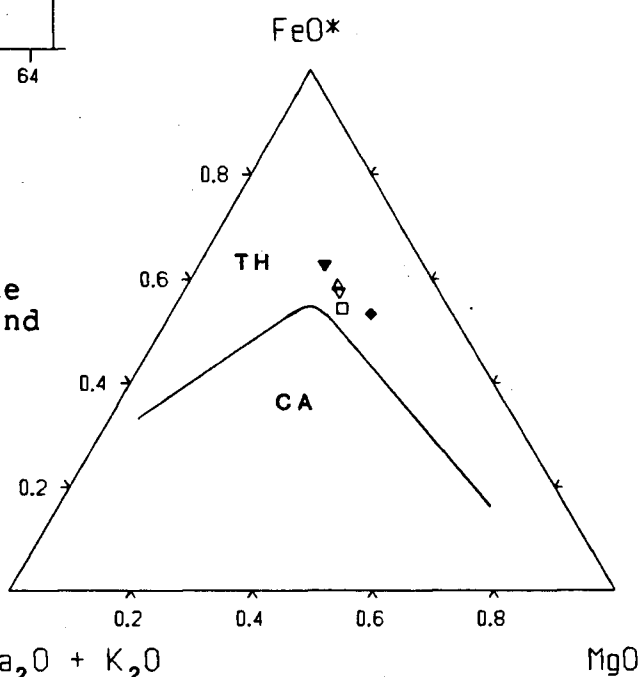


Fig. 6.4. FeO*/MgO vs. SiO₂. Tholeiitic/calcalkaline boundary from Miyashiro (1974).

Four of the five subalkaline and transitional samples lie within the OI field on $\text{MgO-FeO}^*-\text{Al}_2\text{O}_3$ (Fig. 6.7). LEVELD lies within the continental basalt field.

6.2.2 TRACE ELEMENT CLASSIFICATIONS

All twenty-one samples clearly lie within the WPB field on Ti-Zr-Y (Fig. 6.8), therefore Ti-Zr-Sr is not needed.

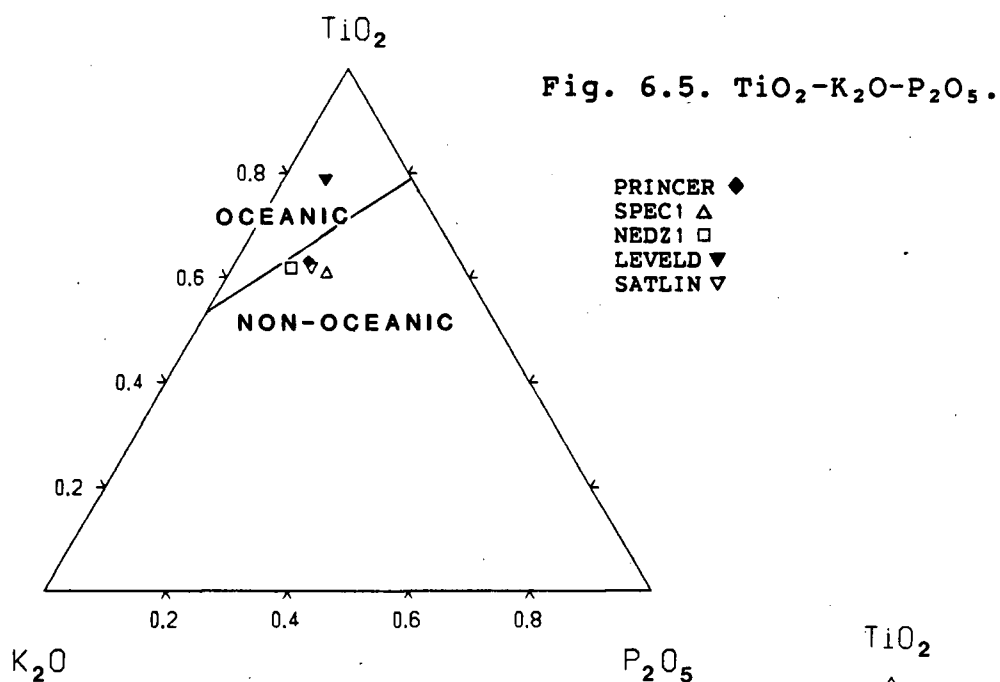
On V vs. Ti/1000 all samples analyzed for V have Ti/V ratios greater than 50 and lie within the WPB field (Fig. 6.9). Tholeiitic samples PRINCER and SATLIN have the lowest Ti/V ratios and are slightly separated from the remaining nineteen samples.

All samples clearly lie within the WPB field on Ti/Y vs. Nb/Y (Fig. 6.10). Samples from the locations just to the north of the Mount Edziza Complex (the NEDZ samples) have the highest Ti/Y and Nb/Y ratios.

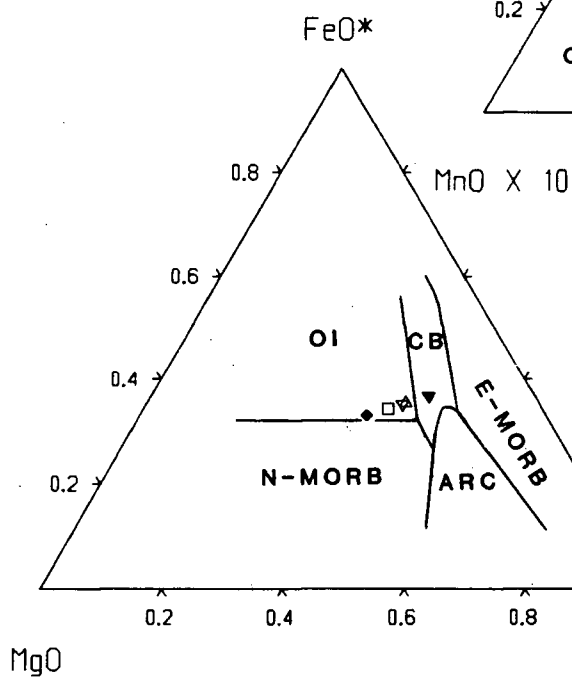
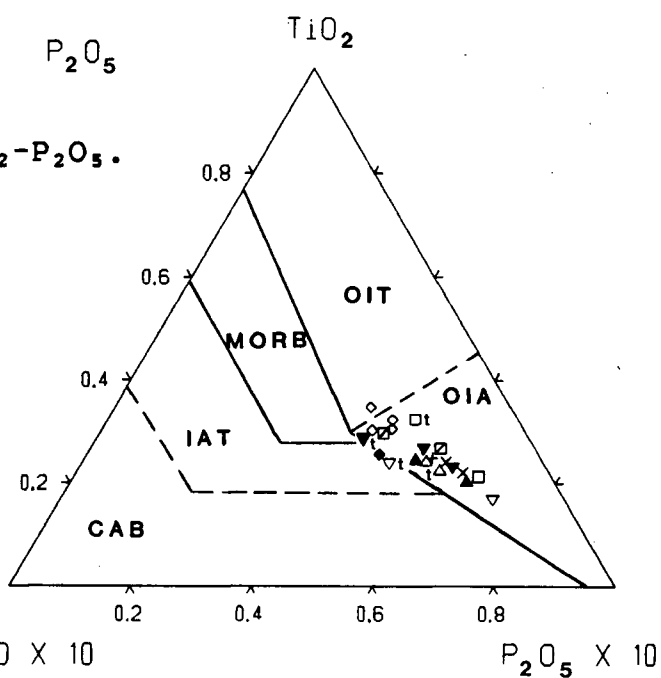
On Ti/Cr vs. Ni all samples plot within the TH MORB field or along the boundary between the IAT and TH MORB fields (Fig. 6.11). AYNH1 and AYNH2 lie far from the remainder of the suite because of their high Ti/Cr ratios.

6.2.3 TRACE AND REE CLASSIFICATIONS

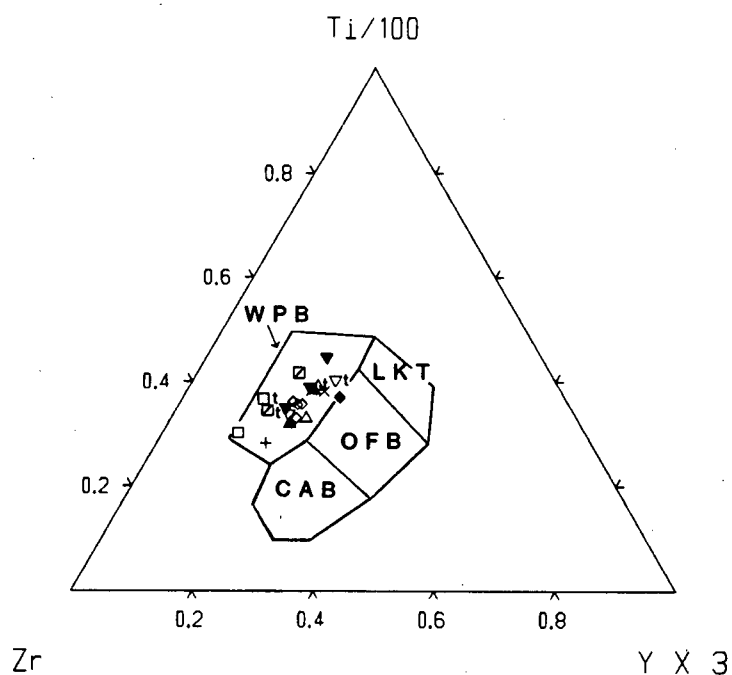
On Cr vs. Ce/Sr approximately two-thirds of the samples lie within or close to the overlapping MORB-WPB

Fig. 6.6. MnO - TiO_2 - P_2O_5 .

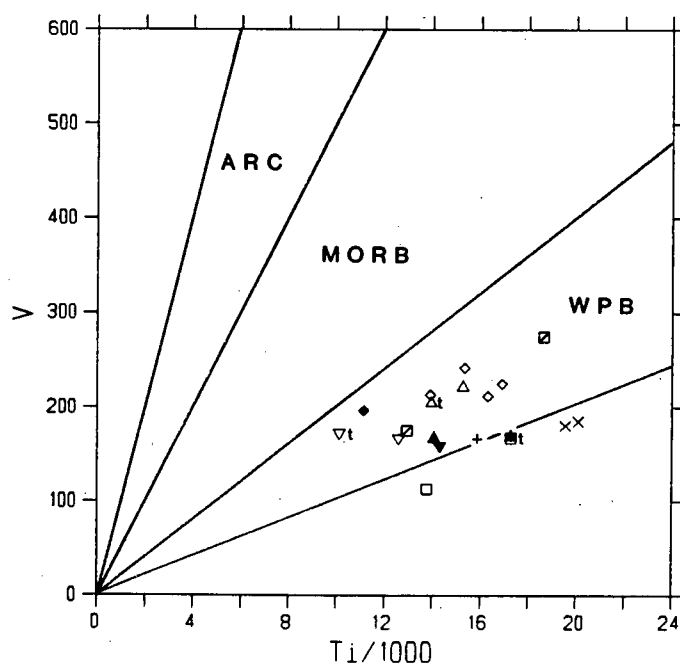
| | |
|-----------------------------|-----------------------------|
| AYNSH1 \times | AYNSH2 \times |
| PRINCER \blacklozenge | MT DUNN \diamond |
| ISKUT \diamond | ISKUTW \diamond |
| BORDERLK \diamond | BOWSER $+$ |
| EDZ1 \blacktriangle | EDZ2 \blacktriangle |
| SPEC1 \triangle | SPEC2 \triangle |
| NEDZ1 \square | NEDZ2 \square |
| NEDZ3 \square | NEDZ4 \square |
| LEVEL1 \blacktriangledown | LEVEL2 \blacktriangledown |
| LEVELD \blacktriangledown | SATLIN \triangledown |
| NATLIN \triangledown | |

Fig. 6.7.
 MgO - FeO^* - Al_2O_3 .

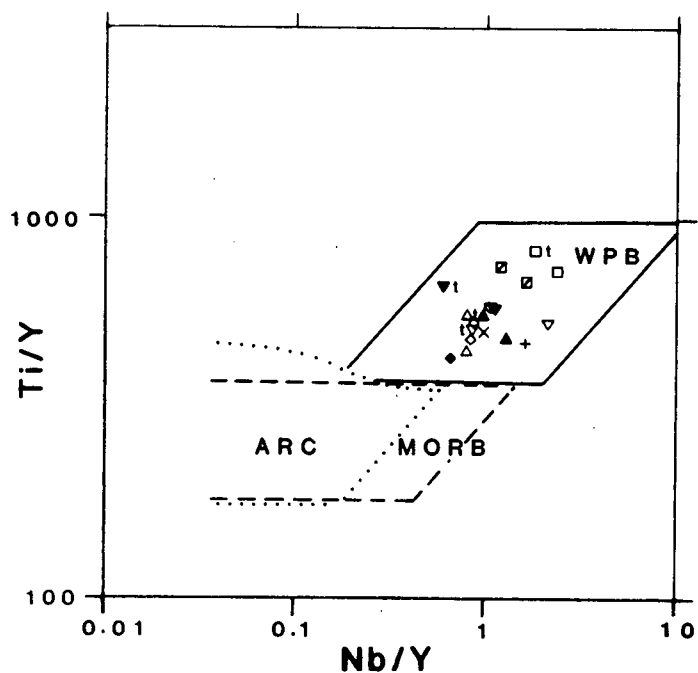
PRINCER \blacklozenge
 SPEC1 \triangle
 NEDZ1 \square
 LEVELD \blacktriangledown
 SATLIN \triangledown



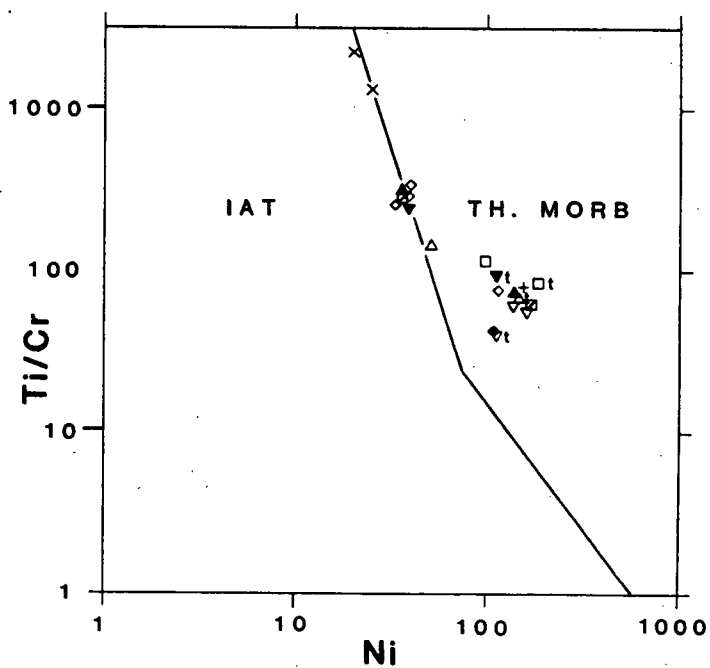
| | |
|------------|-----------|
| AYNSH1 X | AYNSH2 X |
| PRINCER ◆ | MT DUNN ◇ |
| ISKUT ◇ | ISKUTW ◇ |
| BORDERLK ◇ | BOWSER + |
| EDZ1 ▲ | EDZ2 ▲ |
| SPEC1 △† | SPEC2 △ |
| NEDZ1 □† | NEDZ2 □ |
| NEDZ3 □ | NEDZ4 □ |
| LEVEL1 ▼ | LEVEL2 ▼ |
| LEVELD ▼† | SATLIN ▼† |
| NATLIN ▼ | |



Figs. 6.8 and 6.9. Ti-Zr-Y (above) and V vs. Ti/1000 (below).



| | |
|------------|-----------|
| AYNSH1 X | AYNSH2 X |
| PRINCER ◆ | MT DUNN ◇ |
| ISKUT ◇ | ISKUTW ◇ |
| BORDERLK ◇ | BOWSER + |
| EDZ1 ▲ | EDZ2 ▲ |
| SPEC1 △ | SPEC2 △ |
| NEDZ1 □ | NEDZ2 □ |
| NEDZ3 □ | NEDZ4 □ |
| LEVEL1 ▼ | LEVEL2 ▼ |
| LEVELD ▼ | SATLIN ▼ |
| NATLIN ▼ | |



Figs. 6.10 and 6.11. Ti/Y vs. Nb/Y (above) and Ti/Cr vs. Ni (below).

fields (Fig. 6.12). AYNSH1 and AYNSH2 have very low abundances of Cr and lie below the WPB field although their Ce/Sr ratios are within the range of MORB-WPB samples. The five remaining samples lie within the ARC field.

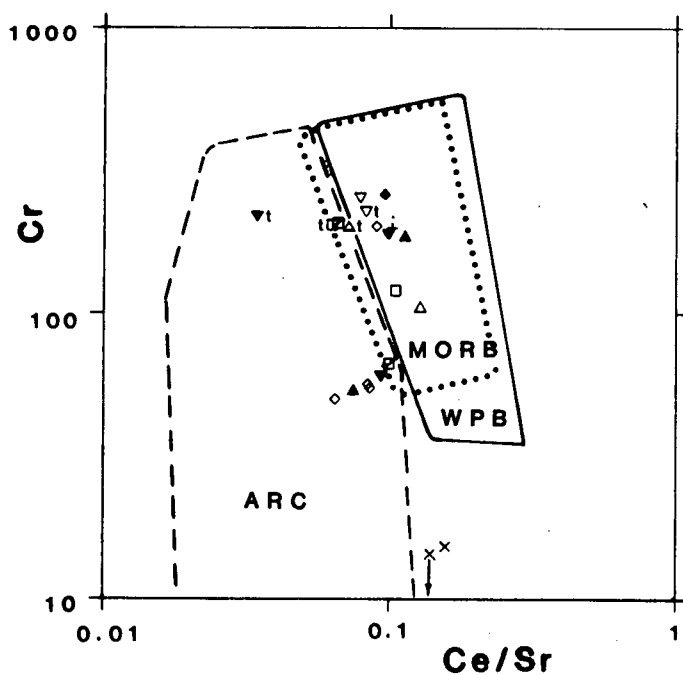
On Cr vs. Y all samples, except NEDZ3, lie within or close to the overlapping ARC-MORB-WPB or ARC-WPB fields (Fig. 6.13). Relative to the other samples NEDZ3 is slightly depleted in both Cr and Y and clearly lies within the ARC field.

Twelve of the twenty-one samples have Ba/La ratios greater than 15 and lie within or close to the orogenic andesite field on La vs. Ba (Fig. 6.14). Seven samples lie within the field for WPB (E-MORB) and two lie within the N-MORB field, with Ba/La ratios less than 11.

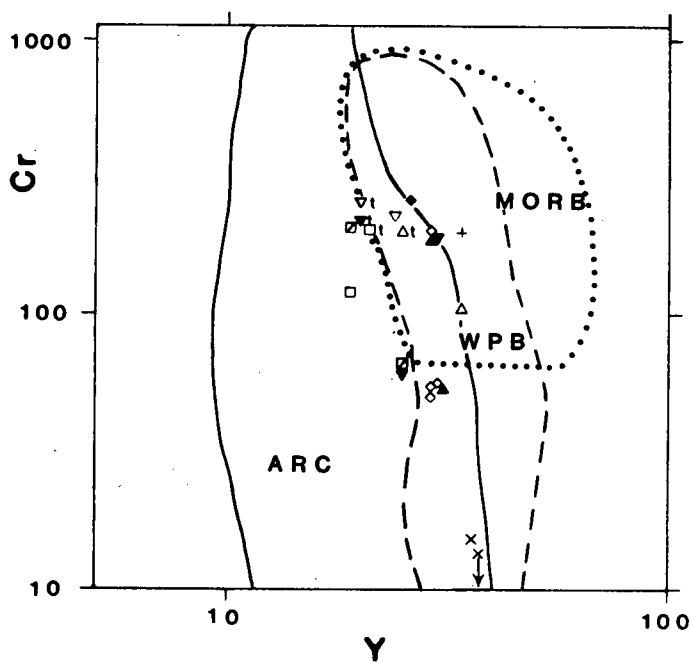
In contrast, on $(\text{Ba/La})_{\text{CH}}$ vs. $(\text{La/Sm})_{\text{CH}}$ nineteen of the twenty-one samples lie within or close to the ocean basalt field and only two (AYNSH1 and AYNSH2) are sufficiently enriched in Ba to clearly lie within the overlapping ocean and ARC fields (Fig. 6.15).

All twenty-one samples are classified as WPB (E-MORB) on La vs. Th (Fig. 6.16). Out of these, only two (NEDZ4 and SATLIN) lie within the overlapping WPB and ARC fields.

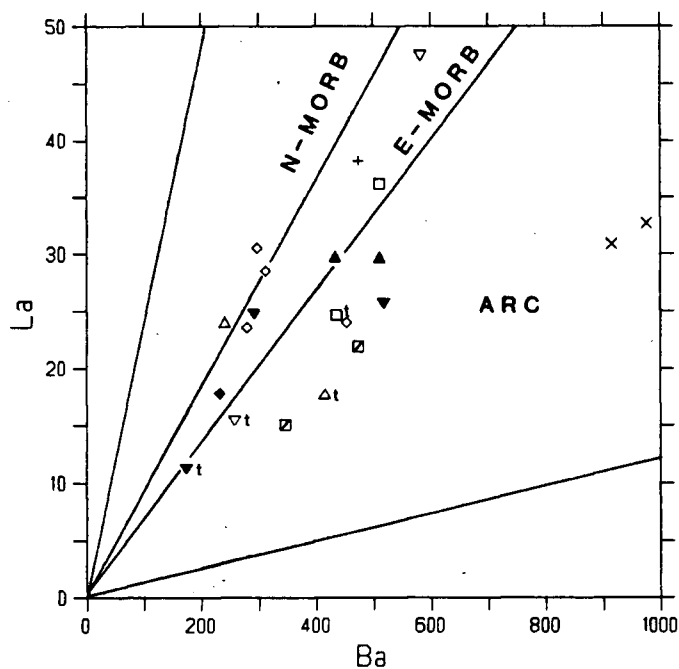
On La vs. Nb all samples lie within or on the border of the WPB (E-MORB) field (Fig. 6.17). Excluding NEDZ1, subalkaline and transitional samples have the



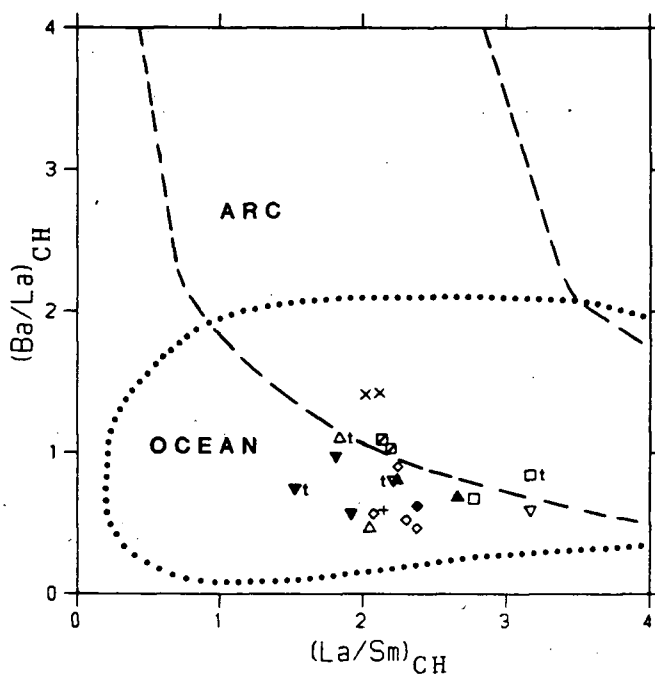
| | |
|------------|-----------|
| AYNSH1 X | AYNSH2 X |
| PRINCER ◆ | MT DUNN ◆ |
| ISKUT ◇ | ISKUTW ◇ |
| BORDERLK ◇ | BOWSER + |
| EDZ1 ▲ | EDZ2 ▲ |
| SPEC1 Δ | SPEC2 Δ |
| NEDZ1 □ | NEDZ2 □ |
| NEDZ3 □ | NEDZ4 □ |
| LEVEL1 ▼ | LEVEL2 ▼ |
| LEVELD ▼ | SATLIN ▼ |
| NATLIN ▼ | |



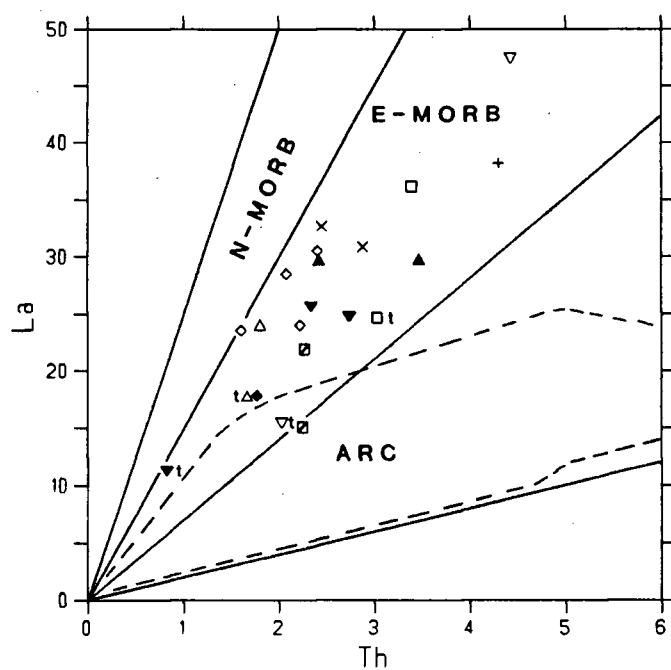
Figs. 6.12 and 6.13. Cr vs. Ce/Sr (above) and Cr vs. Y (below).



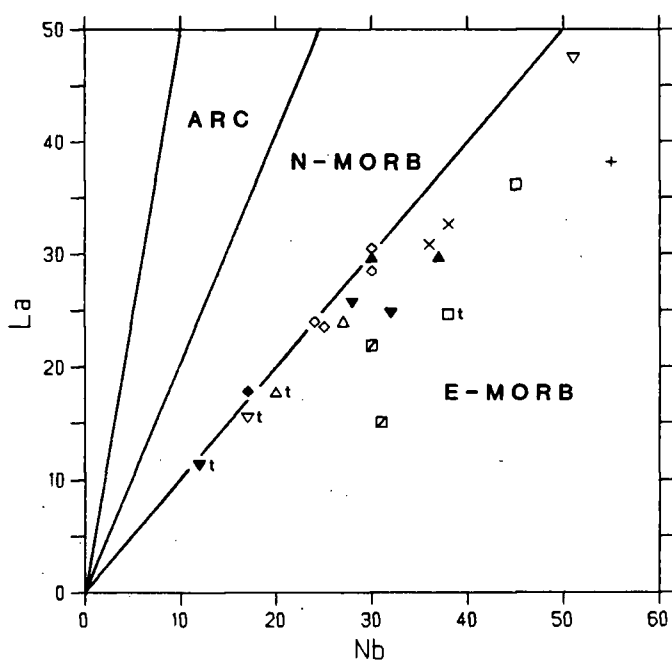
| | |
|-----------------------|-----------------------|
| AYNSH1 x | AYNSH2 x |
| PRINCER ◊ | MT DUNN ◊ |
| ISKUT ◊ | ISKUTW ◊ |
| BORDERLK ◊ | BOWSER + |
| EDZ1 ▲ | EDZ2 ▲ |
| SPEC1 Δ _t | SPEC2 Δ |
| NEDZ1 ◻ _t | NEDZ2 ◻ |
| NEDZ3 ◻ | NEDZ4 ◻ |
| LEVEL1 ▼ | LEVEL2 ▼ |
| LEVELD ▼ _t | SATLIN ▼ _t |
| NATLIN ▼ | |



Figs. 6.14 and 6.15. La vs. Ba (above) and $(\text{Ba}/\text{La})_{\text{CH}}$ vs. $(\text{La}/\text{Sm})_{\text{CH}}$ (below).



| | |
|------------|-----------|
| AYNSH1 X | AYNSH2 X |
| PRINCER ◆ | MT DUNN ◆ |
| ISKUT ◇ | ISKUTW ◇ |
| BORDERLK ◇ | BOWSER + |
| EDZ1 ▲ | EDZ2 ▲ |
| SPEC1 △ | SPEC2 △ |
| NEDZ1 □ | NEDZ2 □ |
| NEDZ3 □ | NEDZ4 □ |
| LEVEL1 ▼ | LEVEL2 ▼ |
| LEVELD ▼ | SATLIN ▼ |
| NATLIN ▼ | |



Figs. 6.16 and 6.17. La vs. Th (above) and La vs. Nb (below).

lowest La and Nb abundances, although their La/Nb ratios are similar to ratios from the alkaline samples.

All samples lie within or just outside of the overlapping WPB - MORB fields on K_2O/Yb vs. Ta^*/Yb (Fig. 6.18). Three samples (NEDZ1, NEDZ3 and NATLIN) have relatively high K_2O/Yb and Ta^*/Yb ratios and lie towards the non-overlapping WPB field, whereas LEVELD has much lower K_2O/Yb and Ta^*/Yb ratios and lies toward the non-overlapping MORB field.

On Th/Yb vs. Ta^*/Yb all samples clearly lie within the overlapping WPB-MORB fields (Fig. 6.19) and on $Th-Hf/3-Ta^*$ all samples lie within the fields for alkaline and tholeiitic WPB (E-MORB) (Fig. 6.20)

6.2.4 BULK EARTH NORMALIZED DIAGRAMS (BEND)

To clarify BEND patterns samples were divided into six groups (Figs. 6.21, 6.22, 6.23, 6.24, 6.25 and 6.26). In general all patterns have convex-up WPB-like shapes, most of them display positive Eu anomalies and all of them show slight enrichment in K relative to an oceanic WPB (Thompson et al., 1983 and 1984).

Tholeiitic samples PRINCER and SATLIN are plotted on Fig. 6.21. These patterns are fairly flat from Ba to La and then slope negatively towards Lu, with a concave-up dip from Sm to Eu. The pattern from transitional sample LEVELD also appears on Fig. 6.21. It is markedly enriched in Ba relative to Rb, has 'peaks'

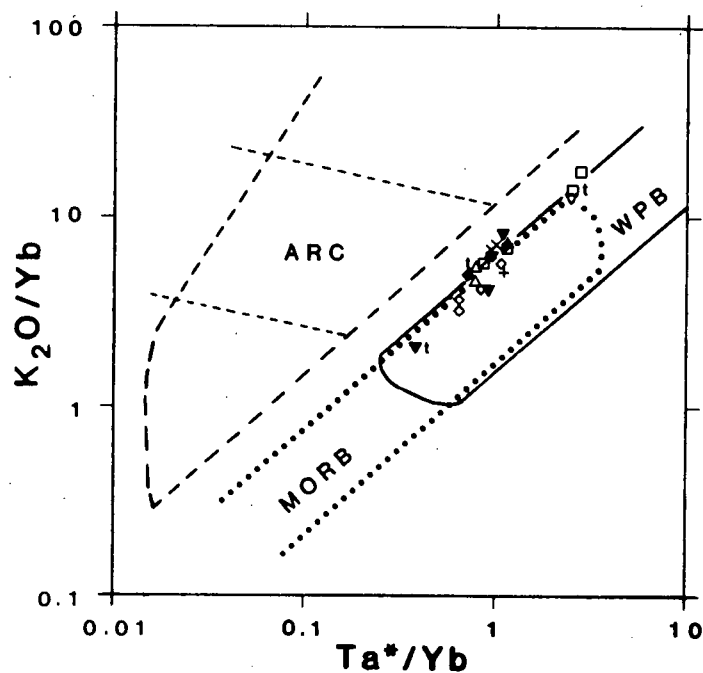


Fig. 6.18. K_2O/Yb vs. Ta^*/Yb .

| | |
|------------|-----------|
| AYNSH1 X | AYNSH2 X |
| PRINCER ◆ | MT DUNN ◆ |
| ISKUT ◆ | ISKUTW ◆ |
| BORDERLK ◆ | BOWSER + |
| EDZ1 ▲ | EDZ2 ▲ |
| SPEC1 ▲ | SPEC2 ▲ |
| NEDZ1 □ | NEDZ2 □ |
| NEDZ3 □ | NEDZ4 □ |
| LEVEL1 ▼ | LEVEL2 ▼ |
| LEVELD ▼ | SATLIN ▼ |
| NATLIN ▼ | |

Fig. 6.19. Th/Yb vs. Ta^*/Yb .

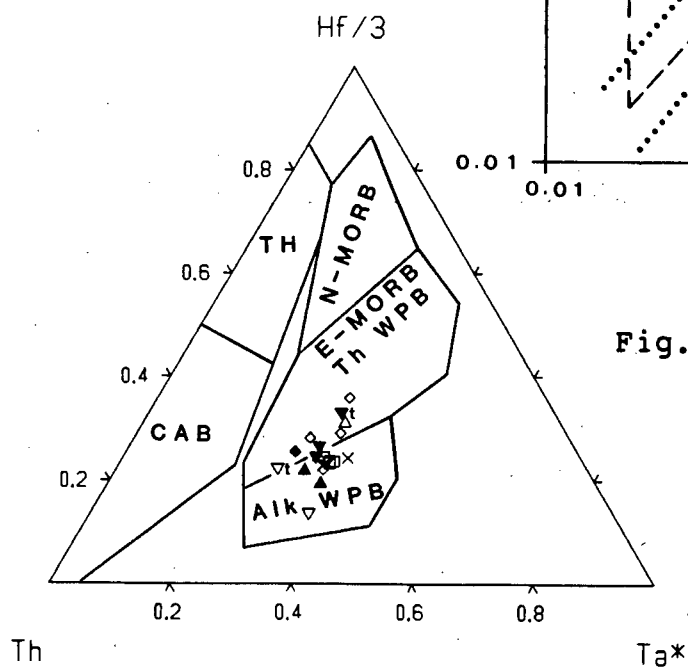
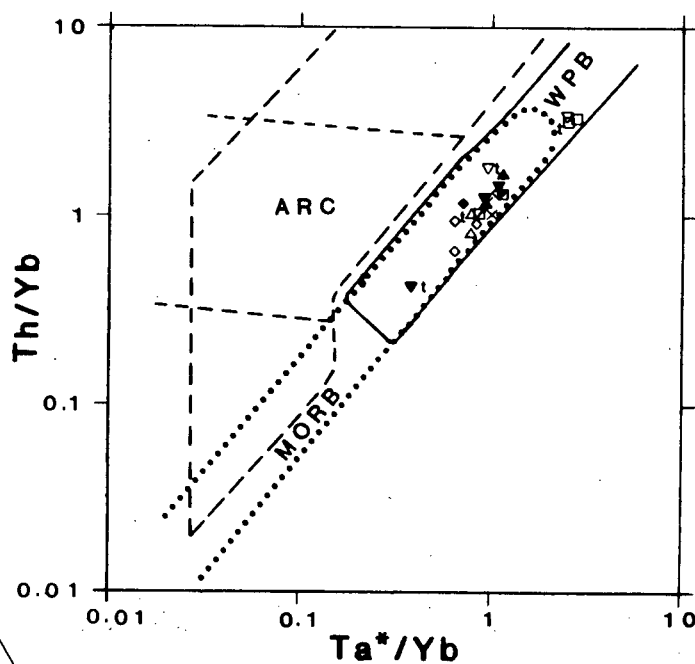


Fig. 6.20. $Th-Hf/3-Ta^*$.

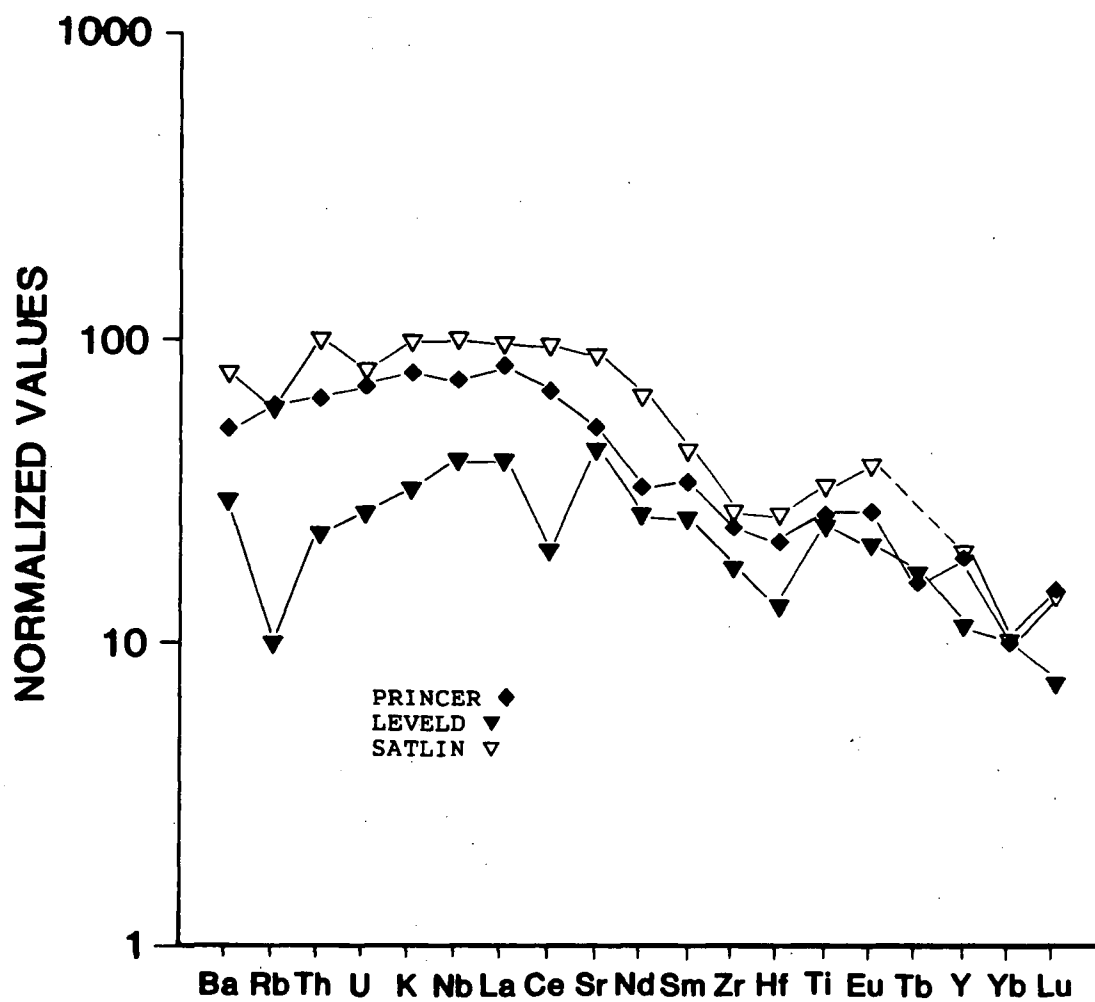


Fig. 6.21. BEN diagram for samples PRINCER, LEVELD and SATLIN.

at Sr and Ti and 'troughs' at Ce and Hf. Excluding Ba enrichment, this latter pattern grossly resembles the BEND pattern from an E-MORB (Fig. 2.25).

Fig. 6.22 has patterns from AYNSh1, AYNSh2 and BOWSER. The former two samples are enriched in Ba relative to Rb and have 'troughs' at Sr. This is unusual because both of them have large positive Eu anomalies. The pattern from BOWSER has a slight 'trough' at Nd and no Eu anomaly.

Samples on Fig. 6.23 are from the Iskut River area. All four patterns are remarkably similar with 'typical' WPB shapes (Thompson et al., 1983). ISKUT is enriched in Ba relative to Rb and MT DUNN has 'troughs' at Ce and Hf.

Patterns displayed on Fig. 6.24 are from the Mount Edziza Volcanic Complex. SPEC1 and EDZ2 are enriched in Ba relative to Rb, but otherwise the patterns are almost identical and similar to those on Fig. 6.23.

Fig. 6.25 has patterns from the samples just to the north of the Mount Edziza Complex. The oldest samples, NEDZ1 and NEDZ3, are separated from the younger samples, NEDZ2 and NEDZ4, because of the formers slightly higher abundances of LIL elements and lower abundances of Yb. NEDZ1 and NEDZ3 have the most fractionated patterns but pattern shapes for all four samples are similar. NEDZ2 and NEDZ4 are slightly enriched in Ba relative to Rb, NEDZ2 has a small 'trough' at Sm and NEDZ1 has small

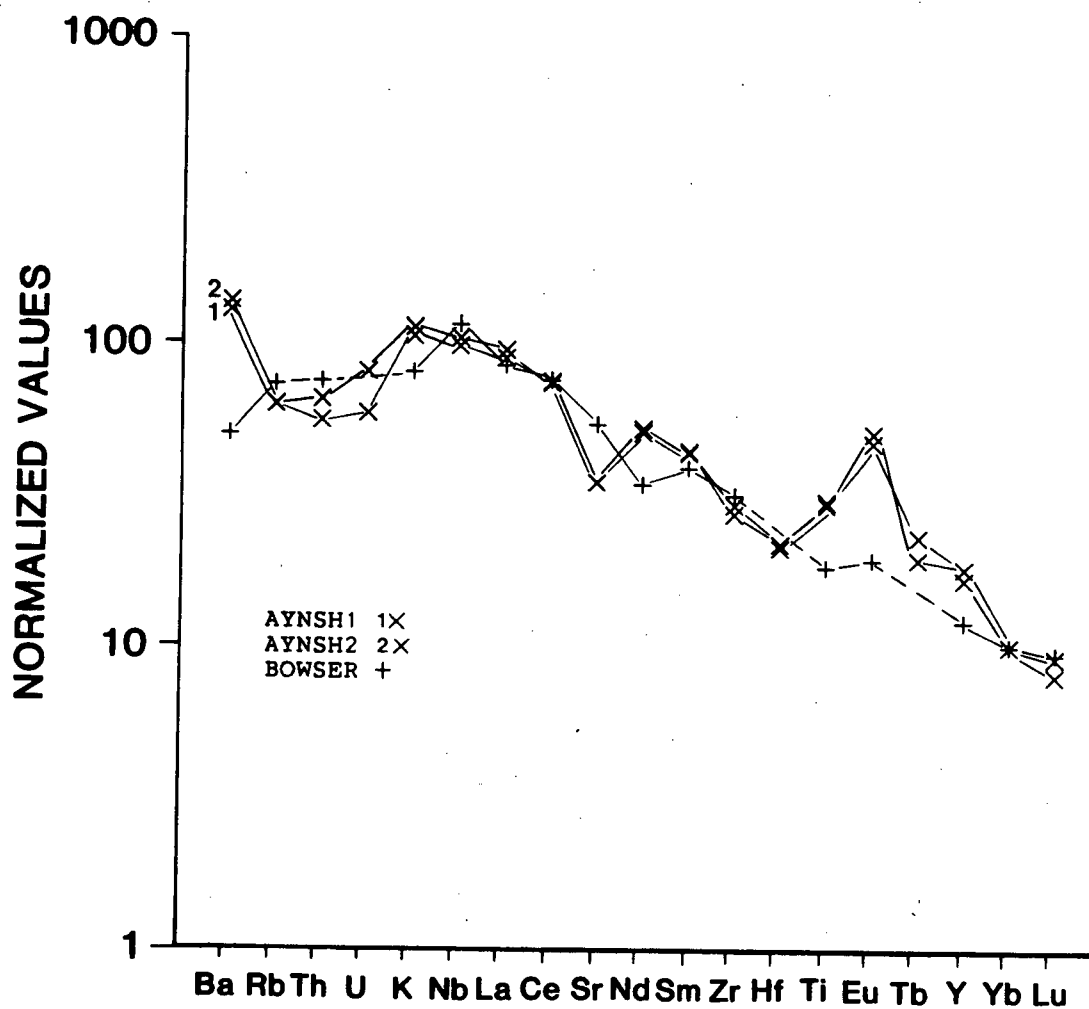


Fig. 6.22. BEN diagram for samples AYNH1, AYNH2 and BOWSER.

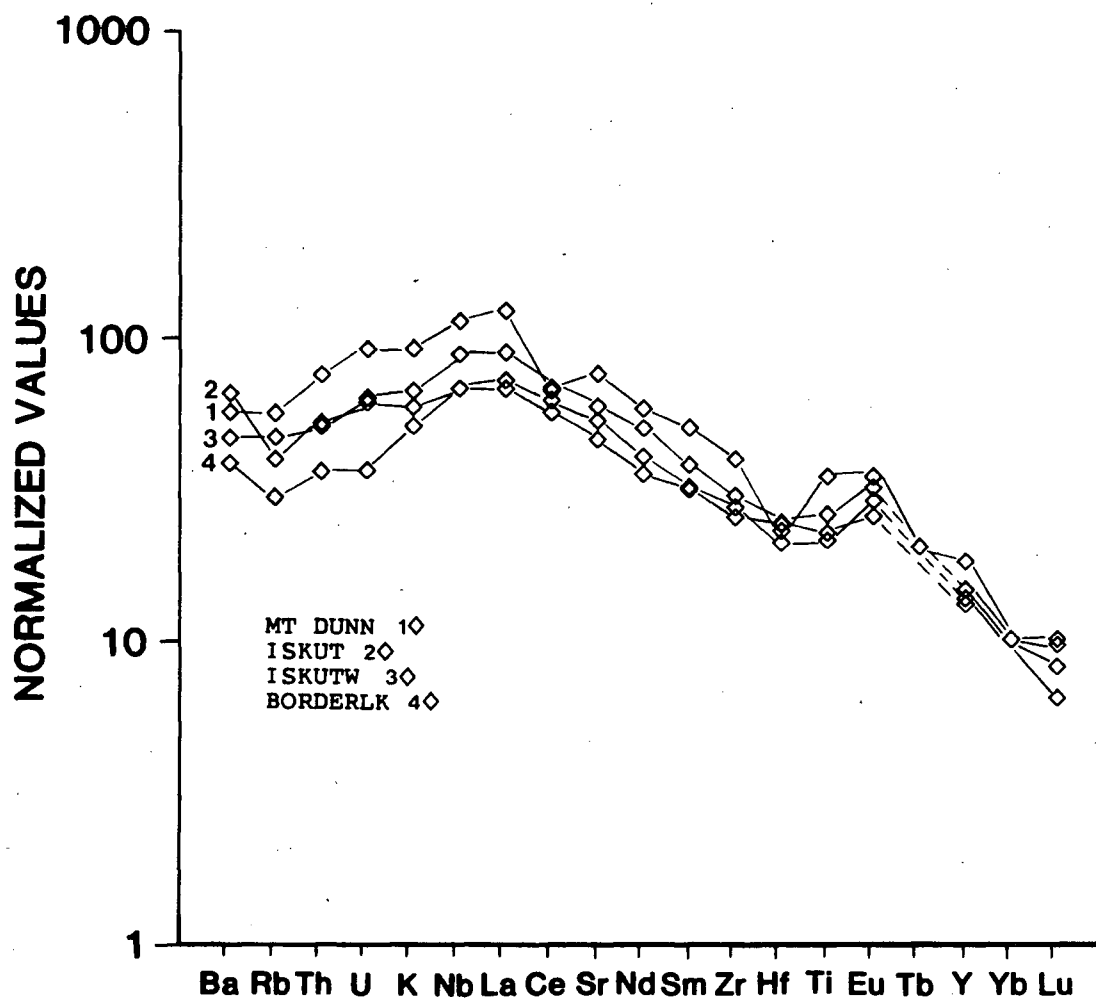


Fig. 6.23. BEN diagram for samples MT DUNN, ISKUT, ISKUTW and BORDERLK.

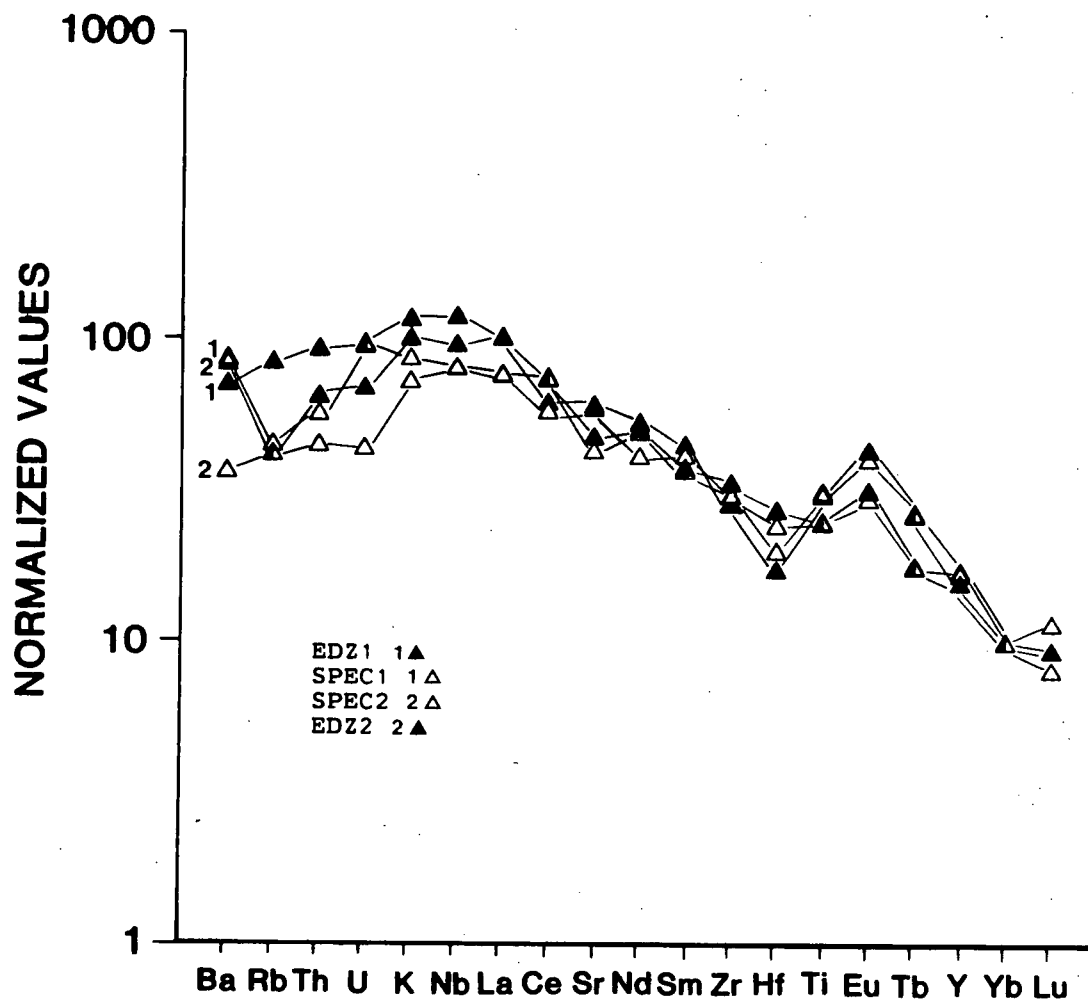


Fig. 6.24. BEN diagram for samples EDZ1, SPEC1, SPEC2, and EDZ2.

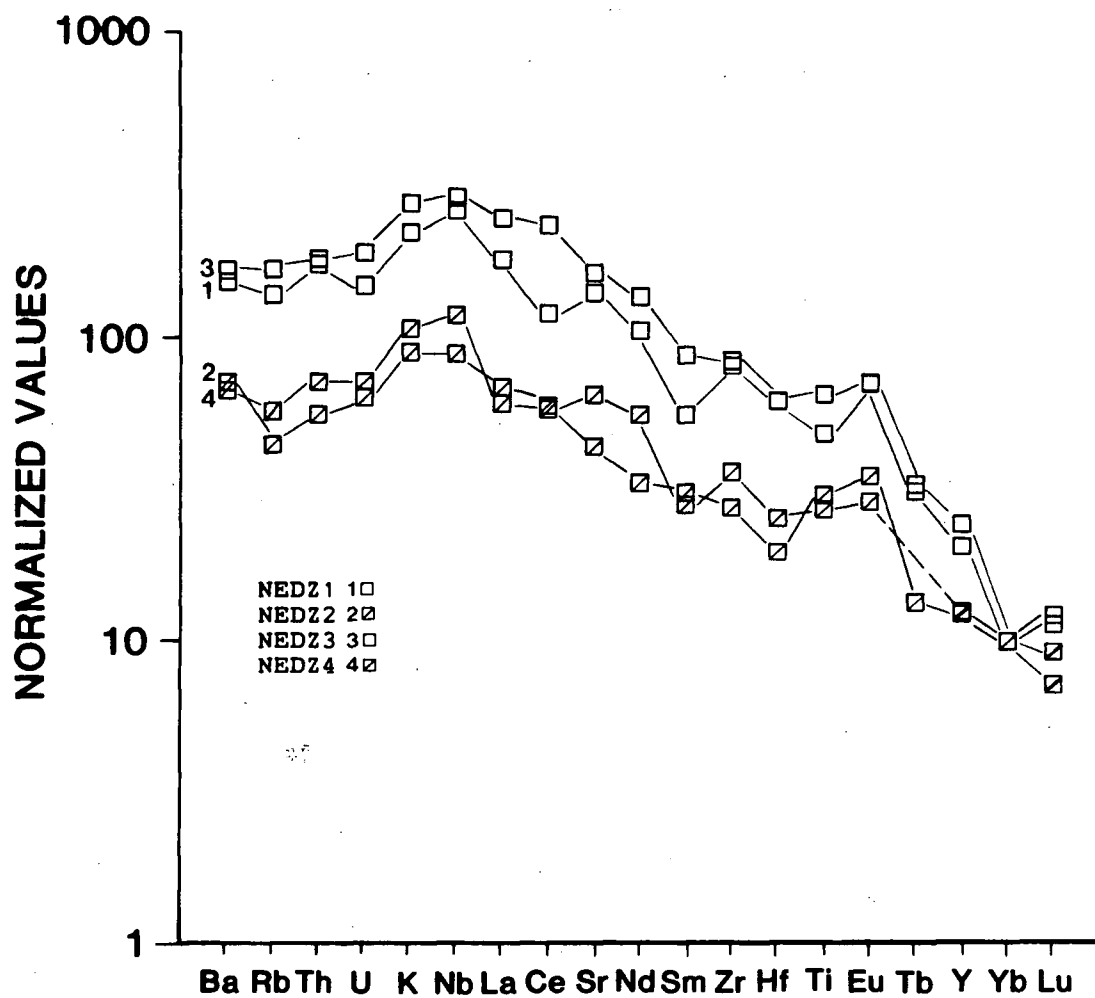


Fig. 6.25. BEN diagram for samples NEDZ1, NEDZ2, NEDZ3, and NEDZ4.

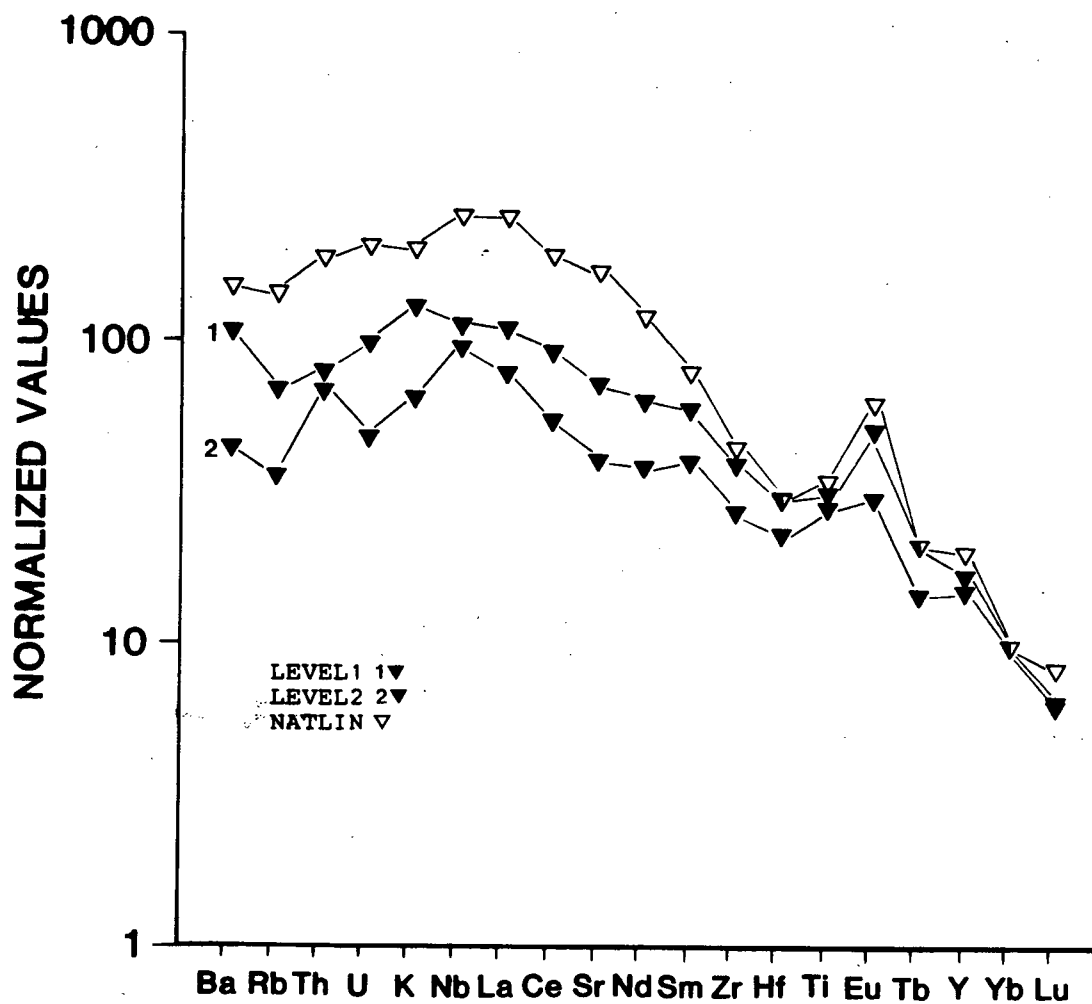


Fig. 6.26. BEN diagram for samples LEVEL1, LEVEL2 and NATLIN.

'peaks' at Sr and Zr.

The two alkaline samples from Level Mountain and the basanite from north of Atlin are plotted on Fig. 6.26. All three patterns have large positive Eu anomalies without a corresponding 'peak' at Sr and LEVEL1 and LEVEL2 are slightly enriched in Ba relative to Rb. Relative to the other 20 BEND patterns, NATLIN's pattern is the most fractionated.

6.3 TRACE ELEMENT CHEMISTRY

As a group the Stikine Belt basalts have abundances of trace and REE and BEND patterns grossly similar to oceanic WPB, but the suite shows considerable internal variation. This is most evident in abundances of Ba, Th, U and Sr. In general the alkaline and transitional samples, excluding LEVELD, have higher abundances of trace and rare earth elements than the two tholeiitic samples (PRINCER and SATLIN), although there is a small amount of overlap.

La abundances in the nineteen alkaline and transitional samples range from 46 to 144 times chondritic, Yb contents lie between 4 and 14 times chondritic and $(La/Yb)_{CH}$ ratios range from 5.9 to 24.5. The highest $(La/Yb)_{CH}$ ratios are from NEDZ1, NEDZ3 and NATLIN, corresponding to their fractionated BEND patterns. Similar abundances and ratios in the two tholeiitic samples are: La = 47 and 54 times chondritic, Yb = 6.8 and 7.7 times chondritic and $(La/Yb)_{CH}$ = 5.9 and 8.

All samples have La/Nb ratios less than or barely greater than 1.0. These ratios are characteristic of ratios in oceanic WPB (Thompson et al., 1983).

Relative to the other twenty samples LEVELD has very low abundances of all LIL elements except Ba. It has an La content of 34.2 times chondritic, a Yb abundance of 9.1 times chondritic and an $(La/Yb)_{CH}$ ratio of 3.83. These geochemical characteristics suggest it came from a source region depleted in LIL by a previous extraction of melt, an interpretation consistent with the E-MORB shape of its BEND pattern (Thirwall and Jones, 1983).

6.3.1 TH AND U

Abundances of Th in samples from the Stikine suite lie between 0.8 and 4.4 ppm and U abundances range from 0.3 to 1.5 ppm (Table V). Th/U ratios are highly variable, range from 1.5 to 4.6 and average 3.0, similar to Th/U ratios from many oceanic WPB (Basaltic Volcanism Study Project, 1981).

6.3.2 TRANSITION ELEMENTS

Samples with low abundances of Cr and Ni, and low Mg' numbers (AYNSH1, AYNH2, IKUTW, MT DUNN, ISKUT, EDZ1, NEDZ2 and LEVEL1) have been more extensively fractionated than the remaining fourteen samples, excluding SPEC2 and NEDZ3, which have higher Cr and Ni abundances and higher Mg' numbers. SPEC2 and NEDZ3,

which are depleted in Ni relative to Cr, probably had a fractionation history which was dominated by the crystallization of olivine rather than clinopyroxene and/or Cr-spinel.

Excluding NEDZ1, NEDZ3 and NATLIN, Sc contents range from 18.1 to 27.1 ppm and average 23 ppm. NEDZ1, NEDZ3 and NATLIN have Sc abundances of 15.7, 11.8 and 17 ppm respectively. These latter three samples also have very low abundances of Yb and Lu, with $(\text{La/Yb})_{\text{CH}}$ ratios greater than 24. Low abundances of Sc suggest fractionation of pyroxene at high pressures, whereas low Yb and Lu abundances and fractionated $(\text{La/Yb})_{\text{CH}}$ ratios suggest small degrees of partial melting of a garnet peridotite (Gast, 1968; Kay and Gast, 1973; Basaltic Volcanism Study Project, 1981; Cullers and Graf, 1984).

6.4 SR ISOTOPES

Available $^{87}\text{Sr}/^{86}\text{Sr}$ ratios from the Stikine Belt samples range from 0.7030 to 0.7039, except sample BOWSER which has an $^{87}\text{Sr}/^{86}\text{Sr}$ ratio of 0.7023 (Table V) (Hamilton, 1981; UBC geochronology lab). These ratios are mostly within the range for ocean islands (0.7028 to 0.706), are the same as those observed in the Anahim Volcanic Belt and Chilcotin Group Basalts and indicate an uncontaminated mantle source for these basalts. The low Sr isotopic ratio in sample BOWSER is typical of a MORB rather than a WPB, and suggests this sample came from an isotopically depleted source.

6.5 DISCUSSION OF DISCRIMINATION DIAGRAMS

Stikine Volcanic Belt samples are classified as WPB on almost all major, trace and rare earth element tectonic discrimination diagrams. Major exceptions to this classification are seen on Cr vs. Ce/Sr (Fig. 6.12), Cr vs. Y (Fig. 6.13) and La vs. Ba (Fig. 6.14) On these diagrams some of the samples lie within the ARC field because of their low Ce/Sr ratios, low Y abundances or high Ba abundances.

Low Ce/Sr ratios, observed on Cr vs. Ce/Sr, are generally caused by an increase in the Sr content, or more unusually as in LEVELD and ISKUTW, by a decrease in the abundance of Ce, both of which are evident on BEND. Increased Sr abundances probably result from an accumulation of plagioclase in the analyzed samples (note also the positive Eu anomalies) but Ce depletion is less easily explained as there are no minerals which preferentially incorporate Ce (Cullers and Graf, 1984). Slightly higher Ce/Sr ratios in samples from the Aiyaniish flow reflect their negative Sr anomalies on BEND. These anomalies suggest plagioclase fractionation and removal in the source, but large positive Eu anomalies in these same samples suggests the analyzed rocks may have contained cumulate plagioclase.

Variations in the Y content, affecting classifications on Cr vs. Y, reflect either a heterogeneous source, variable degree of partial melting, and/or the presence/absence of a residual phase which contains Y, such as garnet, zircon,

sphene or apatite (Pearce, 1982; Clague and Frey, 1982).

Ba enrichment which shows up on La vs. Ba and BEND is atypical for oceanic or continental WPB and suggests interaction with an alkali rich volatile phase (Clague and Frey, 1982). Interaction with such a phase could also produce the slight enrichment in K relative to Nb, seen on BEND and K_2O/Yb vs. Ta^*/Yb . An alkali-rich volatile phase may also provide an explanation for the increased abundances of Sr.

LEVELD lies towards the MORB (oceanic) field on many of the tectonic discrimination diagrams because of its depletion in LIL elements relative to an 'average' WPB. The towards-MORB classification provides additional evidence of its MORB-like depleted source.

The only tholeiitic samples in this suite are located at the western edge of the Stikine Belt. PRINCER is also the southernmost sample and SATLIN, nearly the northernmost, is older than all of the rest. From these observations it is possible that these tholeiites do not strictly represent the Stikine Belt. Because SATLIN is markedly older than all of the other samples and lies near the Miocene Wrangell Belt in the Yukon, it may be an outlier of the Wrangell Arc whose activity is now restricted to Alaska, whereas PRINCER may be the result of the small component of Pacific Plate subduction along the Queen Charlotte fault. However, all tectonic discrimination diagrams classify these two samples as WPB with no evidence for an ARC-like component.

6.6 SUMMARY

Sixteen of the twenty-one basaltic samples from the Stikine Volcanic Belt were classified as alkaline WPB on all chemical and tectonic discrimination diagrams studied. Three of the remaining samples were classified as alkaline/transitional WPB, and the last two were classified as tholeiitic WPB. HOODOO was classified as peralkaline and was not plotted on any of the tectonic discrimination diagrams. Most major, trace and rare earth element abundances and Sr isotope ratios in the basaltic samples are similar to abundances in WPB from the Anahim Volcanic Belt, the Chilcotin Group Basalts and Hawaii.

Enriched contents of Ba, K ± Sr which produce anomalous classifications on Cr vs. Ce/Sr, Cr vs. Y and La vs. Ba are attributed to interaction with an alkali-rich volatile phase. Sr enrichment may also be caused by cumulate plagioclase in the sample, a more likely explanation when there is a corresponding enrichment in Eu (positive Eu anomaly). AYNSH1 and AYNSH2 are depleted in Sr but enriched in Eu, suggesting a complex history involving both plagioclase fractionation and accumulation.

LEVELD is depleted in LIL, has a low $(La/Yb)_{CH}$ ratio, lies towards the MORB field on many of the tectonic discrimination diagrams and has a BEND pattern with an E-MORB shape. These characteristics imply a source region depleted in LIL by a previous extraction of melt.

The two tholeiitic series basalts are unusual in this predominantly alkaline-peralkaline volcanic belt and since they lie nearest to the continental margin may be related to Pacific Plate subduction, although discrimination diagrams do not support this suggestion.

TABLE V STIKINE VOLCANIC BELT

Major, trace and rare earth element abundances, Sr isotope ratios, K/Ar dates and ages.

| Series Name | PRINCER Tholeiite Basalt | AYNSH1 Alkaline Hawaiite | AYNSH2 Alkaline Hawaiite | HOODOO Peralk. Trachyte | BORDERLK Alkaline Alk. Bas. | ISKUTW Alkaline Alk. Bas. | MT DUNN Alkaline Alk. Bas. | ISKUT Alkaline Hawaiite |
|------------------------------------|--------------------------------|--------------------------------|--------------------------------|-------------------------------|-----------------------------------|---------------------------------|----------------------------------|-------------------------------|
| LAT. | 54 26.0 | 55 06.5 | 55 11.0 | 56 46.5 | 56 21.5 | 56 24.0 | 56 29.5 | 56 43.0 |
| LONG. | 130 29.5 | 128 54.0 | 129 12.0 | 131 19.5 | 130 43.0 | 130 53.0 | 130 39 | 130 37.0 |
| SiO ₂ | 48.26 | 47.38 | 48.13 | 59.18 | 46.13 | 46.48 | 46.46 | 48.01 |
| TiO ₂ | 1.86 | 3.35 | 3.26 | 0.33 | 2.56 | 2.72 | 2.82 | 2.32 |
| Al ₂ O ₃ | 13.38 | 14.54 | 14.73 | 15.28 | 14.69 | 16.53 | 15.24 | 16.61 |
| Fe ₂ O ₃ | 13.08 | 15.55 | 14.80 | 10.24 | 13.55 | 13.93 | 14.49 | 13.24 |
| FeO | 0.0 | 0.0 | 0.0 | 0.0 | 0.0 | 0.0 | 0.0 | 0.0 |
| MnO | 0.19 | 0.22 | 0.21 | 0.27 | 0.18 | 0.18 | 0.18 | 0.19 |
| MgO | 10.56 | 4.24 | 3.58 | 0.03 | 8.72 | 6.01 | 7.58 | 5.71 |
| CaO | 8.90 | 7.58 | 7.55 | 1.58 | 9.84 | 9.03 | 8.46 | 9.30 |
| Na ₂ O | 2.67 | 4.71 | 5.09 | 7.79 | 3.15 | 3.86 | 3.35 | 3.43 |
| K ₂ O | 0.74 | 1.60 | 1.70 | 5.28 | 0.78 | 0.94 | 1.01 | 0.86 |
| P ₂ O ₅ | 0.35 | 0.83 | 0.94 | 0.03 | 0.40 | 0.33 | 0.41 | 0.34 |
| Ba | 232.0 | 915.0 | 976.0 | 0.0 | 279.0 | 312.0 | 297.0 | 453.0 |
| Rb | 14.0 | 23.0 | 23.0 | 107.0 | 11.0 | 16.0 | 15.0 | 14.0 |
| Th | 1.8 | 2.9 | 2.4 | 15.4 | 1.6 | 2.1 | 2.4 | 2.2 |
| U | 0.6 | 1.1 | 0.8 | 1.0 | 0.5 | 0.8 | 0.9 | 0.8 |
| Nb | 17.0 | 36.0 | 38.0 | 171.0 | 25.0 | 30.0 | 30.0 | 24.0 |
| La | 17.8 | 30.9 | 32.6 | 128.5 | 23.5 | 28.5 | 30.5 | 24.0 |
| Ce | 38.9 | 68.5 | 67.3 | 294.2 | 52.0 | 57.8 | 44.3 | 54.5 |
| Sr | 406.0 | 437.0 | 435.0 | 0.1 | 581.0 | 689.0 | 687.0 | 641.0 |
| Nd | 13.8 | 35.1 | 33.9 | 117.5 | 23.9 | 31.3 | 28.3 | 26.1 |
| Sm | 4.6 | 9.4 | 9.5 | 27.0 | 7.0 | 7.7 | 7.9 | 6.6 |
| Zr | 112.0 | 215.0 | 200.0 | 1139.0 | 189.0 | 205.0 | 211.0 | 195.0 |
| Hf | 2.9 | 4.6 | 4.7 | 22.8 | 5.3 | 4.9 | 3.6 | 4.4 |
| Eu | 1.4 | 3.7 | 4.0 | 3.0 | 2.1 | 2.4 | 2.0 | 2.2 |
| Tb | 0.5 | 1.2 | 1.0 | N/A | N/A | N/A | 0.8 | N/A |
| Y | 26.0 | 36.0 | 39.0 | 116.0 | 29.0 | 30.0 | 29.0 | 29.0 |
| Yb | 1.5 | 2.4 | 2.4 | 8.9 | 2.4 | 2.3 | 1.8 | 2.3 |
| Lu | 0.3 | 0.3 | 0.3 | 1.2 | 0.2 | 0.3 | 0.3 | 0.3 |
| Co | 49.0 | 40.0 | 34.0 | 2.0 | 53.0 | 50.0 | 236.0 | 46.0 |
| Cr | 260.4 | 15.3 | 8.7 | 0.0 | 201.2 | 56.4 | 50.0 | 54.6 |
| Cu | 59.0 | 44.0 | 44.0 | 11.0 | 34.0 | 22.0 | 37.0 | 23.0 |
| Ni | 109.0 | 25.0 | 20.0 | 27.0 | 115.0 | 39.0 | 40.0 | 33.0 |
| Sc | 23.5 | 23.1 | 22.5 | 0.1 | 24.8 | 21.7 | 19.5 | 24.0 |
| V | 196.0 | 185.0 | 180.0 | 3.0 | 242.0 | 212.0 | 225.0 | 213.0 |
| ⁸⁷ Sr/ ⁸⁶ Sr | 0.7037 | 0.7033 | 0.7031 | 0.7070 | 0.7034 | 0.7035 | N/A | 0.7038 |
| K/Rb | 438.77 | 577.46 | 613.55 | 409.62 | 588.62 | 487.68 | 558.93 | 509.92 |
| (La/Yb) _{CH} | 7.96 | 8.66 | 9.20 | 9.73 | 6.46 | 8.46 | 11.56 | 6.87 |
| La/Nb | 1.05 | 0.86 | 0.86 | 0.75 | 0.94 | 0.95 | 1.02 | 1.00 |
| Mg' | 62 | 35 | 32 | 1 | 56 | 46 | 51 | 46 |
| Dates and Ages (Ma). | 7.2 ± 0.8 | 220 yrs | 220 yrs | 0.02 ± 0.013 | ~.04 | ~.04 | ~.04 | ~.04 |

continued.....

| | BOWSER | SPEC1 | SPEC2 | EDZ1 | EDZ2 | NEDZ1 | NEDZ2 | NEDZ3 |
|------------------------------------|----------------------|---------------------|-----------------------|----------------------|----------------------|---------------------|----------------------|----------------------|
| Series Name | Alkaline Hawaiite | Alk/Trans Basalt | Alkaline- Hawaiite | Alkaline Hawaiite | Alkaline Hawaiite | Alk/Trans Basalt | Alkaline Hawaiite | Alkaline Hawaiite |
| LAT. | 56 54 | 57 17.5 | 57 25.5 | 57 45.5 | 57 56.1 | 57 58.15 | 58 00.0 | 57 59.18 |
| LONG. | 129 22 | 130 32.6 | 130 47.2 | 130 42.0 | 130 37.2 | 130 01.47 | 130 42.4 | 129 55.13 |
| SiO ₂ | 46.94 | 47.11 | 48.07 | 49.32 | 47.99 | 47.29 | 48.35 | 48.97 |
| TiO ₂ | 2.65 | 2.33 | 2.55 | 2.35 | 2.88 | 2.88 | 3.11 | 2.30 |
| Al ₂ O ₃ | 14.85 | 14.93 | 15.78 | 15.23 | 15.75 | 14.44 | 14.90 | 15.18 |
| Fe ₂ O ₃ | 13.94 | 13.95 | 13.00 | 12.72 | 13.19 | 13.59 | 13.00 | 13.05 |
| FeO | 0.0 | 0.0 | 0.0 | 0.0 | 0.0 | 0.0 | 0.0 | 0.0 |
| MnO | 0.19 | 0.18 | 0.21 | 0.18 | 0.20 | 0.15 | 0.18 | 0.13 |
| MgO | 6.92 | 7.65 | 4.72 | 5.54 | 4.17 | 9.04 | 4.61 | 5.73 |
| CaO | 8.53 | 9.37 | 10.22 | 8.75 | 9.94 | 7.66 | 9.51 | 6.93 |
| Na ₂ O | 3.80 | 3.01 | 3.89 | 3.88 | 3.69 | 3.16 | 4.42 | 5.19 |
| K ₂ O | 1.59 | 0.88 | 1.01 | 1.50 | 1.30 | 1.33 | 1.25 | 1.78 |
| P ₂ O ₅ | 0.61 | 0.61 | 0.56 | 0.54 | 0.91 | 0.45 | 0.67 | 0.72 |
| Ba | 474.0 | 415.0 | 241.0 | 434.0 | 511.0 | 436.0 | 474.0 | 511.0 |
| Rb | 35.0 | 11.0 | 14.0 | 26.0 | 13.0 | 20.0 | 15.0 | 26.0 |
| Th | 4.3 | 1.7 | 1.8 | 3.5 | 2.4 | 3.0 | 2.3 | 3.4 |
| U | N/A | 0.4 | 1.2 | 1.1 | 0.8 | 0.8 | 0.8 | 1.1 |
| Nb | 55.0 | 20.0 | 27.0 | 37.0 | 30.0 | 38.0 | 30.0 | 45.0 |
| La | 38.2 | 17.8 | 24.0 | 29.8 | 29.8 | 24.7 | 21.9 | 36.2 |
| Ce | 90.0 | 35.4 | 62.4 | 57.3 | 48.0 | 43.5 | 50.4 | 90.6 |
| Sr | 882.0 | 495.0 | 489.0 | 507.0 | 642.0 | 694.0 | 506.0 | 863.0 |
| Nd | 30.0 | 18.4 | 30.1 | 28.8 | 30.1 | 28.0 | 20.6 | 38.6 |
| Sm | 11.0 | 6.0 | 7.3 | 6.9 | 8.2 | 4.8 | 6.2 | 8.1 |
| Zr | 302.0 | 140.0 | 204.0 | 208.0 | 181.0 | 235.0 | 186.0 | 262.0 |
| Hf | N/A | 2.9 | 4.8 | 5.0 | 3.2 | 5.3 | 3.9 | 5.7 |
| Eu | 2.0 | 2.1 | 2.1 | 2.1 | 2.9 | 2.2 | 2.5 | 2.4 |
| Tb | N/A | 0.9 | 0.8 | 0.8 | 1.2 | 0.7 | 0.6 | 0.7 |
| Y | 34.0 | 25.0 | 34.0 | 29.0 | 31.0 | 21.0 | 25.0 | 19.0 |
| Yb | 3.1 | 1.6 | 2.2 | 2.0 | 2.0 | 0.9 | 2.2 | 1.0 |
| Lu | 0.4 | 0.3 | 0.3 | 0.2 | 0.2 | 0.2 | 0.2 | 0.2 |
| Co | 46.0 | 44.0 | 36.0 | 44.0 | 33.0 | 53.0 | 39.0 | 42.0 |
| Cr | 198.0 | 202.0 | 105.3 | 186.6 | 54.0 | 203.1 | 66.4 | 119.7 |
| Cu | 49.0 | 48.0 | 45.0 | 50.0 | 50.0 | 46.0 | 37.0 | 43.0 |
| Ni | 156.0 | 148.0 | 51.0 | 139.0 | 36.0 | 186.0 | 36.0 | 98.0 |
| Sc | 20.2 | 24.7 | 25.9 | 21.2 | 22.1 | 15.7 | 26.3 | 11.8 |
| V | 166.0 | 206.0 | 223.0 | 168.0 | 170.0 | 167.0 | 275.0 | 113.0 |
| ⁸⁷ Sr/ ⁸⁶ Sr | 0.7023 | N/A | N/A | N/A | N/A | N/A | N/A | N/A |
| K/Rb | 377.10 | 664.08 | 598.86 | 478.90 | 830.10 | 552.02 | 691.75 | 568.30 |
| (La/Yb) _{CH} | 8.21 | 7.46 | 7.39 | 9.84 | 9.83 | 17.41 | 6.71 | 23.80 |
| La/Nb | 0.69 | 0.89 | 0.89 | 0.81 | 0.99 | 0.65 | 0.73 | 0.80 |
| Mg' | 50 | 52 | 42 | 46 | 39 | 57 | 41 | 47 |
| Dates and Ages (Ma). | 1.6 ± 0.3 | 7.8 ± 0.3 | ~3 | 5.9 ± 0.9 | 0.62 ± 0.4 | 5.7 ± 0.2 | 0.43 ± 0.15 | 4.9 ± 0.2 |

continued.....

| | NEDZ4 | LEVELD* | LEVEL1 | LEVEL2* | SATLIN | NATLIN |
|--------------------------------------|----------------------|---------------------|----------------------|----------------------|---------------------|----------------------|
| Series Name | Alkaline Hawaiite | Alk/Trans Basalt | Alkaline Hawaiite | Alkaline Hawaiite | Tholeiite Basalt | Alkaline Hawaiite |
| LAT. | 58 01.8 | 58 19.7 | 58 28.0 | 58 28.9 | 59 19.0 | 59 45.0 |
| LONG. | 130 03.72 | 131 40.0 | 131 26.9 | 131 26.2 | 133 42.75 | 133 20.0 |
| SiO ₂ | 48.12 | 48.60 | 50.17 | 47.80 | 48.99 | 48.39 |
| TiO ₂ | 2.16 | 2.20 | 2.39 | 2.90 | 1.69 | 2.10 |
| Al ₂ O ₃ | 15.00 | 15.60 | 15.48 | 15.40 | 14.67 | 14.32 |
| Fe ₂ O ₃ | 13.31 | 2.60 | 11.94 | 2.40 | 13.32 | 11.36 |
| FeO | N/A | 9.90 | N/A | 10.70 | N/A | N/A |
| MnO | 0.17 | 0.20 | 0.16 | 0.20 | 0.18 | 0.15 |
| MgO | 6.93 | 6.00 | 5.87 | 6.00 | 7.85 | 8.04 |
| CaO | 7.70 | 10.20 | 8.01 | 9.10 | 8.95 | 8.29 |
| Na ₂ O | 5.12 | 3.40 | 4.00 | 3.80 | 3.31 | 4.81 |
| K ₂ O | 1.16 | 0.40 | 1.32 | 0.90 | 0.69 | 1.64 |
| P ₂ O ₅ | 0.34 | 0.30 | 0.64 | 0.60 | 0.36 | 0.90 |
| Ba | 346.0 | 174.0 | 519.0 | 292.0 | 258.0 | 582.0 |
| Rb | 15.0 | 3.0 | 17.0 | 12.0 | 10.0 | 28.0 |
| Th | 2.3 | 0.8 | 2.3 | 2.7 | 2.0 | 4.4 |
| U | 0.7 | 0.3 | 0.9 | 0.6 | 0.5 | 1.5 |
| Nb | 31.0 | 12.0 | 28.0 | 32.0 | 17.0 | 51.0 |
| La | 15.1 | 11.2 | 25.6 | 24.7 | 15.4 | 47.4 |
| Ce | 38.1 | 15.1 | 56.9 | 45.8 | 40.2 | 93.9 |
| Sr | 580.0 | 441.0 | 609.0 | 464.0 | 510.0 | 1135.0 |
| Nd | 26.7 | 14.5 | 28.7 | 23.6 | 20.1 | 43.5 |
| Sm | 4.4 | 4.6 | 8.7 | 8.0 | 4.3 | 9.3 |
| Zr | 189.0 | 106.0 | 195.0 | 185.0 | 92.0 | 178.0 |
| Hf | 3.9 | 2.3 | 4.4 | 4.6 | 2.6 | 3.6 |
| Eu | 1.6 | 1.4 | 2.7 | 2.2 | 1.4 | 2.7 |
| Tb | N/A | 0.7 | 0.8 | 0.7 | N/A | 0.6 |
| Y | 19.0 | 20.0 | 25.0 | 30.0 | 20.0 | 24.0 |
| Yb | 1.7 | 2.0 | 1.6 | 2.2 | 1.1 | 1.3 |
| Lu | 0.2 | 0.2 | 0.2 | 0.2 | 0.2 | 0.1 |
| Co | 49.0 | N/A | 54.0 | N/A | 50.0 | 89.0 |
| Cr | 206.8 | 218.0 | 59.9 | 188.0 | 254.0 | 226.5 |
| Cu | 45.0 | 61.0 | 49.0 | 153.0 | 56.0 | 52.0 |
| Ni | 171.0 | 138.0 | 39.0 | 112.0 | 112.0 | 162.0 |
| Sc | 18.6 | 24.2 | 18.1 | 27.1 | 21.3 | 17.0 |
| V | 175.0 | N/A | 157.0 | N/A | 170.0 | 165.0 |
| Sr ⁸⁷ Sr ⁸⁶ | N/A | 0.70324 | N/A | 0.70302 | 0.7039 | 0.7039 |
| K/Rb | 641.94 | 1106.80 | 644.55 | 622.57 | 572.77 | 486.20 |
| (La/Yb) _{CH} | 5.95 | 3.83 | 10.61 | 7.58 | 9.24 | 24.48 |
| La/Nb | 0.49 | 0.94 | 0.91 | 0.77 | 0.91 | 0.93 |
| Mg' | 51 | 47 | 49 | 45 | 54 | 58 |
| Dates and Ages (Ma) | 0.507±0.07 | ~12 | ~12 | ~12 | 16.5±3.1 | N/A |

* Major element and
some trace element
data from Hamilton
(1981).

N/A = not analyzed

7. ALERT BAY VOLCANIC BELT

Three samples representing the Alert Bay Volcanic Belt were selected for analysis (Fig. 7.1). Two of the samples (ALERT1 and ALERT2) are basaltic in composition (SiO_2 less than 50 wt. %), and the remaining sample (ALERT3) is andesitic ($\text{SiO}_2 = 61.15$ wt. %).

Most of the Alert Bay volcanic rocks were erupted approximately 3.5 ± 1 Ma ago (Table VI). They are a product of volcanism in the arc-trench gap, generated along the descending plate edge (Armstrong et al., in press).

7.1 MAJOR ELEMENT CHEMISTRY

Most major element abundances in basaltic samples ALERT1 and ALERT2 (Table VI) are typical of the range of abundances from tholeiitic and alkaline oceanic WPB (Basaltic Volcanism Study Project, 1981). Al_2O_3 abundances are slightly higher than 'average'. The Mg' number for ALERT1 is 45, but for ALERT2 it is 62 indicating that this latter sample is more primitive. In contrast the major element abundances in andesitic sample ALERT3 are more characteristic of a calcalkaline convergent margin andesite, low TiO_2 and Fe_2O_3 with high Al_2O_3 . This sample has a Mg' number of 49.

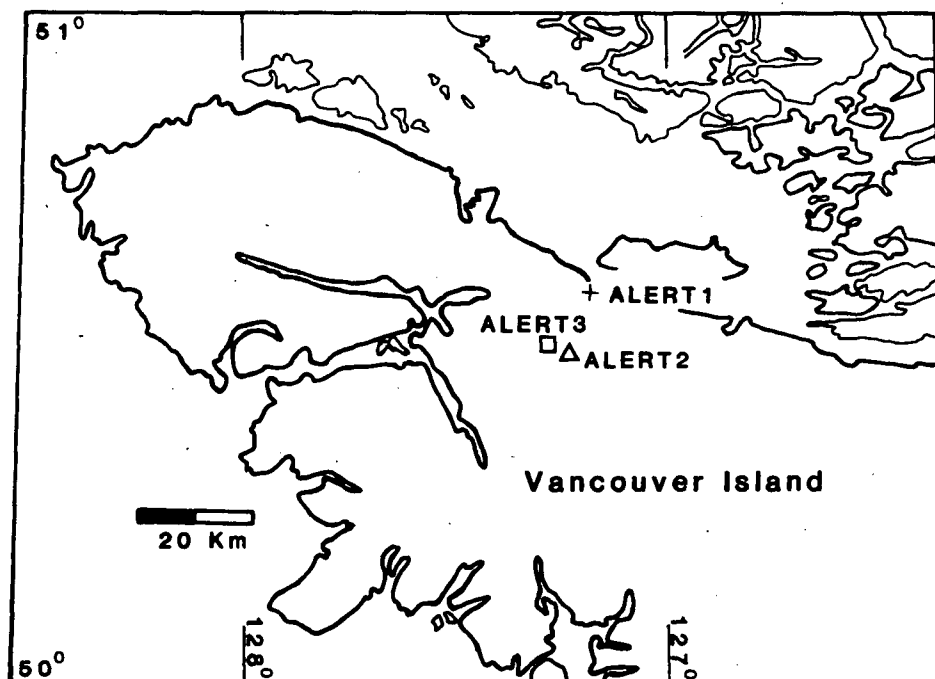


Fig. 7.1. Sample location map for the Alert Bay Volcanic Belt. All subsequent diagrams in this chapter use identical symbols.

7.2 DISCRIMINANT DIAGRAMS

7.2.1 MAJOR ELEMENT CLASSIFICATIONS

On total alkalis vs. silica ALERT1 lies just within the alkaline field, ALERT2 lies on MacDonald's (1968) subalkaline-alkaline field boundary and ALERT3 lies within the subalkaline field (Fig. 7.2). $Ol'-Ne'-Qz$ (not shown) classifies all three samples as subalkaline.

On AFM and FeO^*/MgO vs. SiO_2 diagrams ALERT1 lies within the tholeiitic field, ALERT3 lies within the calcalkaline field and ALERT2 lies on the boundaries between tholeiitic and calcalkaline fields (Figs. 7.3 and 7.4). Additional Alert Bay Group basalts-andesites-dacites and rhyolites plotted on an AFM diagram indicate that ALERT1 belongs to the tholeiitic/transitional Mull trend, whereas ALERT2 and ALERT3 belong to the calcalkaline Cascade trend (Armstrong et al., in press). Al_2O_3 vs. normative plagioclase (not shown) classifies ALERT1 and ALERT2 as tholeiitic and ALERT3 as calcalkaline.

On $TiO_2-K_2O-P_2O_5$ ALERT1 lies within the oceanic field and ALERT2 lies on the boundary between the oceanic and non-oceanic fields (Fig. 7.5).

On $MnO-TiO_2-P_2O_5$ both basaltic samples lie within the OIA field (Fig. 7.6).

ALERT1 is classified as convergent margin and ALERT2 as N-MORB on $FeO^*-MgO-Al_2O_3$ (Fig. 7.7).

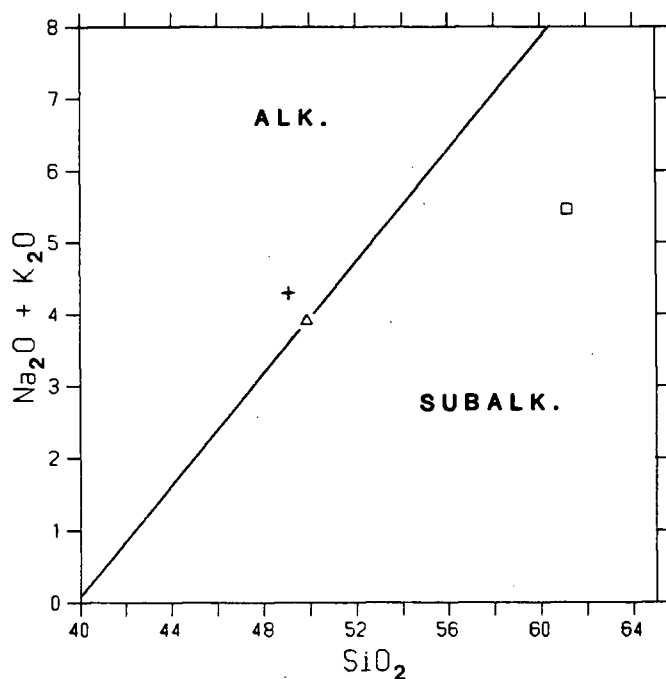


Fig. 7.2. Total alkalis vs. silica. Subalkaline/alkaline boundary from MacDonald (1968).

Fig. 7.3. AFM diagram. Tholeiitic/calcaline boundary from Irvine and Baragar (1971).

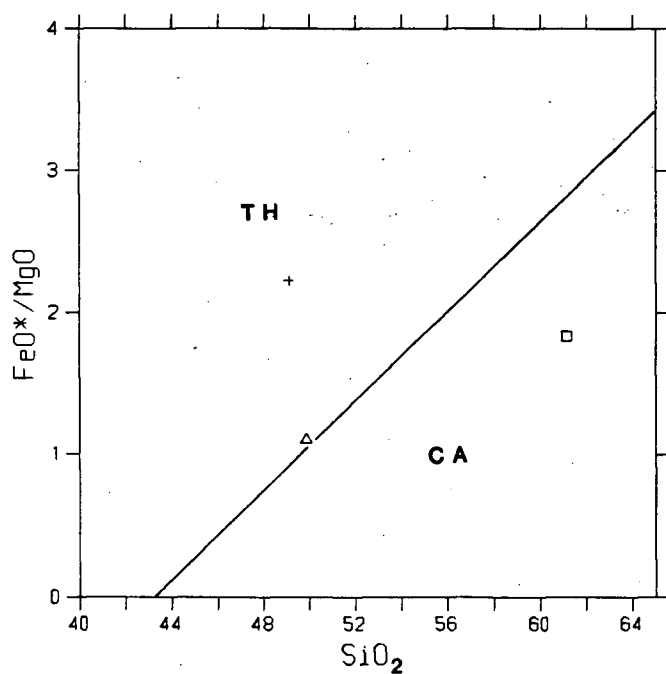
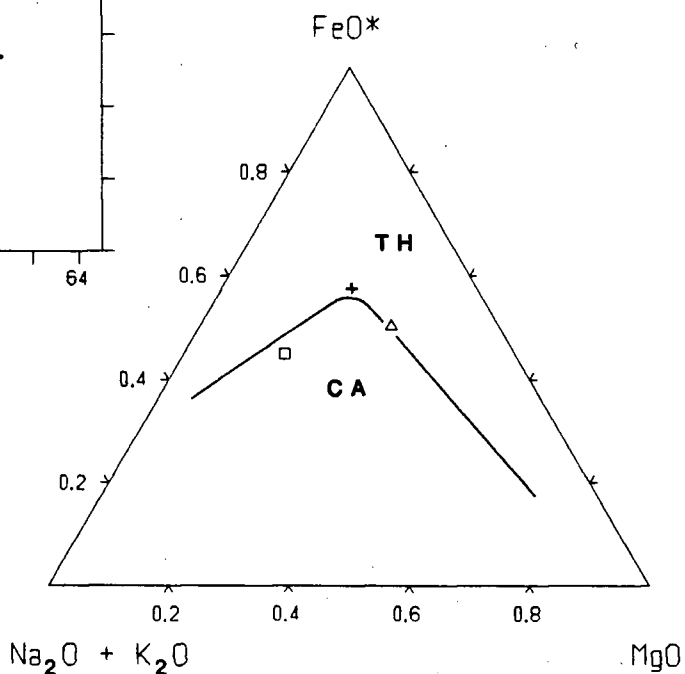
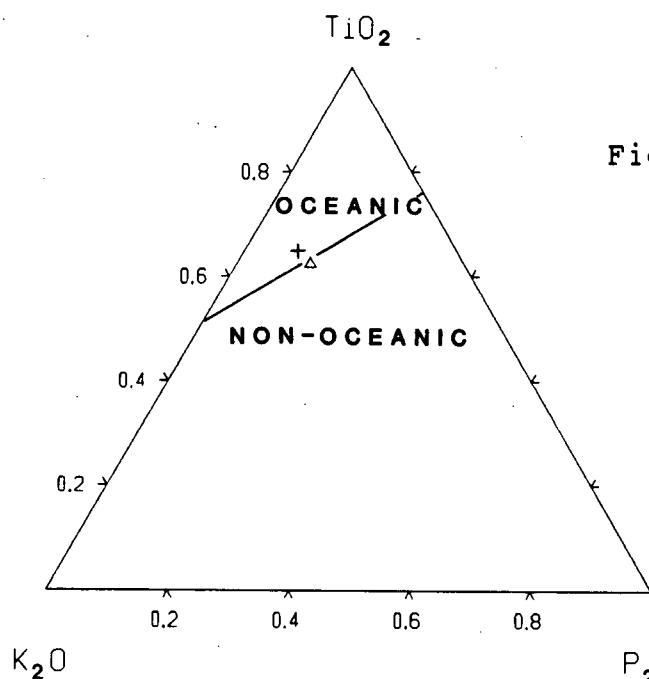
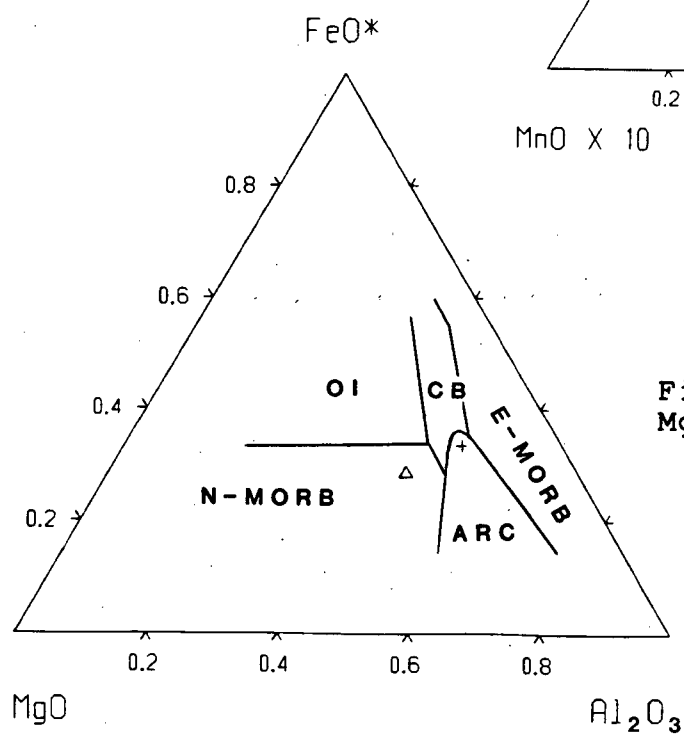
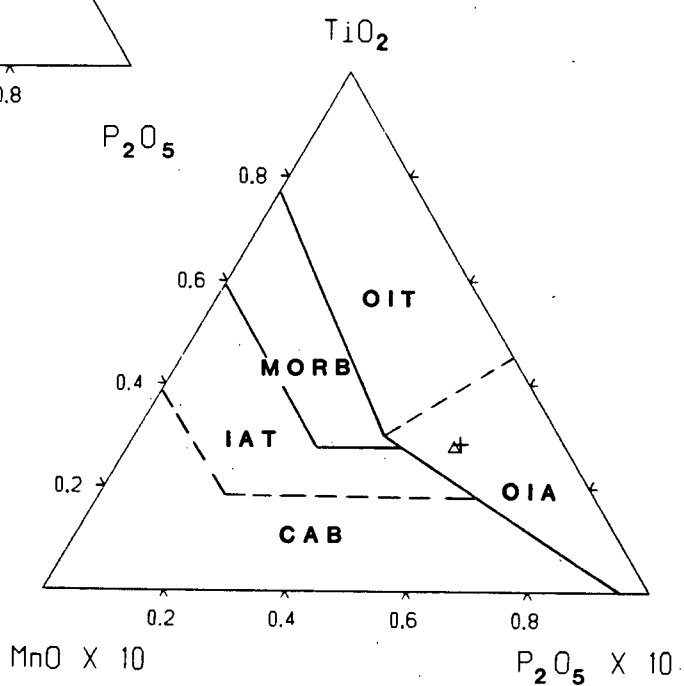


Fig. 7.4. FeO^*/MgO vs. SiO_2 . Tholeiitic/calcaline boundary from Miyashiro (1974).

ALERT1 +
ALERT2 Δ
ALERT3 \square

Fig. 7.5. TiO_2 - K_2O - P_2O_5 .

ALERT1 +
ALERT2 Δ
ALERT3 \square

Fig. 7.6. MnO - TiO_2 - P_2O_5 .Fig. 7.7.
 MgO - FeO^* - Al_2O_3 .

7.2.2 TRACE ELEMENT CLASSIFICATIONS

On Ti-Zr-Y, V vs. Ti/100 and Ti/Y vs. Nb/Y both basaltic samples are classified as WPB (Figs. 7.8, 7.9 and 7.10 respectively).

On Ti/Cr vs. Ni ALERT3 lies within the IAT field and ALERT1 and ALERT2 lie within the TH MORB field (Fig. 7.11).

7.2.3 TRACE AND REE CLASSIFICATIONS

All three samples lie within the convergent margin field on Sm/Ce vs. Sr/Ce (Fig. 7.12), but on Cr vs. Ce/Sr only ALERT3 is unequivocally classified as convergent margin (Fig. 7.13). On the latter diagram ALERT1 lies within the overlapping ARC-MORB fields and ALERT2 lies within the overlapping MORB-WPB fields.

On Cr vs. Y ALERT3 lies within the convergent margin field and ALERT1 and ALERT2 lie within the overlapping ARC-MORB-WPB fields (Fig. 7.14).

All samples lie within the orogenic andesite field on La vs. Ba, close to the boundary with the E-MORB (WPB) field (Fig. 7.15), but on $(Ba/La)_{CH}$ vs. $(La/Sm)_{CH}$ all samples lie within the oceanic (WPB) field (Fig. 7.16). ALERT3 lies just within the overlapping ARC field.

On La vs. Th ALERT1 and ALERT2 lie within the E-MORB (WPB) field with La/Th ratios between 7 and 15 (Fig. 7.17). ALERT3 has an La/Th ratio of 4.6 and

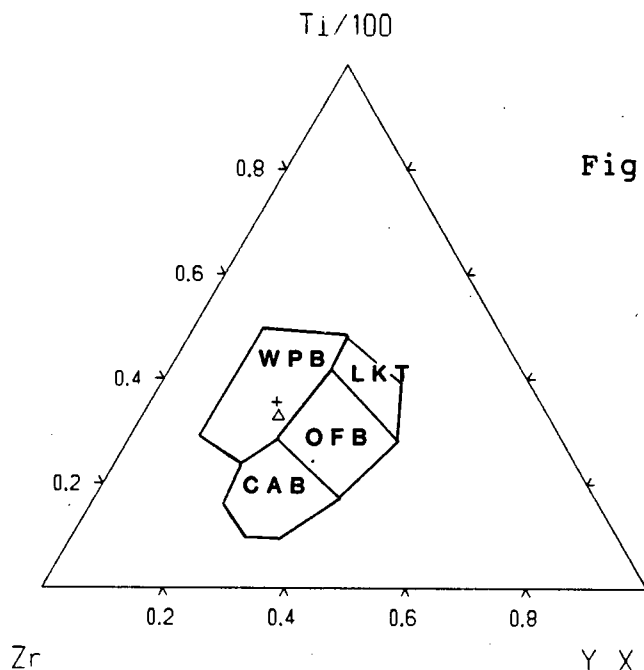


Fig. 7.8. Ti-Zr-Y.

Fig. 7.9. V vs. Ti/1000

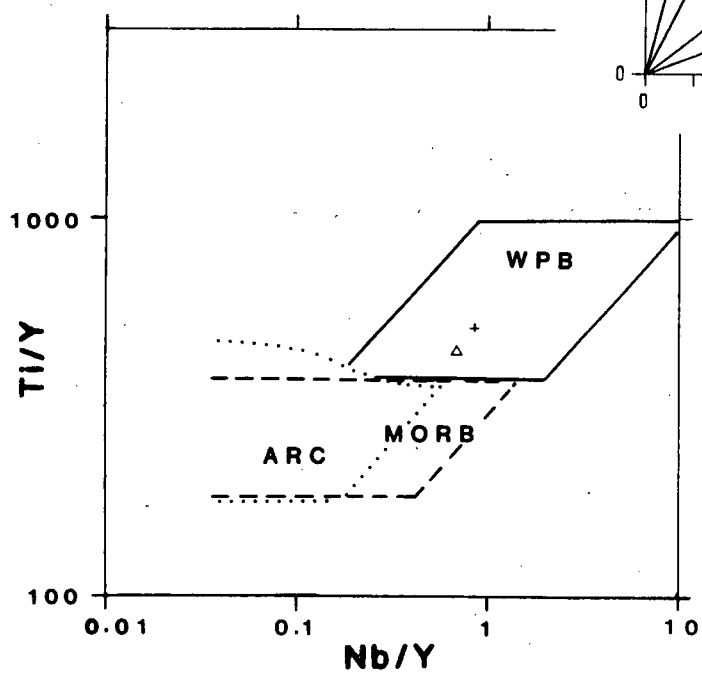
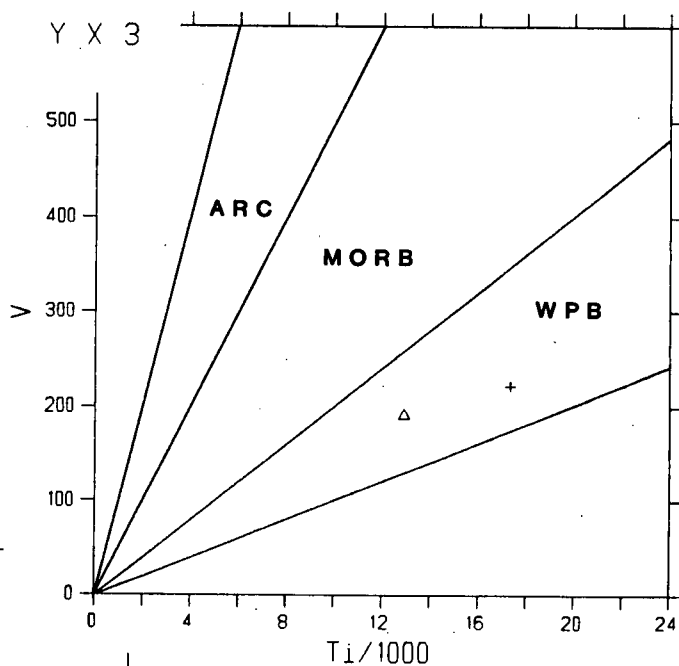
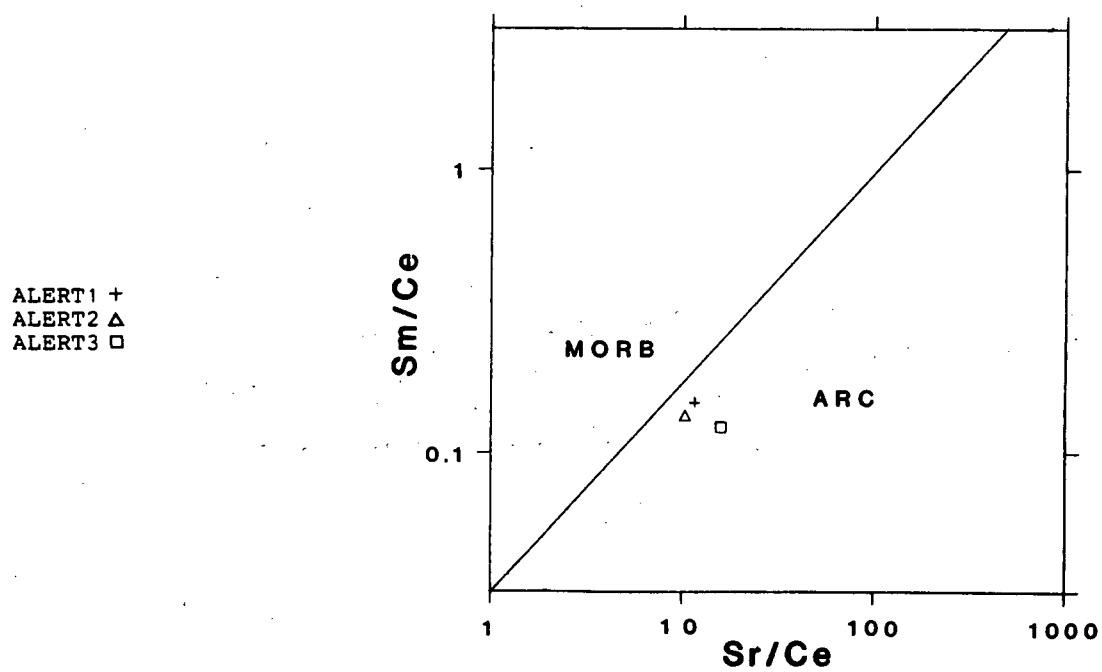
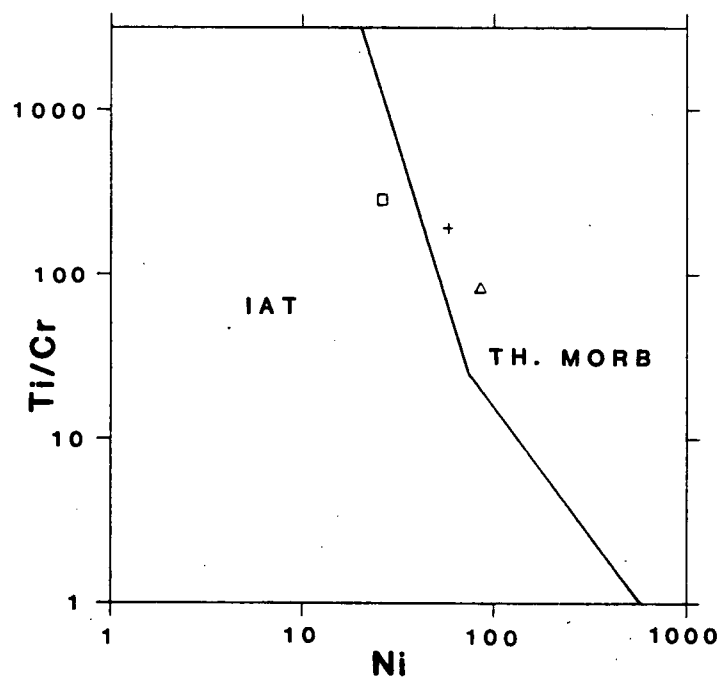
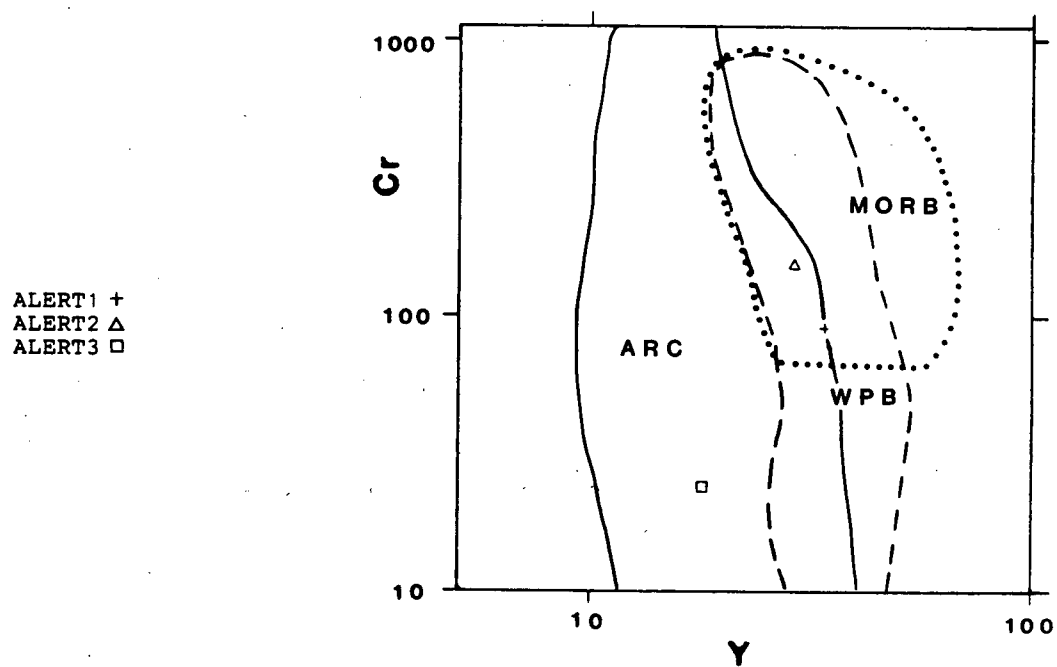
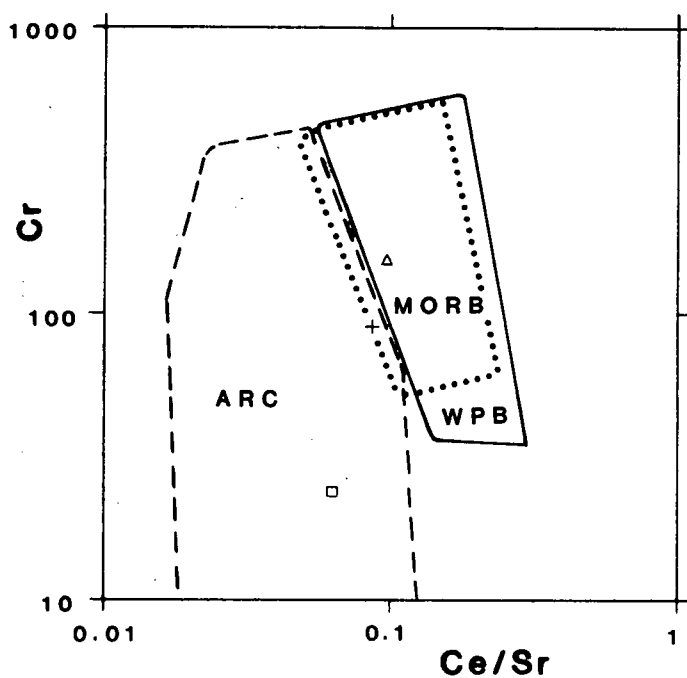


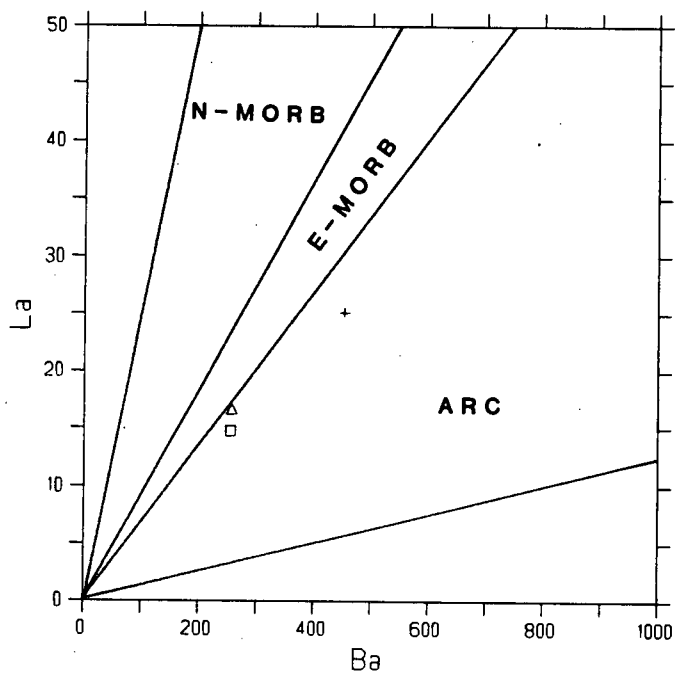
Fig. 7.10. Ti/Y vs. Nb/Y.



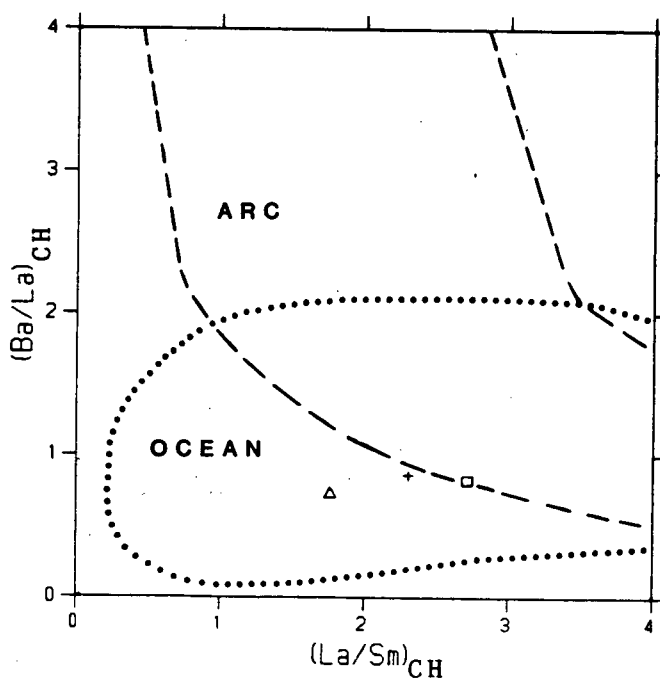
Figs. 7.11 and 7.12. Ti/Cr vs. Ni (above) and Sm/Ce vs. Sr/Ce (below).



Figs. 7.13 and 7.14. Cr vs. Ce/Sr (above) and Cr vs. Y (below).



ALERT1 +
ALERT2 Δ
ALERT3 □



Figs. 7.15 and 7.16. La vs. Ba (above) and $(\text{Ba}/\text{La})_{\text{CH}}$ vs. $(\text{La}/\text{Sm})_{\text{CH}}$ (below).

clearly lies within the orogenic andesite field.

On La vs. Nb ALERT1 and ALERT2 have La/Nb ratios of less than 1 and consequently lie within the E-MORB (WPB) field (Fig. 7.18). ALERT3 has an La/Nb ratio of 1.64 and lies within the N-MORB field.

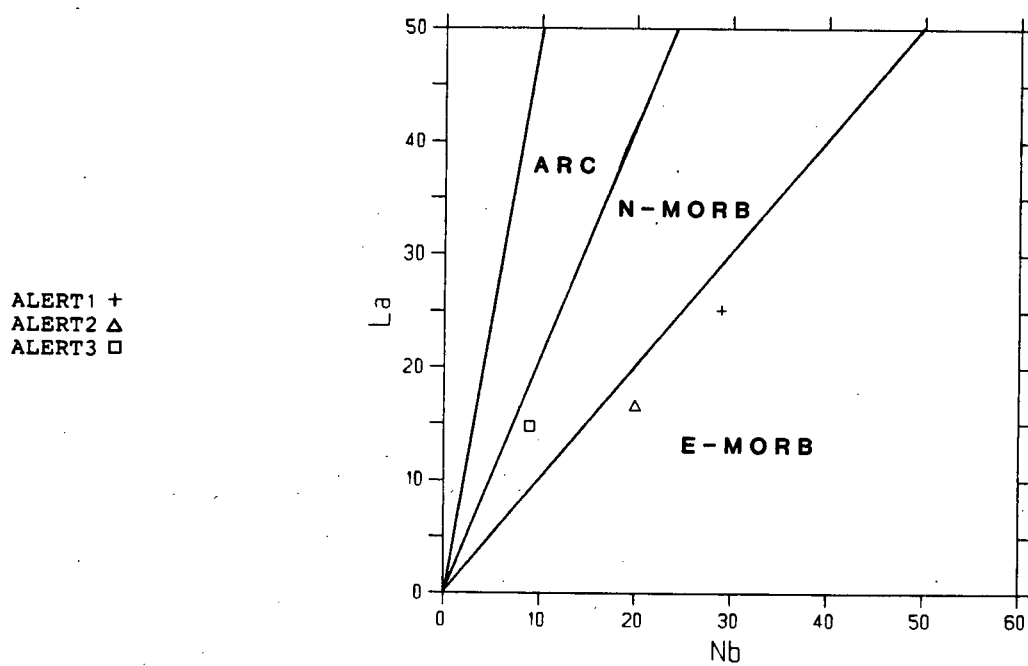
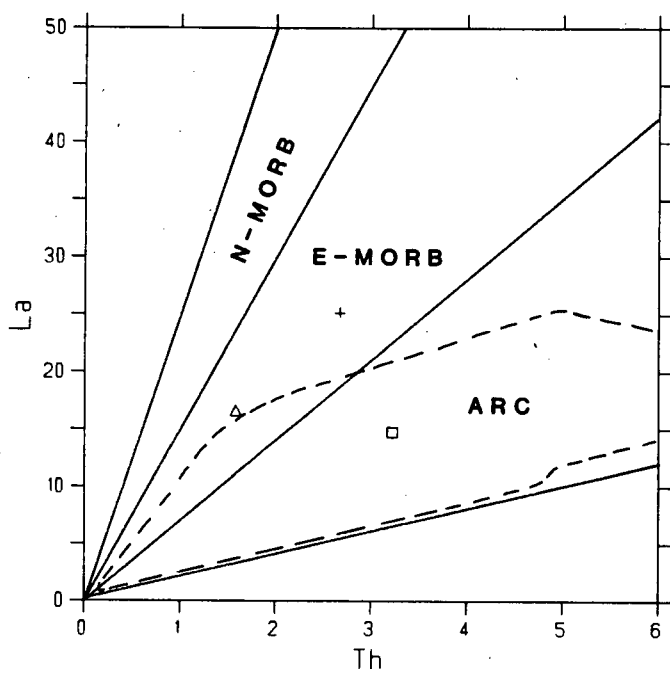
On K_2O/Yb vs. Ta^*/Yb and Th/Yb vs. Ta^*/Yb both basalt samples lie within the overlapping MORB-WPB fields and ALERT3 lies within the ARC field (Figs. 7.19 and 7.20).

ALERT3 lies within the convergent margin (CAB) field on $Th-Hf/3-Ta^*$ and ALERT1 and ALERT2 lie within the E-MORB- tholeiitic WPB field (Fig. 7.21).

7.2.4 BULK EARTH NORMALIZED DIAGRAMS (BEND)

Bend patterns from the three Alert Bay samples are shown on Fig. 7.22. ALERT1 and ALERT2 have virtually identically shaped patterns. They are shallowly convex-up, 'peaking' at Nb, with a concave-up dip from Sm to Eu. Both samples have a 'trough' at U, indicating relative U depletion.

When compared to the two patterns described above the pattern from ALERT3 is noticeably different, especially from Ba to Ti. It is enriched in LIL relative to LREE, has a 'trough' at Nb and Sm and has a convex-up hump from Sm to Ti. From Eu to Yb the pattern from ALERT3 is identical to the patterns from ALERT1 and ALERT2.



Figs. 7.17 and 7.18. La vs. Th (above) and La vs. Nb (below).

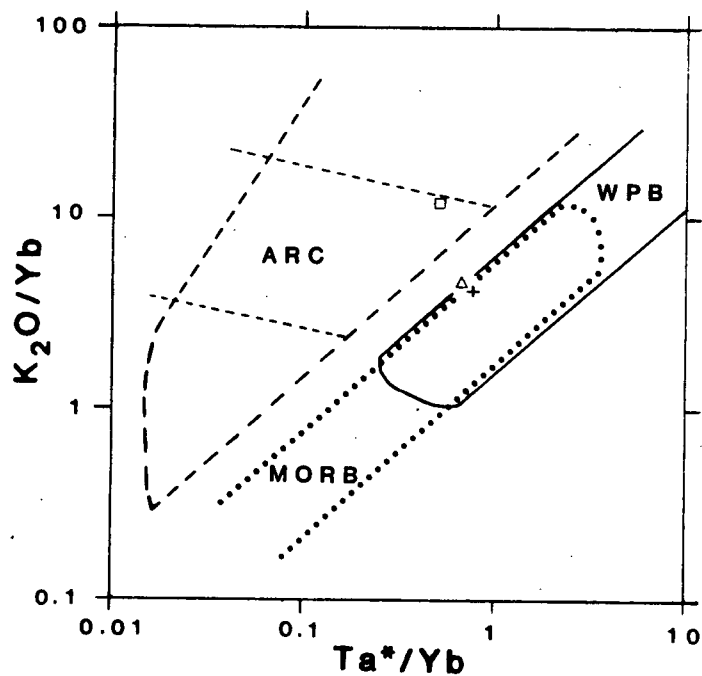


Fig. 7.20. Th/Yb vs. Ta^*/Yb .

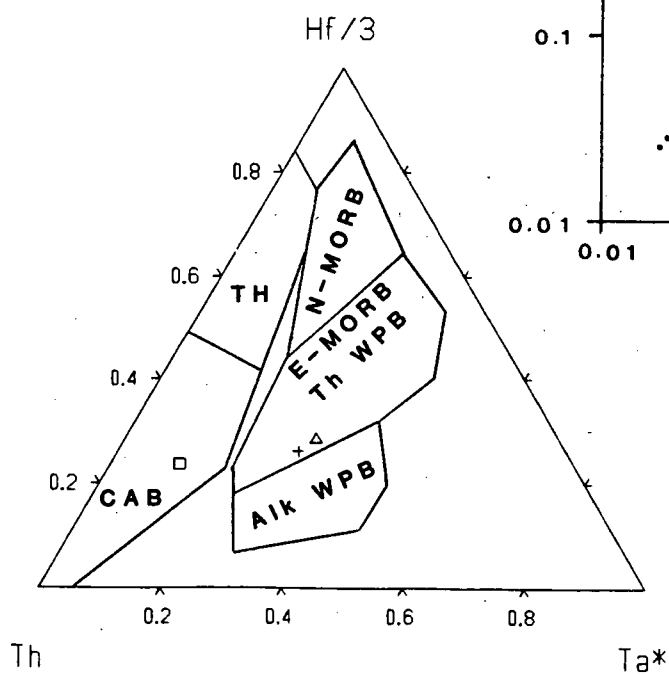
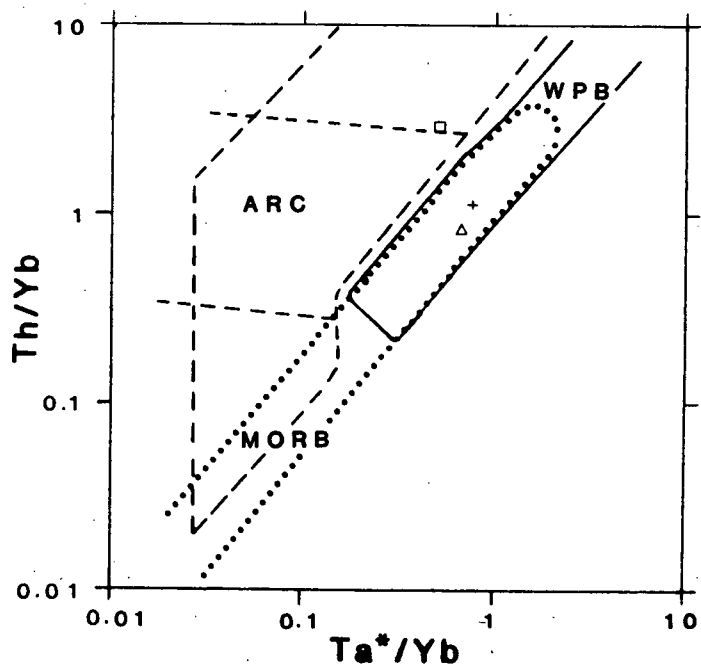


Fig. 7.21. $Th-Hf/3-Ta^*$.

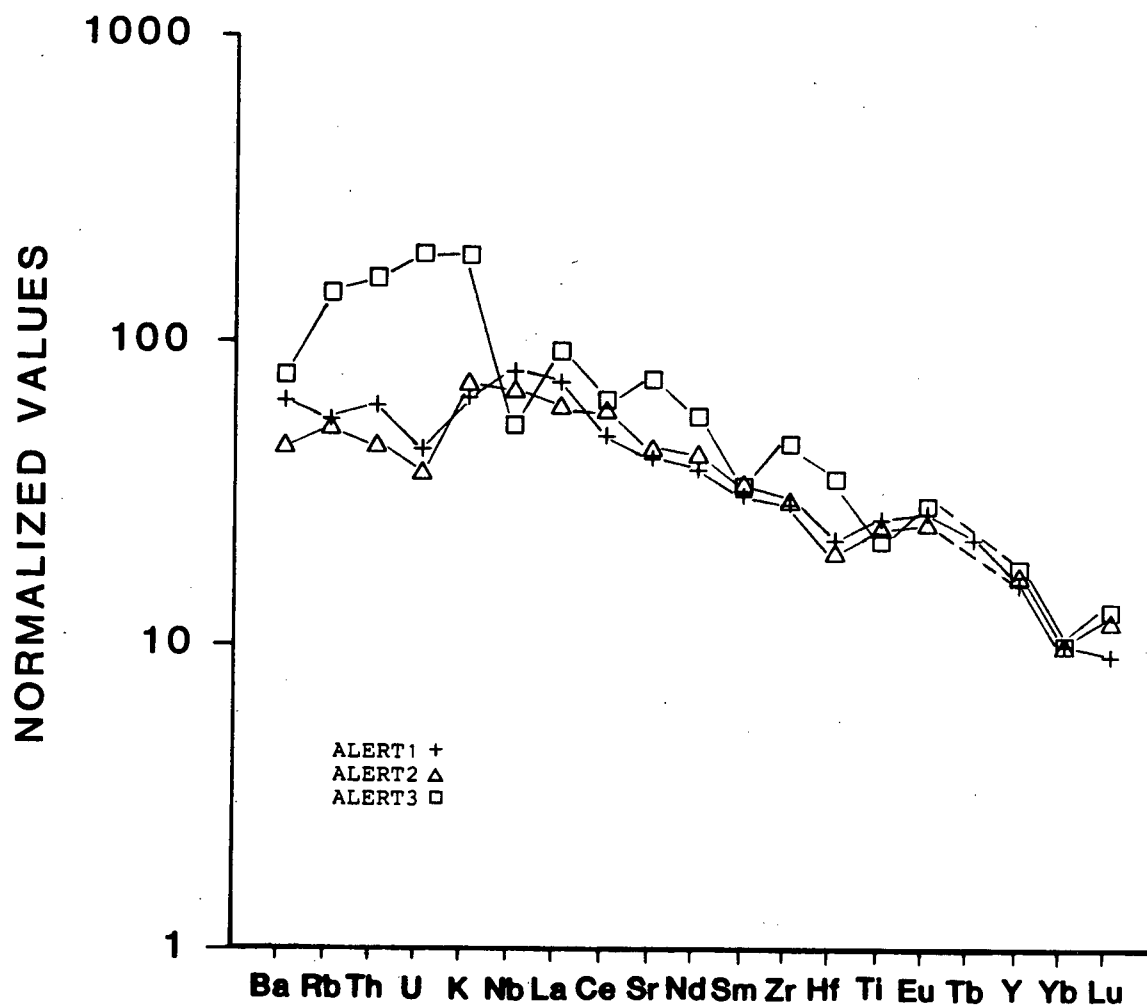


Fig. 7.22. BEN diagram for samples ALERT1, ALERT2 and ALERT3.

All patterns display a slight positive Eu anomaly.

7.3 TRACE ELEMENT CHEMISTRY

Trace and rare earth element abundances for ALERT1 and ALERT2 (Table VI) lie within the range of abundances from WPB erupted at other locations in British Columbia (eg. Stikine Volcanic Belt, Chilcotin Group Basalts and Anahim Volcanic Belt (this study)). BEND patterns also have convex-up WPB-like shapes. La abundances are 76.5 and 50.6 times chondritic, Yb abundances are 10.9 and 8.6 times chondritic and $(La/Yb)_{CH}$ ratios are 7.1 and 5.96 for ALERT1 and ALERT2 respectively. La/Nb ratios of 0.86 and 0.83 and Rb/Nb ratios of 0.69 and 0.75 are within the range of ratios characteristic of oceanic WPB (Thompson et al., 1983).

Relative to ALERT1 and ALERT2, ALERT3 has higher abundances of Rb lower abundances of Nb and REE and similar to lower abundances of Sr, Zr and Hf. Its La content is 44.8 times chondritic, Yb content is 5 times chondritic and $(La/Yb)_{CH}$ ratio is 8.99. It has an La/Nb ratio of 1.64 and an Rb/Nb ratio of 2.67. These ratios are typical of a convergent margin basalt or a within plate basalt which has assimilated continental crust, but it must be remembered that ALERT3 is an andesite, and therefore these ratio discriminants may not apply.

7.3.1 TH AND U

Th abundances in ALERT1 and ALERT2 are 2.7 and 1.6 ppm respectively, U abundances are 0.6 and 0.4 ppm and Th/U ratios are 4.5 and 4.0. These are within the range of abundances and ratios from oceanic WPB. ALERT3 has higher abundances of both Th and U; Th = 3.2 ppm and U = 1.2 ppm, and a lower Th/U ratio; Th/U = 2.7. High abundances of Th and U in a subalkaline rock are more 'typical' in samples from a convergent margin setting.

7.3.2 TRANSITION ELEMENTS

Abundances of Cr and Ni in ALERT1 are lower than equivalent abundances in ALERT2. This reflects ALERT2's more primitive (less fractionated) nature. Sc contents are 24.9 and 22.3 ppm for ALERT1 and ALERT2 respectively. ALERT3 has much lower abundances of both Cr and Ni, indicating a greater amount of both olivine and pyroxene fractionation during its petrogenesis. Its Sc content of 11 ppm provides additional evidence for the fractionation of pyroxene.

7.4 ISOTOPIC DATA

Sr isotope ratios range from 0.7031 to 0.7035, the lowest ratio belonging to ALERT3 (Table VI). These ratios are lower than ratios from most volcanic arcs, but they are like those from the Garibaldi Volcanic Belt and are typical of ratios from WPB magmas (Zhou and Armstrong, 1982; Faure,

1977).

Oxygen isotope analysis done at the University of Alberta and reported by Armstrong et al. (in press) indicate rocks from the Alert Bay Volcanic Belt are enriched in O^{18} compared to typical mantle values (Alert Bay average $O^{18} = 7.1\%$; mantle $O^{18} = 5$ to 6%). This isotopic enrichment is cited as evidence for the assimilation of crustal material.

7.5 DISCUSSION OF DISCRIMINATION DIAGRAMS

On almost all of the major, trace and rare earth element discrimination diagrams basaltic samples ALERT1 and ALERT2 are classified as WPB (E-MORB) and andesitic sample ALERT3 is classified as convergent margin. Discrepancies occur on $MgO-FeO^*-Al_2O_3$ (Fig. 7.7), Sm/Ce vs. Sr/Ce (Fig. 7.12), La vs. Ba (Fig. 7.15), $(Ba/La)_{CH}$ vs. $(La/Sm)_{CH}$ (Fig. 7.16) and La vs. Nb (Fig. 7.18).

On $MgO-FeO^*-Al_2O_3$ neither of the basalts are classified as WPB because their abundances of Al_2O_3 are higher than 'typical' Al_2O_3 abundances in oceanic WPB (OI).

Both basalt samples lie within the ARC field on Sm/Ce vs. Sr/Ce . This disagrees with the WPB classification of most of the other diagrams, but as this diagram does not have a separate field for WPB, the ARC classification should probably be disregarded.

On La vs. Ba all samples are classified as orogenic andesites, but on $(Ba/La)_{CH}$ vs. $(La/Sm)_{CH}$ all samples lie within the oceanic (WPB) field. This indicates Ba abundance

has not been sufficiently enriched to classify any of these samples as 'typical' convergent margin basalt or andesite.

La vs. Nb also suggests the convergent margin-like chemistry of ALERT3 is not really 'typical' of an andesite erupted at a convergent margin setting. Although ALERT3 exhibits an Nb 'trough' on a BEND, which is characteristic of convergent margin basalts and andesites its Nb depletion is not great enough for an orogenic andesite classification on the diagram cited above. This implies either:

- ALERT3 magma came from a within-plate basalt source which was contaminated with continental crust (Thompson et al., 1983), or
- ALERT3 magma is a product of mixing WPB and ARC magmas.

7.6 SUMMARY

The Alert Bay basalt samples are classified as within-plate basalts, whereas the andesitic sample is classified as a convergent margin andesite. Thus, the limited data presented here confirm the observations and conclusions of Armstrong et al. (in press). The above authors recognized two different fractionation trends:

- one following an almost alkaline, tholeiitic trend; explainable by shallow fractionation of an anhydrous aluminous WPB (represented here by ALERT1), and
- the other following a convergent margin Cascade-type trend; explainable by either fractionation of a hydrous aluminous basalt, assimilation of crustal material or

mixing of crustal melt and primary basalt magma
(represented here by ALERT2 (low silica end member) and
ALERT3 (more siliceous member)).

TABLE VI. Alert Bay Volcanic Belt

Major, trace and rare earth element abundances, Sr isotope ratios and K-Ar dates.

| Series Name | ALERT1 | ALERT2 | ALERT3 | |
|------------------------------------|-----------------|----------------|------------------|--------------------|
| | Th/Trans Basalt | Calcalc Basalt | Calcalc Andesite | |
| LAT. | 50 35.2 | 50 30.8 | 50 31 | |
| LONG. | 127 11.6 | 127 12.3 | 127 15.0 | |
| SiO ₂ | 49.11 | 49.86 | 61.15 | |
| TiO ₂ | 2.89 | 2.15 | 1.14 | |
| Al ₂ O ₃ | 16.40 | 15.47 | 16.34 | |
| Fe ₂ O ₃ | 11.92 | 10.90 | 6.21 | N/A = not analyzed |
| FeO | N/A | N/A | N/A | |
| MnO | 0.18 | 0.14 | 0.08 | |
| MgO | 4.82 | 8.87 | 3.06 | |
| CaO | 9.82 | 8.27 | 6.40 | |
| Na ₂ O | 3.38 | 3.06 | 4.14 | |
| K ₂ O | 0.98 | 0.87 | 1.32 | |
| P ₂ O ₅ | 0.50 | 0.41 | 0.17 | |
| Ba | 453.0 | 257.0 | 255.0 | |
| Rb | 20.0 | 15.0 | 24.0 | |
| Th | 2.7 | 1.6 | 3.2 | |
| U | 0.6 | 0.4 | 1.2 | |
| Nb | 29.0 | 20.0 | 9.0 | |
| La | 25.1 | 16.6 | 14.7 | |
| Ce | 44.5 | 42.7 | 27.1 | |
| Sr | 514.0 | 441.0 | 431.0 | |
| Nd | 25.3 | 22.6 | 17.5 | |
| Sm | 6.7 | 5.8 | 3.4 | |
| Zr | 213.0 | 173.0 | 156.0 | |
| Hf | 4.8 | 3.4 | 3.5 | |
| Eu | 2.1 | 1.6 | 1.1 | |
| Tb | 1.1 | N/A | N/A | |
| Y | 34.0 | 29.0 | 18.0 | |
| Yb | 2.4 | 1.9 | 1.1 | |
| Lu | 0.3 | 0.3 | 0.2 | |
| Co | 42.0 | 43.0 | 15.0 | |
| Cr | 90.2 | 155.0 | 24.0 | |
| Cu | 36.0 | 39.0 | 22.0 | |
| Ni | 58.0 | 85.0 | 26.0 | |
| Sc | 24.9 | 22.3 | 11.3 | |
| V | 222.0 | 193.0 | 105.0 | |
| ⁸⁷ Sr/ ⁸⁶ Sr | 0.7035 | 0.7034 | 0.7031 | |
| K/Rb | 406.75 | 481.46 | 456.55 | |
| (La/Yb) _{CH} | 7.10 | 5.96 | 8.99 | |
| La/Nd | 0.86 | 0.83 | 1.64 | |
| Mg* | 45 | 62 | 49 | |
| K/Ar DATE (Ma) | 7 ± 3 | 4.3 ± 0.4 | 3.0 ± 0.4 | |

8. OFFSHORE BASALTS

Eleven samples from the Pacific Ocean seafloor were selected for analysis (Fig. 8.1). Pacific plate basalts are from Brown Bear and Cobb seamounts (2 samples from each) and Explorer seamount (3 samples). The remaining four samples are from southern Explorer Ridge (1 sample), Explorer Rift and Explorer Deep (1 sample each) and Paul Revere Ridge (Fracture Zone) (1 sample).

Most of the samples are probably less than 1 Ma old, except the Paul Revere Ridge sample which may be as old as 4.5 Ma (Riddihough, 1980) and the Explorer seamount samples which are approximately 4 Ma old (R.L. Chase, pers. comm., 1985).

8.1 MAJOR ELEMENT CHEMISTRY

Basalts from Explorer seamount and EXRIFT have characteristic N-MORB major element chemistry (Table VII), i.e. low SiO_2 , K_2O and P_2O_5 and high MgO and CaO (Melson et al., 1976). TiO_2 abundances lie within the TiO_2 abundance range from N-MORB (Christie and Sinton, 1981; Pearce, 1982; Sun et al., 1979). Mg' numbers for Explorer seamount samples range from 60 and 62 but EXRIFT has an Mg' number of 66. This latter basalt is a picrite according to the classification of Irvine and Baragar (1971).

Basalts from the Brown Bear and Cobb seamounts have higher abundances of TiO_2 , FeO^* , K_2O , Na_2O and P_2O_5 and a slightly lower MgO content than N-MORB (Table VII). These



Fig. 8.1. Sample location map for the Ocean Floor Basalt Suite. Key to symbols below.

| | | | |
|----------|---|----------|---|
| EXMOUNT1 | □ | COBB1 | ▽ |
| EXMOUNT2 | ■ | COBB2 | ▼ |
| EXMOUNT3 | ⊠ | SEXRIDGE | + |
| BRBEAR1 | △ | PREVRDG | × |
| BRBEAR2 | ▲ | EXRIFT | ◇ |
| EXDEEP | ◆ | | |

abundances are similar to abundances from E-MORB (Sun et al., 1979). Mg' numbers range from 47 to 54 indicating these basalts are more evolved than the Explorer Seamount and Explorer Rift samples.

Basalts SEXRIDGE and EXDEEP have major element characteristics of both N- and E-MORB; i.e. low total alkalis and high MgO and CaO, but also high K₂O, TiO₂ and P₂O₅ (Table VII). Mg' numbers are 58 and 57 respectively. Following the classification of Melson et al. (1976), Cousens et al. (1984) classify these basalts as low titanium members of the FETI group, or MORB bordering on ferrobasalt.

Relative to N- or E-MORB PREVRDG has higher abundances of TiO₂, Fe₂O₃, MnO, K₂O and P₂O₅, and lower abundances of Al₂O₃, MgO and CaO (Table VII). Mg' equals 36. These chemical characteristics are typical of extreme FETI basalts (Christie and Sinton, 1981), and are suggested by Cousens et al. (1984) to be evidence for a once active, northeasterly propagating rift.

8.2 DISCRIMINATION DIAGRAMS

8.2.1 MAJOR ELEMENT CLASSIFICATIONS

On total alkalis vs. silica three samples are clearly subalkaline (SEXRIDGE, EXRIFT and EXDEEP) and the remaining eight sit astride MacDonald's (1968) subalkaline/alkaline field boundary (Fig. 8.2).

The $Ol'-Ne'-Qz'$ diagram classifies five samples as alkaline (EXMOUNT2, EXMOUNT3, BRBEAR2, COBB1 and COBB2) and the remaining six as subalkaline.

On an AFM diagram all basalts except PREVRDG lie within the field of abyssal tholeiites outlined by Miyashiro et al. (1970) (Fig. 8.3) and on FeO^*/MgO vs. SiO_2 (Fig. 8.4) and Al_2O_3 vs. normative plagioclase, all samples excluding EXMOUNT1, are classified as tholeiites. Thus, the five samples classified as alkaline on $Ol'-Ne'-Qz'$ are designated transitional and will be plotted with the subalkaline samples.

EXMOUNT1 is sufficiently aluminous to lie just within the calcalkaline field on Al_2O_3 vs. normative plagioclase. A calcalkaline classification for an Explorer seamount sample has also been obtained by Armstrong and Nixon (1980).

On $TiO_2-K_2O-P_2O_5$, all samples lie within the oceanic field (Fig. 8.5).

On $MnO-TiO_2-P_2O_5$ COBB1, COBB2, BRBEAR2 and PREVRDG lie astride the MORB-OIT field boundary, BRBEAR1 and EXDEEP lie within the MORB field and samples from the Explorer seamount (EXMOUNT1, EXMOUNT2 and EXMOUNT3) lie astride the MORB-IAT field boundary. (Fig. 8.6). SEXRIDGE and EXRIFT lie within the IAT field.

Samples from Explorer seamount plus sample EXRIFT clearly lie within the MORB field on $MgO-FeO^*-Al_2O_3$ (Fig. 8.7). COBB1 and COBB2 lie within the continental

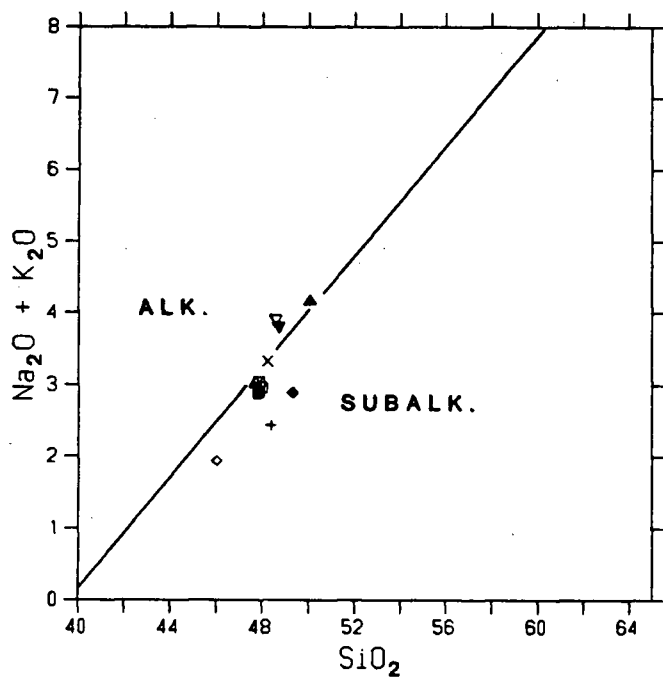


Fig. 8.2. Total alkalis vs. silica. Subalkaline/alkaline boundary from MacDonald (1968).

Fig. 8.3. AFM diagram. Tholeiitic/calcalkaline boundary from Irvine and Baragar (1971).

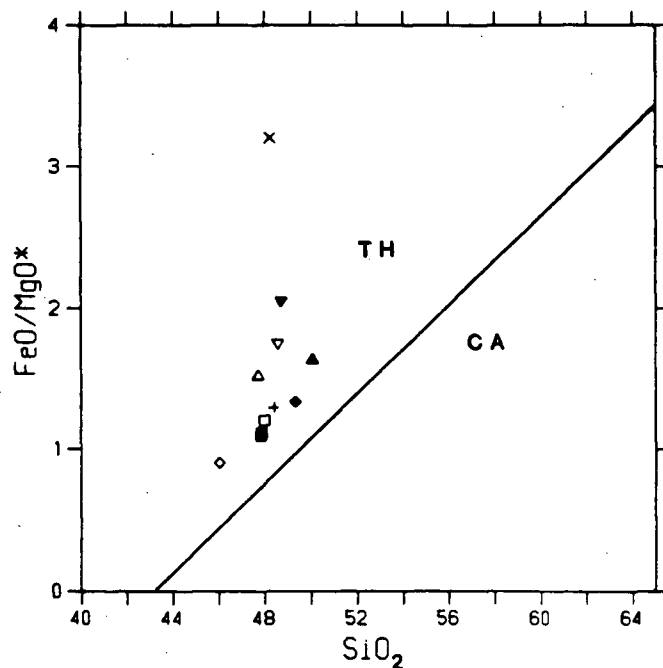
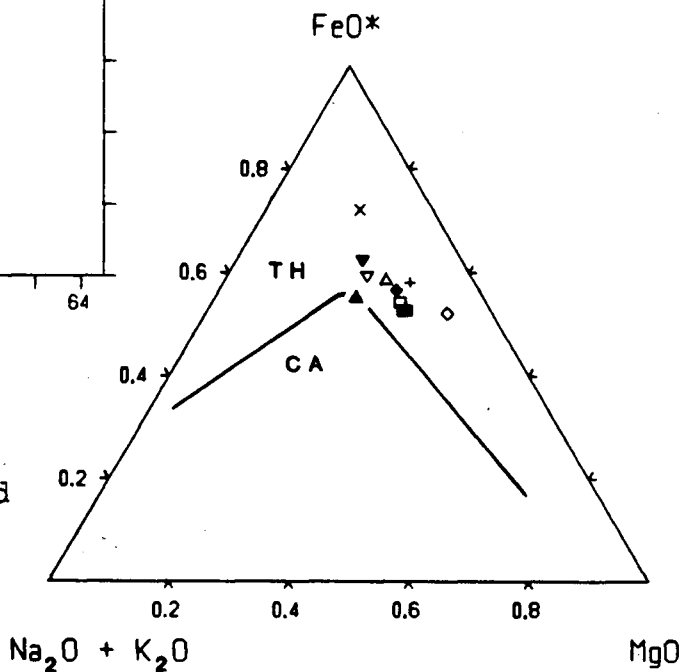
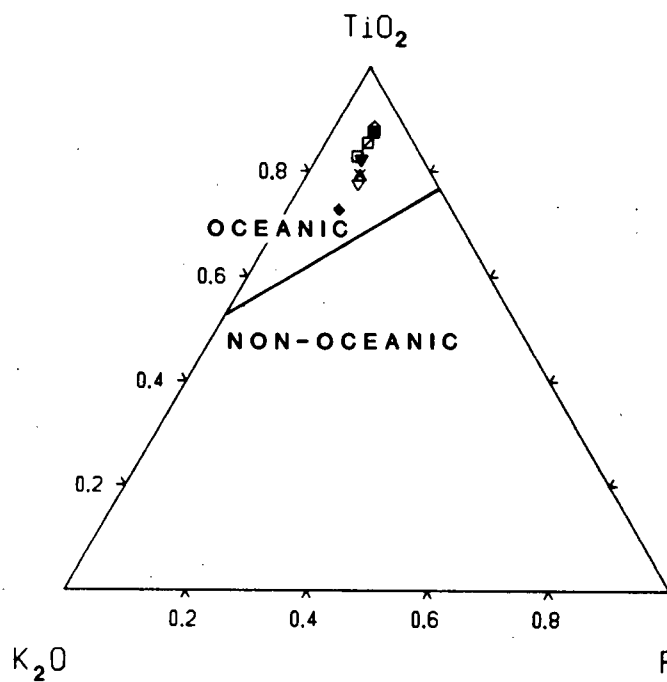
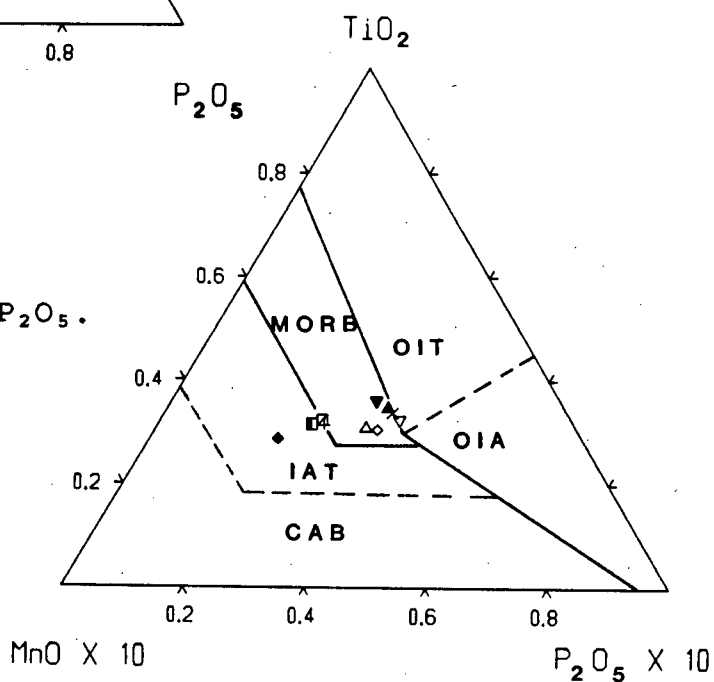
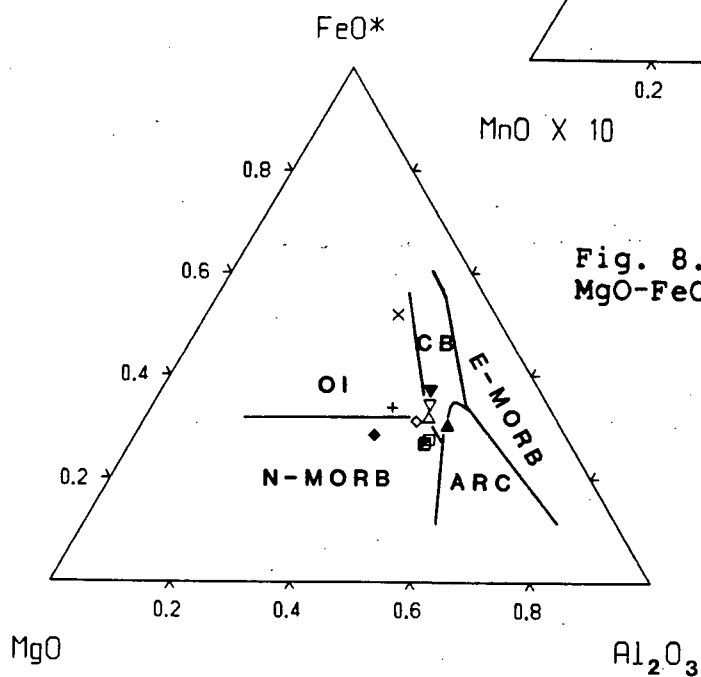


Fig. 8.4. FeO^*/MgO vs. SiO_2 . Tholeiitic/calcalkaline boundary from Miyashiro (1974).

| | |
|------------|------------|
| EXMOUNT1 □ | COBB1 ▽ |
| EXMOUNT2 ■ | COBB2 ▾ |
| EXMOUNT3 ▣ | SEXRIDGE + |
| BRBEAR1 △ | PREVRDG X |
| BRBEAR2 ▲ | EXRIFT ◇ |
| EXDEEP ◆ | |

Fig. 8.5. TiO_2 - K_2O - P_2O_5 .Fig. 8.6. MnO - TiO_2 - P_2O_5 .Fig. 8.7.
 MgO - FeO^* - Al_2O_3 .

| | | | |
|----------|---|----------|---|
| EXMOUNT1 | □ | COBB1 | ▽ |
| EXMOUNT2 | ■ | COBB2 | ▼ |
| EXMOUNT3 | ▣ | SEXRIDGE | + |
| BRBEAR1 | △ | PREVRDG | x |
| BRBEAR2 | ▲ | EXRIFT | ◇ |
| EXDEEP | ◆ | | |

field, EXDEEP and BEBEAR1 plot around the triple point, BRBEAR2 lies just within the orogenic field and SEXRIDGE lies just within the OI field, near to the MORB field. PREVRDG lies far from the other samples, towards FeO*, within the ocean island field.

8.2.2 TRACE ELEMENT CLASSIFICATIONS

All samples lie within the OFB-LKT-CAB field on Ti-Zr-Y (Fig. 8.8). and on Ti-Zr-Sr all samples except PREVRDG lie within the OFB field (Fig. 8.9). PREVRDG plots away from Sr, just outside of the OFB field.

On V vs. Ti/1000 ten samples have ratios between 33 and 41 and plot within the MORB field (Fig. 8.10). The exception is PREVRDG which has a Ti/V ratio of 53 and lies just within the WPB field. Samples from Explorer seamount plus EXRIFT have the lowest Ti and V abundances and are therefore separated from the other seven samples.

All samples lie within the overlapping convergent margin-MORB fields on Ti/Y vs. Nb/Y (Fig. 8.11). Explorer seamount samples have the lowest Ti/Y and Nb/Y ratios and plot away from the other samples. SEXRIDGE sits astride the boundary with the WPB field.

On Ti/Cr vs. Ni all samples except COBB2 clearly lie within the TH MORB field (Fig. 8.12). COBB2 has slightly lower Ni and lies astride the TH MORB-IAT field boundary.

Fig. 8.8. Ti-Zr-Y.

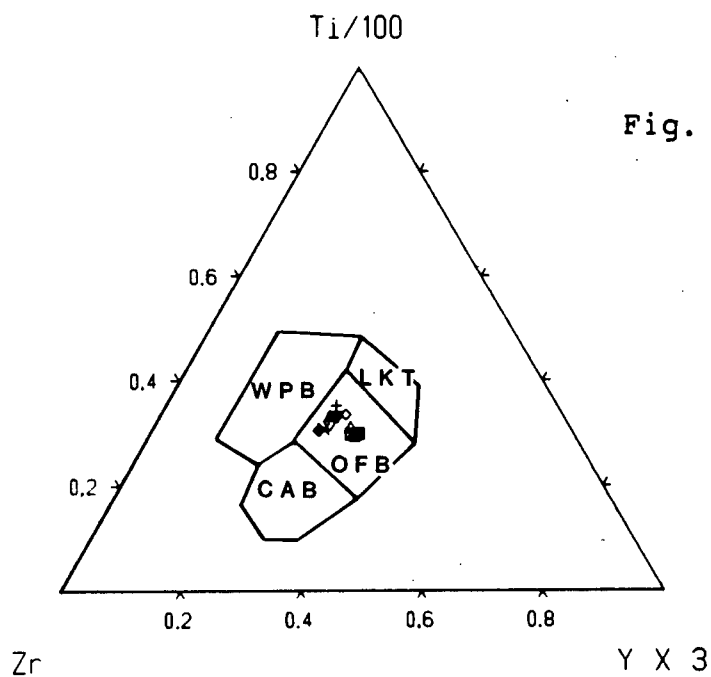


Fig. 8.9. Ti-Zr-Sr.

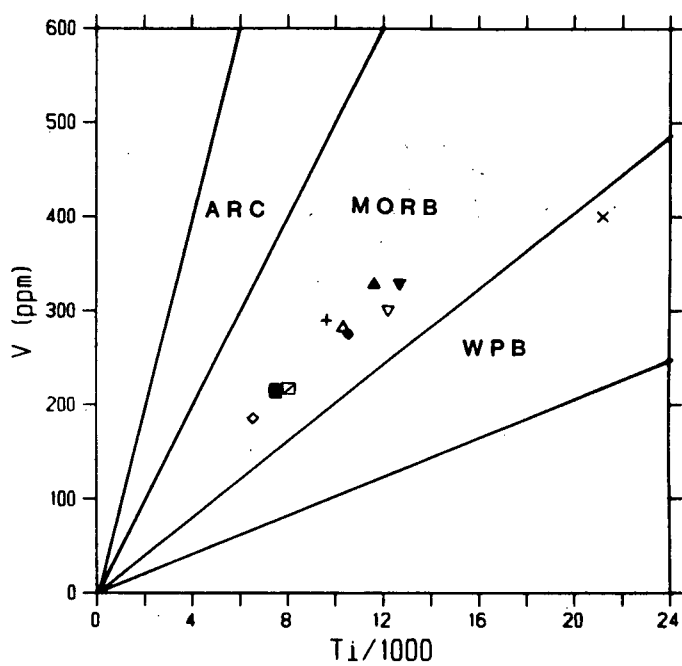
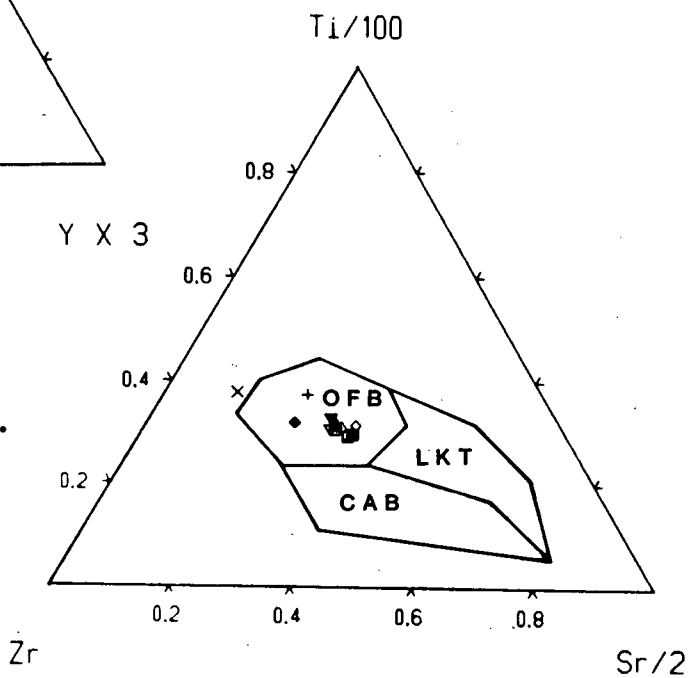
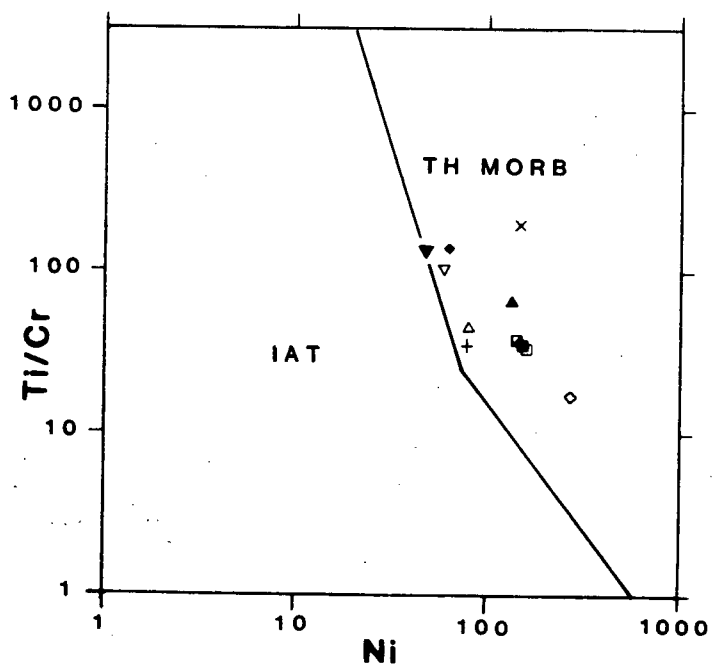
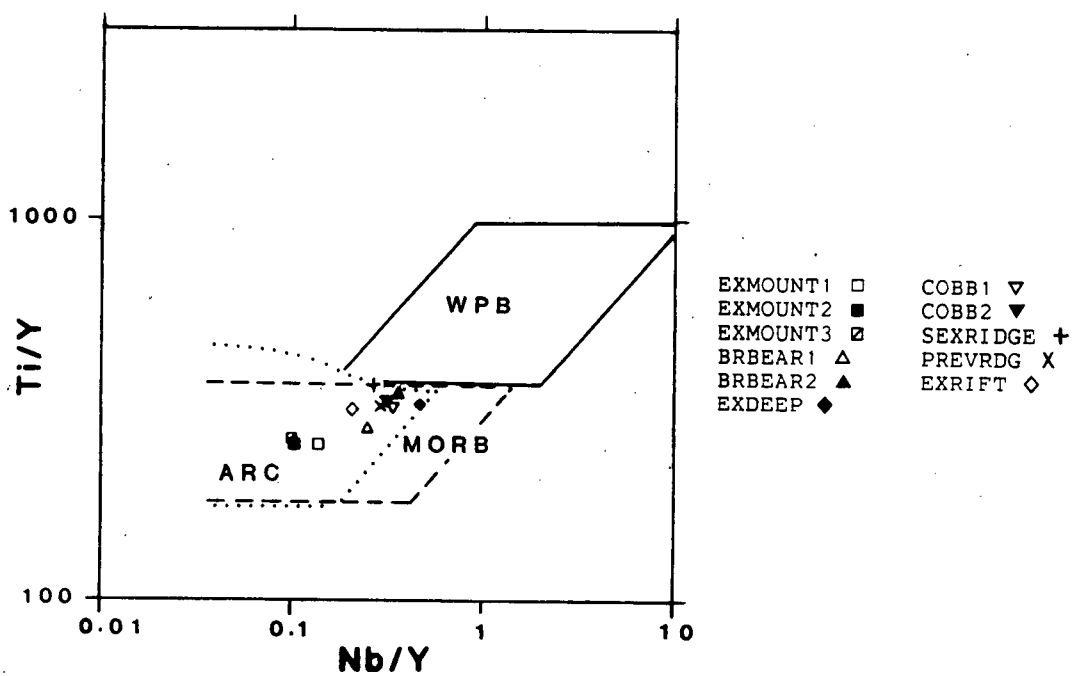


Fig. 8.10. V vs. Ti/1000.

| | | | |
|----------|---|----------|---|
| EXMOUNT1 | □ | COBB1 | ▽ |
| EXMOUNT2 | ■ | COBB2 | ▼ |
| EXMOUNT3 | ◻ | SEXRIDGE | + |
| BRBEAR1 | △ | PREVRDG | × |
| BRBEAR2 | ▲ | EXRIFT | ◇ |
| EXDEEP | ◆ | | |



Figs. 8.11 and 8.12. Ti/Y vs. Nb/Y (above) and Ti/Cr vs. Ni (below).

8.2.3 TRACE AND REE CLASSIFICATIONS

All samples plot within the oceanic field on Sm/Ce vs. Sr/Ce (Fig 8.13).

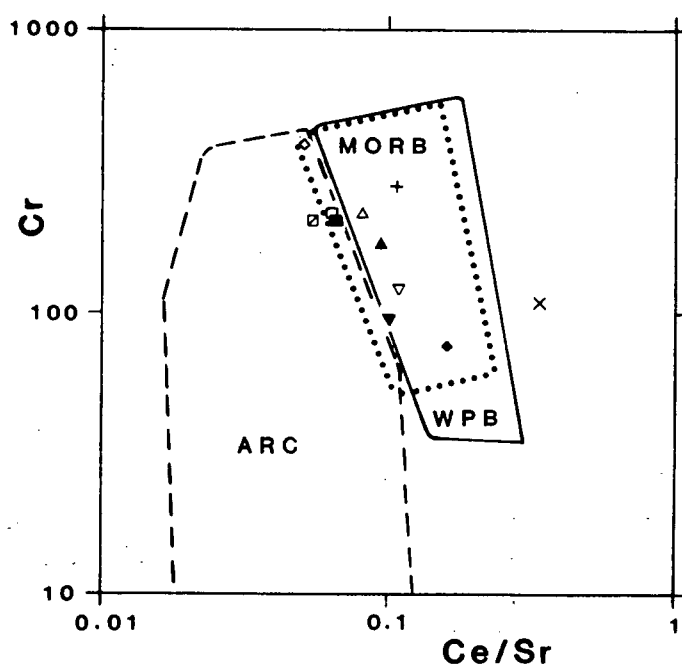
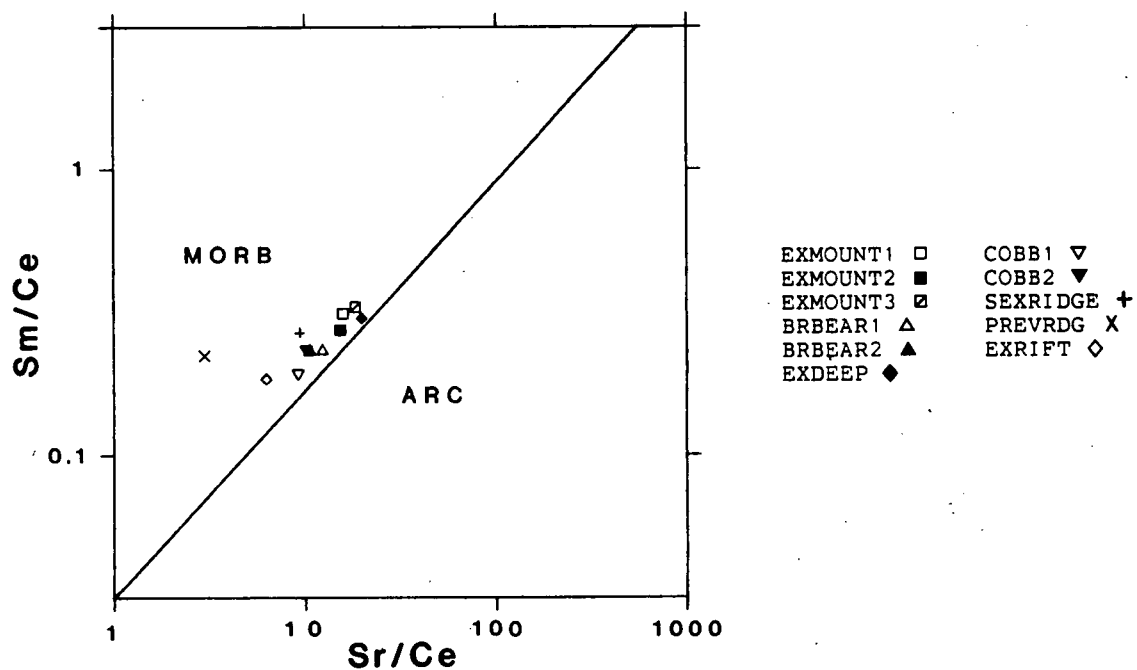
On Cr vs. Ce/Sr BRBEAR and COBB samples plus SEXRIDGE and EXRIFT plot within the overlapping MORB-WPB fields, and Exmount samples plus EXDEEP plot adjacent to the MORB-convergent margin field boundary (Fig. 8.14). PREVRDG has an unusually high Ce/Sr ratio and plots outside of all fields.

On Cr vs. Y all samples lie within the MORB field (Fig. 8.15). PREVRDG has a much higher Y abundance and plots away from the other samples.

On La vs. Ba all samples except PREVRDG have Ba/La ratios between nearly 4 and 11 and plot within or close to the N-MORB field (Fig. 8.16). PREVRDG has a Ba/La ratio of 1.2 and lies outside of all field boundaries.

On $(\text{Ba/La})_{\text{CH}}$ vs. $(\text{La/Sm})_{\text{CH}}$ all samples lie within or close to the ocean field, with $(\text{La/Sm})_{\text{CH}}$ less than 1.5 and $(\text{Ba/La})_{\text{CH}}$ less than 0.5 (Fig. 8.17). BRBEAR1, BRBEAR2, COBB1, COBB2 and EXDEEP have the highest $(\text{Ba/La})_{\text{CH}}$ ratios and PREVRDG has the lowest $(\text{Ba/La})_{\text{CH}}$ ratio. These six samples have the highest $(\text{La/Sm})_{\text{CH}}$ ratios.

On La vs. Th EXMOUNT1 and EXMOUNT2 have La/Th ratios greater than 15 and lie within the N-MORB field (Fig. 8.18). The nine remaining samples have La/Th ratios between 7 and 13 and lie within the E-MORB field.



Figs. 8.13 and 8.14. Sm/Ce vs. Sr/Ce (above) and Cr vs. Ce/Sr (below).

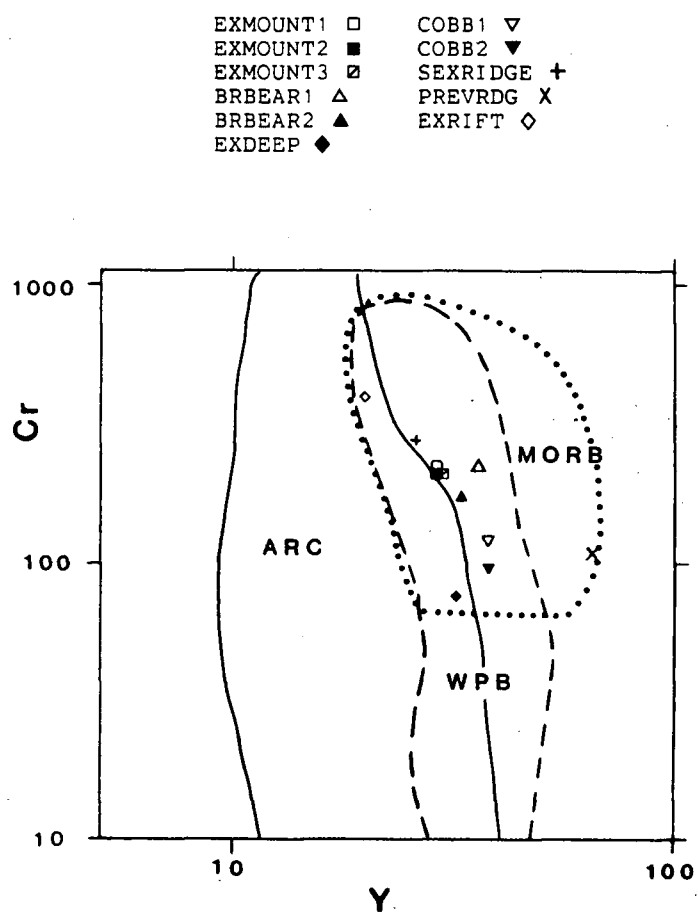
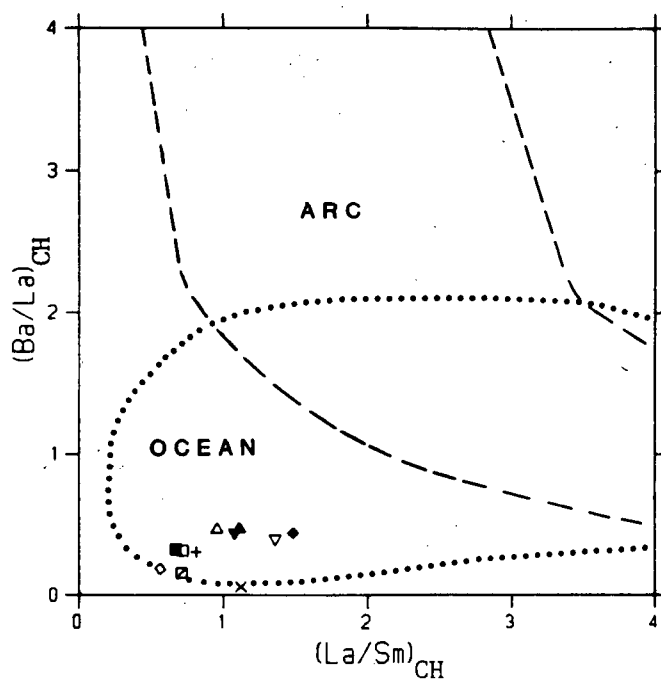
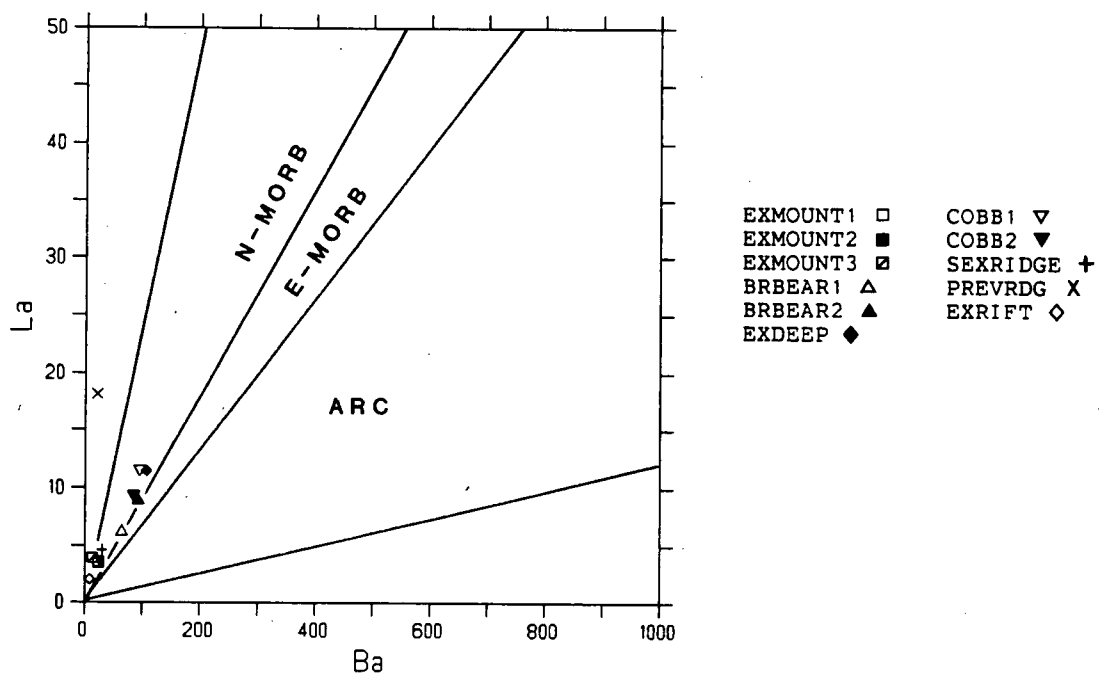


Fig. 8.15. Cr vs. Y.



Figs. 8.16 and 8.17. La vs. Ba (above) and $(Ba/La)_{CH}$ vs. $(La/Sm)_{CH}$ (below).

Five of these nine lie within the part which overlaps the orogenic andesite field.

On La vs. Nb all samples except EXMOUNT2 and EXMOUNT3 have La/Nb ratios less than 1 and lie within the E-MORB field (Fig. 8.19). EXMOUNT2 and EXMOUNT3 have La/Nb ratios of 1.2 and 1.3 respectively and lie just within the N-MORB field.

On K_2O/Yb vs. Ta^*/Yb all samples lie within the MORB field (Fig. 8.20).

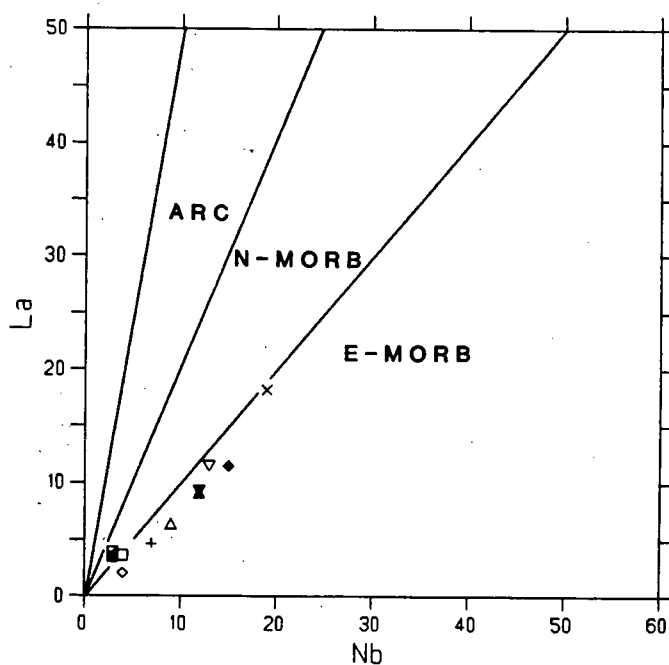
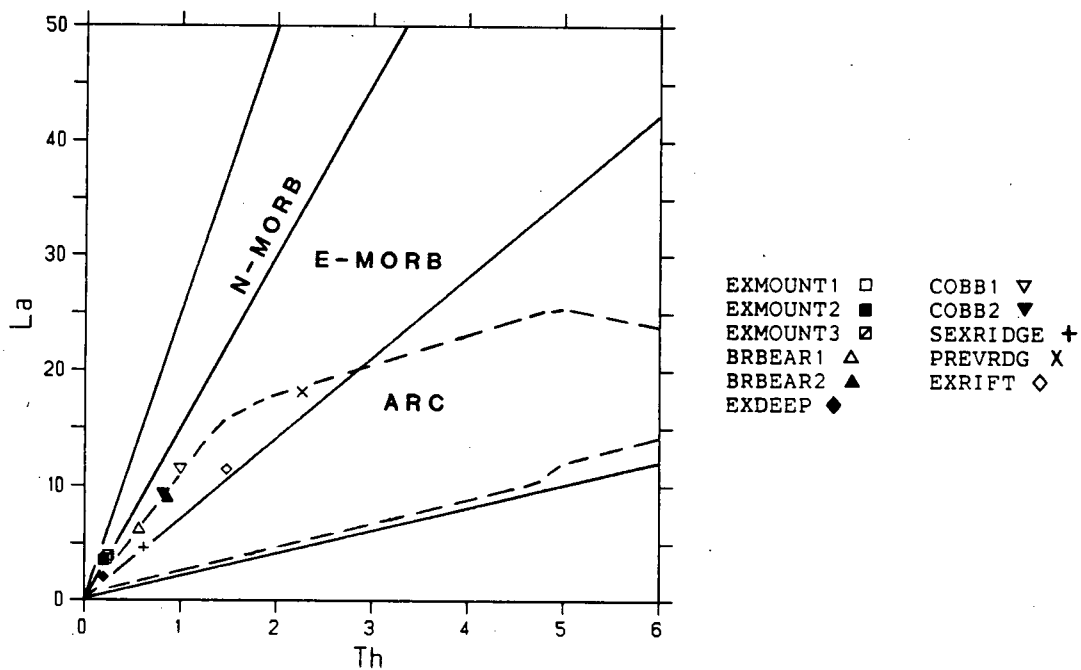
On Th/Yb vs. Ta^*/Yb samples BRBEAR2, COBB1 and EXDEEP lie within the overlapping MORB-WPB fields (Fig. 8.21). The remaining eight samples lie within the MORB field.

Samples lie within both the N- and E-MORB fields on Th-Hf/3-Ta* (Fig. 8.22). Explorer seamount samples and EXRIFT lie within the N-MORB field and BRBEAR(s), COBB(s) and EXDEEP lie within the E-MORB field. SEXRIDGE plots on the boundary line between the N- and E-MORB fields, and PREVRDG lies close to the boundary line, therefore their classifications are not certain.

8.2.4 BULK EARTH NORMALIZED DIAGRAMS (BEND)

Three BEND were plotted for ocean floor data (Fig. 8.23, 8.24 and 8.25).

BEND patterns on Fig. 8.23 are from Explorer Seamount. In general patterns from these samples slope positively from Ba to Sm, slope negatively from Sm to Hf



Figs. 8.18 and 8.19. La vs. Th (above) and La vs. Nb (below).

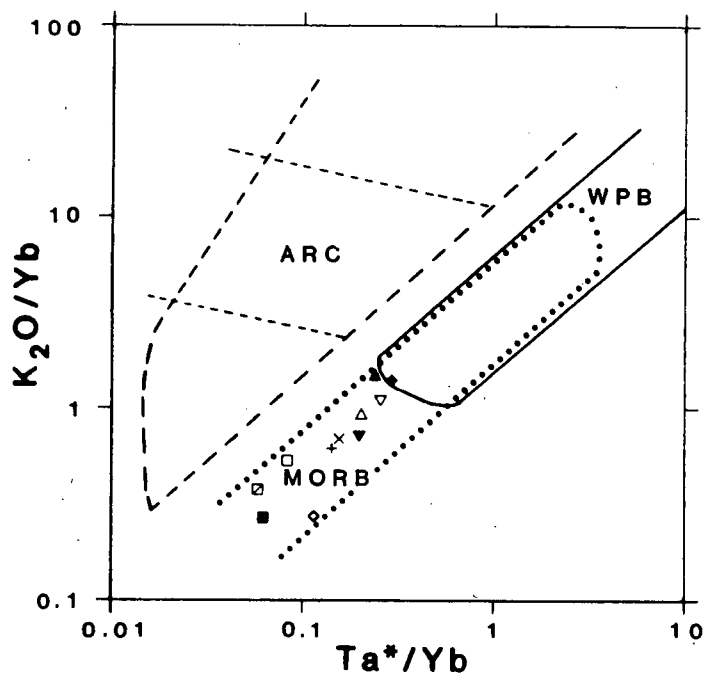


Fig. 8.21. Th/Yb vs. Ta^*/Yb .

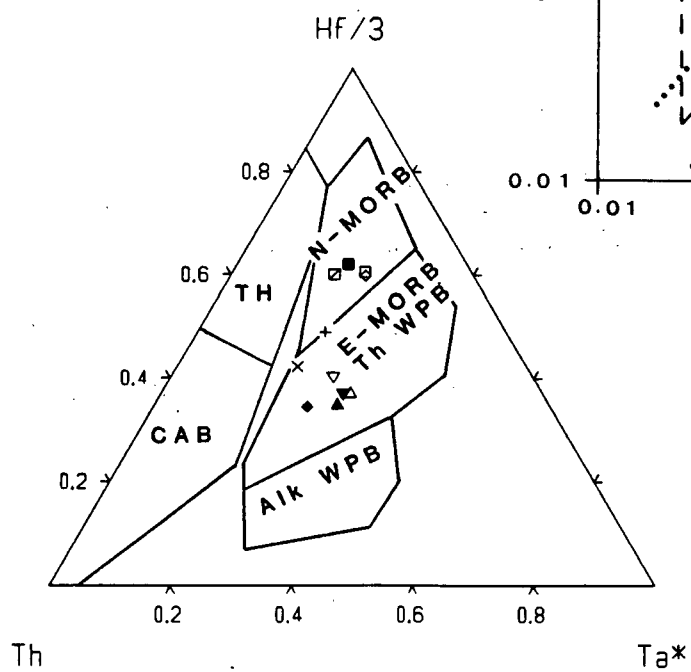
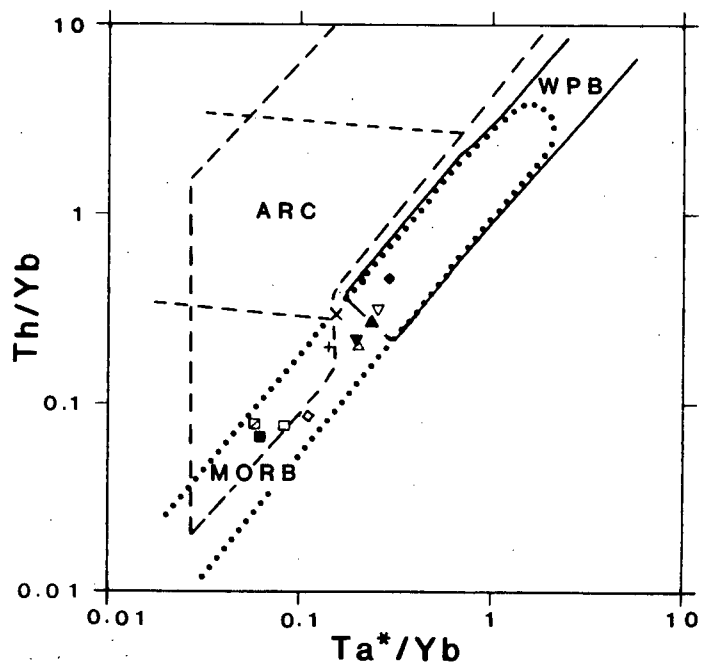


Fig. 8.22. $Th-Hf/3-Ta^*$.

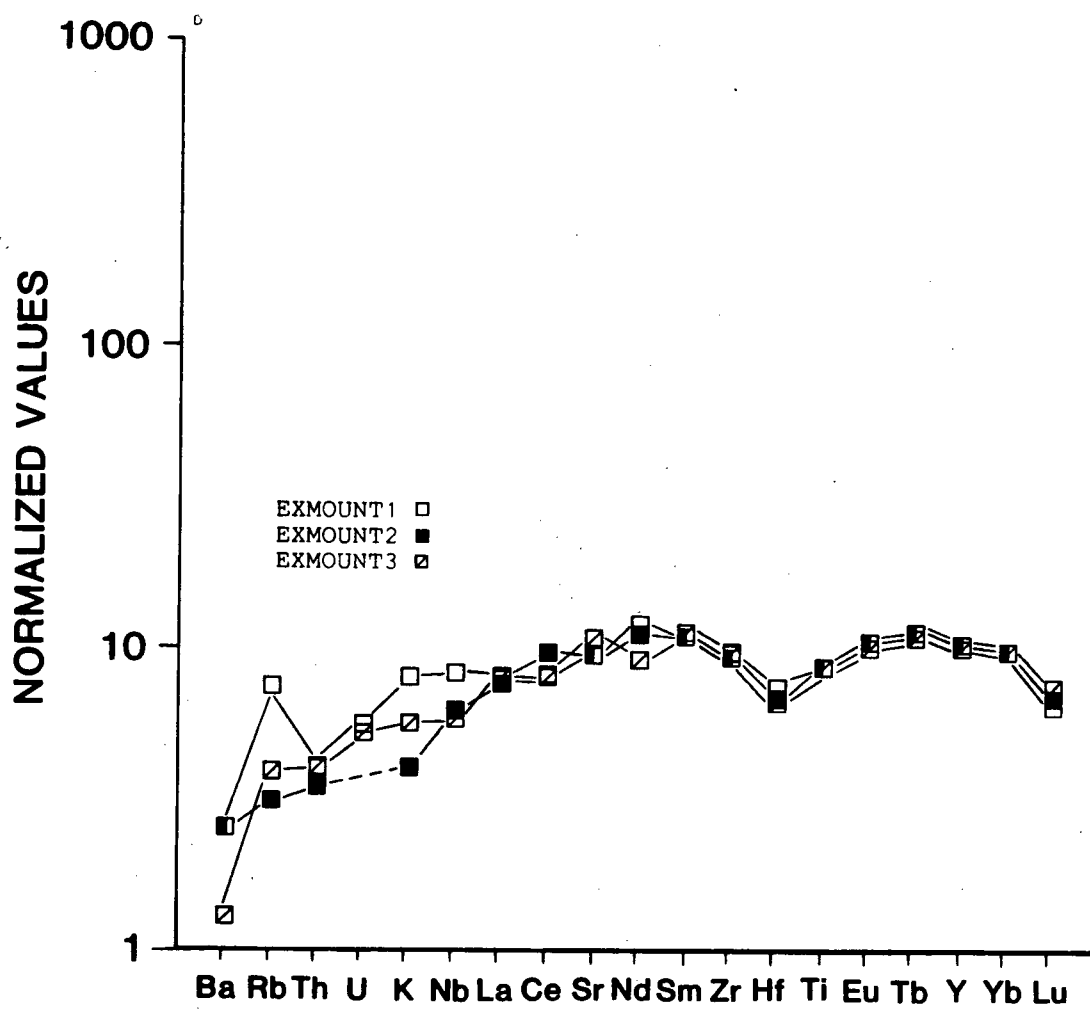


Fig. 8.23. BEN diagram for samples EXMOUNT1, EXMOUNT2 and EXMOUNT3.

and have a convex-up hump from Hf to Lu. EXMOUNT1 has a 'peak' at Rb. None of these patterns have Eu anomalies.

BEND patterns on Fig. 8.24 are from Brown Bear and Cobb seamounts. Patterns have grossly convex-up shapes which 'peak' at Nb and have 'troughs' at Sr and Hf. From Ti to Lu the patterns are relatively unfractionated and have no Eu anomalies, despite their Sr anomalies. In addition, Cobb patterns have a 'trough' at K and BRBEAR1 and COBB2 are slightly enriched in Ba relative to Rb.

BEND patterns from Fig. 8.25 are from Southern Explorer Ridge, Paul Revere Ridge, Explorer Rift and Explorer Deep. The BEND patterns from SEXRIDGE and PREVRDG are grossly similar. Both are relatively unfractionated and both have 'troughs' at Sr, the 'trough' being especially noticeable in the pattern from PREVRDG. PREVRDG has a slight 'trough' at K and a 'peak' at Th whereas SEXRIDGE has a 'peak' at Nb. EXRIFT has 'peaks' at Rb and Nb, but otherwise slopes positively from Ba to Nd and is relatively flat from Sm to Yb. EXDEEP has a pattern with a convex-up shape 'peaking' at Nb, and a 'trough' at Sr. This latter pattern is grossly similar to patterns from Fig. 8.24. None of these patterns have Eu anomalies.

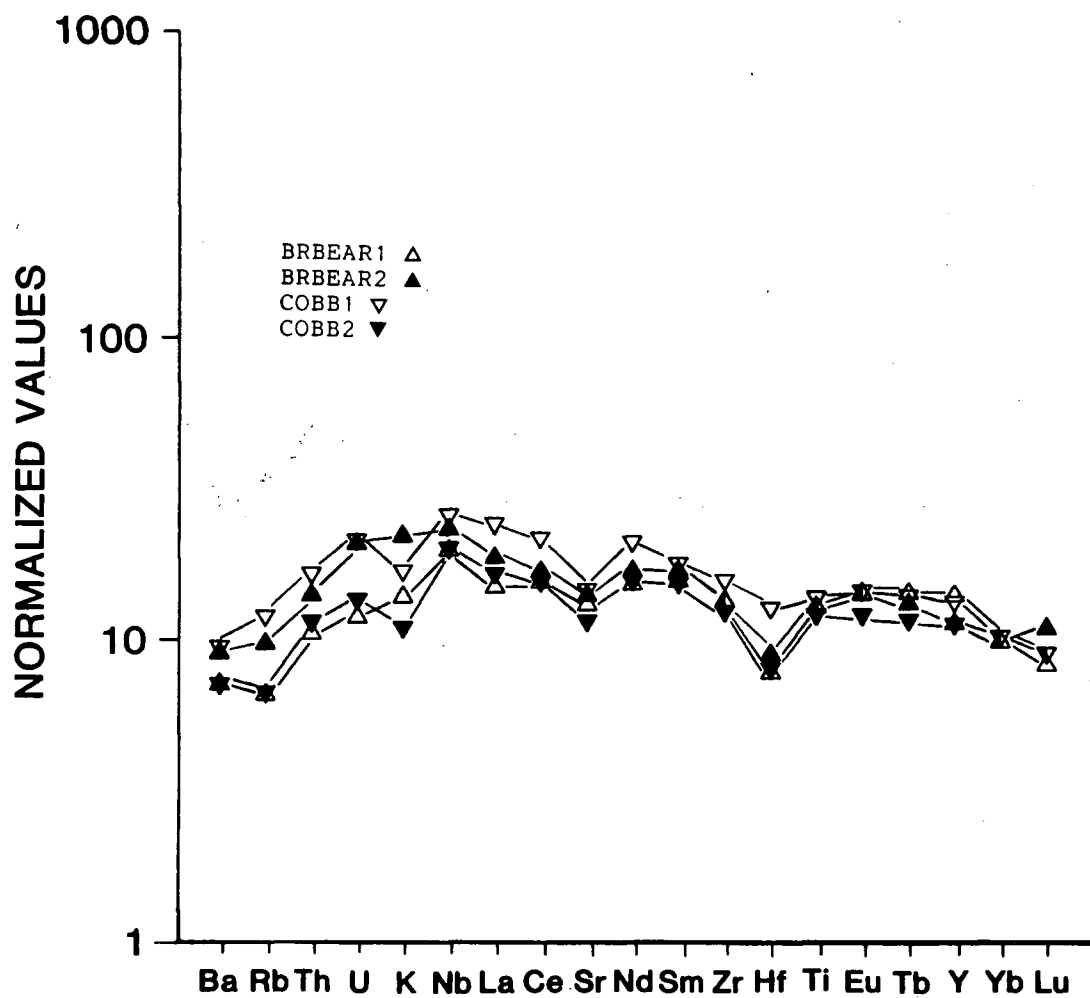


Fig. 8.24. BEN diagram for samples BRBEAR1, BRBEAR2, COBB1 and COBB2.

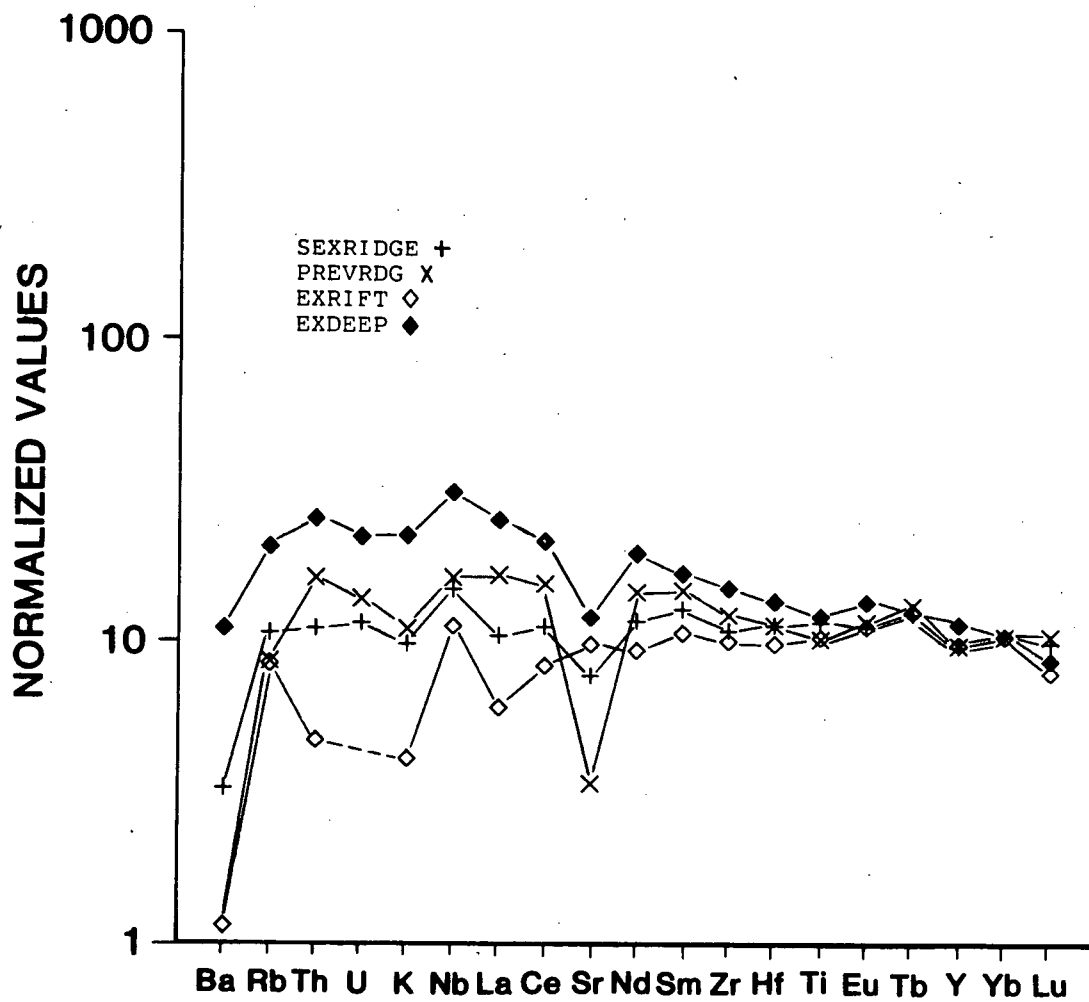


Fig. 8.25. BEN diagram for samples SEXRIDGE, PREVRDG, EXRIFT and EXDEEP.

8.3 TRACE ELEMENT CHEMISTRY

In general the overall abundances of trace and rare earth elements are lower than abundances in samples from any of the other suites in this study.

Trace element abundances and BEND patterns for Explorer seamount samples and EXRIFT grossly resemble abundances in N-MORB, but they have higher concentrations of Ba, Rb and Sr, average to higher abundances of Nb and Zr and lower abundances of Hf (Sun, 1980; Sun et al., 1979; Pearce, 1982; Pearce and Cann, 1973). Zr/Nb ratios between 17.5 and 33 are lower than the average N-MORB ratio of 40 to 50 calculated by Erlank and Kable (1976) suggesting the mantle source region for these basalts is less depleted than the source for most N-MORB. La abundances range from 6.1 to 11.9 times chondritic, Yb abundances are 10.4 to 14.5 times chondritic, $(\text{La/Yb})_{\text{CH}} = 0.58$ to 0.81 and $(\text{La/Ce})_{\text{CH}} = 0.72$ to 0.99 . These ratios are within the range of ratios from N-MORB (Henderson, 1984).

Samples from Brown Bear and Cobb seamounts and Explorer Deep have similar to slightly enriched trace and REE abundances relative to abundances in an 'average' E-MORB, and their BEND patterns resemble E-MORB patterns (Sun, 1980; Thompson et al., 1983; Sun et al., 1979; Pearce, 1982). La abundances lie between 19.2 and 34.7 times chondritic, Yb ranges from 12.7 to 17.3 times chondritic, $(\text{La/Yb})_{\text{CH}}$ ratios range from 1.53 to 2.40, $(\text{La/Ce})_{\text{CH}}$ ratios lie between 0.95 to 1.16 and Zr/Nb ratios lie between 9.6 and 13.2. These

ratios also suggest an E-MORB source (Henderson, 1984; Pearce, 1982; Erlank and Kable, 1976).

Rather than a plume augmented N-MORB source (i.e. E-MORB) for EXDEEP, Cousens et al. (1984) suggest small degrees of partial melting of the mantle source as the cause of high LIL and LREE abundances in this sample. The $^{87}\text{Sr}/^{86}\text{Sr}$ ratios from this area support this explanation.

Relative to N-MORB, SEXRIDGE has higher abundances of all trace elements except Sr. Abundances of LIL are lower than abundances in E-MORB but Zr, Hf and HREE contents are higher (Pearce, 1982; Sun et al., 1979; Sun, 1980). The BEND pattern from this sample does not resemble either an N- or E-MORB pattern but has characteristics of both. Cousens (1982) suggests its shape may be produced by mixing N- and E-MORB magmas, i.e. mixing of EXRIFT and EXDEEP magmas. SEXRIDGE has an La content of 14 times chondritic, Yb equal to 14.1 times chondritic, an $(\text{La}/\text{Yb})_{\text{CH}}$ ratio of 0.9 and an $(\text{La}/\text{Ce})_{\text{CH}}$ ratio of 0.93. Its Zr/Nb ratio equals 14.3. These ratios lie between ratios from EXRIFT and EXDEEP, further support for magma mixing.

Except for Ba and Sr (Ba = 21 ppm, Sr = 133 ppm) PREVRDG has the highest trace and REE concentrations of all samples in this suite. La equals 55.2 times chondritic, Yb is 35 times chondritic, $(\text{La}/\text{Yb})_{\text{CH}}$ equals 1.59 and $(\text{La}/\text{Ce})_{\text{CH}}$ is 1.06. Zr/Nb equals 14.7, similar to Zr/Nb ratios in BRBEAR1 and SEXRIDGE. Schilling et al. (1976) suggest higher trace and rare earth element abundances in propagating rift

segments are evidence for hotspot activity.

8.3.1 TH AND U

Th abundances are 0.3 ppm or less in Explorer seamount samples and EXRIFT and between 0.6 and 1.0 ppm in Brown Bear and Cobb seamount samples and SEXRIDGE (Table VII). These abundances are within the range of N- and E-MORB respectively (Basaltic Volcanism Study Project, 1981). Abundance of Th is 1.5 ppm in EXDEEP and 2.3 ppm in PREVRDG.

U was not analyzed in samples SEXRIDGE, PREVRDG, EXRIFT and EXDEEP but estimated abundances from BEND are 0.2, 0.6, less than 0.1 and 0.4 ppm respectively. U abundance in the remaining seven samples ranges from less than 0.1 to 0.4 ppm. These abundances are within the range of N- and E-MORB from the Pacific Ocean (Jochum et al., 1983).

Th/U ratios range from 2 to 4 and average 3.

8.3.2 TRANSITION ELEMENTS

Cr abundances in Explorer seamount samples, BRBEAR2 and PREVRDG are slightly lower than an 'average' N-MORB, and Ni abundances are marginally higher (Engel et al., 1965). Abundances of Cr and Ni in BRBEAR1 and SEXRIDGE lie within the range from 'average' N-MORB.

COBB1, COBB2 and EXDEEP are depleted in Cr and Ni relative to both N and E-MORB.

EXRIFT has the highest Cr and Ni abundances (Cr = 390 ppm, Ni = 270 ppm) reflecting its (unfractionated) Mg' number of 66.

Sc abundances range from 27.1 to 43.6 ppm and average 37 ppm. This is within the range of MORB (Erlank and Kable, 1976; Pearce, 1982).

Petrography by Cousens (1982) established olivine and plagioclase as the dominant phenocryst phases in Explorer basalts. Pyroxene phenocrysts occurred only rarely. Therefore Ni concentrations are primarily controlled by olivine fractionation and Cr contents are presumably controlled by fractionation of associated Cr-spinel.

8.4 SR ISOTOPES

Sr isotope ratios were not available for samples from Explorer, Brown Bear or Cobb seamounts but Armstrong and Nixon (1980) report an $^{87}\text{Sr}/^{86}\text{Sr}$ ratio of 0.70250 for an Explorer seamount sample located at $49^{\circ} 03' \text{N}$ and $130^{\circ} 54' \text{W}$, and Eaby et al. (1984) report $^{87}\text{Sr}/^{86}\text{Sr}$ ratios of 0.70251 and 0.7023 for Brown Bear and Cobb seamounts respectively. Sr isotope ratios from SEXRIDGE, PREVRDG and EXRIFT lie between 0.70232 and 0.70254 (Table VII) and a sample from Explorer Deep analyzed by Cousens (1982) has an $^{87}\text{Sr}/^{86}\text{Sr}$ ratio of 0.70252. These tightly clustered ratios all lie within the range of ratios from MORB (Hart, 1976) despite the fact that Explorer, Brown Bear and Cobb are seamounts.

8.5 DISCUSSION OF DISCRIMINATION DIAGRAMS

Explorer seamount samples plot within or close to the N-MORB field on all diagrams and do not have the chemical or isotopic characteristics of WPB. This is consistent with their BEND pattern shapes. Although a N-MORB seamount may seem unusual, Batiza (1980) suggests that most small volcanoes on young oceanic crust are chemically similar to MORB.

EXRIFT is classified as N-MORB on all diagrams except MnO-TiO₂-P₂O₅ (IAT) (Fig. 8.6), La vs. Th (E-MORB) (Fig. 8.18) and La vs. Nb (E-MORB) (Fig. 8.19). Relative depletion in P₂O₅ (P₂O₅ = 0.8 wt. %) causes the IAT classification on the first diagram, whereas relative enrichment in Th and Nb respectively classify EXRIFT as E-MORB on the latter two diagrams. However, its BEND pattern is more characteristic of N-MORB than of E-MORB.

On most diagrams Brown Bear and Cobb seamount samples plot far from Explorer seamount samples and sample EXRIFT. They are classified as ocean floor basalts or E-MORB on all diagrams except MgO-FeO*-Al₂O₃ (Fig. 8.7) and La vs. Ba (Fig. 8.16). Higher FeO* and lower Al₂O₃ and MgO abundances result in OI and ARC classifications on the former diagram, whereas relatively low Ba abundances (relative to E-MORB) result in an N-MORB classification on the latter diagram. These low Ba abundances are close to or below detection limits and classifications based on Ba should be judged accordingly. BEND patterns classify these samples as E-MORB

(Fig. 8.24). Brown Bear and Cobb seamounts have low Sr isotope ratios, more characteristic of N-MORB, suggesting that the seamounts are constructed of lavas from depleted sources, rather than from an enriched mantle plume (Eaby et al., 1984).

EXDEEP plots near the Brown Bear and Cobb samples on all of the diagrams, and is thus classified as E-MORB. Its BEND pattern (Fig. 8.25) confirms this classification.

SEXRIDGE lies within the IAT field on $\text{MnO-TiO}_2\text{-P}_2\text{O}_5$ (Fig. 8.6) because of a relatively high MnO abundance (MnO = 0.21 wt. %). Relative to N-MORB it is slightly depleted in Al_2O_3 and enriched in FeO^* , hence its OI classification on $\text{MgO-FeO}^*\text{-Al}_2\text{O}_3$ (Fig. 8.7). On all other diagrams SEXRIDGE plots within the MORB field; as N-MORB on La vs. Ba (Fig. 8.16) and as E-MORB on La vs. Th and La vs. Nb (Figs. 8.18 and 8.19). On Th-Hf/3-Ta* (Fig. 8.22) it lies on the N- and E-MORB field boundary. These chemical characteristics support the mixing hypothesis suggested by this samples BEND pattern and incompatible element ratios.

Sample PREVRDG plots outside of MORB field boundaries on many of the diagrams ($\text{MgO-FeO}^*\text{-Al}_2\text{O}_3$ (Fig. 8.7), Ti-Zr-Sr (Fig. 8.9), Cr vs. Ce/Sr (Fig. 8.14) and La vs. Ba (Fig. 8.16)). On Th-Hf/3-Ta* (Fig. 8.22) it plots close to the boundary between N-MORB and E-MORB. Its BEND pattern and location on all diagrams except Ti-Zr-Sr, Cr vs. Ce/Sr and La vs. Ba suggest mixing of N- and E-MORB sources. The very low Sr content, evident on Ti-Zr-Sr, Cr vs. Ce/Sr and BEND

may be a product of extreme plagioclase fractionation and low Ba abundance may be produced by seawater alteration (Korringa and Noble, 1971; Philpotts et al., 1969). However Sr depletion by plagioclase fractionation usually has an associated negative Eu anomaly and seawater depletion of Ba should supply an accompanying increase in K and Rb. As neither of these accompanying geochemical characteristics are observed both of these suggestions appear unlikely, implying this anomalous chemistry is inherited from the source.

8.6 SUMMARY

In general offshore basalt samples are distinct from all other samples in this study because of their low overall abundances of trace and rare earth elements, and low $^{87}\text{Sr}/^{86}\text{Sr}$ isotope ratios.

On all tectonic discrimination diagrams the samples lie within the MORB field. Diagrams which are able to separate N- from E-MORB (La vs. Ba, La vs. Th, La vs. Nb and Th-Hf/3-Ta*) distinguish three groups of samples. Explorer seamount and Explorer Rift samples are classified as N-MORB, Cobb and Brown Bear Seamount and Explorer Deep samples are classified as E-MORB and Southern Explorer Ridge and Paul Revere Ridge samples are classified as a mixture of N- and E-MORB magmas. BEND pattern shapes confirm these classifications.

Relative to the remainder of the suite PREVRDG has higher abundances of TiO_2 , Fe_2O_3 , MnO and P_2O_5 and lower abundances of Al_2O_3 , MgO and CaO . It also has much higher abundances of all trace and rare earth elements, excluding Ba and Sr. The trace and REE abundances grossly resemble those from an oceanic WPB, but Sr isotope ratios and BEND pattern shape imply a MORB-like source. Extremely high Fe_2O_3 content and lower than 'average' abundance of MgO have been suggested by Cousens et al. (1984) to be evidence for a once active northeasterly directed propogating rift.

TABLE VII. OFFSHORE BASALTS

Major, trace and rare earth element abundances, Sr isotope ratios and estimated ages.

| | EXMOUNT ¹ | EXMOUNT ² | EXMOUNT ³ | BRBEAR ¹ | BRBEAR ² | COBB ¹ | COBB ² |
|---|----------------------|----------------------|----------------------|---------------------|---------------------|-------------------|-------------------|
| Series Name | Tholeiite Basalt | Alk/Trans Basalt | Alk/Trans Basalt | Tholeiite Basalt | Alk/Trans Basalt | Alk/Trans Basalt | Alk/Trans Basalt |
| LAT. | 49 04.0 | 49 04.0 | 49 04.0 | 46 05.7 | 46 05.7 | 46 45.0 | 46 45.0 |
| LONG. | 130 56.0 | 130 56.0 | 130 56.0 | 130 27.8 | 130 27.8 | 130 50.0 | 130 50.0 |
| SiO ₂ | 47.99 | 47.84 | 47.87 | 47.72 | 50.09 | 48.57 | 48.72 |
| TiO ₂ | 1.25 | 1.25 | 1.34 | 1.72 | 1.94 | 2.04 | 2.12 |
| Al ₂ O ₃ | 17.18 | 17.18 | 17.08 | 15.77 | 15.72 | 15.33 | 14.75 |
| Fe ₂ O ₃ | 10.70 | 10.39 | 10.41 | 11.91 | 10.46 | 12.66 | 13.48 |
| FeO | N/A | N/A | N/A | N/A | N/A | N/A | N/A |
| MnO | 0.17 | 0.17 | 0.17 | 0.19 | 0.16 | 0.18 | 0.18 |
| MgO | 8.04 | 8.56 | 8.41 | 7.05 | 5.74 | 6.54 | 5.96 |
| CaO | 11.62 | 11.62 | 11.58 | 11.77 | 11.51 | 10.50 | 10.80 |
| Na ₂ O | 2.80 | 2.81 | 2.91 | 2.78 | 3.71 | 3.54 | 3.51 |
| K ₂ O | 0.16 | 0.08 | 0.12 | 0.26 | 0.47 | 0.35 | 0.27 |
| P ₂ O ₅ | 0.10 | 0.10 | 0.11 | 0.19 | 0.20 | 0.25 | 0.20 |
| H ₂ O | N/A | N/A | N/A | 0.80 | 0.84 | 0.30 | 1.34 |
| Ba | 24.0 | 24.0 | 13.0 | 64.0 | 92.0 | 94.0 | 84.0 |
| Rb | 3.6 | 1.5 | 2.0 | 3.0 | 5.0 | 6.0 | 4.0 |
| Th | 0.2 | 0.2 | 0.3 | 0.6 | 0.9 | 1.0 | 0.8 |
| U | 0.1 | < 0.1* | 0.1 | 0.2 | 0.4 | 0.4 | 0.3 |
| Nb | 4.0 | 3.0 | 3.0 | 9.0 | 12.0 | 13.0 | 12.0 |
| La | 3.6 | 3.5 | 3.9 | 6.3 | 9.1 | 11.4 | 9.2 |
| Ce | 9.8 | 11.6 | 10.3 | 17.4 | 21.4 | 27.1 | 22.9 |
| Sr | 155.0 | 177.0 | 189.0 | 214.0 | 227.0 | 248.0 | 232.0 |
| Nd | 10.5 | 9.7 | 8.6 | 12.4 | 15.7 | 19.1 | 16.8 |
| Sm | 3.1 | 3.2 | 3.4 | 4.1 | 5.0 | 5.2 | 5.3 |
| Zr | 92.0 | 89.0 | 99.0 | 119.0 | 134.0 | 154.0 | 144.0 |
| Hf | 2.1 | 1.9 | 2.0 | 2.0 | 2.6 | 3.6 | 2.7 |
| Eu | 1.1 | 1.0 | 1.1 | 1.3 | 1.5 | 1.5 | 1.5 |
| Tb | 0.7 | 0.8 | 0.8 | 0.9 | 0.9 | 0.9 | 0.9 |
| Y | 29.0 | 29.0 | 30.0 | 36.0 | 33.0 | 38.0 | 38.0 |
| Yb | 3.0 | 3.0 | 3.2 | 2.8 | 3.1 | 3.2 | 3.8 |
| Lu | 0.3 | 0.3 | 0.4 | 0.3 | 0.5 | 0.4 | 0.5 |
| Co | 90.0 | 126.0 | 99.0 | 59.0 | 61.0 | 69.0 | 54.0 |
| Cr | 223.7 | 211.0 | 210.7 | 225.0 | 175.7 | 120.8 | 95.9 |
| Cu | 80.0 | 85.0 | 91.0 | 47.0 | 61.0 | 50.0 | 70.0 |
| Ni | 160.0 | 153.0 | 142.0 | 80.0 | 134.0 | 59.0 | 47.0 |
| Sc | 38.2 | 36.6 | 35.5 | 39.5 | 43.6 | 41.8 | 42.7 |
| V | 213.0 | 216.0 | 219.0 | 283.0 | 330.0 | 300.0 | 328.0 |
| Sr ⁸⁷ _{Sr⁸⁶} | N/A | N/A | N/A | N/A | N/A | N/A | N/A |
| K/Rb | 368.93 | 442.72 | 498.06 | 719.42 | 780.29 | 484.22 | 560.32 |
| (La/Yb) _{CH} | 0.80 | 0.77 | 0.81 | 1.53 | 1.93 | 2.40 | 1.64 |
| La/Nb | 0.90 | 1.15 | 1.30 | 0.70 | 0.75 | 0.88 | 0.77 |
| Mg' | 60 | 62 | 62 | 54 | 52 | 51 | 47 |
| Age (Ma) | 4 | 4 | 4 | < 1 | < 1 | < 1 | < 1 |

* Estimated from BEND

Continued.....

| | SEXRIDGE ² | PREVRDG ² | EXRIFT ² | EXDEEP ² | |
|--------------------------------|-----------------------|----------------------|---------------------|---------------------|---|
| Series Name | Tholeiite Basalt | Tholeiite Basalt | Tholeiite Basalt | Tholeiite Basalt | |
| LAT. | 49 55.2 | 50 00.42 | 50 13.9 | 50 05.5 | |
| LONG. | 130 10.8 | 129 31.5 | 130 15.1 | 129 44.5 | |
| SiO ₂ | 48.41 | 48.24 | 46.03 | 49.32 | Major and some trace element abundances from: |
| TiO ₂ | 1.61 | 3.53 | 1.09 | 1.76 | |
| Al ₂ O ₃ | 13.48 | 10.69 | 15.19 | 15.10 | 1 R.L. Chase (pers. comm., 1984) |
| Fe ₂ O ₃ | 12.63 | 19.33 | 12.27 | 11.51 | 2 B.L. Cousens (1982) |
| FeO | N/A | N/A | N/A | N/A | |
| MnO | 0.21 | 0.30 | 0.19 | 0.19 | |
| MgO | 8.81 | 5.44 | 12.20 | 7.81 | |
| CaO | 12.04 | 8.38 | 12.00 | 11.43 | |
| Na ₂ O | 2.24 | 2.79 | 1.87 | 2.44 | * Estimated from BEND |
| K ₂ O | 0.19 | 0.53 | 0.06 | 0.45 | |
| P ₂ O ₅ | 0.14 | 0.39 | 0.08 | 0.21 | N/A = not analyzed |
| H ₂ O | 0.22 | 1.10 | 0.25 | 0.50 | |
| Ba | 30.0 | 21.0 | 8.0 | 106.0 | |
| Rb | 5.0 | 10.0 | 3.0 | 10.0 | |
| Th | 0.6 | 2.3 | 0.2 | 1.5 | |
| U | 0.2* | 0.6* | < 0.1* | 0.4* | |
| Nb | 7.0 | 19.0 | 4.0 | 15.0 | |
| La | 4.6 | 18.1 | 2.0 | 11.4 | |
| Ce | 13.0 | 44.8 | 7.3 | 25.8 | |
| Sr | 122.0 | 133.0 | 144.0 | 161.0 | |
| Nd | 9.9 | 30.7 | 6.0 | 17.2 | |
| Sm | 3.5 | 10.0 | 2.2 | 4.8 | |
| Zr | 100.0 | 280.0 | 70.0 | 144.0 | |
| Hf | 3.1 | 7.6 | 2.0 | 3.8 | |
| Eu | 1.1 | 2.9 | 0.8 | 1.4 | |
| Tb | 0.8 | 2.1 | 0.6 | 0.8 | |
| Y | 26.0 | 65.0 | 20.0 | 32.0 | |
| Yb | 3.1 | 7.7 | 2.3 | 3.2 | |
| Lu | 0.4 | 1.1 | 0.3 | 0.4 | |
| Co | 42.0 | 42.0 | 52.0 | 41.0 | |
| Cr | 278.0 | 108.9 | 390.2 | 76.2 | |
| Cu | N/A | N/A | N/A | N/A | |
| Ni | 78.0 | 147.0 | 270.0 | 63.0 | |
| Sc | 36.7 | 34.7 | 27.1 | 34.4 | |
| V | 290.0 | 400.0 | 183.0 | 274.0 | |
| Sr ⁸⁷ ₈₆ | 0.70254 | 0.70254 | 0.70232 | N/A | |
| K/Rb | 315.44 | 439.95 | 166.02 | 373.54 | |
| (La/Yb) _{CH} | 1.00 | 1.59 | 0.58 | 2.39 | |
| La/Nb | 0.66 | 0.96 | 0.50 | 0.76 | |
| Mg' | 58 | 36 | 66 | 57 | |
| Age (Ma) | < 1 | 4.5 | < 1 | < 1 | |

9. SUMMARY OF DISCRIMINATION DIAGRAM DISCUSSIONS

Major, trace and rare earth element tectonic discrimination diagrams applied to data from Neogene and Quaternary basalts in British Columbia and the adjacent Pacific Ocean floor correctly identify the tectonic settings of all suites except the Garibaldi Volcanic Belt (Table VIII). However the different WPB tectonic settings (i.e. hotspot, rift, back-arc, plate-edge) cannot be distinguished from each other as data from these WPB suites completely overlap. Garibaldi Belt basalts erupted in a convergent margin setting plot as WPB. This implies that geochemistry alone is not always a valid method for distinguishing ancient tectonic settings.

Analysis for Ta was unsuccessful, but Nb/16 substituted for Ta produced acceptable results on all of the diagrams incorporating Ta.

The alkaline series basalts from all tectonic settings can be distinguished from the tholeiitic series by their higher overall abundances of trace and rare earth elements.

Both N- and E-MORB are distinguished from WPB and convergent margin basalts by their lower overall abundances of trace and rare earth elements. This chemical characteristic clearly separates them from other possible tectonic settings on almost all of the discrimination diagrams plotted. In addition, N-MORB are more depleted in the large low valency cations (Ba, Rb, K and Sr) and Th and U than E-MORB so that tectonic discrimination diagrams using

TABLE VIII.

CLASSIFICATION OF SAMPLE SUITES USING DISCRIMINATION DIAGRAMS

Abbreviations used on the following data pages are listed below:

N/A = not applicable

OFB* = OFB plus CAB plus LKT

and = overlap of data points onto two fields

or = one field for two possible tectonic settings

| | | |
|-----|---|---------------------------|
| ARC | } | convergent margin setting |
| CAB | | |
| IAT | | |

| | | |
|---------|---|---------------------|
| MORB | } | ocean floor setting |
| OFB | | |
| TH MORB | | |

| | | |
|-----|---|----------------------|
| WPB | } | within plate setting |
| OI | | |
| CB | | |

Continued.....

TABLE VIII (cont.)

| SUITE | LIMITATIONS TECTONIC SETTING | TiO_2 - K_2O - P_2O_5 Oc. vs. Non-oc. | MnO - TiO_2 - P_2O_5 MORB-WPB-ARC | MgO - FeO^* - Al_2O_3 MORB-WPB-ARC | Ti - Zr - Y MORB-WPB-ARC | Ti - Zr - Sr MORB-WPB-ARC | V vs. Ti /1000 MORB-WPB-ARC | Ti/Y vs. Nb/Y MORB-WPB-ARC | Ti/Cr vs. Ni MORB vs. ARC | Sr/Ce vs. Sr/Ce MORB vs. ARC |
|-------------------------------|------------------------------------|--|--|--|-----------------------------------|------------------------------------|------------------------------------|-----------------------------------|----------------------------------|-------------------------------------|
| | | not for rocks with alk. >20% on AFM | not for cont. thol. | not for alkaline series | N/A | not for WPB | not for CAB | N/A | Unfract. samples | not for WPB |
| GARIBALDI BELT | ARC | Non-oceanic | WPB and ARC | N-MORB and CB | WPB and OFB* | N/A | WPB and MORB | WPB | TH MORB | ARC |
| COQUIHALLA COMPLEX | ARC | N/A | ARC | ARC | CAB | CAB | N/A | ARC or MORB | IAT | ARC |
| CHILCOTIN BASALTS | WPB (Back-arc?) | Non-oceanic and Oceanic | WPB and MORB and ARC | N-MORB and CB and OI | WPB and OFB* | N/A | WPB | WPB and MORB or ARC | TH MORB and IAT | N/A |
| ANAHIM VOLCANIC BELT | WPB (Hotspot?) | Non-oceanic and Oceanic | WPB and MORB | CB and OI | WPB and OFB* | N/A | WPB and MORB | WPB | TH MORB and IAT | N/A |
| MASSET FORMATION | ARC? WPB? (Hotspot?) | N/A | WPB and ARC | N-MORB and ARC | CAB | CAB | N/A | MORB | IAT | ARC |
| STIKINE VOLCANIC BELT | WPB (Incipient Rift) | Non-oceanic and Oceanic | WPB and MORB | CB and OI | WPB | N/A | WPB | WPB | TH MORB and IAT | N/A |
| ALERT BAY VOLCANIC BELT | WPB (Arc-trench gap) | Non-Oceanic and Oceanic | WPB | N-MORB and ARC | WPB | N/A | WPB | WPB | TH MORB and IAT | ARC |
| OFFSHORE BASALTS | MORB | Oceanic | MORB and ARC | N-MORB and CB and OI and ARC | OFB* | OFB | MORB | MORB or ARC | TH MORB | MORB |

Continued.....

TABLE VIII (cont).

| SUITE | TECTONIC SETTING | Cr vs. Ce/Sr MORB-WPB-ARC | Cr vs. Y WPB or MORB vs. ARC | La vs. Ba E-MORB-N-MORB-ARC | (Ba/La) _{CH} vs. (La/Sm) _{CH} Oceanic-ARC | La vs. Th E-MORB-N-MORB-ARC | La vs. Nb E-MORB-N-MORB-ARC | K ₂ O/Yb vs. Ta*/Yb MORB-WPB-ARC | Th/Yb vs. Ta*/Yb MORB-WPB-ARC | Th-Hf/3-Ta* N-MORB-E-MORB- WPB-ARC |
|-------------------------------|----------------------------|------------------------------------|---------------------------------|---|--|--------------------------------------|---|--|----------------------------------|--|
| GARIBALDI BELT | ARC | WPB and ARC | WPB and ARC | ARC and N-MORB | Oceanic (WPB) | E-MORB or WPB and N-MORB | E-MORB or WPB and N-MORB and ARC | WPB? | WPB | WPB and ARC |
| COQUIHALLA COMPLEX | ARC | ARC | ARC | ARC | ARC | ARC | ARC | ARC | ARC | ARC |
| CHILCOTIN BASALTS | WPB (Back-arc?) | WPB or MORB and/or ARC | WPB and/or ARC | ARC and WPB or E-MORB | Oceanic (WPB) or ARC | E-MORB or WPB and ARC | WPB | WPB? | WPB and ARC | WPB |
| ANAHIM VOLCANIC BELT | WPB (Hotspot?) | WPB or MORB and/or ARC | WPB or ARC or MORB | ARC and N-MORB and E-MORB or WPB | Oceanic (WPB) or ARC | E-MORB or WPB and ARC | E-MORB or WPB and N-MORB | WPB? | WPB | WPB |
| MASSET FORMATION | ARC? WPB? (Hotspot?) | ARC | WPB or ARC | ARC | Oceanic (WPB) | E-MORB or WPB and ARC | N-MORB | WPB? | ARC | ARC? |
| STIKINE VOLCANIC BELT | WPB (Incipient Rift) | WPB and ARC | WPB and/or ARC | ARC and N-MORB and E-MORB or WPB | Oceanic (WPB) or ARC | E-MORB or WPB and ARC | E-MORB or WPB and N-MORB | WPB | WPB | WPB |
| ALERT BAY VOLCANIC BELT | WPB (Arc-trench gap) | WPB or MORB and/or ARC | WPB or MORB and/or ARC | ARC | Oceanic (WPB) | E-MORB or WPB and N-MORB | E-MORB or WPB and N-MORB | WPB and ARC | WPB and ARC | WPB and ARC |
| OFFSHORE BASALTS | MORB | WPB or ARC or MORB | ARC or MORB | N-MORB | Oceanic (MORB) | E-MORB or WPB and N-MORB | N-MORB and E-MORB or WPB | MORB | MORB | N-MORB and E-MORB |

these elements are especially effective in separating these two MORB environments, e.g. La vs. Ba, La vs. Th, La vs. Nb and Th-Hf/3-Ta* (Sun et al., 1979; Wood, 1980; Gill, 1981).

WPB have higher abundances of all trace and rare earth elements than either N- or E-MORB and generally have lower abundances of Ba, Th, K and Sr and higher Nb and Ti abundances than basalts from a convergent margin. These geochemical characteristics readily distinguish WPB from N-MORB and convergent margin basalts on V vs. Ti/1000, Ti/Y vs. Nb/Y, La vs. Ba, La vs. Th, La vs. Nb, K₂O/Yb vs. Ta*/Yb, Th/Yb vs. Ta*/Yb and Th-Hf/3-Ta* (Gill, 1981; Shervais, 1982; Pearce 1982; Wood, 1980; Thompson et al., 1983 and 1984). Distinction of WPB from E-MORB is possible using V vs. Ti/1000, Ti/Y vs. Nb/Y, K₂O/Yb vs. Ta*/Yb, Th/Yb vs. Ta*/Yb and Th-Hf/3-Ta*. Some continental tholeiitic WPB have elemental abundances resembling those in a convergent margin basalt and lie within the convergent margin field on most tectonic discrimination diagrams. Therefore samples in the geologic record which are geochemically identified as convergent margin tholeiites should be judged with this in mind.

Convergent margin basalts are identified by an enrichment in large low valency cations relative to WPB, N- and E-MORB and a depletion in Nb and Ti relative to WPB (Pearce, 1982; Thompson et al., 1983 and 1984; Jakeš and White, 1972; Kay, 1980; Shervais, 1982; Hawkesworth and Powell, 1980). Most basalts from convergent margin settings

have La/Nb greater than 2.0, whereas WPB have La/Nb ratios which are less than or equal to 1.0. Using tectonic discrimination diagrams, separation of convergent margin basalts from WPB is best accomplished using V vs. Ti/1000, La vs. Ba, $(\text{Ba/La})_{\text{CH}}$ vs. $(\text{La/Sm})_{\text{CH}}$, La vs. Th, La vs. Nb, $\text{K}_2\text{O/Yb}$ vs. Ta^*/Yb , Th/Yb vs. Ta^*/Yb and Th-Hf/3-Ta^* . Convergent margin basalts are distinguished from both N- and E-MORB on most of the same diagrams, excluding Ti/Y vs. Nb/Y, and including Sm/Ce vs. Sr/Ce and Cr vs. Ce/Sr.

Table IX presents the studied tectonic discrimination diagrams in order of their overall success at classifying tectonic settings. Suites of basaltic samples are classified with greater certainty than individual samples and relatively unfractionated and unaltered samples are obviously preferred. Characteristic BEND pattern shapes help identify tectonic settings, and are also useful for determining anomalous enrichments and/or depletions in individual samples relative to the remainder of the suite.

The first 8 diagrams listed in Table IX were very to fairly successful at separating convergent margin, ocean floor and within plate basalts and require no further explanations. However, the remaining 10 diagrams were not as successful, because of the various reasons listed below.

Nb depletions and enrichments which result in the misidentification of samples on La vs. Nb are small and within analytical error of 'typical' Nb abundance. By placing the N- and E-MORB field boundary at a La/Nb ratio of

TABLE IX

EFFICIENCY OF TECTONIC DISCRIMINATION DIAGRAMS *

| DISCRIMINANT DIAGRAM USED | WPB | | CONVERGENT MARGIN | | (N-) MORB | (E-) |
|--|------------------------------------|-----------------------------|------------------------------------|-----------------------------|------------------------------------|-----------------------------|
| | % of suite correctly identified | % of other misidentified | % of suite correctly identified | % of other misidentified | % of suite correctly identified | % of other misidentified |
| Th-Hf/3-Ta* | 98% | 5% | 88% | 2% | 100% | 0% |
| { Ti-Zr-Y | 94% | 0% | 100% | 0% | 100% | 6% |
| { Ti-Zr-Sr | --- | --- | 100% | 0% | 100% | 0% |
| Ti/Y vs. Nb/Y | 98% | 0% | 100% | 2% | 100% | 0% |
| Th/Yb vs. Ta*/Yb | 98% | 0% | 80% | 2% | 100% | 0% |
| (Ba/La) _{CH} vs. (La/Sm) _{CH} | 91% | 0% | 100% | 8% | 100% | 0% |
| V vs. Ti/1000 | 94% | 0% | 0% | 0% | 100% | 11% |
| La vs. Th | 89% | 6% | 83% | 9% | 100% | 3% |
| La vs. Nb | 83% | 0% | 80% | 2% | 100% | 12% |
| MnO-TiO ₂ -P ₂ O ₅ | 85% | 0% | 100% | 8% | 73% | 10% |
| Ti/Cr vs. Ni | 83% | 0% | 100% | 14% | 100% | 0% |
| Sm/Ce vs. Sr/Ce | --- | --- | 100% | 0% | 100% | 0% |
| Cr vs. Y | 74% | 0% | 100% | 22% | 100% | 0% |
| K ₂ O/Yb vs. Ta*/Yb | 46% | 0% | 100% | 0% | 100% | 0% |
| Cr vs. Ce/Sr | 50% | 0% | 100% | 44% | 100% | 8% |
| FeO*-MgO-Al ₂ O ₃ | 86% | 23% | 100% | 3% | 45% | 12% |
| La vs. Ba | 13% | 0% | 100% | 57% | 100% | 29% |
| | OCEANIC | | NON-OCEANIC | | | |
| | % of suite correctly identified | % of other misidentified | % of suite correctly identified | % of other misidentified | | |
| K ₂ O-TiO ₂ -P ₂ O ₅ | 100% | 27% | 72% | 0% | | |

* Diagrams are listed in order of overall success

1.2 instead of 1, the percentage of misidentified N-MORB samples would decrease from greater than 70% to less than 20% and the percentage of correctly identified WPB samples would increase from 83% to 93%.

MnO-TiO₂-P₂O₅, which uses major element oxides, is the most successful major element diagram for distinguishing MORB, WPB and convergent margin tectonic settings. Anomalously low P₂O₅ abundances in a few Stikine, Anahim and offshore samples are the primary cause of misidentification and may be a result of apatite removal.

Ti/Cr vs. Ni was successful at separating unfractionated convergent margin basalts from MORB plus WPB. If fractionated samples were included this diagram was less successful, as many WPB plotted within the convergent margin field because of low Ni abundance (almost certainly caused by olivine fractionation).

Sm/Ce vs. Sr/Ce does not contain a field for WPB, but most WPB from this study would have plotted within the MORB field, suggesting this diagram may be even more successful than Ti/Cr vs. Ni for separating convergent margin basalts from WPB plus MORB because Sm/Ce vs. Sr/Ce is unaffected by olivine and/or clinopyroxene fractionation.

Low abundances of Y which affect classifications using Cr vs. Y are probably caused by the presence of one or more minor residual source or magma chamber phases which retain this element (garnet?) (Pearce, 1982). Fractionation of pyroxene ± Cr-spinel also influences a samples position on

this diagram, but most unfractionated samples are correctly identified.

K_2O/Yb vs. Ta^*/Yb correctly identifies only 46% of WPB samples because over 50% lie between the WPB and convergent margin field boundaries. This is caused by an enrichment in K_2O .

Similarly, the low success of Cr vs. Ce/Sr was caused by Sr enrichment, as well as Cr depletion by pyroxene \pm Cr -spinel fractionation.

Eruption through continental crust has been used by Dostal et al. (1977), Jakeš and White (1977) and Gill (1981) to explain the increased abundances of Ba , Rb , Th , U , K and Sr in continental convergent margin magmas. Results from this study suggest that similar increases occur in WPB magmas erupted through continental crust. This is evident on K_2O/Yb vs. Ta^*/Yb , Ce vs. Ce/Sr and La vs. Ba .

$FeO^*-MgO-Al_2O_3$, intended for use in classifying subalkaline basalts proved to be of little value. (This study also plotted the 'transitional' samples). Samples which on other diagrams were classified as WPB plotted in both the CB (continental basalt) and OI (ocean island) fields, with 74% of the studied samples lying within the OI field, and none of the ocean floor samples plotted within the E-MORB field despite their E-MORB classification on La vs. Th , La vs. Nb and $Th-Hf/3-Ta^*$. When all subalkaline samples were plotted together most of them clustered around the CB, OI, N-MORB triple junction so that identification of

tectonic setting was impossible. Overall this diagram was not successful for classifying the basalts studied and should only be used if these are the only major element oxides which have been analyzed, and if large numbers of samples are being compared.

La vs. Ba was the least successful trace and rare earth element tectonic discrimination diagram because most of the WPB samples plotted within the convergent margin field. This was caused by their anomalous enrichments in Ba (mentioned above).

$\text{TiO}_2\text{-K}_2\text{O-P}_2\text{O}_5$, which also uses major element oxides, was 72% effective in separating non-oceanic from oceanic subalkaline basalts but as WPB, convergent margin basalts and MORB cannot be separated, this diagram was not a successful discriminator.

Ti/Y vs. Nb/Y , $(\text{Ba/La})_{\text{CH}}$ vs. $(\text{La/Sm})_{\text{CH}}$, Ti/Cr vs. Ni , Cr vs. Y and Cr vs. Ce/Sr appear to be successful for distinguishing MORB, WPB and convergent margin basalt tectonic environments (Table IX). However, they all contain overlapping fields, and consequently are only useful if combined with some other indication of tectonic setting.

Positive Eu anomalies occur in BEND patterns from all of the suites, and although Eu anomalies are important in fractionation studies of evolved magmas they are of little use for distinguishing tectonic origins. Eu anomalies are absent in many BEND patterns which have positive Sr anomalies; a further suggestion that eruption through

continental crust, rather than plagioclase accumulation, causes the Sr enrichment observed in some of the samples.

10. CONCLUSIONS

Eight suites of basaltic rocks from British Columbia and its offshore ocean floor were distinguished one from the other using eighteen tectonic discrimination diagrams and bulk earth normalized diagrams (BEND). Basalts from the ocean floor were classified as N- and E-MORB, those from the Coquihalla Complex and the Masset Formation as ARC and the remainder were classified as WPB (Garibaldi Belt, Chilcotin Basalts, Anahim Volcanic Belt, Stikine Volcanic Belt, Alert Bay Volcanic Belt). Of all tectonic discrimination diagram studied, none was able to separate the various within plate environments (i.e. hotspot (Anahim Belt), incipient rift (Stikine Belt), back-arc (Chilcotin Group), plate-edge (Alert Bay Belt)).

The Garibaldi Belt basalts, in a convergent margin setting, were consistently classified as WPB, suggesting that geochemical tectonic classifications of ancient basalts be applied with caution and supporting evidence, such as chemistry of associated more-fractionated rocks, should be included.

Some within plate basalts erupted through continental crust have higher than 'average' abundances of Ba, Th, U, K and Sr. In most cases these 'continental' enrichments are not large enough to affect the overall classification of a suite on tectonic discrimination diagrams.

Although REE abundances from INAA are important for quantitative models of within-suite fractionation paths

(e.g. Eu anomalies, Yb abundances and $(La/Yb)_{CH}$ ratios) most are not important for establishing tectonic setting. The only exception is La, used in the ratio La/Nb. La/Nb ratios less than 1.2 correctly separate 93% of WPB, including E-MORB, from N-MORB (La/Nb of 1.2 to 2) and convergent margin (La/Nb > 2) basalts.

Major and trace element abundances from XRF analysis are generally sufficient for distinguishing the tectonic environment.

If only major element oxide abundances are available, tectonic settings can be determined fairly successfully using MnO-TiO₂-P₂O₅.

Better discrimination is obtained using the paired Ti-Zr-Y and Ti-Zr-Sr diagrams. This pair of diagrams is very successful for separating within plate from convergent margin from oceanic basalts, but N- and E-MORB are not separated one from the other.

The most effective diagram for distinguishing basalts and more fractionated magmas of within plate, convergent margin, N-MORB and E-MORB is Th-Hf/3-Ta. These trace elements are from INAA, but acceptable results were produced using the XRF element ratios Nb/16 and Zr/39, substituted for Ta and Hf respectively. No XRF substitution was found for Th but it may conveniently be determined via γ counting.

The least effective tectonic discriminant diagrams are FeO*-MgO-Al₂O₃ and La vs. Ba. Those using Cr and Ni (Ti/Cr vs. Ni, Cr vs. Ce/Sr and Cr vs. Y) are very sensitive to

fractionation, but if properly applied they are able to distinguish convergent margin from MORB plus WPB basalts.

REFERENCES

- Abbey, S., 1976, SY-2, SY-3 and MRG-1. A report on the collaborative analysis of three Canadian rock samples for use as certified reference materials - supplement 1, Canadian Center for Mineral and Energy Technology, Report 76-36, 27 p.
- Abbey, S., 1980, Studies in "standard samples" for use in the general analysis of silicate rocks and minerals. *Geostandards Newsletter*, v. 4, p. 163-190.
- Abbey, S., 1983, Studies in "standard samples" of silicate rocks and minerals 1969-1982. Geological Survey of Canada Paper 83-15, 114 p.
- Addition, M.K. and Seil, R.O., 1979, Columbia River basalt reference sample. Rockwell International Publication No. RHO-SA-93 13 p.
- Alibert, C., Michard, A. and Albarede, F., 1983, The transition from alkali basalts to kimberlites: Trace element evidence from melilitites. *Contributions to Mineralogy and Petrology*, v. 82, p. 176-186.
- Anderson, R.G., 1975, The geology of the volcanics in the Meager Creek map-area, southwestern British Columbia. Unpublished B.Sc. thesis, University of British Columbia, Vancouver, Canada, 130 p.
- Arculus, R.J., Delong, S.E., Kay, R.W. Brook, C. and Sun, S.-S., 1977, The alkalic rock suite of Bogoslof Island, eastern Aleutian arc, Alaska. *Journal of Geology*, v. 85, p. 177-186.
- Armstrong, R.L., 1971, Isotopic and chemical constraints on models of magma genesis in volcanic arcs. *Earth and Planetary Science Letters*, v. 12, p. 137-142.
- Armstrong, R.L. and Nixon, G.T., 1980, Chemical and Sr-isotopic composition of igneous rocks from Deep Sea Drilling Project Legs 59 and 60. *in* Kroenke, L., Scott, R. et al. (eds.), Initial Reports of the Deep Sea Drilling Project, U.S. Government Printing Office, Washington, D.C., V. 59, p. 719-727.
- Armstrong, R.L., Muller, J.E., Harakal, J.E. and Muehlenbachs, K., in press, The Neogene Alert Bay Volcanic Belt of northern Vancouver Island, Canada: Descending plate edge volcanism in the arc trench gap.
- Basaltic Volcanism Study Project, 1981, Basaltic Volcanism On The Terrestrial Planets. Pergamon Press, Inc., New

York, 1286 p.

Batiza, R., 1980, Origin and petrology of young oceanic central volcanoes: Are most tholeiitic rather than alkalic? *Geology*, v. 8, p. 477-482.

Beccaluva, L., Ohnenstetter, D. and Ohnenstetter, M., 1979, Geochemical discrimination between ocean floor and island arc tholeiites - application to some ophiolites. *Canadian Journal of Earth Sciences*, v. 32, p. 114-120.

Berman, R.G., 1979, The Coquihalla Volcanic Complex, southwestern British Columbia. Unpublished M.Sc. thesis, Department of Geology, University of British Columbia, Vancouver, Canada, 170 p.

Berman, R.G. and Armstrong, R.L., 1980, Geology of the Coquihalla volcanic complex, southwestern British Columbia. *Canadian Journal of Earth Sciences*, v. 17, p. 985-995.

Best, M.G. and Brimhall, W.H., 1974, Late Cenozoic alkalic basaltic magmas in the western Colorado plateaus and the Basin and Range transition zone, U.S.A. and their bearing on mantle dynamics. *Geological Society of America Bulletin*, v. 85, p. 1677-1690.

Bevier, M.L., 1978, Field relations and petrology of the Rainbow Range shield volcano, west-central British Columbia. Unpublished M.Sc. thesis, Department of Geology, University of British Columbia, Vancouver, Canada, 100 p.

Bevier, M.L., 1982, Geology and petrogenesis of Mio-Pliocene Chilcotin Group basalts, British Columbia. Ph.D. thesis, Department of Geology, University of California, Santa Barbara, 110 p.

Bevier, M.L., Armstrong, R.L. and Souther, J.G., 1979, Miocene peralkaline volcanism in west central British Columbia - it's temporal and plate tectonic setting. *Geology*, v. 7, p. 389-392.

Carmichael, I.S.E., Turner, F.J. and Verhoogen, J., 1974, *Igneous Petrology*. McGraw-Hill Inc., 739 p.

Christie, D.M. and Sinton, M.J., 1981, Evolution of abyssal lavas along propagating segments of the Galapagos spreading center. *Earth and Planetary Science Letters*, v. 56, p. 321-335.

Clague, D.A. and Frey, F.A., 1982, Petrology and trace element Geochemistry of the Honolulu Volcanics, Oahu: Implications for the Oceanic Mantle Below Hawaii. *J. of*

- Pet., v.23, p. 447-504.
- Cohen, R.S. and O'Nions, R.K., 1982, Identification of recycled crustal material in the mantle from Sr, Nd and Pb isotopic investigation. *Earth and Planetary Science Letters*, v. 61, p. 73-84.
- Cousens, B.L., 1982, Major and trace element geochemistry of basalts from the Explorer area, northeast Pacific ocean. Unpublished M.Sc. thesis, Department of Geology, University of British Columbia, Vancouver, Canada, 100 p.
- Cousens, B.L., Chase, R.L. and Schilling, J.-G., 1984, Basalt geochemistry of the Explorer Ridge area, northeast Pacific ocean. *Canadian Journal of Earth Sciences*, v. 21, p. 157-170.
- Covell, D.F., 1959, Determination of Gamma ray abundance directly from the total absorption peak. *Analytical Chemistry*, v. 31, p. 1785-1790.
- Cullers, R.L. and Graf, J.L., 1984, Rare earth elements in rocks of the continental crust: Predominantly basic and ultrabasic rocks. *in* Henderson, P. (ed.), *Developments in Geochemistry 2: Rare Earth Element Geochemistry*, Elsevier Science Publishers, Amsterdam, p. 237-274.
- Davies, O.L. (ed.), 1961, *Statistical methods in research and production*. Hafner publishing company, New York, 396 p.
- DeLong, S.E., Hodges, F.M. and Arculus, R.J., 1975, Ultramafic and mafic inclusions, Kanaga Island, Alaska, and the occurrence of alkaline rocks in island arcs. *Journal of Geology*, v. 83, p. 721-736.
- Dostal, J., Zentelli, M., Caelles, J.C. and Clark, A.H., 1977, Geochemistry and origin of volcanic rocks of the Andes (26° -28° S). *Contributions to Mineralogy and Petrology*, V. 63, p. 113-128.
- Dupuy, C. and Dostal, J., 1984, Trace element geochemistry of some continental tholeiites. *Earth and Planetary Science Letters*, v. 67, p. 61-69.
- Eaby, J., Clague, D.A. and Delaney, J.R., 1984, Sr isotopic variations along the Juan de Fuca Ridge. *Journal of Geophysical Research*, v. 789, p. 7883-7890.
- Engel, A.E.J., Engel, C.G. and Havens, R.G., 1965, Chemical characteristics of oceanic basalts and the upper mantle. *Geological Society of America Bulletin*, v.76, p. 719-734.

- Erlank, A.J. and Kable, E.J.D., 1976, The significance of incompatible elements in mid-Atlantic ridge basalts from 45° N with particular reference to Zr/Nb. *Contributions to Mineralogy and Petrology*, v. 54, p. 281-291.
- Faure, G., 1977, *Isotope geology*. New York, Wiley, 464 p.
- Ferrara, G. and Treuil, M., 1974, Petrological implications of trace element and Sr isotope distributions in basalt-pantellerite series. *Bulletin Volcanologique*, v. 38 No. 3, p. 548-574.
- Fiesinger, D.W., 1975, Petrology of the Quaternary volcanic centers in the Quesnel highlands and Garibaldi Provincial Park areas, British Columbia. Ph.D. thesis, Department of Geology, University of Calgary, Calgary, Canada, 132 p.
- Flanagan, F.J., 1974, Reference samples for the earth sciences. *Geochimica et Cosmochimica Acta*, v. 38, p. 1731-1744.
- Flanagan, F.J. (ed.), 1976, Descriptions and analyses of eight new USGS rock standards. Geological Survey of Canada Professional Paper 840, 192 p.
- Gast, P.W., 1968, Trace element fractionation and the origin of tholeiitic and alkaline magma types. *Geochimica et Cosmochimica Acta*, v. 32, p. 1057-1086.
- Gill, J.B., 1981, *Orogenic andesites and plate tectonics*. Springer Verlag, Berlin - Heidelberg - New York, 390 P.
- Gladney, E.S. and Goode, W.E., 1981, Elemental concentrations in eight new United States Geological Survey rock standards: A review. *Geostandards Newsletter*, v. 5, p. 31-64.
- Govindaraju, K. (chief ed.), 1984, Compilation of working values and sample description for 170 international reference samples of mainly silicate rocks and minerals. *Geostandards Newsletter Special Issue*, July 1984, 88 p.
- Green, N.L., 1981, Geology and petrology of Quaternary volcanic rocks, Garibaldi lake area, southwestern British Columbia. *Geological Society of America Bulletin Part II*, V. 92, p. 1359-1470.
- Grove, E.W., 1974, Deglaciation - A possible triggering mechanism for recent volcanism. *in* Proceedings of the symposium on Andean and Antarctic volcanology problems (Santiago, Chile, September, 1974), p. 88-97.

- Hakli, T.A. and Wright, T.L., 1970, The fractionation of nickel between olivine and augite as a geothermometer. *Geochimica et Cosmochimica Acta*, v. 31, p. 877-884.
- Hamilton, T.S., 1981, Late Cenozoic alkaline volcanics of Level Mountain range, northwestern British Columbia: Geology, petrology and paleomagnetism. Ph.D. thesis, Department of Geology, University of Alberta, Edmonton, Canada, 490 p.
- Hawkesworth, C.J., Norry, M.J., Roddick, J.C., Baker, P.E., Francis, P.W. and Thorpe, R.S., 1979, $^{143}\text{Nd}/^{144}\text{Nd}$, $^{87}\text{Sr}/^{86}\text{Sr}$ and incompatible element variations in calc-alkaline andesites and plateau lavas from South America. *Earth and Planetary Science Letters*, v. 42, p. 45-57.
- Hawkesworth, C.J., O'Nions, R.K., Pankhurst, R.J., Hamilton, P.J. and Evensen, N.M., 1977, A geochemical study of island arcs and back arc tholeiites from the Scotia Sea. *Earth and Planetary Science Letters*, v. 36, p. 45-57.
- Hawkesworth, C.J. and Powell, M., 1980, Magma genesis in the Lesser Antilles island arc. *Earth and Planetary Science Letters*, v. 51, p.297-308.
- Henderson, P., 1984, General geochemical properties and abundances of the rare earth elements. *in* Henderson, P. (ed.), *Developments in geochemistry 2: Rare earth element geochemistry*, Elsevier Science Publishers, Amsterdam, p. 1-32.
- Henderson, P. and Pankhurst, R.J., 1984, Analytical chemistry. *in* Henderson, P. (ed.), *Developments in geochemistry 2: Rare earth element geochemistry*, Elsevier Science Publishers, Amsterdam, p. 467-499.
- Hole, M.J., Saunders, A.D., Marriner, G.F. and Tarney, J., 1984, Subduction of pelagic sediments: implications for the origin of Ce-anomalous basalts from the Mariana Islands. *Journal of the Geological Society of London*, v. 141, p. 453-472.
- Holme, P.E., 1982, Non-recognition of continental tholeiites using the Ti-Y-Zr diagram. *Contributions to Mineralogy and Petrology*, v. 79, p. 308-310.
- Horn, J.R. and Bird, D.N., 1981, Seismic refraction results across the southern Queen Charlotte transform fault zone. *Geological Association of Canada, Programs With Abstracts*, V. 6, p. A-26.
- Hyndman, R.D., Riddihough, R.P. and Herzer, R., 1979, The Nootka fault zone; A new plate boundary off western

- Canada. The Geophysical Journal of the Royal Astronomical Society, V. 58, p. 667-683.
- Irvine, T.N. and Baragar, W.R.A., 1971, A guide to the chemical classification of the common volcanic rocks. Canadian Journal of Earth Sciences, v. 8, p. 523-548.
- Isachsen, C.E., 1984, Geology, geochemistry and geochronology of the Westcoast Crystalline Complex and related rocks, Vancouver Island, British Columbia. Unpublished M.Sc. thesis, Department of Geology, University of British Columbia, Vancouver, Canada, 144 p.
- Jakeš, P. and White, A.J.R., 1969, Structure of the Melanesian arcs and correlation with distribution of magma types. Tectonophysics, v. 8, p. 223-236.
- Jakeš, P. and White, A.J.R., 1972, Major and trace element abundances in volcanic rocks of orogenic areas. Geological Society of America Bulletin, v. 83, p. 29-40.
- Jochum, K.P., Hofmann, A.W., Ito, E., Seufert, H.M. and White, W.M., 1983, K, U, and Th in mid-ocean ridge basalt glasses and heat production, K/U and K/Rb in the mantle. Nature, v. 306, p. 431-436.
- Kay, R.W., 1980, Volcanic arc magmas: Implications of a melting mixing model for element recycling in the crust - upper mantle system. Journal of Geology, v. 88, p. 497-522.
- Kay, R.W., 1984, elemental abundances relevant to identification of magma sources. Philosophical Transactions of the Royal Society of London Series A, v. 310, p. 535-547.
- Kay, R.W. and Gast, P.W., 1973, The rare earth content and origin of alkali - rich rocks. Journal of Geology, v. 81, p. 653-682.
- Kennedy, G. and Fowler, A., 1983, Interference from Uranium in neutron activation analysis of rare-earths in silicate rocks. Journal of Radioanalytical Chemistry, v. 78, p. 165-169.
- Korringa, M.K. and Noble, D.C., 1971, Distribution of Sr and Ba between natural feldspar and igneous melt. Earth and Planetary Science Letters, V. 11, p. 147-151.
- Kramar, U. and Puchelt, H. (1982) Reproducibility tests for INAA determinations with AGV-1, BCR-1 and GSP-1 and new data for 17 geochemical reference materials.

Geostandards Newsletter, v. 6, p. 221-227.

Kuno, H., 1968, Differentiation of basaltic magmas. *in* Hess, H.H. (ed.), The Poldervaart treatise on rocks of basaltic composition, Interscience, New York, p. 623-688.

Langmuir, C.H., Bender, J.F., Bence, A.E., Hanson, G.N. and Taylor, S.R., 1977, petrogenesis of basalts from the FAMOUS area; mid-Atlantic ridge. *Earth and Planetary Science Letters*, v. 36. p. 133-156.

Lawrence, R.B., 1979, Garibaldi group volcanic rocks of the Salal creek map area (northern half), southwestern British Columbia. Unpublished B.Sc. thesis, Department of Geology, University of British Columbia, Vancouver, Canada, 83 p.

Lawrence, R.B., Armstrong, R.L. and Berman, R.G., 1984, Garibaldi group volcanic rocks of the Salal creek area, southwestern British Columbia: Alkaline lavas on the fringe of the predominantly calc-alkaline Garibaldi (Cascade) volcanic arc. *Journal of Volcanology and Geothermal Research*, v. 21, p. 255-276.

Lederer, C.M. and Shirley, V.S., 1978, Table of isotopes. Wiley and Sons Inc., New York, 1599 p.

MacDonald, G.A., 1968, Composition and origin of Hawaiian lavas. *Geological Society of America Memoir* 116, p. 477-522.

MacDonald, G.A. and Katsura, T., 1964, Chemical composition of Hawaiian lavas. *Journal of Petrology*, v. 5, p. 82-133.

MacDonald, R., 1974, Nomenclature and petrochemistry of the peralkaline oversaturated extrusive rocks. *Bulletin Volcanologique*, v. 38, p. 498-516.

McDougall, I., 1976, Geochemistry and origin of basalt of the Columbia river group, Oregon and Washington. *Geological Society of America Bulletin*, v. 87, p. 777-792.

McKenzie, D. and O'Nions, R.K., 1983, Mantle reservoirs and ocean island basalts. *Nature*, v. 301, p. 229-231.

Melson, W.G., Vallier, T.L., Wright, T.L., Byerly, G. and Nelen, J., 1976, Chemical diversity of abyssal volcanic glasses erupted along Pacific, Atlantic and Indian sea-floor spreading centers. *American Geophysical Union Monograph*, v. 19, p. 351-368.

Milne, W.G., Weichert, D.H., Basham, P.W., Berry, M.J. and

- Hasegawa, H.S., 1981, Seismic zoning in Canada; some modifications to current maps. *in* Proceedings of Conference XIII: Evaluation of regional seismic hazards and risk, Hays, W.W. (ed.), United States Geological Survey Open File Report No. 81-0437, p. 138-142.
- Miyashiro, A., 1974, Volcanic rock series in island arcs and active continental margins. *American Journal of Science*, v. 274, p. 321-355.
- Miyashiro, A. and Shido, F., 1975, Tholeiitic and calc-alkaline series in relation to the behaviors of titanium, vanadium, chromium and nickel. *American Journal of Science*, v. 275, p. 265-277.
- Mullen, E.D., 1983, MnO/TiO₂/P₂O₅: A minor element discriminant for basaltic rocks of oceanic environments and its implication for petrogenesis. *Earth and Planetary Science Letters*, v. 62, p. 53-62.
- Nicholls, J., Stout, M.Z. and Fiesinger, D.W., 1982, Petrologic variations in Quaternary volcanic rocks, British Columbia and the nature of the underlying upper mantle. *Contributions to Mineralogy and Petrology*, v. 79, p. 201-218.
- Norry, M.J. and Fitton, J.G., 1983, Compositional differences between oceanic and continental basaltic lavas and their significance. *in* Continental Basalts and Mantle Xenoliths. Hawkesworth, C.J. and Norry, M.J. (eds.), Shiva Press, p. 158-185.
- O'Nions, R.K., Evensen, N.M. and Hamilton, P.J., 1980, Differentiation and evolution of the mantle. *Philosophical Transactions of the Royal Society of London Series A*, v. 297, p. 479-493.
- Parrish, R.R., 1982, Cenozoic thermal and tectonic history of the Coast Mountains of British Columbia as revealed by fission track and geological data and quantitative thermal models. Ph.D. thesis, University of British Columbia, Vancouver, Canada, 166 p.
- Pearce, J.A., 1982, Trace element characteristics of lavas from destructive plate boundaries. *in* Andesites: Orogenic andesites and related rocks, Thorpe, R.S. (ed.), John Wiley and Sons, p. 525-548.
- Pearce, J.A., 1983, Role of the sub-continental lithosphere in magma genesis at active continental margins. *in* Continental Basalts and Mantle Xenoliths. Hawkesworth, C.J. and Norry, M.J. (eds.), Shiva Press, p. 230-249.
- Pearce, J.A. and Cann, J.R., 1973, Tectonic setting of basic

- volcanic Rocks determined using trace element analysis. Earth and Planetary Science Letters, v. 28, p.459-469.
- Pearce, J.A. and Norry, M.J., 1979, Petrogenetic implications of Ti, Zr, Y and Nb variation in volcanic rocks. Contributions to Mineralogy and Petrology, v. 69, p. 33-47.
- Pearce, T.H., Gorman, B.E. and Birkett, T.C., 1975, The TiO_2 - K_2O - P_2O_5 diagram: A method of discriminating between oceanic and non-oceanic basalts. Earth and Planetary Science Letters, v. 24, p. 419-426.
- Pearce, T.H., Gorman, B.E. and Birkett, T.C., 1977, The relationship between major element chemistry and tectonic environment of basic and intermediate volcanic rocks. Earth and Planetary Science Letters, V. 36, p. 121-132.
- Parker, R.L. and Fleischer, M., 1968, Geochemistry of niobium and tantalum. U.S. Geological Survey Professional Paper 612, p. 1 43.
- Philpotts, J.A., Schnetzler, C.C. and Hart, S.R., 1969, Submarine basalts: Some K, Rb, Sr, Ba, rare-earth, H_2O and CO_2 data bearing on their alteration, modification by plagioclase, and possible source materials. Earth and Planetary Science Letters, v. 7, p. 293-299.
- Plafker, G., Hudson, T., Bruns, T. and Rubin, M., 1978, Late Quaternary offsets along the Fairweather fault and crustal interactions in southern Alaska. Canadian Journal of Earth Sciences, v. 17, p. 681-689.
- Potts, P.J., Thorpe, O.W. and Watson, J.S., 1981, Determination of the rare earth element abundances in 29 international rock standards by instrumental neutron activation analysis: A critical appraisal of calibration errors. Chemical Geology, v. 34, p. 331-352.
- Rhodes, J.M., Blanchard, D.P., Rodgers, K.V., Jacobs, J.W. and Brannon, J.C., 1976, Petrology and chemistry of basalts from the Nazca plate: Part - 2 major and trace element chemistry. in Yeats, R.S., Hart, S.R., et al. (eds.) Initial Reports of the Deep Sea Drilling Project, v. 34, United States Government Printing Office, Washington, D.C., p. 239-244.
- Riddihough, R.P., 1977, Lithospheric plate interactions off Canada's west coast during the last 10 million years. Canadian Journal of Earth Sciences, v. 14, p. 384-396.
- Riddihough, R.P., 1979, Gravity and structure of an active margin - British Columbia and Washington. Canadian

- Journal of Earth Sciences, v. 16, p. 350-363.
- Riddihough, P.J., Currie, R.G. and Hyndman, R.D., 1980, The Dellwood Knolls and their role in triple junction tectonics off northern Vancouver Island. Canadian Journal of Earth Sciences, v. 17, p. 577-593.
- Rozenberg, R.J. and Zilliacus, R., 1980, Instrumental neutron activation determination of 23 elements in 8 new USGS standard rocks. Geostandards Newsletter, v. 4, p. 191-198.
- Saunders, A.D. and Tarney, J., 1978, The geochemistry of basalts from a back-arc spreading center in the east Scotia Sea. Geochimica et Cosmochimica Acta, v. 43, p. 555-572.
- Saunders, A.D., Tarney, J. and Weaver, S.D., 1980, Transverse geochemical variation across the Antarctic Peninsula: Implication for the genesis of calc-alkaline magmas. Earth and Planetary Science Letters, v. 46, p. 344-360.
- Schilling, J.G., Anderson, R.N. and Vogt, P., 1976, Rare earth, Fe and Ti variations along the Galapagos spreading center and their relationship to the Galapagos mantle plume. Nature, v. 261, p. 108-113.
- Shervais, J.W., 1982, Ti - V plots and the petrogenesis of modern and ophiolitic lavas. Earth and Planetary Science Letters, v. 59, p. 101-118.
- Shimizu, N. and Arculus, R.J., 1975, Rare earth element concentrations in a suite of basanitoids and alkali olivine basalts from Grenada, Lesser Antilles. Contributions to Mineralogy and Petrology, v. 50, p. 231-240.
- Sienko, M.J. and Plane, R.A., 1957, Chemistry. McGraw - Hill Book Company, U.S.A., 621 p.
- Souther, J.G., 1977, Volcanism and tectonic environments in the Canadian cordillera - A second look. *in* Baragar, W.R.A., Coleman, L.C. and Hall, J.M. (eds.) Volcanic Regimes in Canada. Geological Association of Canada Special Paper 16, p. 3-24.
- Souther, J.G., in press, The western Anahim Belt: rootzone of a peralkaline magma system. Canadian Journal of Earth Sciences.
- Souther, J.G., Armstrong, R.L. and Harakal, J., 1984, Chronology of the peralkaline, Late Cenozoic Mount Edziza volcanic complex, northern British Columbia,

- Canada. Geological Society of America Bulletin, v. 95, p. 337-349.
- Srivastava, S.P., 1973, Interpretation of gravity and magnetic measurements across the continental margin of British Columbia. Canadian Journal of Earth Sciences, v. 10, p. 1664-1677.
- Stacey, R.A., 1974, Plate tectonics, volcanism and the lithosphere in British Columbia. Nature, v. 250, p. 133-134.
- Steele, T.W., Wilson, A., Goudvis, R., Ellis, P.J. and Radford, A.J., 1978, Trace element data (1966-1977) for the six 'NIMROC' reference samples. Geostandards Newsletter, v. 2, p. 71-106.
- Sun, S.-S., 1980, Lead isotopic study of young volcanic rocks from mid-ocean ridges, ocean islands and island arcs. Philosophical Transactions of the Royal Society of London Series A, v. 297, p. 409-445.
- Sun, S.-S., Nesbitt, R.W. and Sharaskin, A.Y., 1979, Geochemical characteristics of mid-ocean ridge basalts. Earth and Planetary Science Letters, v. 44, p. 119-138.
- Sutherland-Brown, A., 1969, Aiyansh lava flow, British Columbia. Canadian Journal of Earth Sciences, v. 6, p. 1460-1468.
- Thompson, R.N., Esson, J. and Dunham, A.C., 1972, Major element and chemical variation in the Eocene lavas of the Isle of Skye, Scotland. Journal of Petrology, v. 13, p. 219-253.
- Thirwall, M.F. and Jones, N.W., 1983, Isotope geochemistry and contamination mechanics of Tertiary lavas from Skye, northwest Scotland. in Continental Basalts and Mantle Xenoliths. Hawkesworth, C.J. and Norry, M.J. (eds.), Shiva Press, p. 186-208.
- Thompson, R.N., Morrison, M.A., Dickin, A.P. and Hendry, G.L., 1983, Continental flood basalts.....arachnids rule O.K.? in Continental Basalts and Mantle Xenoliths. Hawkesworth, C.J. and Norry, M.J. (eds.), Shiva Press, p. 158-185.
- Thompson, R.N., Morrison, M.A., Hendry, G.L. and Parry, S.J., 1984, An assesment of the relative roles of crust and mantle in magma genesis: An elemental approach. Philosophical Transactions of the Royal Society of London Series A, v. 310, p. 549-590.
- Thornton, C.P. and Tuttle, O.F., 1960, Chemistry of igneous

- rocks: I. differentiation index. American Journal of Science, v. 258, p. 664-684.
- van der Heyden, P., 1982, Tectonic and stratigraphic relations between the Coast Plutonic Complex and Intermontane Belt, West Central British Columbia. Unpublished M.Sc. thesis, Department of Geology, University of British Columbia, Vancouver, Canada, 172 p.
- Wager, L.R. and Deer, W.A., 1939, The petrology of the Skaergaard intrusion, Kangerdlugssuag, East Greenland. Meddl. om Gronland, v. 105, No. 4, p. 1-352.
- Weaver, B.C. and Tarney, J., 1983, Chemistry of the sub-continental mantle: inferences from Archaean and Proterozoic dykes and continental flood basalts. *in* Continental Basalts and Mantle Xenoliths. Hawkesworth, C.J. and Norry, M.J. (eds.), Shiva Press, p. 209-229.
- White, W.M. and Bryan, W.B., 1977, Sr Isotope, K, Rb, Cs, Sr, Ba and rare earth geochemistry of basalts from the FAMOUS area. Geological Society of America Bulletin, v. 88, p. 571-576.
- White, W.M. and Patchett, J., 1984, Hf-Nd-Sr isotopes and incompatible element abundances in island arcs: implications for magma origins and crust-mantle evolution. Earth and Planetary Science Letters, v. 67, p. 167-185.
- Wilson, M. and Davidson, J.P., 1984, The relative roles of crust and upper mantle in the generation of oceanic island arc magmas. Philosophical Transactions of the Royal Society of London Series A, v. 310, p. 661-674.
- Wood, D.A., 1980, The application of a Th-Hf-Ta diagram to problems of tectonomagmatic classification and to establishing the nature of crustal contamination of basaltic lavas of the British Tertiary volcanic province. Earth and Planetary Science Letters, v. 50, p. 11-30.
- Wood, D.A., Joran, J.-L. and Treuil, M., 1979, A re-appraisal of the use of trace elements to classify and discriminate between magma series erupted in different tectonic settings. Earth and Planetary Science Letters, v. 45, p. 326-336.
- Yoder, H.S. and Tilley, C.E., 1962, Origin of basaltic magmas - an experimental study of natural and synthetic systems. Journal of Petrology, V. 3, p. 342-532.
- Yorath, C.J. and Chase, R.L., 1981, Tectonic history of the

Queen Charlotte islands and sdjacent sreass - a model.
Canadian Journal of Earth Sciences, v. 18, p.
1717-1739.

Yorath, C.J. and Hyndman, R.D., 1983, Subsidence and thermal
history of Queen Charlotte basin. Canadian Journal of
Earth Sciences, v. 20, p. 135-159.

Young, I., 1981, Structure of the western margin of the
Queen Charlotte basin. Unpublished M.Sc. thesis,
Department of Geology, University of British Columbia,
Vancouver, Canada, 380 p.

Zhou, X. and Armstrong, R.L., 1982, Cenozoic volcanic rocks
of eastern China; secular and geographic trends in
chemistry and strontium isotopic composition. Earth and
Panetary Science Letters, v. 58, p. 301-329.

APPENDIX I

SAMPLE SOURCES AND PREVIOUS ANALYSES

On the following pages samples are listed in the order they appear in the text.

SAMPLE - sample name used in this study.

ORIGINAL NUMBER - sample name used by the original collector.

FORM - form the sample was in when selected for this study.

Whole rock - small rock fragments.

Powder - powdered rock sample, no rock fragments.

Pellet - pressed powder pellet used in previous XRF analysis.

PREPARATION - method used to powder the rock samples for analysis:

N/A - not known.

W-Carb. - tungsten carbide ring mill.

BICO - steel disc mill.

Agate - Motor driven agate mortar.

BCDM - Prepared by the B.C. Department of Mines.

GSC - Prepared by the Geological Survey of Canada.

COLLECTOR - individual who collected the sample in the field.

PREVIOUS ANALYSES - previous analytical work.

N/A - not known, or no previous analyses.

Major Elements - all major element oxides in weight %.

REFERENCE - reference(s) which include this sample.

N/A - no published reference.

GARIBALDI AND PEMBERTON BELTS

| SAMPLE | ORIGINAL NUMBER | FORM | PREPARATION | COLLECTOR | PREVIOUS ANALYSIS | REFERENCE |
|----------------------------|------------------------|--------|----------------|--------------|--|--|
| ELAHO | RD-44084-VI | Powder | W-Carb. | R. Anderson | Major Elements, K-Ar date, Sr isotope ratio | Anderson, 1975 |
| GARIBALD | MG-74-36-4 | Powder | N/A | N. Green | Major Elements, Ba, Cr, Cu, Nb, Ni, Rb, Sr, V, Y, Zn, Zr | Green, 1981 |
| CHEAK | GV-7 | Powder | N/A | D. Fiesinger | Major Elements | Fiesinger, 1975 Nicholls et al., 1982 |
| MEAGER | RD-4B1 | Powder | W-Carb. | R. Anderson | Major Elements, K-Ar date, Sr isotope ratio | Anderson, 1975 |
| CAYLEY | SE1501-79 | Powder | BICO, Agate | J.G. Souther | N/A | N/A |
| SALAL1 SALAL2 SALAL3 | C5-5 M1-12 M5-14 | Pellet | BICO, Agate | R. Lawrence | Major Elements, Ba, Cr, Nb, Ni, Rb, Sr, V, Y, Zr, Sr isotope ratio | Lawrence, 1979 Lawrence et al., 1984 |
| SILVERA SILVERH | SE77-1-1 SE77-1-7B | Powder | BICO, Agate | J.G. Souther | K-Ar date, Sr isotope ratio | N/A |
| COQ251 COQ632 COQ61 | 251 632 61 | Pellet | N/A | R. Berman | Major Elements, Ba, Ce, Cr, Nb, Nd, Ni, Rb, Sr, V, Y, Zr, Sr isotope ratio | Berman, 1979 Berman and Armstrong, 1980 |

CHILCOTIN BASALTS

| SAMPLE | ORIGINAL NUMBER | FORM | PREPARATION | COLLECTOR | PREVIOUS ANALYSES | REFERENCE |
|-----------------|-----------------|------------|-------------|----------------|--|-------------------------------|
| REDSTONE | 93B | Powder | N/A | T. Hamilton | N/A | N/A |
| BULL CAN | BC-6 | Powder | N/A | M.L. Bevier | Major Elements, Nb, Ni, Rb, Sr, Y, Zr, K-Ar date, Sr isotope ratio | Bevier, 1982 Parrish, 1982 |
| NAZKO | Nazko | Whole rock | W-Carb. | W.H. Mathews | Major Elements, K-Ar date | N/A |
| QUESW | WHM-76-1 | Powder | BICO, Agate | W.H. Mathews | Major Elements, K-Ar date, Sr isotope ratio | N/A |
| CARD | CTM-76TD | Powder | GSC | J.G. Souther | K-Ar date, Sr isotope ratio | N/A |
| CAMEL DOG CK | CA-1 DC-1 | Powder | N/A | M.L. Bevier | Major Elements, Nb, Ni, Rb, Sr, Y, Zr, K-Ar date, Sr isotope ratio | Bevier, 1982 |
| EDMUND | Edmund | Whole rock | W-Carb. | W.H. Mathews | Major Elements, K-Ar date | N/A |
| DEADMAN | DR-11 | Powder | N/A | M.L. Bevier | Major Elements, Nb, Ni, Rb, Sr, Y, Zr, K-Ar date, Sr isotope ratio | Bevier, 1982 |
| WOOD LK | Wood Lk | Whole rock | W-Carb. | W.H. Mathews | Major Elements, K-Ar date | N/A |
| BLIZZARD | Blizzard | Powder | BICO, Agate | R.L. Armstrong | K-Ar date, Sr isotope ratio | N/A |

ANAHIM VOLCANIC BELT

| SAMPLE | ORIGINAL NUMBER | FORM | PREPARATION | COLLECTOR | PREVIOUS ANALYSES | REFERENCE |
|------------------------------|----------------------------------|------------|----------------|---------------------------|---|-------------------------------|
| MASSET1 MASSET2 | MR3 MR8 | Pellet | BICO, Agate | I. Young | K-Ar date, Sr isotope ratio | Young, 1981 |
| ARIS IS KITASU LAKE IS | SE090265 SE050365 SE030865 | Pellet | GSC | J.G. Souther | Sr isotope ratio | N/A |
| RAINBOW ANAHIM | R25 AP15 | Pellet | BICO, Agate | M.L. Bevier | Major Elements, Ba, Nb, Ni, Rb, Sr, K-Ar date, Sr isotope ratio | Bevier, 1978 |
| ITCHA1 | IMV 76-11 | Powder | BICO, Agate | J. Nicholls B. Proffet | K-Ar date, Sr isotope ratio | Proffet, unfinished thesis |
| ITCHA2 | Itcha 11b | Powder | N/A | T. Hamilton | N/A | N/A |
| ALEX | TD58CA6 | Pellet | GSC | H.W. Tipper | Sr isotope ratio | N/A |
| QUESLK | JSG 80-37 | Whole rock | W-Carb. | J. Getsinger | N/A | N/A |
| SPAN CK | 118cAcB-1 | Powder | GSC | J.G. Souther | Sr isotope ratio | N/A |
| WGRAYN TROPY | BCV-12 BCV-2 | Powder | N/A | D. Fiesinger | Major Elements, Sr isotope ratio | Fiesinger, 1975 |

STIKINE VOLCANIC BELT

| SAMPLE | ORIGINAL NUMBER | FORM | PREPARATION | COLLECTOR | PREVIOUS ANALYSES | REFERENCE |
|----------------------------------|--|--------|----------------|--------------------------------|--|--------------------------|
| PRINCER | CD575 | Powder | BICO, Agate | C. Dingee | K-Ar date, Sr isotope ratio | N/A |
| AYNSH1 AYNSH2 | NR-6 NR-2B | Powder | N/A | J. Nicholls | Sr isotope ratio | N/A |
| HOODOO | SE1701-76 | Pellet | BICO, Agate | J.G. Souther R.L. Armstrong | K-Ar date, Sr isotope ratio | N/A |
| BORDERLK ISKUT ISKUTW | 11285M 11297M 11288M | Powder | BCDM | E.W. Grove | Sr isotope ratio | Grove, 1974 |
| MT DUNN | Mt. Dunn | Powder | N/A | T. Hamilton | N/A | N/A |
| BOWSER | GE1 | Pellet | BICO, Agate | G. Eisbacher | K-Ar date, Sr isotope ratio | N/A |
| SPEC1 SPEC2 EDZ1 EDZ2 | SE1603-73 SE1504a-72 SE04076-76 ML0614-66 | Powder | BICO, Agate | J.G. Souther | K-Ar date | Souther et al., 1984 |
| NEDZ1 NEDZ2 NEDZ3 NEDZ4 | H81-4KAr H81-169 H81-8KAr H80-87F | Powder | BICO, Agate | P.B. Read | K-Ar date | N/A |
| LEVEL1 | 8/28-68/5815 | Powder | N/A | T. Hamilton | Major Elements | Hamilton, 1981 |
| LEVELD LEVEL2 | KD-1 8/25-50/6397 | Powder | N/A | T. Hamilton | Major Elements, Ba, Cr, Cu, Nb, Ni, Rb, Sr, Th, U, Y | Hamilton, 1981 |
| NATLIN | A-1 | Powder | N/A | J. Nicholls | Major Elements, Sr isotope ratio | Nicholls et al., 1982 |
| SATLIN | T75 215-1 | Powder | N/A | T. Bultman | N/A | N/A |

ALERT BAY VOLCANIC BELT

| SAMPLE | ORIGINAL NUMBER | FORM | PREPARATION | COLLECTOR | PREVIOUS ANALYSES | REFERENCE |
|----------------------------|-------------------------------|--------|----------------|-----------|--|---------------------------------|
| ALERT1 ALERT2 ALERT3 | 69-7A1 69-31-D 69-31-F1 | Powder | BICO, Agate | J. Muller | Major Elements, Ba, Cr, Nb, Ni, Rb, Sr, V, Y, Zr, K-Ar date, Sr isotope ratio | Armstrong et al., (in press) |

OFFSHORE BASALTS

| SAMPLE | ORIGINAL NUMBER | FORM | PREPARATION | COLLECTOR | PREVIOUS ANALYSES | REFERENCE |
|----------------------------------|--|------------|-----------------------|--------------------|--|--|
| EXMOUNT1 EXMOUNT2 EXMOUNT3 | RLC-1 RLC-2 RLC-4 | Whole rock | W-Carb. | R.L. Chase | Major Elements, Ce, Cr, Nb, Nd, Ni, Rb, Sr, Th, Y, Zr | N/A |
| BR BEAR1 BR BEAR2 COBB1 | RLC-1155-1 RLC-1155-2 RLC-1152-360 | Whole rock | W-Carb. | R.L. Chase | Major Elements, Ba, Cr, Cu, Nb, Ni, Rb, Sr, V, Y, Zr | N/A |
| COBB2 | RLC-1152-500 | Powder | N/A | R.L. Chase | | |
| SEXRIDGE | 77-14-36-X | Powder | Cr-steel ring mill | R.L. Chase | Major Elements, Ba, Ce, Co, Cr, Nb, Nd, Ni, Rb, Sc, Sr, V, Y, Zr, La, Sm, Eu, Tb, Yb, Lu, Sr isotope ratio | Cousens, 1982 Cousens et al., 1984 |
| PREVRDG EXRIFT EXDEEP | 72-22-7-1 70-25-4-62G 70-25-17-1 | Powder | Cr-steel ring mill | A.G. Thomlinson | | |

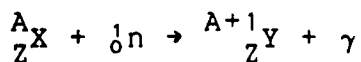
APPENDIX II - NEUTRON ACTIVATION ANALYSIS

Each sample was analyzed by instrumental neutron activation analysis (INAA) to determine the content of selected rare earth (La, Sm, Eu, Tb, Yb, Lu) and trace (Th, Ta, Hf, Sc) elements.

When an element is bombarded by neutrons, whose flux is expressed as the number of neutrons passing through an area of 1 cm² during one second, the neutrons are absorbed by a fraction of the target nuclei, the efficiency of capture being expressed as a capture cross section for the atom of the element. This is expressed as: $a^* = a^0 * B * F$, where

- a^0 = number of atoms
- a^* = number of atoms absorbing neutrons
- B = the capture cross section and
- F = the integrated neutron flux (flux * time).

The absorbed neutrons are held by a binding energy which has a value from about 7.5 to 8.8 MeV and this extra energy leaves the resulting isotopes in an excited state. De-excitation is accomplished by an almost instantaneous emission of a gamma ray. The above process can be written as the following equation:



where A (the mass number) = number of protons plus neutrons, n is the absorbed neutron and γ is the emitted gamma ray.

Isotopes produced in this manner may be stable or unstable. In some cases the first daughter product of a radioactive isotope is also unstable and will undergo a further decay forming another daughter product and so on, until a stable nuclide is produced. The final stable nuclide is initially in an excited state and subsequently emits gamma rays with characteristic energies until its ground state is reached.

Radioactive decay involves emission of one or more particles. Each particle is associated with a complimentary gamma ray with specific mean energy. This means that each radioactive isotope has its own characteristic gamma energy spectrum making it possible to uniquely detect the presence of that particular isotope. The amount of an element present in a sample is directly proportional to gamma energy emitted. To determine the concentration of elements in an irradiated unknown sample a standard with known concentration of elements is similarly irradiated and analyzed. The ratio of unknown to standard radioactivity, after any necessary corrections for radioactive decay between counting times, is used to calculate the concentration (Henderson and Pankhurst, 1984). Table X contains the list of isotopes used, their corresponding half-lives and the energies of the photopeaks used for determining abundances of elements.

TABLE X

ELEMENT ISOTOPE DATA (Lederer and Shirley, 1978)

| ACTIVATION REACTION | HALF-LIFE (hrs.) | ENERGY OF γ -RAY PEAKS (keV) |
|---|---------------------|--|
| $^{151}_{63}\text{Eu} \rightarrow ^{152}_{63}\text{Eu}$ | 122736 | 122, 344, 1408 |
| $^{180}_{72}\text{Hf} \rightarrow ^{181}_{72}\text{Hf}$ | 1017.6 | 133, 482 |
| $^{139}_{57}\text{La} \rightarrow ^{140}_{57}\text{La}$ | 40.2 | 487, 1596 |
| $^{176}_{71}\text{Lu} \rightarrow ^{177}_{71}\text{Lu}$ | 158.88 | 208, 113 |
| $^{45}_{21}\text{Sc} \rightarrow ^{46}_{21}\text{Sc}$ | 2011.68 | 889 |
| $^{152}_{62}\text{Sm} \rightarrow ^{153}_{62}\text{Sm}$ | 46.7 | 103, 69 |
| $^{181}_{73}\text{Ta} \rightarrow ^{182}_{73}\text{Ta}$ | 2760 | 1121, 1221 |
| $^{159}_{65}\text{Tb} \rightarrow ^{160}_{65}\text{Tb}$ | 1728 | 879, 298 |
| $^{232}_{90}\text{Th} \rightarrow ^{233}_{91}\text{Pa}$ | 648 | 312, 300 |
| $^{174}_{70}\text{Yb} \rightarrow ^{175}_{70}\text{Yb}$ | 100.56 | 396, 282 |

SAMPLE IRRADIATION AND COUNTING TECHNIQUES

1.000 gm of accurately weighed <80 mesh whole rock sample was placed in a small plastic irradiation vial and heat-sealed to prevent leakage. The sample vials were then packed in four layers in a larger Nalgene bottle, each layer containing twelve to fourteen unknown samples and five to six standards. Additional standards as unknowns were included in the first bottle in order to check analytical precision and systematic errors.

Each layer contained at least:

1. a standard prepared by Chemex called LIQUID 1 which was used to determine the concentrations of La, Eu, Sm, Tb, Yb and Lu.
2. Standard NIML for Th and Hf abundances (Abbey, 1983).
3. Chemex standard SC50 for Sc abundances.
4. Chemex standards TA2 or TA10 for concentrations of Ta.
5. SY2 (Abbey, 1983).

Abundances of selected trace and rare earth elements in these standards are listed in Table XI.

The bottles were sent to Washington State University at Pullman, Washington where they were subjected to a neutron flux of 6.7×10^{12} neutrons/cm²/sec ($\pm 15\%$) for 20 minutes. Although there is no measureable flux gradient at the irradiation location the sample bottles were also rotated during irradiation to insure flux homogeneity.

After irradiation the bottle was returned to NOVATRAK (a subsidiary of Chemex Labs Ltd.) at TRIUMF, U.B.C. and allowed

TABLE XI
ABUNDANCES OF SELECTED TRACE AND RARE EARTH ELEMENTS IN STANDARDS USED
FOR INAA

Abundances in ppm

| | LIQ1 ¹ | NIML ² | SY2 ³ | SC50 ¹ | TA2 ¹ | TA10 ¹ |
|----|-------------------|-------------------|------------------|-------------------|------------------|-------------------|
| Th | | 65 | 380? | | | |
| Ta | | | | | 245 | 122 |
| La | 200 | | 85 | | | |
| Sm | 50 | | 15 | | | |
| Hf | | 190? | 8? | | | |
| Eu | 10 | | 2.2 | | | |
| Tb | 50 | | 2.7 | | | |
| Yb | 50 | | 17 | | | |
| Lu | 50 | | 3? | | | |
| Sc | | | 7? | 50 | | |

¹Chemex prepared standard

²NIML a lujavrite from South African Committee for Certified Reference Materials (Abbey, 1983).

³SY2 a syenite from Canadian Certified Reference Materials Project (Abbey, 1976; Abbey, 1983).

? = questionable value

to cool for five to seven days. The samples and standards were then unpacked from the large irradiation bottles and their gamma ray emissions were measured using a coaxial Ge(Li) detector (Ortec® 7040 series). Pulses from the detector went via an amplification stage to a 4000 channel multichannel analyzer (Ortec® 7000 series)

It would have been advantageous to have a planar Ge(Li) or pure Ge detector rather than a coaxial one to analyze for the elements Ta, Eu, Lu, Yb, Hf and Ce, as a planar detector allows better resolution in the energy range 50-350 keV (Potts et al., 1981; Henderson and Pankhurst, 1984). Most peaks in this energy range analyzed by the coaxial detector had to be corrected for interference. With a planar detector the interferences would have been smaller and the final results more accurate.

Each sample was counted for 1000 seconds.¹ The rare earth elements La, Sm, Yb, and Lu which have half-lives ranging from 40 to 159 hours were counted immediately after the initial cooling period. Analyses of the remaining elements (Th, Ta, Hf, Eu, Tb and Sc) were done after a further 4 to 5 week cooling period.

An attempt was made to determine Cs content in each sample, but it appeared that abundances of Cs were below the detection limit, as no Cs gamma ray emissions were recorded.

¹ Samples BOWSER, COQ61, COQ632 and COQ251 were counted by NOVATRAK staff. All others were counted by the author.

Gamma rays emitted by samples are displayed and recorded as photopeaks on an energy spectrum, the net area under the photopeak being proportional to the flux of gamma rays emitted per unit time, which in turn is proportional to the concentration of the parent nuclide. Net area of photopeaks (the area of the peak above the background, **NOT** the total count above the baseline) (Covell, 1959) was calculated using an EGG Ortec® multichannel analyzer. Whenever possible the net areas for two photopeaks of the same isotope were recorded and concentrations were calculated separately for each photopeak. Differences in concentration between peak pairs ranged from 0% to 10%. Only one useable photopeak was found for the elements Th, Ta, Tb, and Sc.

Each photopeak net area in the standards and samples was corrected for decay back to an arbitrary initial time t_0 . The correction is:

$$e^{\lambda(t-t_0)} Na = Na_0$$

where: $\lambda = \ln 2 / \text{half-life}$

- t = time that counting of the sample began
- t_0 = chosen initial time
- Na = measured net peak area
- Na_0 = calculated net peak area at t_0

When the net peak area for all of the photopeaks in the

samples and standards have been calculated back to an initial time, t_0 , the concentration of elements in the samples can be determined by the following equation:

$$\frac{(\text{Net Area})_{\text{sam}}}{(\text{Net Area})_{\text{stand}}} = \frac{(\text{Conc. of element})_{\text{sam}}}{(\text{Conc. of element})_{\text{stand}}}$$

U abundances were determined by delayed neutron activation at the reactor site in Pullman, Washington. This analysis was performed by NOVATRAK staff.

INTERFERENCE OF PHOTOPEAKS

Interference of the Ta, Sm, Yb and Lu photopeaks by coincident photopeaks of Sc, Pa plus Np, Pa and Np respectively must be corrected before abundances of Ta, Sm, Yb and Lu can be calculated. Chemical separation to remove the interfering element will of course give the best results, but this is not always efficient. A quicker method involves irradiating a pure form of the interfering element and determining a ratio of the coincident photopeak to another photopeak. This ratio can then be applied to all samples. As no pure forms of U and Th (hence Np and Pa) were available, an estimate of the correction ratio was calculated from Lederer and Shirley (1978) and Kennedy and Fowler (1983). These were used for the duration of the analyses.

A Ta-free Sc standard was included in each of the irradiated layers so that a correction ratio to apply to the Sc peak at 889 keV could be uniquely determined for each layer

TABLE XII

TABLE OF INTERFERENCES *

| ISOTOPE | ENERGY OF γ -RAY (keV) | INTERFERRING PHOTOPEAKS AT ENERGY OF | PEAK MEASURED FOR CORRECTIONS | RATIO ¹ |
|------------------------|----------------------------------|--|----------------------------------|--------------------|
| $^{177}_{71}\text{Lu}$ | 208 | ^{239}Np @ 210 | 278 keV | 0.345 |
| $^{153}_{62}\text{Sm}$ | 103 | ^{233}Pa @ 104 | 312 keV | 0.021 |
| | | ^{239}Np @ 106 | 106 keV | 0.854 |
| $^{182}_{73}\text{Ta}$ | 1121 | ^{46}Sc @ 1121 | 889 keV | 0.802 |
| | | | | 0.805 |
| | | | | 0.797 |
| | | | | 0.795 |
| | | | | 0.795 |
| | | | | 0.794 |
| | | | | 0.798 |
| | | | | 0.794 |
| | | | | 0.781 |
| | | | | 0.791 |
| | | | | 0.793 |
| | | | | 0.789 |
| $^{175}_{70}\text{Yb}$ | 396 | ^{233}Pa @ 398 | 312 keV | 0.032 |

¹ A different ratio for Sc was determined for each layer with an approximate error of ± 0.04 . In the table the Sc ratios are given in order of bottles and layers, starting with bottle 1 - layer 1 and continuing to bottle 4 - layer 3.

* Interferring photopeaks and corresponding peak(s) to measure for corrections compiled from Kennedy and Fowler (1983), Lederer and Shirley (1983) and NOVATRAK data sheets.

of samples. This ratio ranged from 0.781 to 0.805 ± 0.04 . The above information is given in Table XII.

ACCURACY and PRECISION

According to Henderson and Pankhurst (1984) analytical precision of INAA at the level of REE concentrations found in basalts will be about 2-4% for the elements La, Ce, Nd, Sm, Eu, and Yb and 3-6% for Tb and Lu, all at an accuracy of about 5%.

Analytical precision in this study was based on replicate analyses of standards NIML and SY2 as well as intralab geology standards P-1 and WP1, all of which were included in all of the irradiations. Precision of analyses is $\pm 5\%$ for Th, La, Hf and Sc; $\pm 7\%$ for Sm; $\pm 10\%$ for Ta, Eu, Tb and Yb; and $\pm 15\%$ for Lu (Table XIV). Table XIII lists the data used to calculate the above precisions. As only one calculated abundance was recorded for each of the other standards and unknowns (no replicate analyses were done) the above precisions are assumed to apply to all of the samples analyzed.

Analytical accuracy is dependent on calibration of the single or multi-element standards used in calculating the concentrations of elements in the unknowns. To confirm the calibrations numerous interlaboratory rock standards of known concentration were analyzed as unknowns (Abbey, 1983; Flanagan, 1974; Flanagan, 1976; Kramar and Puchelt, 1982; Rozenberg and Zilliacus, 1980; Steele et al., 1978; Gladney

and Goode, 1981; Govindaraju, 1984; Alibert et al., 1983). Calculated concentrations vs. reference concentrations were tabulated (Table XV) and systematic errors in analyses were calculated for each element, (Table XVI). Systematic errors were less than the precision for Th, Sm, Eu, Tb and Lu but were greater than the precision for Ta, La, Hf, Yb and Sc. Consequently, calculated abundances of the latter elements were revised by an amount equal to the systematic error; -16% for Ta, +14.5% for La, +8% for Hf, +12% for Yb and +19.5% for Sc.

TABLE XIII (cont.)

PRECISION OF INAA BASED ON REPLICATE ANALYSES

Abundances in ppm

| SAMPLE | Th | Ta | La | Sm | Hf | Eu | Tb | Yb | Lu | Sc | Run | Layer |
|------------|------|------|------|------|------|------|------|------|-----|------|-----|-------|
| WP1 | 1.79 | 1.06 | 11.4 | 3.2 | 1.5 | 0.7 | N/A | 1.4 | 0.2 | 7.6 | 1 | 2 |
| WP1 | 2.68 | 1.44 | 11.9 | 3.2 | 2.1 | 0.7 | N/A | 1.3 | 0.2 | 7.8 | 1 | 2 |
| WP1 | 2.39 | 1.31 | 11.6 | 3.1 | 2.2 | 0.6 | N/A | 1.3 | 0.2 | 7.6 | 1 | 2 |
| WP1 | 2.04 | 0.98 | 11.1 | 3.1 | 2.1 | 0.6 | N/A | 1.5 | 0.2 | 7.8 | 1 | 2 |
| WP1 | 2.34 | N/D | 11.2 | 3.0 | 1.8 | 0.6 | N/A | 1.2 | 0.2 | 7.8 | 1 | 2 |
| WP1 | 2.46 | N/D | 11.4 | 3.2 | 1.9 | 0.6 | N/A | 1.3 | 0.2 | 8.0 | 1 | 2 |
| WP1 | 2.18 | 0.12 | 11.3 | 3.3 | 2.6 | 0.7 | N/A | 1.4 | 0.2 | 7.6 | 1 | 3 |
| WP1 | 1.73 | N/D | 10.7 | 3.1 | 2.1 | 0.8 | N/A | 1.2 | 0.2 | 7.5 | 1 | 3 |
| WP1 | 2.16 | N/D | 11.5 | 3.1 | 2.6 | 0.6 | 0.3 | 1.4 | 0.2 | 7.5 | 2 | 1 |
| WP1 | 2.38 | 0.56 | 11.6 | 3.1 | 2.8 | 0.7 | 0.3 | 1.3 | 0.2 | 7.3 | 2 | 2 |
| WP1 | 2.22 | N/D | 11.3 | 3.0 | 2.8 | 0.7 | 0.4 | 1.2 | 0.2 | 7.7 | 2 | 3 |
| WP1 | 2.25 | 1.59 | 10.3 | 3.1 | 2.5 | 1.0 | 1.0 | 1.0 | 0.2 | 7.9 | 3 | 1 |
| Mean | 2.22 | 0.59 | 11.2 | 3.1 | 2.3 | 0.7 | 0.5 | 1.3 | 0.2 | 7.7 | | |
| 1 σ | 0.27 | 0.64 | 0.43 | 0.09 | 0.42 | 0.12 | 0.34 | 0.13 | 0.0 | 0.20 | | |

N/D = not detected

N/A = not analyzed

continue.....

TABLE XIII (cont.)

PRECISION OF INAA BASED ON REPLICATE ANALYSES

Abundances in ppm

| SAMPLE | Th | Ta | La | Sm | Hf | Eu | Tb | Yb | Lu | Sc | Run | Layer |
|------------|------|------|------|------|------|------|-----|------|-----|------|-----|-------|
| P-1 | 3.3 | 4.3 | 10.7 | 2.6 | 2.2 | 0.5 | N/A | 1.8 | 0.3 | 9.1 | 1 | 2 |
| P-1 | 3.9 | 1.1 | 10.4 | 2.8 | 2.8 | 0.6 | N/A | 1.8 | 0.3 | 8.3 | 2 | 1 |
| P-1 | 3.6 | 1.2 | 10.7 | 2.7 | 2.8 | 0.7 | N/A | 2.0 | 0.3 | 8.1 | 2 | 1 |
| P-1 | 3.7 | 2.1 | 10.6 | 2.7 | 3.0 | 0.6 | N/A | 2.1 | 0.3 | 8.5 | 2 | 2 |
| P-1 | 3.8 | 0.4 | 10.3 | 2.6 | 3.0 | 0.6 | N/A | 1.9 | 0.3 | 8.4 | 2 | 2 |
| P-1 | 3.7 | 0.1 | 10.0 | 2.9 | 2.9 | 0.6 | N/A | 1.8 | 0.3 | 9.1 | 2 | 3 |
| P-1 | 3.8 | N/D | 10.9 | 2.9 | 3.0 | 0.7 | N/A | 2.0 | 0.3 | 9.1 | 2 | 3 |
| P-1 | 3.7 | N/D | 10.4 | 2.5 | 3.3 | 0.6 | N/A | 1.8 | 0.3 | 8.9 | 2 | 3 |
| Mean | 3.7 | 1.15 | 10.5 | 2.7 | 2.9 | 0.6 | | 1.9 | 0.3 | 8.7 | | |
| 1 σ | 0.18 | 1.47 | 0.28 | 0.15 | 0.32 | 0.06 | | 0.12 | 0.0 | 0.41 | | |

N/D = not detected

N/A = not analyzed

continue.....

TABLE XIII (cont.)

PRECISION OF INAA BASED ON REPLICATE ANALYSES

Abundances in ppm

| SAMPLE | Th | Ta | La | Sm | Hf | Eu | Tb | Yb | Lu | Sc | Run | Layer |
|------------|-------|-----|------|------|-----|------|------|------|------|------|-----|-------|
| SY2 | 362.6 | N/D | 65 | 15.0 | N/A | 1.6 | N/A | N/A | N/A | 5.4 | 1 | 1 |
| SY2 | 365.8 | N/D | 65 | 16.3 | 6.6 | 2.2 | N/A | 19.3 | N/A | 5.1 | 1 | 2 |
| SY2 | 366 | N/D | 72.1 | 16.6 | 6.9 | 2.0 | N/A | 13.6 | 3.0 | 5.3 | 1 | 3 |
| SY2 | 380 | N/D | 73.2 | 15.4 | 7.2 | 2.3 | 2.5 | 16.9 | 2.1 | 5.4 | 2 | 1 |
| SY2 | 385 | N/D | 70.3 | 15.3 | 7.3 | 2.3 | 3.0 | 15.1 | 1.9 | 5.2 | 2 | 2 |
| SY2 | 386 | N/D | 73.9 | 18.1 | 7.6 | 2.5 | 2.5 | 14.2 | 3.1 | 5.6 | 2 | 3 |
| SY2 | 374 | N/D | 76.4 | 17.5 | 6.9 | 2.1 | 3.0 | 13.5 | 3.0 | 5.7 | 2 | 4 |
| SY2 | 399 | N/D | 64.2 | 15.6 | 7.3 | 2.3 | 2.8 | 15.3 | 2.2 | 5.8 | 3 | 1 |
| SY2 | 364 | N/D | 68.1 | 15.4 | 7.2 | 2.4 | 3.0 | 15.2 | 3.0 | 5.8 | 4 | 1 |
| SY2 | 373 | N/D | 65.7 | 15.0 | 7.9 | 2.1 | 3.3 | 16.1 | 2.7 | 7.5 | 4 | 2 |
| SY2 | 366.5 | N/D | 73.0 | 16.8 | 8.3 | 2.6 | 3.4 | 17.1 | 2.3 | 7.6 | 4 | 3 |
| Mean | 374.7 | | 69.7 | 16.1 | 7.3 | 2.2 | 2.9 | 15.6 | 2.6 | 5.8 | | |
| 1 σ | 11.6 | | 4.3 | 1.1 | 0.5 | 0.27 | 0.33 | 1.79 | 0.46 | 0.87 | | |

N/D = not detected

N/A = not analyzed

continue.....

TABLE XIII

PRECISION OF INAA BASED ON REPLICATE ANALYSES

Abundances in ppm

| SAMPLE | Th | Ta | La | Sm | Hf | Eu | Tb | Yb | Lu | Sc | Run | Layer |
|------------|-----|------|-----|------|-----|------|-----|-----|------|------|-----|-------|
| NIML | STD | 27.6 | 202 | 4.8 | STD | 1.2 | N/D | 3.6 | 0.4 | 0.2 | 1 | 1 |
| NIML | STD | 25.0 | 201 | 5.3 | STD | 0.8 | N/D | 3.5 | 0.4 | 0.2 | 1 | 2 |
| NIML | STD | 26.5 | 189 | 4.8 | STD | 1.0 | N/D | 2.5 | 0.5 | 0.2 | 1 | 3 |
| NIML | STD | 26.1 | 201 | 4.6 | STD | 1.1 | N/D | 2.8 | 0.4 | 0.2 | 2 | 1 |
| NIML | STD | 26.3 | 187 | 4.7 | STD | 0.9 | N/D | 3.6 | 0.4 | 0.1 | 2 | 2 |
| NIML | STD | 26.3 | 192 | 4.5 | STD | 1.0 | N/D | 2.6 | 0.5 | 0.2 | 2 | 3 |
| NIML | STD | 24.7 | 197 | 5.1 | STD | 0.9 | N/D | 2.2 | 0.5 | 0.2 | 2 | 4 |
| NIML | STD | 27.7 | 177 | 5.6 | STD | 1.1 | N/D | 2.0 | 0.5 | 0.1 | 3 | 1 |
| NIML | STD | 26.7 | 209 | 4.2 | STD | 1.0 | N/D | 2.7 | 0.4 | 0.3 | 1 | 1 |
| NIML | STD | 21.9 | 206 | 4.8 | STD | 0.9 | N/D | 2.7 | 0.6 | 0.2 | 4 | 1 |
| NIML | STD | 22.5 | 190 | 4.1 | STD | 1.0 | N/D | 3.2 | 0.4 | 0.3 | 4 | 2 |
| NIML | STD | 21.3 | 210 | 4.8 | STD | 1.2 | N/D | 3.1 | 0.4 | 0.3 | 4 | 3 |
| Mean | | 25.2 | 197 | 4.8 | | 1.0 | | 2.9 | 0.45 | 0.22 | | |
| 1 σ | | 2.2 | 9.9 | 0.42 | | 0.12 | | 0.5 | 0.07 | 0.06 | | |

N/D = not detected

STD = sample used as a standard

TABLE XIV

RELATIVE PRECISIONS BASED
ON REPLICATE ANALYSESConcentration and 1σ in ppm
Precisions¹ in %

| | Th | | | Ta | | | La | | | Sm | | | Hf | | |
|--------------------|-----------------------|-----------|-------|-----------------------|-----------|--------|-----------------------|-----------|-------|-----------------------|-----------|-----------|----------------------|-----------|-------|
| | Conc. | 1σ | Prec. | Conc. | 1σ | Prec. | Conc. | 1σ | Prec. | Conc. | 1σ | Prec. | Conc. | 1σ | Prec. |
| NIML | STD | | | 25.2 | 2.2 | 8.7 | 197 | 9.9 | 5 | 4.8 | 0.4 | 8.7 | STD | | |
| SY2 | 374.7 | 11.6 | 3.1 | N/D | | | 69.7 | 4.3 | 6 | 16.1 | 1.1 | 6.8 | 7.3 | 0.5 | 6.8 |
| WP1 | 2.2 | 0.3 | 13.6 | (0.59)* | (0.64)* | (108)* | 12.8 | 0.4 | 3.1 | 3.1 | 0.1 | 2.9 | 2.5 | 0.4 | 16 |
| P-1 | 3.7 | 0.18 | 4.9 | (1.15)* | (1.47)* | (128)* | 12.0 | 0.3 | 2.5 | 2.7 | 0.2 | 5.5 | 3.1 | 0.3 | 10 |
| Relative Precision | $\pm 5\%$ or 0.3 ppm | | | $\pm 10\%$ or 0.6 ppm | | | $\pm 5\%$ or 0.4 ppm | | | $\pm 7\%$ or 0.2 ppm | | | $\pm 5\%$ or 0.4 ppm | | |
| | Eu | | | Tb | | | Yb | | | Lu | | | Sc | | |
| | Conc. | 1σ | Prec. | Conc. | 1σ | Prec. | Conc. | 1σ | Prec. | Conc. | 1σ | Prec. | Conc. | 1σ | Prec. |
| NIML | 1.0 | 0.1 | 12 | N/D | | | 2.9 | 0.5 | 17 | 0.45 | 0.07 | 15.5 | 0.22 | 0.06 | 27 |
| SY2 | 2.2 | 0.3 | 12.3 | 2.9 | 0.3 | 11.4 | 15.6 | 1.8 | 11.5 | 2.6 | 0.5 | 17.7 | 5.8 | 0.9 | 15 |
| WP1 | 0.7 | 0.1 | 17 | 0.5 | 0.3 | 68 | 1.5 | 0.1 | 6.6 | 0.2 | 0.0 | ≤ 25 | 9.2 | 0.2 | 2.2 |
| P-1 | 0.6 | 0.1 | 10 | N/D | | | 2.1 | 0.1 | 4.8 | 0.3 | 0.0 | ≤ 17 | 10.4 | 0.4 | 3.8 |
| Relative Precision | $\pm 10\%$ or 0.2 ppm | | | $\pm 10\%$ or 0.3 ppm | | | $\pm 10\%$ or 0.4 ppm | | | $\pm 15\%$ or 0.1 ppm | | | $\pm 5\%$ or 0.1 ppm | | |

N/A = not analyzed

STD = Sample used as a standard

N/D = below detection limit

* = contaminated sample

¹These precisions are calculated from data contained in the previous Tables, $(\sigma/\text{mean}) \times 100$.

TABLE XV
TEST OF ANALYTICAL ACCURACY FOR INAA

| Abundances in ppm | | | | | | | | | | | |
|-------------------|-------------------|--------------------|-------------------|--------------------|-------------------|-------------------|-----|------------------|-------------------|-------------------|-----------|
| SAMPLE | Th | Ta | La | Sm | Hf | Eu | Tb | Yb | Lu | Sc | Run-layer |
| NIMG | 51.4±2.6 | 5.1±0.6 | 104±5 | 15±1 | 10.9±0.5 | 0.4±0.2 | N/A | 14.5±1.5 | 1.8±0.1 | 0.4±0.1 | 1-1 |
| Ref. | 52 ³ | 4.64 ¹² | 107 ¹² | 15.4 ⁵ | 12? ³ | 0.4? ³ | | 14 ³ | 2? ³ | 0.5 ¹² | |
| NIMS | 1.2±0.3 | N/D | 4.6±0.6 | 1.3±0.2 | 0.4±0.3 | N/D | N/A | N/D | N/D | 2.9±0.1 | 1-1 |
| Ref. | 0.9? ³ | | 4? ² | 1.2 ¹² | 0.3 ¹² | | | | | 3.8 ¹² | |
| SY3 | 985±49 | N/D | 1226±61 | 82.7±6 | 8.3±0.4 | 16.2±1.6 | N/A | N/D | N/D | 5.1±0.3 | 1-1 |
| Ref. | 990 ³ | | 1350 ³ | 95 ¹ | 9? ³ | 14? ³ | | | | 7? ³ | |
| RGM-1 | 13.6±0.7 | 1.0±0.6 | 19.1±1 | 4.0±0.3 | 5.5±0.4 | 0.5±0.2 | N/A | 1.5±0.4 | N/D | 3.3±0.2 | 1-3 |
| Ref. | 15? ³ | 1.0 ³ | 23? ³ | 4.3? ³ | 6.0? ³ | 0.7? ³ | | 2.3 ⁷ | | 4.7 ³ | |
| QLO-1 | 5.4±0.3 | 0.7±0.6 | 24.2±1.2 | 5.2±0.4 | 4.7±0.4 | 1.3±0.2 | N/A | 1.9±0.4 | 0.4±0.1 | 7.0±0.4 | 1-3 |
| Ref. | 4.8? ³ | 0.63 ⁷ | 27? ³ | 5.1? ³ | 4.6? ³ | 1.5? ³ | | 2.2 ⁷ | 0.4 ⁸ | 9? ³ | |
| BHVO-1 | 1.1±0.3 | 1.0±0.6 | 13.9±0.7 | 6.7±0.5 | 4.2±0.4 | 2.0±0.2 | N/A | 1.7±0.4 | 0.3±0.1 | 26.3±1.3 | 1-3 |
| Ref. | 1.0 ³ | 1.1? ³ | 17? ³ | 6.1 ³ | 4.3 ³ | 2.0 ³ | | 1.9 ³ | 0.3 ⁶ | 31 ⁶ | |
| GSP-1 | 109±5 | 1.6±0.6 | 155±8 | 28±2 | 13.6±0.7 | 2.2±0.2 | N/A | 1.6±0.4 | 0.2±0.1 | 4.9±0.2 | 1-3 |
| Ref. | 105 ³ | 1? ³ | 191 ¹⁰ | 26.8? ⁹ | 14? ³ | 2.2 ¹⁰ | | 1.9 ³ | 0.2? ³ | 6.6 ³ | |
| STM-1 | 29.3±1.5 | 21.6±0.6 | 145±7 | 13±1 | 23.6±1.2 | 3.0±0.3 | N/A | 3.7±0.4 | 0.5±0.1 | 0.4±0.1 | 1-3 |
| Ref. | 31? ³ | 18? ³ | 146 ¹¹ | 13 ³ | 27? ³ | 3.7 ³ | | 4.3 ³ | 0.7 ⁸ | 0.5 ¹¹ | |

N/D = not detected

N/A = not analyzed

? = questionable value

continued.....

TABLE XV (cont.)
TEST OF ANALYTICAL ACCURACY FOR INAA

Abundances in ppm

| SAMPLE | Th | Ta | La | Sm | Hf | Eu | Tb | Yb | Lu | Sc | R-L |
|---------|----------------------|-------------------|-----------------------|-------------------|-------------------|-------------------|--------------------|----------------------|--------------------|---------------------|------|
| BCR-1 | 6.9±0.3 | 1.3±0.6 | 24±1 | 7.3±0.5 | 3.8±0.4 | 2.1±0.2 | 0.7±0.3 | 3.4±0.3 | 0.5±0.1 | 29.4±1.5 | 4-2 |
| Ref. | 6.1 ³ | 0.8? ³ | 27 ³ | 6.5 ³ | 5 ³ | 2.0 ³ | 1.0 ³ | 3.4 ³ | 0.5? ³ | 33 ³ | |
| ARCHO-1 | 7.6±0.4 | 2.6±0.6 | 38.5±2 | 9.9±0.7 | 9.7±0.5 | 4.4±0.4 | 1.5±0.4 | 3.9±0.4 | 0.6±0.1 | 31.9±1.6 | 4-3 |
| Ref. | 7.3±0.1 ⁴ | 1.18 ⁴ | 45.8±0.6 ⁴ | 9.83 ⁴ | 11.1 ⁴ | 4.31 ⁴ | 1.47? ⁴ | 4.2±0.1 ⁴ | 0.63? ⁴ | 28.93 ⁴ | |
| NIML | STD | 25.2±0.6 | 197±3 | 4.8 | STD | 1.0 | N/D | 2.9±0.1 | 0.45±0.02 | 0.22±0.02 | n=12 |
| Ref. | | 22? ³ | 200? ³ | 4.8 ¹² | | 1? ³ | | 3.5 ¹² | 0.4? ¹² | 0.27? ¹² | |
| SY2 | 374.7±3.5 | N/D | 69.7±1.3 | 16.1±0.3 | 7.3±0.2 | 2.2 | 2.9±0.1 | 15.6±0.6 | 2.6±0.1 | 5.8±0.3 | n=11 |
| Ref. | 380? ³ | | 85 ¹ | 15? ³ | 8? ³ | 2.2 ¹ | 2.7 ¹ | 17 ³ | 3? ³ | 7? ³ | |

R-L = Run-layer

N/D = not detected

N/A = not analyzed

STD = sample used as a standard

? = questionable value

¹ Abbey, 1976

² Abbey, 1980

³ Abbey, 1983

⁴ Additon and Seil, 1979

⁵ Alibert et al., 1983

⁶ Flanagan, 1974

⁷ Flanagan, 1976

⁸ Gladney and Goode, 1981

⁹ Govindaraju, 1984

¹⁰ Kramar and Puchelt, 1982

¹¹ Rozenberg and Zilliacus, 1980

¹² Steele et al., 1978

ABUNDANCES FROM DUPLICATE ANALYSES
(INAA)

| | | Abundances in ppm | | | | | | |
|----------|-----------|-------------------|------|------|------|-----|------|------|
| | | La | Sm | Eu | Tb | Yb | Lu | Sc |
| SEXRIDGE | U. B. C. | 4.6 | 3.5 | 1.1 | 0.8 | 3.1 | 0.4 | 36.7 |
| | Schilling | 4.6 | 3.7 | 1.30 | 0.79 | 3.1 | 0.43 | 43 |
| PREVRDG | U. B. C. | 18.1 | 10.0 | 2.9 | 2.1 | 7.7 | 1.1 | 34.7 |
| | Schilling | 15.2 | 9.9 | 3.02 | 2.09 | 7.8 | 1.08 | 36 |
| EXRIFT | U. B. C. | 2.0 | 2.2 | 0.8 | 0.6 | 2.3 | 0.3 | 27.1 |
| | Schilling | 1.9 | 2.5 | 1.01 | 0.61 | 2.4 | 0.34 | 31 |
| EXDEEP | U. B. C. | 11.4 | 4.8 | 1.4 | 0.8 | 3.2 | 0.4 | 34.4 |
| | Schilling | 9.7 | 4.8 | 1.68 | 0.93 | 3.7 | 0.54 | 39 |

U. B. C. = INAA by the author.
Schilling = INAA by J.G. Schilling, presented in Cousens et al., 1984.

TABLE XVI
SYSTEMATIC ERROR IN INAA ANALYSES

| SAMPLE | Th | Ta | La | Sm | Hf | Eu | Tb | Yb | Lu | Sc |
|---------------------------------|----------|----------|-----------|----------|----------|----------|----------|----------|----------|----------|
| NIMG | -1%±5% | +9.9%±5% | -3%±5% | -3%±7% | -9%±5% | 0%±15% | N/A | +4%±10% | -10%±15% | -20%±10% |
| NIMS | +33%±25% | N/D | -15%±13% | +8%±15% | N/D | N/D | N/A | N/D | N/D | -24%±14% |
| SY3 | -0.5%±5% | N/D | -9%±5% | -13%±7% | -8%±8% | +15%±10% | N/A | N/D | N/D | -27%±8% |
| RGM-1 | -9%±5% | +0%±3% | -17%±5% | -7%±7% | -8%±7% | -28%±12% | N/A | -35%±13% | N/D | -42%±12% |
| QLO-1 | +13%±5% | +11%±20% | -10%±5% | +2%±7% | +2%±7% | -13%±10% | N/A | -14%±10% | 0%±10% | -22%±6% |
| BHVO-1 | +10%±27% | -9%±5% | -18%±5% | +10%±7% | -2%±7% | 0%±15% | N/A | -10%±10% | 0%±10% | -15%±5% |
| GSP-1 | +4%±5% | +60%±20% | -23%±5% | +4%±7% | -3%±5% | 0%±10% | N/A | -16%±10% | 0%±20% | -26%±8% |
| STM-1 | -5%±5% | +20%±10% | -0.7%±5% | 0%±7% | -13%±5% | -19%±15% | N/A | -14%±10% | -28%±5% | -25%±10% |
| BCR-1 | +13%±5% | +62%±15% | -11%±5% | +12%±7% | -24%±15% | +5%±12% | -30%±20% | 0%±10% | 0%±20% | -11%±5% |
| ARCHO-1 | +4%±5% | +54%±20% | -1.9%±5% | +0.7%±7% | -14%±5% | +2%±10% | +2%±15% | -7%±10% | -5%±16% | -10%±5% |
| NIML | STD | +14%±2% | -18%±1.5% | 0%±7% | STD | 0%±10% | N/D | -17%±3% | +13%±4% | -19%±9% |
| SY2 | -0.2%±1% | N/D | -18%±1.8% | +7%±2% | -9%±3% | 0%±10% | +7%±3% | -8%±4% | -13%±4% | -17%±5% |
| MEAN | +2.8% | +33% | -13% | +1.7% | -9% | -4% | +6% | -12% | -6% | -21.5% |
| WGTD. MEAN | +1.4% | +16.3% | -14.4% | +2.4% | -8.3% | -1.5% | +3% | -12.2% | -6.2% | -19.4% |
| 1σ UNCERTAINTY OF WGTD. MEAN | ±3.8% | ±5.9% | ±3.6% | ±6.0% | ±5.7% | ±11.4% | ±15.0% | ±7.4% | ±7.8% | ±7.1% |

N/D = not determined

N/A = not analyzed

STD = sample used as a standard

NOVATRAK ANALYSES

Samples BOWSER, COQ251, COQ632 and COQ61 were analyzed by NOVATRAK. All four samples have two to three times the Yb content of other samples and samples BOWSER and COQ61 exhibit a similar enrichment in Th. None of the samples analyzed by the author are enriched to the same extent, suggesting the enrichment is a product of NOVATRAK analysis. Therefore these abundances were not recorded. To plot BEND patterns for these samples an estimated Yb content was calculated using the ratio $Y/Yb = 13$, the average ratio from all other samples.

ELEMENT ABUNDANCES IN STANDARDS WP1 AND P-1

Intralab standards P-1 and WP1 were analyzed numerous times throughout the study period to establish them as secondary standards. Although major element oxide abundances had been previously determined no prior analyses had determined abundances of Th, Ta, La, Sm, Hf, Eu, Tb, Yb, Lu and Sc. Calculated abundances from this study are recorded in Table 4 and revised abundances are listed in Table XVII.

TABLE XVII
ELEMENT ABUNDANCES IN INTRALAB STANDARDS WP1 and P-1

| ELEMENT | STANDARDS | |
|---------|----------------|----------------|
| | WP1 | P-1 |
| Eu | 0.7 ± 0.1 | 0.6 ± 0.1 |
| Hf | 2.5 ± 0.1 | 3.1 ± 0.1 |
| La | 12.8 ± 0.1 | 12.0 ± 0.1 |
| Lu | 0.2 ± 0.1 | 0.3 ± 0.1 |
| Sc | 9.2 ± 0.1 | 10.4 ± 0.1 |
| Sm | 3.1 ± 0.1 | 2.7 ± 0.1 |
| Tb | 0.5 ± 0.1 | N/D |
| Th | 2.2 ± 0.1 | 3.7 ± 0.1 |
| Yb | 1.5 ± 0.1 | 2.1 ± 0.1 |

Abundances in ppm
N/D = not detected

APPENDIX III - MAJOR AND TRACE ELEMENT ANALYSIS BY XRF

PREPARATION FOR ANALYSIS

Nearly all of the samples selected for analysis had been crushed and powdered during previous studies. The remainder were small whole rock fragments which were powdered to approximately 200 mesh by grinding them first in a tungsten carbide ring mill and then in an agate mortar. All powdered samples were subsequently made into pellets as described in the U.B.C. XRF lab instruction sheets. Pellet preparation was done by the author.

MAJOR ELEMENT ANALYSIS

Major element oxide concentrations were determined by X-ray fluorescence spectroscopy on an automated Phillips® spectrometer, using the pressed powder method of van der Heyden (1982). This analysis was performed by B. Cousens in the department of Oceanography at the University of British Columbia. Analyses for H₂O and CO₂ were not performed. The method and operating conditions as well as a complete description of the computer program used in data reduction are contained in van der Heyden (1982).

Included in the sample set were four standards analyzed as unknowns and fourteen samples for which major element abundances had previously been determined. Estimated precisions were calculated from these duplicate analyses by

finding the mean range (w) and dividing this number by a constant (d_n) (Davies, 1961). These estimated precisions are listed in Table XVIII, along with % mean deviations from the recommended values for standards used in constructing the working curves (Abbey, 1983).

TRACE ELEMENT ANALYSIS

Concentrations of Ba, Rb, Nb, Ce, Sr, Nd, Zr, Y, Co, Cr, Cu, Ni and V were determined by XRF analyses of pressed powder pellets. These pellets were the same as those used for major element oxide determinations. All of the above elements, except Ce and Nd, were analyzed by B. Cousens of U.B.C. Ce and Nd analyses were done by the author at the department of Geological Sciences, U.B.C. Raw data was reduced using a computer program written by Berman (1979) and modified by B. Cousens (pers. comm.).

Included with the unknown samples were five standards and sixteen samples in which abundances of all or some of the trace elements had been previously determined.

Table XIX lists 1 σ errors on the analyses of standards used to create the working curves, as well as analytical precision estimates based on duplicate analyses. Precision for Ba is poor due to low counting intensities.

TABLE XVIII

PRECISION OF MAJOR ELEMENT ANALYSES

MAJOR ELEMENTS: % mean deviation from working curves constructed using the recommended values for the same standards (Abbey, 1983). Estimated precisions are from duplicate analyses of unknown samples.

| | % MEAN DEVIATION | ESTIMATED PRECISION |
|--------------------------------|---------------------|---------------------|
| SiO ₂ | 1% | 1.7% |
| TiO ₂ | 2.5% | 2.5% |
| Al ₂ O ₃ | 3.7% | 3.5% |
| Fe ₂ O ₃ | 2% | 2.8% |
| MnO | 1% | 10% |
| MgO | 1.3% | 9.5% |
| CaO | 2.8% | 2.7% |
| Na ₂ O | 4.0% | 8.7% |
| K ₂ O | 4.1% | 5% |
| P ₂ O ₅ | 10.4% | 10.0% |

On the following pages are:

1. Computed major element abundances in the analyzed standards which were used to calculate % mean deviation, and
2. Abundances from duplicate analyses.

FINAL DATA FOR STANDARDS USED IN CONSTRUCTION
OF WORKING CURVES FOR MAJOR ELEMENT ANALYSIS

| IDENT | SI | AL | FE | MG | CA | NA | K | STANDARDS | | P | H2O | CO2 | TOTAL | |
|--------|-------|-------|-------|-------|-------|-------|-------|-----------|-------|-------|------|------|--------|---------------|
| | | | | | | | | TI | MN | | | | | |
| BHVO-1 | 49.81 | 14.64 | 12.05 | 7.18 | 11.21 | 2.44 | 0.46 | 2.61 | 0.16 | 0.21 | 0.20 | 0.04 | 101.01 | FINAL VALUE |
| | 49.31 | 14.49 | 11.93 | 7.11 | 11.10 | 2.42 | 0.46 | 2.58 | 0.16 | 0.21 | 0.20 | 0.04 | | NORM. VALUE |
| | 49.90 | 13.70 | 12.10 | 7.20 | 11.40 | 2.30 | 0.53 | 2.70 | 0.17 | 0.28 | 0.20 | 0.04 | 100.52 | RECCOM. VALUE |
| | -0.59 | 0.79 | -0.17 | -0.09 | -0.30 | 0.12 | -0.07 | -0.12 | -0.01 | -0.07 | 0.0 | 0.0 | | NORM.-RECC. |
| BCR-1 | 54.34 | 13.61 | 13.16 | 3.48 | 7.03 | 3.45 | 1.68 | 2.23 | 0.18 | 0.37 | 0.67 | 0.02 | 100.23 | FINAL VALUE |
| | 54.22 | 13.58 | 13.13 | 3.47 | 7.01 | 3.44 | 1.67 | 2.23 | 0.18 | 0.37 | 0.67 | 0.02 | | NORM. VALUE |
| | 54.53 | 13.72 | 13.44 | 3.48 | 6.97 | 3.30 | 1.70 | 2.26 | 0.18 | 0.36 | 0.67 | 0.02 | 100.63 | RECCOM. VALUE |
| | -0.31 | -0.14 | -0.31 | -0.01 | 0.04 | 0.14 | -0.03 | -0.03 | 0.00 | 0.01 | 0.0 | 0.0 | | NORM.-RECC. |
| MRG-1 | 39.61 | 8.24 | 18.01 | 13.54 | 14.94 | 0.31 | 0.17 | 3.73 | 0.17 | 0.06 | 0.98 | 1.00 | 100.77 | FINAL VALUE |
| | 39.31 | 8.18 | 17.87 | 13.44 | 14.83 | 0.30 | 0.17 | 3.70 | 0.17 | 0.06 | 0.98 | 1.00 | | NORM. VALUE |
| | 39.32 | 8.50 | 17.85 | 13.49 | 14.77 | 0.71 | 0.18 | 3.69 | 0.17 | 0.06 | 0.98 | 1.00 | 100.72 | RECCOM. VALUE |
| | -0.01 | -0.32 | 0.02 | -0.05 | 0.06 | -0.41 | -0.01 | 0.01 | 0.00 | 0.00 | 0.0 | 0.0 | | NORM.-RECC. |
| JB-1 | 53.01 | 14.92 | 9.12 | 7.50 | 9.08 | 2.60 | 1.47 | 1.37 | 0.15 | 0.28 | 1.01 | 0.18 | 100.70 | FINAL VALUE |
| | 52.64 | 14.81 | 9.06 | 7.45 | 9.02 | 2.58 | 1.46 | 1.36 | 0.15 | 0.28 | 1.01 | 0.18 | | NORM. VALUE |
| | 52.60 | 14.62 | 9.05 | 7.76 | 9.35 | 2.79 | 1.42 | 1.34 | 0.15 | 0.26 | 1.01 | 0.18 | 100.53 | RECCOM. VALUE |
| | 0.04 | 0.19 | 0.01 | -0.31 | -0.33 | -0.21 | 0.04 | 0.02 | 0.00 | 0.02 | 0.0 | 0.0 | | NORM.-RECC. |
| W-1 | 52.06 | 15.48 | 10.93 | 6.74 | 10.92 | 2.20 | 0.65 | 1.08 | 0.17 | 0.18 | 0.53 | 0.06 | 101.00 | FINAL VALUE |
| | 51.55 | 15.33 | 10.82 | 6.67 | 10.81 | 2.18 | 0.65 | 1.07 | 0.17 | 0.18 | 0.53 | 0.06 | | NORM. VALUE |
| | 52.72 | 15.02 | 11.10 | 6.63 | 10.98 | 2.15 | 0.64 | 1.07 | 0.17 | 0.14 | 0.53 | 0.06 | 101.21 | RECCOM. VALUE |
| | -1.17 | 0.31 | -0.28 | 0.04 | -0.17 | 0.03 | 0.01 | -0.00 | -0.00 | 0.04 | 0.0 | 0.0 | | NORM.-RECC. |
| AGV-1 | 59.88 | 15.82 | 7.20 | 1.88 | 5.35 | 4.26 | 2.92 | 1.14 | 0.10 | 0.50 | 0.78 | 0.02 | 99.83 | FINAL VALUE |
| | 59.98 | 15.84 | 7.21 | 1.88 | 5.36 | 4.26 | 2.92 | 1.14 | 0.10 | 0.50 | 0.78 | 0.02 | | NORM. VALUE |
| | 59.61 | 17.19 | 6.82 | 1.52 | 4.94 | 4.34 | 2.92 | 1.06 | 0.10 | 0.51 | 0.78 | 0.02 | 99.81 | RECCOM. VALUE |
| | 0.37 | -1.35 | 0.39 | 0.36 | 0.42 | -0.08 | 0.00 | 0.08 | -0.00 | -0.01 | 0.0 | 0.0 | | NORM.-RECC. |

ABUNDANCES FROM DUPLICATE ANALYSES
ESTIMATE OF ANALYTICAL PRECISION
XRF MAJOR ELEMENTS

Major element oxides in wt. %.

| SAMPLE | SiO ₂ | TiO ₂ | Al ₂ O ₃ | Fe ₂ O ₃ | MnO | MgO | CaO | Na ₂ O | K ₂ O | P ₂ O ₅ |
|-------------------|------------------|------------------|--------------------------------|--------------------------------|--------|------|-------|-------------------|------------------|-------------------------------|
| NBS688 | 47.79 | 1.19 | 17.99 | 10.61 | 0.17 | 7.54 | 12.35 | 2.02 | 0.19 | 0.15 |
| Ref. ¹ | 48.4 | 1.17 | 17.36 | 10.35 | 0.167 | 8.4 | 12.17 | 2.15 | 0.187 | 0.134 |
| NIML | 53.82 | 0.49 | 14.72 | 10.02 | (1.03) | 0.43 | 3.35 | (10.80) | 5.31 | 0.04 |
| Ref. ¹ | 52.4 | 0.48 | 13.64 | 9.75 | (0.77) | 0.28 | 3.22 | (8.37) | 5.51 | 0.06 |
| NIMC | 73.79 | 0.12 | 13.28 | 2.46 | 0.02 | 0.07 | 1.05 | 3.63 | 5.58 | 0.01 |
| Ref. ¹ | 75.70 | 0.09 | 12.08 | 1.74 | 0.02 | 0.06 | 0.78 | 3.36 | 4.99 | 0.01 |
| SY3 | 59.16 | 0.13 | 12.28 | 6.67 | 0.37 | 3.38 | 8.63 | 4.48 | 4.30 | 0.60 |
| Ref. ¹ | 59.68 | 0.15 | 11.80 | 5.66 | 0.32 | 2.67 | 8.26 | 4.15 | 4.20 | 0.54 |
| COQ61 | 57.75 | 0.83 | 15.38 | 8.05 | 0.14 | 6.11 | 6.42 | 2.96 | 2.16 | 0.21 |
| Ref. ² | 58.51 | 0.82 | 16.22 | 7.91 | 0.15 | 4.30 | 6.51 | 3.08 | 2.27 | 0.22 |
| COQ251 | 53.53 | 1.02 | 16.38 | 8.89 | 0.19 | 6.75 | 9.70 | 2.26 | 0.96 | 0.31 |
| Ref. ² | 53.98 | 1.01 | 17.74 | 8.87 | 0.18 | 4.40 | 9.60 | 2.89 | 1.04 | 0.28 |
| COQ632 | 55.40 | 1.02 | 16.34 | 8.38 | 0.15 | 5.47 | 8.12 | 3.08 | 1.67 | 0.37 |
| Ref. ² | 54.58 | 1.03 | 16.98 | 9.63 | 0.15 | 4.58 | 8.02 | 3.17 | 1.61 | 0.28 |

() These numbers were not used in the calculation of estimated precisions.

continue.....

MAJOR cont.

| | SiO ₂ | TiO ₂ | Al ₂ O ₃ | Fe ₂ O ₃ | MnO | MgO | CaO | Na ₂ O | K ₂ O | P ₂ O ₅ |
|-------------------|------------------|------------------|--------------------------------|--------------------------------|--------|---------|---------|-------------------|------------------|-------------------------------|
| WOOD LK. | 48.19 | 2.66 | 16.01 | 13.65 | 0.18 | 4.60 | 7.60 | 4.93 | 1.38 | 0.80 |
| Ref. ⁴ | 46.40 | 2.67 | 15.13 | 13.95 | 0.16 | 4.21 | 7.31 | 4.79 | 1.20 | 0.58 |
| EDMUND | 50.55 | 1.53 | 15.64 | 11.78 | 0.16 | 6.28 | 8.95 | 4.03 | 0.67 | 0.42 |
| Ref. ⁴ | 48.79 | 1.66 | 14.94 | 12.10 | 0.17 | 7.34 | 8.61 | 3.97 | 0.55 | 0.24 |
| NAZKO | 51.24 | 1.84 | 15.07 | 12.12 | 0.16 | 6.82 | 8.46 | 3.38 | 0.62 | 0.30 |
| Ref. ⁴ | 49.50 | 1.85 | 14.27 | 12.26 | 0.17 | 8.14 | 8.34 | 3.36 | 0.53 | 0.21 |
| V8M | 50.59 | 0.89 | 15.22 | 12.50 | (0.25) | 7.66 | 8.61 | 2.69 | 1.26 | 0.33 |
| Ref. ³ | 50.86 | 0.87 | 15.38 | 12.58 | (0.09) | 6.99 | 7.95 | 3.16 | 1.17 | 0.25 |
| 12-2 | (43.27) | 0.13 | 12.62 | (14.45) | 0.23 | (18.76) | (10.15) | 0.27 | 0.10 | 0.11 |
| Ref. ³ | (37.55) | 0.17 | 12.05 | (12.74) | 0.14 | (23.67) | (8.41) | 0.56 | 0.11 | 0.03 |
| 27-22 | 45.92 | 0.79 | 15.20 | 11.99 | 0.21 | 11.64 | 12.92 | 0.94 | 0.34 | 0.05 |
| Ref. ³ | 45.05 | 0.76 | 15.57 | 12.01 | 0.16 | 11.99 | 12.62 | 1.60 | 0.35 | 0.05 |
| 35-19b | 44.41 | 0.96 | 15.11 | 14.64 | 0.23 | 10.83 | 12.46 | 1.11 | 0.20 | 0.05 |
| Ref. ³ | 42.81 | 0.91 | 15.39 | 14.73 | 0.15 | 10.95 | 12.00 | 1.79 | 0.21 | 0.06 |
| DOG CK | 51.25 | 1.93 | 14.69 | 12.82 | 0.16 | 6.70 | 8.47 | 3.27 | 0.57 | 0.14 |
| Ref. ⁵ | 50.65 | 1.92 | 14.67 | 12.77 | 0.16 | 8.28 | 8.58 | 3.15 | 0.65 | 0.22 |
| BULL CAN | 49.71 | 1.35 | 15.58 | 13.20 | 0.17 | 7.42 | 8.56 | 3.42 | 0.41 | 0.17 |
| Ref. ⁵ | 49.67 | 1.28 | 15.58 | 13.00 | 0.17 | 8.32 | 8.88 | 3.46 | 0.38 | 0.14 |
| CAMEL | 51.89 | 1.93 | 15.25 | 11.04 | 0.14 | 6.02 | 8.51 | (4.25) | 0.81 | 0.15 |
| Ref. ⁵ | 51.94 | 1.94 | 16.13 | 11.06 | 0.14 | 6.38 | 9.50 | (2.69) | 0.82 | 0.30 |
| DEADMAN | 48.41 | 1.90 | 14.62 | (13.84) | 0.18 | 9.81 | (7.54) | 2.19 | 1.04 | 0.34 |
| Ref. ⁵ | 49.11 | 1.98 | 14.98 | (12.14) | 0.16 | 9.34 | (9.48) | 2.40 | 1.05 | 0.34 |

¹ Abbey, 1983; ² Berman, 1979; ³ Isachsen, 1984; ⁴ W. H. Mathews (pers. comm.);

⁵ Bevier, 1982

TABLE XIX

PRECISION OF TRACE ELEMENT ANALYSES

TRACE ELEMENTS: Approximate 1σ scatter of standards about working curves as generated by Berman (1979) program. Abundances in standards are from Abbey (1983). Estimated precisions are from duplicate analyses of samples.

| | APPROX. 1σ ERRORS | ESTIMATED PRECISION |
|-----------------|-----------------------------|---------------------|
| Ba | 50 ppm | 26.1 ppm |
| Rb | 1 ppm | 2.3 ppm |
| Nb | 3 ppm | 1.9 ppm |
| Ce | 10 ppm | N/D* |
| Sr | 4 ppm | 6.6 ppm |
| Nd | 5 ppm | N/D* |
| Zr | 2 ppm | 8.5 ppm |
| Y | 2 ppm | 2.2 ppm |
| Co ¹ | 4 ppm | 5.7 ppm |
| Cr ¹ | 9 ppm | 10.2 ppm |
| Cu ¹ | 6 ppm | 11.3 ppm |
| Ni | 5 ppm | 4.8 ppm |
| V | 4 ppm | 8.4 ppm |

¹ Estimated precisions for Co, Cr, and Cu are based on relatively few duplicate analyses.

* N/D=not determined

On the following pages are:

1. Computed trace element abundance in the analyzed standards which were used to calculate 1σ , and
2. Abundances from duplicate analyses.

TRACE ELEMENT REGRESSION ANALYSIS - MINOR BASALT DATA BATCH 1

NUMBER OF STANDARDS= 13

BA SLOPE= 5.8234 INTERCEPT=-45.2678 R= 0.99929 AVG. DEVIATION= 38.01 STAN. DEV.= 49.646

STANDARD ERROR IN SLOPE= 0.0827 STANDARD ERROR IN INTERCEPT= 1.0189

| STANDARD | PPM | CALCULATED | DIFFERENCE |
|----------|---------|------------|------------|
| BHVO | 135.00 | 191.10 | 56.10 |
| BCR-1 | 680.00 | 713.73 | 33.73 |
| JB-1 | 490.00 | 553.08 | 63.08 |
| W-1 | 160.00 | 175.85 | 15.85 |
| AGV-1 | 1200.00 | 1157.21 | -42.79 |
| SY-3 | 430.00 | 358.99 | -71.01 |
| NIM-L | 450.00 | 431.61 | -18.39 |
| DTS-1 | 5.00 | -33.84 | -38.84 |
| MGMICA | 4000.00 | 4002.29 | 2.29 |

REJECTED STANDARDS ARE: (0.0)

CO SLOPE= 0.2970 INTERCEPT= 0.2420 R= 0.99535 AVG. DEVIATION= 3.52 STAN. DEV.= 4.374

STANDARD ERROR IN SLOPE= 0.0096 STANDARD ERROR IN INTERCEPT= 0.1215

| STANDARD | PPM | CALCULATED | DIFFERENCE |
|----------|--------|------------|------------|
| BCR-1 | 36.00 | 38.06 | 2.06 |
| MRG-1 | 86.00 | 88.31 | 2.31 |
| JB-1 | 39.00 | 37.33 | -1.67 |
| W-1 | 47.00 | 41.16 | -5.84 |
| AGV-1 | 16.00 | 20.91 | 4.91 |
| SY-3 | 12.00 | 10.91 | -1.09 |
| NIM-L | 8.00 | 9.34 | 1.34 |
| DTS-1 | 135.00 | 129.48 | -5.52 |
| PCC-1 | 110.00 | 115.49 | 5.49 |
| FEMICA | 20.00 | 14.77 | -5.23 |
| MGMICA | 20.00 | 23.23 | 3.23 |

REJECTED STANDARDS ARE: QLO-1 (15.75)
BHVO (-8.78)

CR SLOPE= 0.2729 INTERCEPT=-25.7192 R= 0.99996 AVG. DEVIATION= 6.53 STAN. DEV.= 9.183

STANDARD ERROR IN SLOPE= 0.0010 STANDARD ERROR IN INTERCEPT= 0.0396

| STANDARD | PPM | CALCULATED | DIFFERENCE |
|----------|---------|------------|------------|
| BHVO | 300.00 | 289.98 | -10.02 |
| BCR-1 | 15.00 | 20.72 | 5.72 |
| W-1 | 115.00 | 124.46 | 9.46 |
| AGV-1 | 10.00 | -3.62 | -13.62 |
| NIM-L | 10.00 | 18.04 | 8.04 |
| QLO-1 | 4.00 | 1.54 | -2.46 |
| PCC-1 | 2800.00 | 2800.41 | 0.41 |
| MGMICA | 100.00 | 102.47 | 2.47 |

REJECTED STANDARDS ARE: SY-3 (-33.62)
JB-1 (19.49)

CU SLOPE= 1.1973 INTERCEPT= -1.0425 R= 0.99529 AVG. DEVIATION= 3.67 STAN. DEV.= 5.698

STANDARD ERROR IN SLOPE= 0.0521 STANDARD ERROR IN INTERCEPT= 0.3456

| STANDARD | PPM | CALCULATED | DIFFERENCE |
|----------|--------|------------|------------|
| BHVO | 140.00 | 132.32 | -7.68 |
| JB-1 | 56.00 | 64.41 | 8.41 |
| W-1 | 110.00 | 114.30 | 4.30 |
| SY-3 | 16.00 | 15.99 | -0.01 |
| QLO-1 | 27.00 | 27.12 | 0.12 |
| PCC-1 | 8.00 | 4.79 | -3.21 |
| FEMICA | 4.00 | 2.07 | -1.93 |

REJECTED STANDARDS ARE: AGV-1 (13.64)
BCR-1 (11.27)

continue.....

NB SLOPE= 2.3422 INTERCEPT= 3.3493 R= 0.99963 AVG. DEVIATION= 2.00 STAN. DEV.= 2.908

STANDARD ERROR IN SLOPE= 0.0286 STANDARD ERROR IN INTERCEPT= 0.1500

| STANDARD | PPM | CALCULATED | DIFFERENCE |
|----------|--------|------------|------------|
| BHVO | 19.00 | 20.26 | 1.26 |
| BCR-1 | 19.00 | 14.67 | -4.33 |
| MRG-1 | 20.00 | 21.14 | 1.14 |
| AGV-1 | 16.00 | 16.04 | 0.04 |
| QLD-1 | 10.00 | 13.53 | 3.53 |
| FEMICA | 270.00 | 271.03 | 1.03 |
| MGMICA | 120.00 | 117.33 | -2.67 |

REJECTED STANDARDS ARE: W-1 (6.68)

NI SLOPE= 0.5439 INTERCEPT=-11.9338 R= 0.99998 AVG. DEVIATION= 4.02 STAN. DEV.= 5.428

STANDARD ERROR IN SLOPE= 0.0013 STANDARD ERROR IN INTERCEPT= 0.0336

| STANDARD | PPM | CALCULATED | DIFFERENCE |
|----------|---------|------------|------------|
| BHVO | 120.00 | 114.65 | -5.35 |
| BCR-1 | 10.00 | 17.99 | 7.99 |
| MRG-1 | 195.00 | 189.91 | -5.09 |
| JB-1 | 135.00 | 128.39 | -6.61 |
| W-1 | 76.00 | 76.00 | 0.00 |
| AGV-1 | 15.00 | 13.99 | -1.01 |
| NIM-L | 11.00 | 17.07 | 6.07 |
| QLD-1 | 6.00 | 9.11 | 3.11 |
| PCC-1 | 2400.00 | 2400.91 | 0.91 |

REJECTED STANDARDS ARE: DTS-1 (46.20)

continue.....

RB SLOPE= 5.7249 INTERCEPT= 0.3191 R= 0.99961 AVG. DEVIATION= 0.58 STAN. DEV.= 0.810

STANDARD ERROR IN SLOPE= 0.0716 STANDARD ERROR IN INTERCEPT= 0.1844

| STANDARD | PPM | CALCULATED | DIFFERENCE |
|----------|-------|------------|------------|
| BHVO | 10.00 | 9.04 | -0.96 |
| BCR-1 | 47.00 | 48.04 | 1.04 |
| MRG-1 | 8.00 | 7.85 | -0.15 |
| JB-1 | 41.00 | 41.21 | 0.21 |
| W-1 | 21.00 | 21.78 | 0.78 |
| AGV-1 | 67.00 | 66.85 | 0.15 |
| QLO-1 | 74.00 | 73.24 | -0.76 |

REJECTED STANDARDS ARE: DTS-1 (9.41)

SR SLOPE= 69.5064 INTERCEPT= 1.3856 R= 0.99991 AVG. DEVIATION= 2.60 STAN. DEV.= 3.787

STANDARD ERROR IN SLOPE= 0.4240 STANDARD ERROR IN INTERCEPT= 0.7788

| STANDARD | PPM | CALCULATED | DIFFERENCE |
|----------|--------|------------|------------|
| BCR-1 | 330.00 | 327.60 | -2.40 |
| JB-1 | 440.00 | 446.23 | 6.23 |
| W-1 | 190.00 | 188.95 | -1.05 |
| AGV-1 | 660.00 | 657.16 | -2.84 |
| PCC-1 | 1.00 | 1.13 | 0.13 |
| FEMICA | 5.00 | 2.19 | -2.81 |
| MGMICA | 25.00 | 27.74 | 2.74 |

REJECTED STANDARDS ARE: BHVO (-29.09)
MRG-1 (9.84)

continue.....

V SLOPE= 2.6309 INTERCEPT=-12.1511 R= 0.99966 AVG. DEVIATION= 3.43 STAN. DEV.= 4.252

STANDARD ERROR IN SLOPE= 0.0307 STANDARD ERROR IN INTERCEPT= 0.2472

| STANDARD | PPM | CALCULATED | DIFFERENCE |
|----------|--------|------------|------------|
| BCR-1 | 420.00 | 421.77 | 1.77 |
| JB-1 | 210.00 | 214.52 | 4.52 |
| W-1 | 260.00 | 255.57 | -4.43 |
| AGV-1 | 125.00 | 120.27 | -4.73 |
| SY-3 | 51.00 | 48.17 | -2.83 |
| DTS-1 | 11.00 | 14.36 | 3.36 |
| PCC-1 | 29.00 | 31.34 | 2.34 |

REJECTED STANDARDS ARE: MRG-1 (33.70)
 BHVO (18.50)
 QLO-1 (9.57)

Y SLOPE= 3.2198 INTERCEPT= 3.7667 R= 0.99997 AVG. DEVIATION= 1.39 STAN. DEV.= 2.171

STANDARD ERROR IN SLOPE= 0.0106 STANDARD ERROR IN INTERCEPT= 0.0655

| STANDARD | PPM | CALCULATED | DIFFERENCE |
|----------|--------|------------|------------|
| BHVO | 27.00 | 29.46 | 2.46 |
| BCR-1 | 40.00 | 37.07 | -2.93 |
| MRG-1 | 16.00 | 15.59 | -0.41 |
| JB-1 | 26.00 | 24.46 | -1.54 |
| AGV-1 | 19.00 | 21.20 | 2.20 |
| SY-3 | 740.00 | 740.04 | 0.04 |
| QLO-1 | 24.00 | 24.17 | 0.17 |

REJECTED STANDARDS ARE: (0.0)

continue.....

ZR SLOPE= 21.3804 INTERCEPT= 7.4686 R= 0.99998 AVG. DEVIATION= 1.22 STAN. DEV.= 1.935

STANDARD ERROR IN SLOPE= 0.0600 STANDARD ERROR IN INTERCEPT= 0.1770

| STANDARD | PPM | CALCULATED | DIFFERENCE |
|----------|--------|------------|------------|
| BCR-1 | 185.00 | 185.38 | 0.38 |
| MRG-1 | 105.00 | 105.52 | 0.52 |
| AGV-1 | 230.00 | 231.71 | 1.71 |
| DTS-1 | 10.00 | 6.39 | -3.61 |
| PCC-1 | 6.00 | 6.86 | 0.86 |
| FEMICA | 800.00 | 799.35 | -0.65 |
| MGMICA | 20.00 | 20.79 | 0.79 |

REJECTED STANDARDS ARE: QLO-1 (47.79)
 JB-1 (-13.06)
 BHVO (-10.42)
 W-1 (-11.70)

ABUNDANCES FROM DUPLICATE ANALYSES

ESTIMATE OF ANALYTICAL PRECISION

XRF TRACE ELEMENTS

Abundances in ppm

| SAMPLE | Ba | Rb | Nb | Sr | Y | Co | Cr | Cu | Ni | V | Zr |
|---------------------|------|-------|-------|--------|-----|-----|--------|------|--------|-------|---------|
| NIML ₅ | 355 | 195 | (767) | (4419) | 20 | 2 | (0) | (76) | 6 | 85 | (10557) |
| Ref. ₅ | 450 | 190 | (960) | (4600) | 25? | 8? | (10?) | (13) | 11 | 81 | (11000) |
| NIMD ₅ | 0 | 0 | 3 | 3 | 4 | 194 | (3209) | 2 | (2701) | 45 | 20 |
| Ref. ₅ | 10? | N/R | N/R | 3? | N/R | 208 | (2900) | 10 | (2040) | 40 | 20? |
| NIMG ₅ | 82 | 340 | 59 | 11 | 144 | 5 | (0) | 3 | 6 | 2 | 287 |
| Ref. ₅ | 120? | 325 | 53 | 10 | 147 | 4? | (12) | 12 | 8? | 2? | 300 |
| SY3 ₁ | 388 | (127) | 136 | (141) | 748 | 13 | 0 | (3) | (88) | 49 | (252) |
| Ref. ₁ | 430 | (208) | 130 | (306) | 740 | 12 | 10 | (16) | (11) | 51 | (320) |
| NBS688 ₁ | 180 | 2 | 6 | 170 | 22 | 42 | (85) | 81 | 145 | (216) | 60 |
| Ref. ₁ | 200 | 1.9 | N/R | 169 | N/R | 50 | (330) | 96 | 150 | (250) | N/R |
| COQ61 ₂ | 842 | 54 | 6 | 479 | 28 | * | 65 | * | 12 | 191 | 149 |
| Ref. ₂ | 873 | 53 | 7 | 480 | 28 | | 64 | | 9 | 197 | 156 |
| COQ251 ₂ | 576 | 21 | 5 | 605 | 23 | * | 39 | * | 27 | 241 | 95 |
| Ref. ₂ | 589 | 21 | 5 | 578 | 26 | | 50 | | 23 | 241 | 107 |
| COQ632 ₂ | 646 | 42 | 6 | 500 | 28 | * | 4 | * | 12 | 213 | 120 |
| Ref. ₂ | 668 | 44 | 7 | 512 | 30 | | 22 | | 13 | 225 | 132 |
| V8M ₄ | 525 | 41 | 6 | 447 | 27 | * | * | * | 50 | 276 | 54 |
| Ref. ₄ | 534 | 36 | 4.1 | 420 | 25 | | | | 54 | 267 | 65 |
| 12-2 ₄ | 1 | 3 | 2 | 49 | 10 | * | * | * | (316) | 144 | 12 |
| Ref. ₄ | 13 | 1.72 | 3.4 | 46.2 | 4.6 | | | | (281) | 143 | 22.2 |

continue.....

TRACE cont.

| SAMPLE | Ba | Rb | Nb | Sr | Y | Co | Cr | Cu | Ni | V | Zr |
|--------------------|------|-----|-----|-------|------|----|-------|----|-------|-------|------|
| 27-22 ₄ | 92 | 5 | 3 | 374 | 15 | * | * | * | 65 | 300 | 17 |
| Ref. ⁴ | 86 | 5.1 | 1.9 | 353 | 13 | | | | 56 | 324 | 30 |
| 35-19b | 106 | 4 | 3 | 216 | 24 | * | * | * | 221 | 295 | 25 |
| Ref. ⁴ | 72 | 3 | 3.1 | 211 | 22 | | | | 211 | 307 | 38 |
| 35-17a | (26) | 3 | 2 | (541) | 4 | * | * | * | 23 | (80) | 4 |
| Ref. ⁴ | (75) | 4.9 | 2.4 | (665) | 2.7 | | | | 26 | (130) | 21.8 |
| 34-3b | 290 | 36 | 7 | 394 | 16 | * | * | * | 98 | 276 | 57 |
| Ref. ⁴ | 294 | 35 | 7.8 | 403 | 15 | | | | 101 | 272 | 73 |
| EXMOUNT1 | * | 4 | 4 | (155) | 29 | * | 262 | * | 160 | * | 92 |
| Ref. ³ | | 3.6 | 1.8 | (181) | 26.9 | | 275.7 | | 150.9 | | 87.4 |
| EXMOUNT2 | * | 1 | 3 | 177 | 29 | * | 261 | * | 153 | * | 89 |
| Ref. ³ | | 1.9 | 3 | 177 | 26.5 | | 275.6 | | 143.9 | | 85.7 |
| EXMOUNT3 | * | 2 | 3 | 189 | 30 | * | 263 | * | 142 | * | 99 |
| Ref. ³ | | 1.7 | 2 | 189 | 26.2 | | 280.9 | | 134.5 | | 97.4 |
| BRBEAR1 | 64 | 3 | 9 | 214 | 36 | * | * | 47 | 90 | 283 | 119 |
| Ref. ³ | 50 | 2 | 6 | 208 | 32 | | | 59 | 80 | 256 | 111 |
| BRBEAR2 | 92 | 5 | 12 | 227 | 33 | * | (176) | 61 | 55 | (330) | 134 |
| Ref. ³ | 51 | 9 | 8 | 235 | 34 | | (238) | 70 | 49 | (269) | 128 |
| COBB1 | 94 | 6 | 13 | 248 | 38 | * | (118) | 50 | 59 | 300 | 154 |
| Ref. ³ | 40 | 3 | 9 | 248 | 32 | | (271) | 64 | 57 | 274 | 140 |
| COBB2 | 84 | 4 | 12 | 232 | 38 | * | 105 | 70 | (47) | (328) | 144 |
| Ref. ³ | 29 | 2 | 8 | 226 | 38 | | 110 | 82 | (28) | (276) | 133 |

N/R = standard has no referenced value

* = sample was not analyzed previously

? = questionable value

¹Abbey, 1983²Berman, 1979³R.L. Chase (pers. comm.)⁴Isachsen, 1984⁵Steele et al., 1978

APPENDIX IV - TA CONTAMINATION

New INAA Ta data plotted on discrimination diagrams showed both enormous enrichment and great scatter in Ta relative to abundances in the samples which were used to define tectonic fields. (Wood, 1980; Wood et al., 1979; Pearce, 1979). This suggested either:

- the mantle source region beneath B.C. is enriched in Ta and heterogeneous,
- analysis for Ta was done incorrectly, or
- the samples had been contaminated with Ta during preparation.

Mantle enrichment in Ta would likely be accompanied by enrichments in other incompatible elements, but as these 'other' enrichments are not observed it is presumed that the mantle beneath B.C. is not enriched in Ta. Precision of the Ta analysis for reference standards is $\pm 10\%$, implying that the analytical technique was not at fault, but in intralab standards P-1 and WP1 the analytical scatter is larger than $\pm 100\%$. This hinted that sample contamination during preparation was the most probable cause of the enrichment and variation.

Most of the samples had been powdered for analysis in previous studies and incomplete records were kept concerning the equipment used in their preparation (whether BICO disc mill and/or agate mortar, or steel ring mill, or tungsten carbide ring mill). The samples prepared specifically for this

study were all crushed in a tungsten-carbide ring mill and they all have anomalously high Ta abundances (see Table XX), suggesting it was the tungsten-carbide which contaminated the sample. In addition, Wood et al. have (1979) have stressed that preparation in a tungsten carbide shatter box was a major source of Ta contamination and should be avoided. To confirm this suggested source of contamination, silica sand was acid washed and crushed in the same tungsten-carbide ring mill and the resulting powder was analyzed by XRF. As suspected a peak corresponding to tens of ppm of Ta was present, which could only be there as a result of contamination (C.J. Hickson and S.J. Juras, in preparation). Therefore in order to use Ta discrimination diagrams a substitution or correction must be made.

Sienko and Plane (1957) and Parker and Fleischer (1968) note that Nb and Ta are a pair of elements which have similar ionic radii (Nb=0.69 Å; Ta=0.68 Å), identical valence states, are very incompatible, and always occur together in minerals. They substitute for Ti in clinopyroxene, hornblende, Mg-Fe mica, titanomagnetite and sphene.

Abundances and ratios of Nb and Ta occurring in various rock types were compiled by Parker and Fleischer (1968). Average abundances of Nb:Ta in subalkaline continental gabbros and basalts were reported as 17 ppm and 1 ppm respectively whereas granites, quartz monzonites and granodiorites averaged 12 ppm Nb and 1.3 ppm Ta. In the alkaline equivalents of the above rock types the Nb and Ta abundances increased by

approximately five times, however the Nb/Ta ratios ranged from 10 to 15 independent of the rock series. More recently Wood (1980) and Gill (1981) report the average Nb/Ta ratio equal to 16.

A compilation of recent analyses of Nb and Ta in some igneous rock standards is presented in Table XXI. Nb concentrations range from a low of 9.4 ppm in RGM-1, a rhyolite, to 380 ppm in SG-1A, an albitized granite, and Ta concentrations range from 0.50 ppm in W-1, a diabase, to 26 ppm in SG-1A, the albitized granite standard. However Nb/Ta ratios show a much closer agreement ranging from 9.4 to 23.75 and averaging 15.1.

Table XXII records similar data for average Lewisian gneisses, granulite xenoliths and basalts from the Isle of Skye, Iceland and the Emperor seamount (Wood, 1980). Although the contents of Nb and Ta are generally much less in the Lewisian rocks than in the basalts the Nb/Ta ratios are similar, averaging 15.6, with a range from 11.3 to 20.

The average Nb/Ta ratio for all basaltic samples listed in Tables XXI and XXII is 15.8.

Approximately 50% of the Nb/Ta ratios in the analyzed rocks from this study do not lie within the range of ratios defined by the standards but abundances of Nb are similar to reported Nb abundances in basalts, confirming the probable contamination with Ta. With Nb/16 substituted for calculated Ta in the Ta-bearing discriminant diagrams, all of the data points plotted within the appropriate tectonic fields. (This

substitution for Ta is denoted by Ta* elsewhere in the thesis). The use of Nb in discriminant diagrams which involve Ta is acceptable provided that the concentrations of Nb are 1 ppm or greater (Wood et al., 1979).

TABLE XX

CALCULATED Nb AND Ta ABUNDANCES IN ANALYZED BASALTIC SAMPLES *

| SAMPLE | Nb (ppm) | Ta (ppm) | Nb/Ta |
|---------------------|----------|----------|-------|
| ARIS IS | 15 | N/D | > 15 |
| KITASU | 57 | 5 | 11.4 |
| LAKE IS | 23 | 82 | 0.3 |
| RAINBOW | 25 | 1 | 25 |
| ANAHIM | 33 | 2 | 16.5 |
| ITCHA1 ² | 45 | 4 | 11.3 |
| ITCHA2 | 61 | 3 | 20.3 |
| ALEX | 20 | N/D | > 20 |
| QUES LK | 21 | 3 | 7 |
| SPAN CK | 42 | 3 | 14 |
| WGRAYN | 22 | 4 | 5.5 |
| TROPHY | 16 | 1 | 16 |
| MASSET1 | 14 | 2 | 7 |
| MASSET2 | 15 | 1 | 15 |
| SATLIN | 12 | N/D | > 12 |
| PRINCER | 17 | 4 | 4.3 |
| AYNSH1 | 41 | 2 | 20.5 |
| AYNSH2 | 38 | 4 | 9.5 |
| ISKUTW | 30 | N/D | > 30 |
| BORDERLK | 25 | 5 | 5 |
| MT. DUNN | 30 | 3 | 10 |
| ISKUT | 24 | 1 | 24 |
| HOODOO ³ | 171 | 9 | 19 |
| BOWSER | 55 | 1 | 55 |
| SPEC1 | 20 | N/D | > 20 |
| SPEC2 | 27 | N/D | > 27 |
| EDZ1 | 37 | 2 | 18.5 |
| EDZ2 | 30 | 1 | 30 |
| NEDZ1 | 38 | 3 | 12.7 |
| NEDZ2 | 30 | 2 | 15 |
| NEDZ3 | 45 | 5 | 9 |
| NEDZ4 | 31 | 4 | 7.8 |
| LEVEL1 | 28 | 1 | 28 |
| LEVELD | 12 | N/D | > 12 |
| LEVEL2 | 32 | 2 | 16 |
| NATLIN | 51 | 4 | 12.8 |

* = Methods of preparation in Appendix 1

N/D = not detected

² Mugearite³ Peralkaline

TABLE XX (cont.)

| SAMPLE | Nb (ppm) | Ta (ppm) | Nb/Ta |
|----------------------|----------|----------|-------|
| CHEAK | 10 | 1 | 10 |
| GARIBALD | 9 | 7 | 1.3 |
| CAYLEY ¹ | 6 | 1 | 6 |
| ELAHO | 12 | N/D | > 12 |
| MEAGER | 15 | 13 | 1.2 |
| SALAL1 | 25 | 2 | 12.5 |
| SALAL2 | 21 | 1 | 21 |
| SALAL3 | 27 | 2 | 13.5 |
| SILVERA ¹ | 20 | 3 | 6.7 |
| SILVERH | 23 | 4 | 5.8 |
| COQ251 | 5 | 8 | 0.6 |
| COQ61 | 6 | 1 | 6 |
| COQ632 | 6 | 3 | 2 |
| BLIZZARD | 29 | 5 | 5.8 |
| CARD | 19 | 2 | 9.5 |
| WOOD LK. | 37 | 7 | 5.3 |
| DEADMAN | 22 | 5 | 4.4 |
| REDSTONE | 18 | 6 | 3 |
| BULLCAN | 6 | 6 | 1 |
| DOGCK | 12 | 1 | 12 |
| CAMEL | 9 | 5 | 1.8 |
| EDMUND | 3 | 5 | 0.6 |
| NAZKO | 13 | 2 | 6.5 |
| QUESW | 23 | 2 | 11.5 |
| ALERT1 ¹ | 9 | 5 | 1.8 |
| ALERT2 | 20 | 1 | 20 |
| ALERT3 | 29 | N/D | > 29 |
| BRBEAR1 | 9 | 5 | 1.8 |
| BRBEAR2 | 12 | N/D | > 12 |
| COBB1 | 13 | 4 | 3.3 |
| COBB2 | 12 | N/D | > 12 |
| EXMOUNT1 | 4 | 1 | 4 |
| EXMOUNT2 | 3 | 2 | 1.5 |
| EXMOUNT3 | 3 | 4 | 0.75 |
| SEXRIDGE | 7 | 13 | 0.5 |
| PREVRDG | 19 | 9 | 2.1 |
| EXDEEP | 15 | 15 | 1 |
| EXRIFT | 4 | 7 | 0.6 |

N/D = not detected

¹ Andesite

TABLE XX (cont.) (VANCOUVER ISLAND)

| SAMPLE | Nb (ppm) | Ta (ppm) | Nb/Ta |
|----------------------|----------|----------|-------|
| M598 | 10 | 3 | 3.3 |
| M600 | 4 | 19 | 0.3 |
| M605 | 8 | 10 | 0.8 |
| M606 | 4.4 | 2 | 2.2 |
| K609 | 12 | 17 | 0.7 |
| K613 | 10 | 6 | 1.7 |
| K614 | 11 | 8 | 1.4 |
| K615 | 11 | 3 | 3.7 |
| B618 | 5 | N/D | > 5 |
| B619 ¹ | 7 | 4 | 1.8 |
| B620 | 7 | N/D | > 7 |
| B621 | 7 | N/D | > 7 |
| S630 | 7 | 4 | 1.8 |
| S631 ¹ | 5 | 4 | 1.3 |
| S632 | 13 | 18 | 0.7 |
| 79-H-39 | 29 | 12 | 2.4 |
| 79H-10A ¹ | 10 | 1.38 | 7.25 |
| SICKER1 | 25 | 2 | 12.5 |
| SICKER3 | 6 | 3 | 2 |
| 10-1265 | 4 | N/D | > 4 |
| R-136 | 5 | 1 | 5 |
| 683422 ⁵ | 7 | N/D | > 7 |
| 683241 ⁵ | 8 | N/D | > 8 |
| 682132 ¹ | 9 | 1 | 9 |
| GMIC#4 ⁶ | 7 | 1 | 7 |
| 34-3b | 7.8 | 6 | 1.3 |
| WCT-3 | 7.6 | 4 | 1.9 |
| 15-12a | 3.4 | 4 | 0.8 |
| 35-19b | 3.1 | 9 | 0.3 |
| 12-2 | 3.4 | 2 | 1.7 |
| 27-22 ⁴ | 1.9 | N/D | > 1.9 |
| V8M | 4 | 7 | 0.6 |
| V8F ¹ | 4 | N/D | > 4 |
| IIP ⁵ | 7.1 | 6 | 1.2 |

N/D = not detected

¹ Andesite⁴ Ankaramite⁵ Diorite⁶ Granodiorite

TABLE XXI

ABUNDANCES OF Nb AND Ta IN STANDARDS (Abbey, 1983)

| SAMPLE | ROCK TYPE | Nb (ppm) | Ta (ppm) | Nb/Ta |
|--------|-------------------|----------|----------|-------|
| BHVO-1 | Basalt | 19 | 1.1? | 17.3 |
| BCR-1 | Basalt | 19? | 0.8? | 23.8 |
| BE-N | Basalt | 100 | 5.5? | 18.2 |
| W-1 | Diabase | 9.5 | 0.50 | 19 |
| AGV-1 | Andesite | 16? | 1.4? | 11.4 |
| G-1 | Granite | 24 | 1.5 | 16.0 |
| G-2 | Granite | 13? | 0.8? | 16.3 |
| NIM-G | Granite | 53 | 4.5? | 11.8 |
| SG-1A | Albitized Granite | 380 | 26 | 14.6 |
| QLO-1 | Quartz Latite | 10.5? | 0.9? | 11.7 |
| STM-1 | Syenite | 270? | 18? | 15.0 |
| RGM-1 | Rhyolite | 9.4? | 1.0? | 9.4 |

? = questionable value

TABLE XXII

ABUNDANCES OF Nb AND Ta IN TERRESTRIAL ROCKS (Wood, 1980)

| SAMPLE | ROCK TYPE | Nb (ppm) | Ta(ppm) | Nb/Ta |
|------------|---------------------|----------|---------|-------|
| LEWISIAN 2 | 4 Basic Gneisses | 2 | 0.1 | 20 |
| LEWISIAN 3 | Basic Gneiss | 2 | 0.12 | 16.7 |
| LESOTHO | Granulite Xenoliths | 5 | 0.3 | 16.7 |
| SKYE 1 | Alkali Basalt | 9 | 0.80 | 11.3 |
| SKYE2 | Hawaiite | 30 | 2.04 | 14.7 |
| EMPORER | Hawaiite | 29 | 2.01 | 14.4 |
| ICELAND 1 | Th. Basalt | 11 | 0.76 | 14.5 |
| ICELAND 2 | Shield tholeiite | 2 | 0.12 | 16.7 |